The application of fossil grass-phytolith analysis in the reconstruction of late Cainozoic environments in the South African interior

By

LLOYD ROSSOUW

Submitted in fulfillment of the requirements for the degree

PHILOSOPHIAE DOCTOR

In the Faculty of Natural and Agricultural Sciences
(Department of Plant Sciences)
University of the Free State, Bloemfontein
South Africa

May 2009

Promoter: Prof. L. Scott
(Department of Plant Sciences, University of the Free State)

Declaration

I declare that the thesis* hereby submitted by me for the Ph.D degree at the University of the Free State is my own independent work and has not previously been submitted by me at another university or faculty. I furthermore cede copyright of the thesis in favour of the University of the Free State.

Lloyd Rossouw
C/o National Museum, Bloemfontein and Department of Plant Sciences,
University of the Free State, Bloemfontein
29 May 2009

* Title: The application of fossil grass-phytolith analysis in the reconstruction of late Cainozoic environments in the South African interior.

ABSTRACT

Grass-dominated ecosystems occupy a primary position with regard to current debates concerning key events in faunal turnover and human evolution in Africa. Our knowledge of how grass-dominated ecosystems in southern Africa have reacted to periods of global warming and cooling in the past is provided by a broad range of proxy data sources, most notably pollen and stable isotope records. Phytolith analyses provide an alternative fossil record of environmental change and are now progressively becoming a conventional analytical approach in palaeoenvironmental research. The grass family (Poaceae) produces abundant silica bodies, especially within specific and specialized silica cells located in costal zones of the leaf epidermis. In addition to being highly resistant to decomposition, grass phytoliths show markedly varied and distinct morphologies. In this study a central hypothesis, namely that the morphology of grass short-cell phytoliths consistently follows meaningful environmental traits that are rooted in the relationship between phytolith shape and the ecological niche of grasses, was investigated by interpreting morphologically diagnostic grass phytolith assemblages according to their association with the ecological requirements of the grass species that produces them, irrespective of taxonomic affiliation. An effort was therefore made to assign ecological meaning to short-cell phytoliths by comparing a range of ecological preferences in modern grasses with the phytoliths that they produce, rather than just using phytoliths to discriminate between grass subfamilies, tribes or genera. This entailed a

systematic investigation of grass leaf epidermis from a collection of 309 species, followed by an assessment of the ecological significance of grass-short-cell phytoliths within a quantitative model. The model allowed for comparison of geographically diverse grass phytolith assemblages by converting them into one homogenous group represented by ecological categories. Several meaningful ecological trends were demonstrated by results in this study, and it is suggested that short cell phytolith association in grasses is primarily driven by a temperature gradient, marked by cool versus warm growing temperatures and reflected by grasses utilizing the C_3 and C_4 photosynthetic pathway. The study gives emphasis to the importance of investigating phytolith systematics with the aid of adequate comparative reference collections.

TABLE OF CONTENTS

GENERAL INTRODUCTION 1

Introduction 1

Grass silica short cells 9

Aims of the study 10

Structure of thesis 14

METHODOLOGY 16

Introduction 16

Description of Ecological Categories 18

Photosynthesis 19

Rainfall 20

Habitat 21

CLASSIFICATION OF GSSC-MORPHOTYPES 39

Introduction 39

Morphological Description 42

Background 42

GSSC-phytoliths analysed in this study 44

Lobate Class 46

Saddle Class 48

Trapeziform Class 48

QUANTITATIVE ANALYSES 56

Introduction **56**

Analysis of variance 56

Correspondence Analysis 56

Results **57**

Association between Morphotypes 58

Association between Morphotype and Subfamily 61

Ecological Categories 65

DISCUSSION AND CONCLUSION **99**

Production and affiliation between GSSC- phytoliths 99

GSSC-phytoliths and the environment 100

Applicability to fossil phytolith assemblages 101

Conclusion 103

REFERENCES **108**

APPENDICES

Appendix 1: Atlas of GSSC-phytoliths extracted from grass leaves. **131**

Appendix 2: Atlas of 227 grass leaf epidermis slide vouchers. **171**

Appendix 3: Indicator matrix of GSSC-morphotypes recorded in 309 grass species. **210**

Appendix 4: Spearman's rank-order correlation between association through rate of recurrence of morphotypes and relative abundance of morphotypes. **220**

Appendix 5: Basic statistics of the number of GSSC-morphotypes counted for each GSSC-morphotype subcategory. **224**

Appendix 6: GSSC-phytolith abundance as a proportion of all morphotypes per category. **229**

Appendix 7: Basic statistics of the number of GSSC-morphotypes counted for each subfamily subcategory. 235

Appendix 8: Subfamily: Tukey's HSD test for unequal sample sizes. 238

Appendix 9: Basic statistics of the number of GSSC-morphotypes counted for each photosynthetic pathway subcategory, including C_4 subtypes. 249

Appendix 10: Tukey's HSD test for unequal sample sizes in the Photosynthetic pathway-category (including C_3 and C_4). 252

Appendix 11: Tukey's HSD test for unequal sample sizes in the photosynthetic pathway - category (C_4 only). 264

Appendix 12: Basic statistics of the number of GSSC-morphotypes counted for each Rainfall subcategory. 271

Appendix 13: Tukey's HSD test for unequal sample sizes in the Rainfall-category 273

Appendix 14: Basic statistics of the number of GSSC-morphotypes counted for each habitat subcategory. 280

Appendix 15: Tukey's HSD test for unequal sample sizes in the Habitat-category. 285

Appendix 16: Comparison of GSSC-phytoliths against three Palaeoenvironmental Scenarios. 295

LIST OF TABLES

Table 1. Subdivision of subfamilies, tribes and genera representing three hundred and nine species used in this study. Classification after Clayton and Renvoize (1986) and GPWG (2001). **29**

Table 2. List of GSSC-morphotypes selected for this study and their equivalent descriptions according to the International Code for Phytolith Nomenclature (Madella et al. 2005). **33**

Table 3. Association through rate of recurrence. Association between GSSC-morphotypes based on their frequency within each category. **34**

Table 4. Relative abundance of GSSC-morphotypes based on proportional representation within each category. The frequencies are standardized, so that their sum in each row is equal to 100%. **35**

Table 5. Association through rate of recurrence. Association between GSSC-morphotypes based on their occurrence within the categories subfamily, photosynthesis, rainfall and habitat, expressed in percentage. **36**

Table 6. Relative abundance of GSSC-morphotypes based on their proportional representation within the categories subfamily, photosynthesis, rainfall and habitat (one hundred GSSC-bodies counted per species, averaged and standerdized so that the sum for each row is equal to 100%). **37**

Table 7. Summary of Spearman's rank-order correlation between association through the rate of recurrence of GSSC-morphotypes (Table 3) and relative abundance of GSSC-morphotypes (Table 4). **75**

Table 8. One-way ANOVA of the number of morphotypes as a proportion of the total number of phytoliths produced by dataset of 309 grass species. Marked differences are significant at $p < .05000$. **78**

Table 9. Dimension contributions to inertia in CA for GSSC-morphotypes. **79**

Table 10. One-way ANOVA for the Subfamily category. Marked differences are

significant at p < .05000. **81**

Table 11. Dimension contributions to inertia in CA using only morphotypes found to significantly differentiate between six subfamilies. **82**

Table 12. Proportional representation of GSSC-morphotypes and their mean carbon isotope δ 13C ratio in ($^{0}/_{00}$) Delta value data from Vogel *et al.* (1978); Ellis *et al.* (1980) and Schulze *et al.* (1996). **85**

Table 13. One-way ANOVA for the Photosynthetic pathway category. Marked differences are significant at p < .05000. **86**

Table 14. Dimension contributions to inertia in CA using only morphotypes found to significantly differentiate between C_3 and C_4 subcategories. **87**

Table 15. One-way ANOVA for the Photosynthetic pathway category including only C4 subtypes. Marked differences are significant at p < .05000. **89**

Table 16. Dimension contributions to inertia in CA using only morphotypes found to significantly differentiate between C_4 subtypes. **90**

Table 17. One-way ANOVA for the Rainfall category. Marked differences are significant at p < .05000. **92**

Table 18. Dimension contributions to inertia in CA using only morphotypes found to significantly differentiate between Rainfall subcategories. **93**

Table 19. One-way ANOVA for the Habitat category. Marked differences are significant at p < .05000. **95**

Table 20. Dimension contributions to inertia in CA using only morphotypes found to significantly differentiate between Habitat subcategories. **96**

Table 21. Number of dimensions that explain 100% of the variability, and the sum total of inertia for the first two dimensions that were extracted from each of the six sets of CA carried out in the study. **104**

Table 22. Summary meaningful association between GSSC-morphotypes and

subcategories based on CA of relative frequencies (dimension contributions). **106**

LIST OF FIGURES

Figure 1. Photomicrographs of prepared grass leaf epidermis. Planar view of in situ short cell silica bodies within the leaf epidermis. The long axis of the leaf is horizontal. Scale = 10ų. **12**

Figure 2. The biomes of South Africa. Map and biome categories after Mucina and Rutherford (2006). Rainfall data after Vogel *et al*. (1978) and Gibbs Russell (1990). **38**

Figure 3. Orientation of short cell phytoliths. Abaxial / adaxial aspects, are defined as the planar view (surface or plateau) or top view according to Mulholland (1989). The four sides connecting the planar aspect to the base of the silica body are described as side views for the long opposite faces, compared to end views for the short opposite faces. **51**

Figure 4. The Lobate Class. Bilobate variant 1: (1) planar view; (2) side view. Bilobate variant 2: (3-7) planar view; (8-10) oblique view; (11-12) side view. Bilobate variant 3: (13-15) planar view; (16) oblique view. Polylobate: (17-18) planar view; (19-20) oblique view. Cross: (21-24) planar view; (25) side view; (26) oblique view. The so-called *Stipa*-type is represented by 7, 11-12 and 18. **52**

Figure 5. The Saddle Class. Saddle variant 1: (1-5) planarview; (6-8) side view; (9) end view; (10) oblique view. Saddle variant 2: (11-13) planar view; (14-15) side view. **53**

Figure 6. Basic morphological features of the Saddle Variant 1. **54**

Figure 7. Basic morphological features of the Saddle Variant 2. **54**

Figure 8. The Trapeziform Class. Trapezoid: (1-4) planar view; (5-6) oblique view; (7-12) side view. Rondel: (13-14) planar view; (15-17) oblique view; (18) side view. Oblong: trapeziform sinuate, (19-21,26) planar view; trapeziform smooth, (22, 25, 27) oblique view; trapeziform polylobate, (23, 24) oblique view; Reniform: (28-30) planar view; (31) side view. **55**

Figure 9. Bivariate plot of the number of morphotypes (mean %) with sample size. Regression line with 0.95 conf. int.; r2 = 0.1657; r = 0.4070, p = 0.2241. **76**

Figure 10. Box plot with whiskers showing relative abundance of GSSC-morphotypes as a proportion of the total number of morphotypes in grasses that produce them. **77**

Figure 11. A two-dimensional distribution of CA demonstrating the relationship between GSSC-morphotypes. **80**

Figure 12. First two dimensions of CA using only morphotypes found to significantly differentiate between six subfamilies. **83**

Figure 13. Bivariate plot of relative abundance of morphotypes and average carbon isotope δ 13C ratios in species that produce them. C3 grasses show an average of -26.5 %0 (δ< -20 %0) and C4 grasses an average of -12.5 %0 (δ< -16 %0) (Vogel *et al*. 1978). **84**

Figure 14. First two dimensions of CA using only morphotypes found to significantly differentiate between C3 and C4 photosynthetic types. **88**

Figure 15. First two dimensions of CA using only morphotypes found to significantly differentiate between C_4 subtypes (aspartate (NAD and PCK) and malate formers (NADP). **91**

Figure 16. First two dimensions of CA using only morphotypes found to significantly differentiate between Rainfall subcategories. **94**

Figure 17. First two dimensions of CA using only morphotypes found to significantly differentiate between Habitat subcategories. **97**

Figure 18. First two dimensions of CA using only morphotypes found to significantly differentiate between Habitat subcategories. **98**

Figure 19. A two-dimensional distribution of CA demonstrating the relationship between the categories habitat, rainfall and photosynthesis, based on the occurrence of eleven GSSC-morphotypes in 309 grass species. **105**

Figure 20. Bivariate plot of the number of C4- (A) and C3-grass species (B) with <500mm summer rainfall areas. Regression line with 0.95 confidence interval. **107**

General Introduction

Introduction

A large amount of research has been generated with regard to southern hemisphere climate changes during the late Cenozoic, which shows that the impact of orbital forcing and the influences of high-latitude ice volumes were major driving mechanisms of southern hemisphere climate evolution (DeMenocal 1995; Partridge *et al.* 1997). In addition, the evolution of grass-dominated ecosystems has received considerable attention over the past two decades, especially concerning the time period that is for the most part relevant to human evolution (Retallack 2001; Cerling *et al.* 1997; Vrba 1995; Jacobs *et al.* 1999). The reason is because grass-dominated ecosystems occupy a primary position with regard to current debates concerning key events in faunal turnover and human evolution in Africa (Vrba 1995; Scott 2002; Bobe and Behrensmeyer 2004).

During the last five million years several major cooling and warming episodes have impacted on the Earth's climate within an overall trend towards global cooling and aridification (DeMenocal 1995; Partridge *et al.* 1997). These cycles, also known as Milankovitch cycles, are astronomical permutations of the earth's orbital eccentricity, tilt and orientation of its spin axis that influenced climate changes at different times with the shortest cycle of 23 000 years prominent prior to 2.8 million years ago, a 41 000 year cycle dominating between 2.8 million and one million years ago and a 100 000 year cycle governing from one million years onwards (DeMenocal 1995; Partridge *et al.* 1997). Biotic reactions to climate changes of this magnitude varied

from extinction to speciation - responses that, according to the habitat hypothesis, are major driving mechanisms of evolutionary change (Vrba 1995).

In this instance the expansion and contraction of grasslands in Africa played an important role in creating prospects for vicariance and speciation (Cerling *et al*. 1997, Vrba 1995). Our knowledge of how grass-dominated ecosystems in southern Africa have reacted to periods of global warming and cooling in the past is provided by a broad range of proxy data sources, including sedimentary, biological and archaeological evidence (Deacon & Lancaster 1988; Vrba *et al*. 1995; Shaw & Thomas 1996; Partridge *et al*. 1997, 2004; Scott 1999a, 1999b, 2002). The most comprehensive records of late Neogene grasslands in the central interior of South Africa are derived from faunal studies, pollen sequences and stable isotope records (Brink 1987, 1988; Brink and Rossouw 2000; Scott 2002; Lee-Thorpe and Talma 2000; Rossouw 2006; Hopley *et al*. 2007). Whereas fossil vertebrate fauna and stable carbon isotopes from fossil enamel, paleosols, speleothems and fossil hyrax dung have added considerably to the proxy data record of palaeo-grassland environments, pollen records have presented the most direct access to plant communities of the past and is one of the most common methods of palaeoenvironmental reconstruction, providing key records of vegetation change and climatic fluctuations since the Cretaceous in southern Africa (Coetzee 1967; Klein 1984; Scholtz 1985; Van Zinderen Bakker 1984, 1989, 1995; Scott *et al*. 1995, 1999b, 2002; Lee Thorp and Talma 2000).

Refinement of regional patterns in grassland history is hampered by lack of identification of grass pollen data below family level and the incapability of carbon

isotope analysis to distinguish between C_3 grass and dicotyledonous vegetation (Mulholland 1989; Scott 2002). The problem is compounded by an overall scarcity of terrestrial pollen records, which also impedes palynological investigations of early grassland expansion on the subcontinent (Chase and Meadows 2007). Lately, phytolith analyses have provided an alternative fossil record of environmental change throughout the Neogene and are now progressively becoming a conventional analytical approach in palaeoenvironmental research (Piperno 1988, 2006).

The term phytolith is a general description for soluble, hydrated silica that is deposited within a variety of plant types (Piperno 1988, 2006). Hydrated silica is also described as opal phytoliths, plant opal, colloidal silica or biogenic opal. These terms generally include both the typical silica bodies formed in specialized silica cells as well as uncharacteristic silica bodies sometimes present in other epidermal cells of living plants. Phytoliths are useful for palaeoenvironmental studies because it is inorganic, resistant to oxidation and can be found in a variety of sedimentary contexts that lack pollen (Jones and Beavers 1963; Rovner 1971, 1983, 1988; Pearsall 1982; Mulholland 1989; Piperno 1988, 2006).

The study of phytoliths is a comparatively young discipline with regards to palaeoenvironmental studies and has also developed as a tool in a wide variety of applications (Bryant 1993). Phytoliths were already known from historical observations of plant material and was observed in living plants by a German botanist, called Struve, in 1835 and Ehrenberg in 1841 and 1846 (Piperno 1988). Silica bodies noted in horsetails and grasses were referred to as ‘silex’ by John Lindley, a professor of botany at the University of London until 1860 (Piperno 1988).

The siliceous tissue of plants in windblown dust is also mentioned by Charles Darwin during his travels on the H.M.S. Beagle over two hundred and fifty years ago (Piperno 1988). Ehrenberg developed the first classification system for phytoliths in 1854 and recognized several dozen types of phytoliths (Piperno 1988).

Already at an early stage, opal phytoliths were used as an "index mineral" by comparing amounts, shapes and sizes of opal extracted from soils with those from plants (Beavers and Stephan 1958). Smithson (1958) and Wynn Parry and Smithson (1958, 1964) showed that phytoliths from British soils could be assigned to particular grass tribes or groups of tribes. Baker (1959) analyzed phytoliths in soils for shape distribution and found that the phytolith forms identified can be an effective indicator of the vegetation history. Jones (1964) noted the palaeoenvironmental potential of phytoliths after identifying silica bodies in Cenozoic sedimentary rocks. Oberholster (1968) explained the occurrence of plant opal in two soil profiles from Springbok Flats, South Africa in terms of pedoturbation. Fossil sediments from Western Victoria in Australia were analyzed to test the stability of opal phytoliths in terms of long term preservation (Gill 1967). Armitage (1975) demonstrated the potential use of phytoliths as indicators of herbivore diets when phytoliths were extracted from dental calculus on the teeth of modern cattle. Rovner (1971, 1988) attempted to show the level at which opal phytoliths are taxonomically significant in palaeoecological studies and provided a discussion of phytoliths from various archaeological sites. Phytoliths from soils were used to reconstruct prehistoric and early historic agricultural activities in Hawaii (Pearsall and Trimble 1984). Plant material and soils were analyzed for maize and wild grasses phytoliths in a comparative study in order to recognize

archaeological maize in Panama (Piperno 1984). Fossil pollen and phytoliths were used to document vegetation changes throughout a period of loess accumulation during the Pleistocene in Nebraska, USA (Fredlund *et al.* 1985). Ollendorf (1987) conducted a comparative study of phytoliths obtained from archaeological sediments at the Iron Age site of Tel Miqne in Israel. Palaeodiet preferences in Pleistocene herbivores were explored looking at dental boluses and the silica remains it contain (Akersten *et al.* 1988). A textbook on phytolith analysis provided a comprehensive summary of the discipline and an up to date account of past phytolith research (Piperno 1988). Research on tropical angiosperms from Panama provided an account of the occurrence and morphology of phytoliths in their reproductive structures (Piperno 1989). Using stereological identification methods, Russ and Rovner (1989) distinguished wild *Zea* varieties from cultivated primitive maize for archaeological comparison. In a quantitative study, the taphonomy and morphology of phytoliths from coastal dune sediments were investigated to determine ancient human occupation in the UK (Powers *et al.* 1989). Ciochon *et al*. (1990) identified phytoliths from the enamel surfaces of the teeth of the extinct Asian ape from Liucheng Cave in China. Retallack *et al.* (1990) and Retallack (1992) described wooded grassland conditions at Fort Ternan, Kenya, 14 million years ago by the identification of grass short cell phytoliths. Dugas and Retallack (1993) undertook a SEM investigation of fossilized grass plant material in Middle Miocene paleosols from Fort Ternan, Kenya, showing details of grass short cell phytoliths with comparison to the most similar living grass genera. Fredlund and Tieszen (1994) used modern phytolith assemblages from the North American Great Plains as proxies for past

environmental changes and followed it up with a statistical analysis of modern phytolith assemblages to interpret fossil phytolith assemblages in terms of Late Pleistocene climate changes (Fredlund and Tieszen 1997). Piperno and Pearsall (1993) showed differences and similarities in the reproductive structures of maize and teosinte from North and South America. Fox *et al.* (1994) identified grass-like phytoliths on the surface of historical human teeth from Spain, using SEM and Middleton and Rovner (1994) described a method for the extraction of phytoliths from herbivore dental calculus. Rovner (1994) used phytolith analyses to reconstruct 200 years of floral history of the Harpers Ferry historical site in West Virginia, USA. In an attempt to identify rice phytoliths from early agricultural sites in Thailand, Kaelhofer and Piperno (1994) conducted a comparative study of mainly grasses from the region. Alexandre *et al.* (1997) conducted quantitative analyses of grass and dicotyledonous phytoliths using indices to provide a palaeoenvironmental history of Holocene lake sediments in Senegal and the Congo. Phytoliths in contemporary, Holocene and Pleistocene sediments from Ethiopia were applied to facilitate the temporal differentiation of regional vegetation over time (Barboni *et al.* 1999). Runge (1999) presented a classification scheme of soil phytolith assemblages as a guide to characterize rain forest and grassland vegetation in central Africa. Late Pleistocene and Holocene sediment cores from Tswaing Crater in South Africa provided grass phytoliths that were used as a proxy for palaeoclimatological processes (McLean and Scott 1999). Mercader *et al.* (2000) applied phytoliths of grasses and arboreal plants, extracted from Late Pleistocene and Holocene sediments, as a proxy for palaeovegetation dynamics in the Ituri Forest of the Congo. The application of grass

phytolith assemblages as proxies for palaeoclimatic shifts, was further explored by Mulder and Ellis (2000) using South-West African grass leaf phytoliths. McClaren and Umlauf (2000) investigated the potential for carbon isotopes in phytoliths to estimate long-term desert grassland dynamics in southwestern North America. Gobetz and Bozarth (2001) extracted phytoliths from dental calculus removed from the teeth of Late Pleistocene mastodons. Wallis (2001) studied phytolith assemblages as an alternative source of vegetation history for tropical savannah regions in northwestern Australia. Madella *et al.* (2002) carried out a phytolith analysis of archaeological sediments to interpret subsistence behaviour and mobility patterns of Neanderthals from Amud Cave in Israel. Carnelli *et al.* (2002) suggested a new microanalytical technique for application in palaeoenvironmental research by showing that woody and herbaceous phytoliths can be distinguished based on the amount of aluminum found in the phytoliths they produce. Chemical analysis of occluded carbon in phytoliths suggested important ramifications for the application of $\delta^{13}C$ analysis on C_3 and C_4 plant matter due to the highly depleted state of the occluded organic carbon in charred organic material (Krull *et al.* 2003). Albert *et al*. (2003) conducted a quantitative analysis of grass and dicotyledonous phytoliths from Mid to Late Pleistocene hearths and associated sediments at Hayonim Cave in Israel. In a related study, Elbaum *et al* (2003) presented a method to distinguish between burnt and unburnt phytolith assemblages in archaeological sites by measuring the refractive indices of individual phytoliths. Abrantes (2003) provided a 340 000 year continental climate record from tropical Africa based on a quantitative analysis of C3 and C4 grass phytoliths from Mid to Late Pleistocene sediment cores in the

Equatorial Antlantic. In Urugauy, Iriarte (2003) studied a range of grass taxa and nine modern soil samples by applying multivariate analysis to discriminate between cross-shaped phytolith assemblages in the identification of maize from archaeological sites. Phytoliths extracted from plant remains and archaeological sediments from Panama were analyzed in a comparative study in order to identify maize in neotropical regions (Pearsall *et al.* 2003). Piperno (2003) presented a review of the earliest remains of maize found in Ecuador based on phytoliths recovered from food residues, as well as comments made on the technique which identifies remains of vegetative structures of maize. In an additional investigation, Pearsall *et al*. (2004) identified phytoliths and starch granules recovered from stone tools at Real Alto in Ecuador. Thorn (2004a) provided an annotated bibliography of phytolith studies with photographic atlas of selected New Zealand subantarctic and subalpine phytoliths. Through a quantitative analysis of grass phytoliths from fossil sediments, Thorn (2004b) also suggested that C_4-grasslands, and a minor woody component, were regionally predominant in Queensland, Australia during late Holocene times. Stromberg (2004, 2005) presented a record of grassland evolution in the central Great Plains of the USA, based on the analysis of soil phytolith assemblages from late Tertiary sediments. Harvey and Fuller (2005) based the development of rice and millet processing models for Neolithic sites in North-Central India on phytolith assemblages while Boyd (2005) used phytoliths from aeolian sediments to study regional palaeoenvironmental change during the Holocene in the northern Great Plains of Canada. Bremond *et al.* (2005) demonstrated two phytolith indices to distinguish between grasslands in tropical areas and presented a new phytolith proxy to gain insight into grass water

stress. Prasad *et al.* (2005) reported the presence of phytoliths, including that of grasses, identified in fossilized coprolites of titanosaurid sauropods that lived about 65 to 71 million years ago in central India. Late Holocene human coprolites from southwestern North America show phytoliths as well as calcium oxalate bodies from desert suculents in human diet, and suggest that calcium oxalate phytoliths from desert succulents caused dental microwear (Reinhard and Danielson 2005). Tsartsidou *et al*. (2006) examined a modern reference collection of plants in order to evaluate the contribution of phytoliths in archaeological studies in Greece. Webb and Longstaffe (2006) looked at oxygen isotope signatures in phytoliths for application in paleoclimate studies. Albert *et al.* (2006) and Bamford *et al.* (2006) constructed a taphonomical model based on the post-depositional preservation of grass, sedge, palm and dicotyledonous phytoliths from Plio-Pleistocene sediments at Olduvai Gorge in Tanzania. In a comparative study of modern phytoliths, a range of soil phytolith assemblages were analyzed from various phytogeographical zones from inter-tropical Africa to discriminate vegetation types (Barboni *et al.* 2007).

Grass silica short cells

The grass family (Poaceae) produces abundant silica bodies, especially within specific and specialized silica cells located in costal zones of the leaf epidermis (Metcalfe 1960; Kok 1972; Ellis 1979). In addition to being highly resistant to decomposition, grass phytoliths show markedly varied and distinct morphologies and several morphological studies have indicated that a number of grass morphotypes are characteristic of certain taxa (Twiss *et al*. 1969; Brown 1984; Mulholland 1989; Mulholland and Rapp 1992). Numerous types of silicification are found in grasses.

Silica infilling of intercellular spaces between sub-epidermal cells can also occur, including those from intercostal zones, but these atypical silica bodies are generally not characteristic in shape (Parry and Smithson 1964; Ellis 1979; Clayton and Renvoize 1986). Intracellular silicification of various types of epidermal cells, more often than not conforms closely to the shape of the original cell, and is sometimes very useful in palaeoecological studies (Bremond *et al.* 2005). This includes long cells, bulliform cells, stomatal guard cells, cork cells, macrohairs, microhairs and prickles (Ellis 1979).

Analyses of grass silica short cell (GSSC) phytoliths have been particularly forthcoming with regard to grassland history and associated palaeoclimatic changes, while complementing pollen studies in overall vegetative reconstructions (Figure 1). GSSC-phytoliths, are specialized silica cells (idioblasts) located in both the costal zone and intercostal zones of the leaf epidermis, overlying the vascular bundles and their associated sclerenchyma (Metcalfe 1960; Kok 1972; Ellis 1979; Clayton and Renvoize 1986). These cells comprise only a portion of the total siliceous residue and have restricted distributions within grasses, but they provide the most taxonomically useful types of grass phytoliths (Twiss *et al*. 1969, Rovner 1971, Ellis 1979; Brown 1984; Piperno 1988; Mulholland 1989; Mulholland and Rapp 1992; Fredlund and Tieszen 1997; Barboni *et al.* 1999; Stromberg 2002, 2004; Bremond *et al*. 2005).

Aims of the study

Palaeo-grassland inferences, using phytoliths, have been derived from quantitative assessments of phytolith assemblages using multivariate analyses and ratio models that provide indices to predict particular environmental conditions (Fredlund *et al*.

1985; Twiss 1992; Powers-Jones and Padmore 1993; Alexandre *et al*. 1997; Barboni *et al.* 1999, 2007; Fredlund and Tieszen 1997; Mercader *et al*. 2000; Boyd 2005; Bremond *et al.* 2008). However, the analysis of fossil phytolith assemblages tend be site-specific, and designed around specific taxonomic analogues in order to identify phytoliths that discriminate between different taxonomic groups (Stromberg 2004; Piperno 2006).

The original aim of this study involved a general approach for analyzing fossil phytoliths, but a lack of standardized methodology lead to a change of focus with the result that my endeavor culminated in the development of a uniform model for interpreting GSSC-phytolith assemblages within a singular ecological framework. The title of this thesis may therefore be misleading as this investigation eventually focused on establishing a standard methodology for fossil phytolith analyses and not on the analysis of fossil phytoliths from the central interior of southern Africa, itself.

My approach followed on previous phytolith studies that have emphasized the importance of studying modern phytolith assemblage variability in order to interpret fossil assemblages on a regional scale, through 'vegetative' rather than 'floristic' reconstructions of grass communities (Fredlund and Tieszen 1994; 1997). Reasons for using GSSC-phytoliths were based on three assumptions. Firstly, unlike many other phytolith-producing plant taxa, grasses occur in a variety of habitats throughout South Africa and are suitable indicators of a diversity of environmental conditions (Acocks 1988; Gibbs Russell *et al*. 1990). Secondly, studies have shown that, within the grass family, GSSC-phytoliths are proven to be highly diagnostic and hardy morphotypes (Twiss *et al.* 1969; Mulholland 1989; Fredlund and Tieszen 1994).

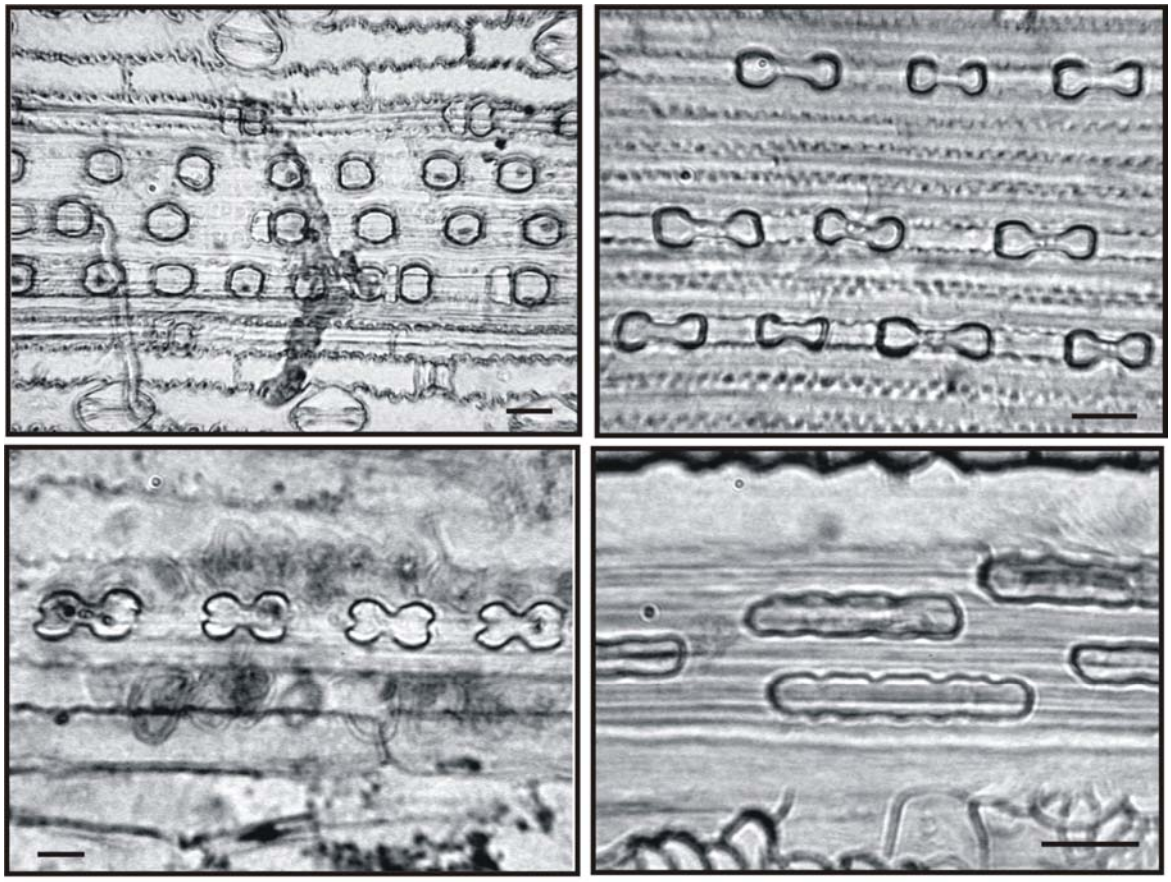

Figure 1. Photomicrographs of prepared grass leaf epidermis. Planar view of *in situ* short cell silica bodies within the leaf epidermis. The long axis of the leaf is horizontal. Scale = 10ų.

Thirdly, the effect of 'inheritance' on phytolith assemblages, where settling of phytolith assemblages in topsoils over time, is influenced by variables such as surface stability and chemical dissolution, (Fredlund and Tieszen 1994). As a result, interpretation of phytolith assemblages are complicated by several biases, including variable production rates of phytoliths in different plant groups, discrete size distributions in phytolith assemblages from different ecological contexts, post-depositional transport and variable preservation (Jones and Handreck 1963; Twiss *et al.* 1969; Bartoli

and Wilding 1980; Piperno 1988; Alexandre *et al.* 1997; Hansen *et al.* 1998). This inconsistent preservation of phytoliths owing to different taxonomic origins or morphology may strongly influence the interpretation of fossil phytolith assemblages (Jones and Handreck 1963; Bartoli and Wilding 1980).

An important effect as a result of these factors, together with the tendency for prolific grass phytolith production in general, is the tendency for grass phytoliths to be over-represented in soil assemblages (Piperno 1988). Focusing on phytoliths that are derived from a single plant group, circumvent potential bias related to differential preservation between different plant taxa. Additionally, grass phytolith assemblages provide abundant quantities of diagnostic GSSC-phytoliths.

Central to this study was the intention to refine the predictive power of GSSC-phytoliths by providing a quantitative model for predicting general patterns of past environmental conditions by interpreting morphologically diagnostic grass phytolith assemblages according to their association with the ecological requirements of the grass species that produces them, irrespective of taxonomic affiliation. An effort was therefore made to assign ecological meaning to GSSC-phytoliths by comparing a range of ecological preferences in modern grasses with the phytoliths that they produce, rather than just using phytoliths to discriminate between grass subfamilies, tribes or genera.

I attempted a methodology that is comparable to ecological structure analysis. Through this method, habitats and environmental conditions are reconstructed by conveying ecological attributes to extant organisms and comparing it to fossil communities (Andrews and Nesbit-Evans 1979; Van Couvering 1980; Andrews

1989; Reed 1997; 1998). These studies have shown that unlike methods using taxonomic analogues, the analysis of ecological association allows for the comparison of temporally or geographically diverse assemblages without being concerned with taxonomical differences. I subsequently devised a comparable method to explore and test the following assumption:

The biogeographical distribution of grasses in southern Africa, is linked to several climatic parameters (Vogel et al. 1978; Ellis et al. 1980; Gibbs Russell 1988; Gibbs Russell et al. 1990). Consequently, the morphology of South African grass short-cell phytoliths consistently follows meaningful environmental traits due to the relationship between phytolith shape and the ecological niche occupied by various taxonomic groups within the grass family. Grass short-cell phytoliths are therefore appropriate indicators of grass-community responses to periods of environmental change. This assumption forms the basis of the study and was tested through the following objectives in Chapters 3 and 4:

- Provision and explanation of a modern phytolith reference collection as a frame of reference for comparison;
- Assessment of the environmental significance of grass phytoliths, based on a botanical index of modern grass chorology, and using standard methods of observation, description and statistics to explore the relationship between grass short-cell morphology and grass chorology in southern Africa.

Structure of thesis

The remainder of the thesis is composed of seven chapters. Chapter 2 discusses methods and materials used for analyzing the ecological significance of modern

grass phytoliths. A description of grass short cell morphology, based on a modern reference collection that is included in two appendices, is presented in Chapter 3. Chapter 4 provides a quantitative analysis of the morphological data and the implications of these results are discussed and concluding remarks offered in Chapter 5. A list of references and appendices are presented in Chapters 6 and 7.

Methodology

Introduction

Assessment of the environmental significance of GSSC-phytoliths, was based on a botanical index of grass biogeography, extracted from a dataset of three hundred and nine grass species, comprising eight subfamilies, nineteen tribes and one hundred and two genera (Table 1). Morphological descriptions of the GSSC-phytoliths were guided by observations represented in two reference collections (Appendices 1 and 2). One collection consists of slide preparations of five-centimetre leaf sections taken from voucher specimens of mature individuals housed at the herbarium of the Department of Botany at the National Museum in Bloemfontein, the National Herbarium of Pretoria and the Bolus Herbarium at the University of Cape Town (Appendix 1). Standard dry-ashing procedures (described in Appendix 1) were followed to extract phytoliths from these herbarium samples (Parr *et al.* 2001). Additional comparisons were done on a collection of prepared slide vouchers of fully-articulated grass leaf epidermis sections from the Roger Ellis collection housed at the National Herbarium of Pretoria (Appendix 2) A set quantity of one hundred GSSC-bodies were counted per slide, each slide representing one species. This included the articulated short cell bodies located along the costal zones of each epidermis section from the Roger Ellis collection, and the disarticulated short cell bodies counted along randomly selected traverses in the dry-ashed collection.

Biogeographical data for each species was collated from published research, herbarium records and the National Herbarium Computerized Information System

(Chippendall and Crook 1976; Gibbs Russell 1985; Gibbs Russell *et al.* 1990). The latter is a robust vegetation database that includes distribution data of one thousand eight hundred and eleven species, based on the records of more than sixty-two thousand grass specimens collected in southern Africa. This system provides a checklist of grasses that occur in each of the 3900-quarter degree grids that cover southern Africa (Gibbs Russell 1985; 1988; Gibbs Russell *et al*. 1990).

As a first step, species were converted into numeric profiles, using eleven GSSC-morphotype variables to represent each species according to their rate of recurrence (presence or absence) into a binary indicator matrix (summarized in Table 3, listed in lefthand-column in Appendix 3). However, this quantification method produces only frequency data. As a result, the procedure was repeated by counting one hundred individual GSSC-phytoliths per slide to ascertain the relative abundance (rate of production) of each of the eleven morphotypes, in order to provide a dataset that could be tested for significant differences between means (ANOVA) (summarized in Table 4, listed in righthand-column in Appendix 3). A non-parametric Spearman's rank-order correlation-coefficient, r_S, was used to confirm expected positive covariation between the values of the corresponding GSSC-phytolith types in two phytolith datasets (Table 3 and 4) (see Quantitative Analysis).

From the data, I created GSSC-profiles for six subfamilies, as well as for nineteen ecological categories, their diversity reflected by photosynthesis, rainfall and habitat. The GSSC-morphotype variables were grouped into five categories, namely morphotype, subfamily, photosynthesis, rainfall and habitat. In order to eventually infer ecological trends from GSSC phytoliths, percentages of morphotypes were

calculated for each category, and in return, percentages of each adaptation, (i.e. morphotype), were analyzed by ecological category. This was achieved by tabulating the percentages of GSSC-phytoliths according to their distribution and the ecological adaptation of the grasses that produce them. The results are summarized in Table 5 and 6 and presented in Appendices 7, 9, 12 and 14.

Thus, each category was allocated a numerical profile based on morphotype association that reflects a non-phylogenetic community structure. This means that ecological preferences are differentiated based on the resulting phytolith assemblage structure. The approach allowed me to determine the degree of association between GSSC-morphotype and ecological condition, and enabled me to compare modern ecological categories directly with each other as well as with fossil phytolith assemblages because the parameters that were used are not taxon-specific and therefore not effected by temporal or geographical separation.

Description of Ecological Categories

Climate is perceived as the principal dynamic component and obvious independent variable shaping vegetation on all scales (Schulze 1997). South Africa, being the southernmost sovereign region on the African continent covers a total surface area of approximately 1,2 million square kilometers with the effect that its topography and latitudinal position (between 18º and 35º south) strongly influences general climate patterns (Figure 2). In addition, the country has an extensive coastline, constituting the western, southern and eastern boundaries of the country. Consequently, the effects of oceanic circulation systems and offshore currents are well reflected in the

overall climate distribution of the region (Deacon and Lancaster 1988; Scott 1995; Barrable *et al.* 2002; Scott and Lee Thorp 2004; Chase and Meadows 2007).

Since grasses are adapted to react relatively swiftly to environmental changes, including variation in atmospheric carbon dioxide, moisture availability and temperature, the taxonomic composition of grassy ecosystems indirectly reflects a variety of regional climatic conditions by means of their ecological preferences (Vogel *et al*. 1978; Gibbs Russell 1988, 1990; Ficken *et al*. 2002; Scott 2002; Wooller and Beuning 2002). Nineteen ecological preferences (categories) were selected, representing different biochemical variants of the photosynthetic pathway, rainfall variability and habitat preferences associated with grass distribution in South Africa.

Photosynthesis

Distribution of grasses in southern Africa is primarily linked to growing season temperature and seems to account for the geographic distribution of C_3 and C_4 grasses, where elevated temperatures during the growing season favour the C_4 photosynthetic pathway (Vogel *et al*. 1978; Ellis *et al.* 1980; Cerling *et. al*. 1997; Ehleringer *et al.* 1991, Ehleringer *et al.* 1997; Sage and Monson 1999; Sage 2004). C_3 and C_4 respectively refer to three-carbon and a four-carbon molecules being the first products in photosynthesis (Ehleringer and Monson 1993). They represent two photosynthetic pathways that exist among grasses - the ancestral C_3 (Calvin–Benson) photosynthetic pathway which is utilized by grasses generally thriving under cool, dry to mesic winter-rainfall conditions, and the C_4 (Hatch–Slack) photosynthetic pathway, which is subdivided into aspartate formers and malate formers (Vogel *et al*. 1978; Ellis *et al.* 1980; Schulze *et al*. 1996). The aspartate formers dominate grass

flora in arid summer rainfall regions with conditions of low soil moisture availability, while the malate formers (NADP-me type) attain their maximum frequency in high summer rainfall areas (Vogel *et al*. 1978; Ellis *et al.* 1980; Gibbs Russell *et al.* 1990) Two subtypes are recognized for the aspartate formers, namely the NAD-me-type, dominating in warm, arid areas with low and unpredictable summer rainfall and the PCK-type (phosphoenolpyruvate-carboxykinase), associated with grasses adapted to intermediate rainfall levels and occurring in moist habitats with summer rainfall less than 350mm per year, (Ellis *et al.* 1980). The PCK-type appears to be an intermediate between the NAD-me type and the malate forming NADP-me type (Ellis *et al.* 1980).

Rainfall

South Africa is part of a generally semi-arid subcontinent, with less than five percent of the region receiving annual rainfall of greater than 800 mm and more than ninety percent of rainfall returning to the atmosphere as part of evaporative loss (Schultz 1997). Although dry climates dominate southern Africa, the region covers a wide range of climatic zones, ranging from true desert to temperate and subtropical to tropical systems, with strongly seasonal precipitation regimes (Rutherford and Westfall 1994; Oldfield and Thompson 2004; Mucina and Rutherford 2006). The region's rainfall is determined by seasonal shifts of the South Atlantic and Indian Ocean anti-cyclonic, high-pressure systems (Deacon and Lancaster 1988). The northern and eastern parts of southern Africa receive mostly summer rainfall where the eastern escarpment with its Drakensberg range is responsible for major orographic effects. Mean annual precipitation is highest along the eastern

escarpment and generally decreases westwards from the escarpment across the plateau (Schulze 1997). Another rainfall maximum occurs in the southwestern Cape where rainfall increases from 400 mm on the Cape Flats to over 2000 mm in the Cape Fold Mountains (Deacon and Lancaster 1988). Eighty percent of the annual precipitation in the southwestern Cape occurs during the winter season (Schulze 1997; Rutherford and Westfall 1994).

Three rainfall subcategories were selected based on the arrangement of grass subfamily regions according to Gibbs Russell (1988) (Figure 2). The subcategories consists of a higher than forty percent winter rainfall group (>40%W), a less than five hundred millimeters summer rainfall group (<500mm S), and a higher than five hundred millimeters summer rainfall group (>500mm S). Distribution of grass subfamilies in southern Africa suggests that the Panicoideae subfamily is most abundant in summer rainfall areas with more than 500 mm of rainfall per year, while the Chloridoideae and Aristidoideae are most abundant in summer rainfall areas with rainfall less than 500 mm per year. This corresponds to the division between dry and moist grassland of the Grassland Biome where sour (unpalatable) andropogonoid grasses predominate above 600 mm of rainfall and sweet (palatable), chloridoid grasses are more common below 600 mm of rainfall (Rutherford and Westphall 1996). The Arundinoideae, Bambusoideae, Danthionoideae, Ehrhartoideae and introduced pooids prefer regions with more than forty percent of rainfall occurring in winter while indigenous pooids are most abundant in the high Drakensberg mountain range on the eastern escarpment (Gibss Russell *et al.* 1990).

Habitat

The South African region represents a highly diverse and endemic, southern temperate and subtropical flora, which is reflected by several distinctive ecological regions or biomes (Cowling and Hilton-Taylor 1997; Rutherford 1997; Mucina and Rutherford 2006) (Figure 2). Defined on the basis of climate, corresponding life-form patterns and vegetation structure, biomes offer an ecological framework for biotic communities, including grasses (Rutherford and Westfall 1994; Low and Rebelo 1996). Grasses occur ubiquitously throughout most of South Africa. It is the predominant plant life form in the Grassland Biome, and is, except for the Desert Biome, also widespread in all the major biomes of southern Africa (Rutherford and Westfall 1994; Rutherford 1997).

Twelve habitat subcategories were selected for the study (see Habitat category in Table 5). Except for edaphic and montane grasslands, and grasses adapted to shady habitats, description of habitat types was based on their association with seven well-defined biomes according to the categorization by Rutherford and Westfall (1994) and Rutherford (1997). These were the categories used by Gibbs Russell *et al*. (1990) in their reference guide of southern African grasses (Figure 2). The latest categorization of South African biomes includes all seven biomes described by Rutherford and Westfall (1994), but with the inclusion of two new biomes that were previously elements of the Savanna Biome, namely the Albany Thicket Biome and Indian Ocean Coastal Belt Biome (Rutherford *et al.* 2006a, Figure 2).

Strictly speaking, the term ‘grassland’ refers to vegetation dominated by grasses in a single layered structure or sometimes with an open, woody plant cover (Rutherford and Westfall 1994) Therefore, in describing the habitat categories, the term

'grassland' was used to refer only to montane, edaphic, and savanna grasslands and the grasslands of the Grassland Biome. In contrast, grass communities occurring in the Desert, Succulent Karoo and Nama-Karoo biomes make up a very small fraction of the total vegetation component and cannot be described as grasslands.

Grassland

One hundred and thirty four grass species from the sample group were associated with the Grassland Biome. The temperate grasslands of South Africa cover the high central plateau of South Africa, inland areas of Kwazulu-Natal and the mountainous regions of the Eastern Cape Province, occupying about 24 percent of the country's surface area (Rutherford and Westfall 1994; Mucina *et al.* 2006a). It is strongly seasonal with summer rainfall and late summer maximum in vegetation, followed by near complete termination of activity in winter accompanied by winter drought (O'Connor and Bredenkamp 1997). Thunderstorms and hail are common in summer and frost is common in winter, while fire is vital to its structure. Division between dry and moist grassland are made on the basis of annual rainfall, with 500 to 700 mm of rainfall marking the boundary (Rutherford and Westfall 1994) (Figure 2). Perennial grasses are the dominant plant form, but annuals are important components of the vegetation where disturbance occurs. The grasslands are moisture-dependant and decreases with lower annual rainfall. Woody species are limited to specialized niches, but forbs form an important component of the grasslands (Rutherford and Westfall 1994).

Montane and High altitude grassland

Eighty eight grass species from the sample group were associated with these grasslands. The montane grasslands of South Africa generally correspond to the

Grassland Biome in terms of their floristic composition, the obvious distinction pertaining to mountainous regions of generally high altitudes with relatively cool mean annual temperatures, where rainfall may occur at any time of the year and orographic mists supplement rainfall (Meadows and Linder 1993; Mucina *et al*. 2006a; Rutherford *et al.* 2006a). Two broadly defined sub-categories were delineated in this study: (1) montane grasslands that are primarily associated with the Great Escarpment of the Drakensberg region, including montane grassland communities on Karoo inselbergs, and the Cape Folded Belt in the southwestern and southern Cape; (2) high-altitude montane grasslands that are associated with the very highest plateaus and mountain ridges of the Drakensberg region found generally above 2000m above sea level (Figure 2). The high-altitude montane grasslands category mostly corresponds with Acocks' 'Themeda—Festuca Alpine' Veld (Acocks 1988), the 'Alti Mountain Grassland' of Low and Rebelo (1988) and the 'Drakensberg Afroalpine Heathland' Sub-biome of Mucina *et al*. (2006a). The majority of the centres of endemism recognized in the Grassland Biome are linked to high altitudes.

Savanna Grassland

One hundred and fifty seven grass species from the sample group were associated with the Savanna Biome. The Savanna Biome represents the southernmost extension of the largest biome in Africa and nearly encloses the temperate Grassland Biome where it grades into the Albany Thicket and Indian Ocean Coastal Belt Biomes (Rutherford *et al*. 2006b). Savannas are characterized by wooded subtropical grasslands, also called savanna woodland, shrub savanna or bushveld in many areas of the country. It accounts for almost 33 percent of the South African

landscape, does not occur at high altitude and is found mostly below 1500 m with temperatures generally higher than the adjacent Grassland Biome (Rutherford and Westfall 1994). The biome is characterized by seasonal rainfall with wet summer and dry winter periods. Development of the modern savanna is closely linked to the evolution of C_4 photosynthesis in grasses (Sage and Monson 1999; Sage 2004).

Nama-Karoo

Eighty five grass species from the sample group were associated with this biome. The Nama-Karoo covers most of the vast central plateau region of the Western and Northern Cape Provinces. It is an arid biome that forms an ecotone between the fynbos flora to the south, and the subtropical savanna in the north (Mucina *et al*. 2006b). Climate influence is continental, with low unreliable rainfall that mostly occurs in late summer. Summers are hot with a mean January maximum of > 30°C. Local endemism is very low with Asteraceae, Fabaceae and Poaceae the dominant plant families.

Desert

Twenty six grass species from the sample group were associated with this biome. The Desert Biome adjoins the western Atlantic seaboard, southern Angola, Namibia and within South Africa, stretches from the Atlantic coast along the Orange River inland towards the town of Pofadder in northern Bushmanland (Jurgens *et al*. 2006). It is defined by less than 70mm of annual rainfall in the easternmost parts and by sparse perennial vegetation of less than ten percent canopy cover (Jurgens *et al*. 2006). The southern margin of the biome is bordering on the temperate winter-rainfall region of the most arid parts of the Succulent Karoo Biome (Jurgens *et al*. 1997). A

small variety of grass species, with *Stipagrostis* the most common genus, occurs in this hyperarid region of low rainfall and high evapotranspiration rates.

Succulent Karoo

Forty six grass species from the sample group were associated with this biome. The Succulent Karoo Biome is a semi-desert region restricted to the year-round and winter rainfall with very high levels of summer aridity (Milton *et al.* 1997). Mean annual rainfall is low, varying between 100 mm and 200 mm with the overall biome average about 170 mm. The biome occurs mostly west of the western escarpment through the western belt of the Western Cape, inland towards the Little Karoo, and interfaces with the Fynbos Biome with which it shares its greatest floristic affinity (Mucina *et al.* 2006a). A high diversity of dwarf leaf-succulent shrubs dominates the vegetation, mainly represented by the Aizoaceae, Euphorbiaceae, Crassulaceae and succulent members of the Asteraceae.

Fynbos

One hundred and four grass species from the sample group were associated with the Fynbos Biome. It has dry and hot summers, associated with a high frequency of trade winds, and winter rainfall, which is brought on by the occurrence of westerly cyclonic fronts (Rutherford and Westfall 1994). Mean annual rainfall averaged over the total area of the biome is about 480 mm. The biome is situated almost exclusively in the south-western and southern parts of the Western Cape Province, and comprises three major vegetation complexes, namely fynbos, renosterveld and strandveld (Rebelo *et al*. 2006). Fynbos consist of an evergreen, fire-prone shrubland dominated by the Restionaceae family, and shrubs of the Ericaceae, Asteraceae, Rhamnaceae and Rutaceae families (Rebelo *et al*. 2006). Trees are rare and grasses comprise

a relatively small part of the biomass. Grassy fynbos occurs on soils of finer texture, higher nutrient levels and under conditions of less summer drought. Grasses also occur in renosterveld vegetation, which refers to *Elytropappus rhinocerotis*, the dominant plant in this complex (Rebelo *et al*. 2006). Strandveld vegetation is usually found close to the sea and consists of dense to closed shrublands dominated by sclerophyllous, broad-leaved shrubs (Rebelo *et al*. 2006).

Forest

Afrotemperate Forests are highly distinctive, but characterized by very small and patchy occurrences over the wetter parts of the winter- and summer-rainfall areas of the country (Mucina and Geldenhuys 2006). Fifteen grass species were associated with this category. Forests occur scattered along the eastern and southern margins of South Africa, with the majority smaller than one hundred hectares in size. Forests are characterized by vegetation dominated by evergreen trees and a large specific set of distinctive flora where graminoids are usually rare (Rutherford and Westfall 1994). Their distribution is mostly determined by high water availability and persists in areas with mean annual rainfall of more than 525 mm with strong winter rainfall, and more than 725 mm with summer rainfall, while orographic precipitation also plays a major role. (Mucina and Geldenhuys 2006).

Edaphic habitats

One hundred and three grass species from the sample group were associated with this subcategory. Edaphic grasslands are not related to any particular climatic region. For this subcategory, edaphic grasslands were determined largely by the condition of the substratum, in this case seasonally or permanently waterlogged soils. In terms of vegetation structure it is associated with seasonal pans, swamps, vleis or wetlands

(White 1983; habitat subcategories *Damp soils* and *Swamps / Vleis* in Table 5 and 6) and corresponds to the Inland Azonal Vegetation category of Mucina *et al.* (2006c).

Shady habitats

Forty three grass species were associated with this habitat preference. As with the edaphic grassland category, this habitat type is not related to any particular climatic region or regional vegetation structure. Unlike the Forest habitat subcategory, this preference was selected on the basis of grass adaptation to shady habitats that include open woodland or riparian canopy and rock crevices in open environments (Gibbs Russell *et al.*1990).

Table 1. Subdivision of subfamilies, tribes and genera representing three hundred and nine species used in this study. Classification after Clayton and Renvoize (1986) and GPWG (2001).

Clade	Subfamily	Tribe	Genus	Pathway
BEP	Bambusoideae Luerss.	Bambuseae Dumort.	Thamnocalamus	C3
			Bambusa	C3
			Olyra	C3
	Ehrhartoideae Link	Ehrharteae Nevski	Ehrharta	C3
		Centotheceae Ridley	Megastachya	C3
		Oryzeae Dumort.	Leersia	C3
			Oryza	C3
			Prosphytochloa	C3
	Pooideae Benth.	Brachypodieae (Hack.) Hayek	Brachypodium	C3
		Bromeae Dumort.	Bromus	C3
		Meliceae Link ex Endl.	Melica	C3
		Poeae R. Br.	Colpodium	C3
			Festuca	C3
			Poa	C3
			Puccinellia	C3
		Stipeae Dumort.	Stipa	C3
		Aveneae Link	Agrostis	C3
			Anthoxantum	C3
			Helictotrichon	C3
PACCAD	Arundinoideae Burmeist.	Arundineae Dumort. (identical to subfamily and thus redundant)	Dregechloa	C3
			Phragmites	C3
			Elytrophorus	C3
			Styppeiochloa	C3

Table 1 continued

PACCAD	Danthonioideae Barker & H.P.Linder	Danthonieae Zotov (identical to subfamily and thus redundant)	Danthonia	C3	
			Karroochloa	C3	
			Pentaschistis	C3	
			Tribolium	C3	
			Pentameris	C3	
			Pseudopentameris	C3	
			Schismus	C3	
			Chaetobromus	C3	
			Merxmuellera	C3	minus *M. rangei* (incl. Chloridoideae)
			Prionanthium	C3	
	Aristidoideae Caro	Aristideae C.E. Hubbard (identical to subfamily and thus redundant)	Aristida	C4	
			Stipagrostis	C4	
			Sartidia	C3	
	Panicoideae Link	Andropogoneae Dumort.	Andropogon	C4	
			Bothriochloa		
			Cymbopogon	C4	
			Dichantium	C4	
			Diheteropogon	C4	
			Elionurus	C4	
			Eriochrysis	C4	
			Heteropogon	C4	
			Hyparrhenia	C4	
			Hyperthelia	C4	
			Imperata	C4	
			Ischaemum	C4	
			Monocymbium	C4	
			Sorghastrum	C4	
			Themeda	C4	
			Vetiveria	C4	

Table 1 continued

PACCAD	Panicoideae Link (cont.)	Arundinelleae Stapf	Loudetia	C4
			Trichopterix	C4
			Tristachya	C4
		Paniceae R. Br.	Alloteropsis	C3/C4
			Anthephora	C4
			Brachiaria	C4
			Digitaria	C4
			Echinochloa	C4
			Entolasia	C3
			Eriochloa	C4
			Leucophrys	C4
			Melinis	C4
			Oplismenus	C3
			Panicum	C3/C4
			Pennisetum	C4
			Sacciolepis	C3
			Setaria	C4
			Stenotaphrum	C4
			Tarigidia	C4
			Tricholaena	C4
			Urochloa	C4
	Chloridoideae Kunth ex Beilschm.	Cynodonteae Dumort.	Harpochloa	C4
			Chloris	C4
			Eustachys	C4
			Schoenefeldia	C4
			Enteropogon	C4
			Cynodon	C4
			Ctenium	C4
			Michrochloa	C4
			Spartina	C4
			Rendlia	C4
			Tragus	C4
			Perotis	C4

Table 1 Continued

Chloridoideae Kunth ex Beilschm.	**Pappophoreae Kunth**	**Enneapogon**	**C4**	
		Schmidtia	**C4**	
	Eragrostideae Stapf	**Eragrostis**	**C4**	**except *E. walteri* = C3 (Ellis 1984)**
		Entoplacamia	**C4**	
		Fingerhuthia	**C4**	
		Oropetium	**C4**	
		Coelachyrum	**C4**	
		Triraphis	**C4**	
		Dinebra	**C4**	
		Brachyochloa	**C4**	
		Cladoraphis	**C4**	
		Eleusine	**C4**	
		Dactyloctenium	**C4**	
		Pogonarthria	**C4**	
		Sporobolus	**C4**	
		Lophachme	**C4**	
		Diplachne	**C4**	

Table 2. List of GSSC-morphotypes selected for this study and their equivalent descriptions according to the International Code for Phytolith Nomenclature (Madella *et al.* 2005).

			International Code for Phytolith Nomenclature (2005)		
		Current Study	ICPN Names	Shape 3D	Shape 2D
LOBATE	1	Bilobate Variant 1	Dumbbell	Tabular, Trapezoidal	Bilobate
	2	Bilobate Variant 2	Dumbbell	Tabular, Trapezoidal	Bilobate
	3	Bilobate Variant 3	Dumbbell	Tabular, Trapezoidal	Bilobate
	4	Polylobate	Polylobate	Trapezoidal, Cylindrical	Polylobate
	5	Cross	Cross	——	Quadra-lobate
SADDLE	6	Saddle Variant 1	Saddle	Equidimensional, dorsally & ventrally concave	Saddle, Concave
	7	Saddle Variant 2	——	Equidimensional, dorsally & ventrally concave	Square, Rectangular
TRAPEZIFORM	8	Trapezoid	Trapeziform	Trapezoidal, Cubic, Concave	Square, Rectangular
	9	Rondel	Rondel	Conical	Orbicular, Ovate
	10	Oblong	Trapeziform Sinuate	Carinate, Tabular, Trapezoidal	Oblong, Elongated, Rectangular
	11	Reniform	——	Reniform, Trapezoidal	Crescentic

Table 3. Association through rate of recurrence. Association between GSSC-morphotypes based on their frequency (absence / presence) within each category. For example, 36.5% of grass species that produce the Bilobate Variant 1 morphotype (n = 52), also produce the Bilobate Variant 2 morphotype.

Morphotype			Lobate %					Saddle %		Trapeziform %			
	1 Abbrev.	2 Species	3 Bilobate Var1	4 Bilobate Var2	5 Bilobate Var3	6 Polylobate	7 Cross	8 Saddle Var1	9 Saddle Var2	10 Trapezoid	11 Rondel	12 Oblong	13 Reniform
Bilobate Var1	B1	52	100.0	36.5	5.8	26.9	5.8	1.9	1.9	0.0	0.0	1.9	1.9
Bilobate Var2	B2	139	14.4	100.0	19.4	24.5	15.8	0.0	1.4	9.4	4.3	5.0	4.3
Bilobate Var3	B3	40	5.0	77.5	100.0	12.5	15.0	10.0	5.0	15.0	5.0	10.0	15.0
Polylobate	Po	51	23.5	72.5	11.8	100.0	5.9	0.0	2.0	11.8	5.9	15.7	0.0
Cross	Cr	25	4.0	96.0	20.0	12.0	100.0	0.0	0.0	4.0	0.0	4.0	0.0
Saddle Var1	S1	49	2.0	2.0	8.2	0.0	0.0	100.0	34.7	0.0	0.0	0.0	4.1
Saddle Var2	S2	46	0.0	6.5	0.0	0.0	0.0	43.5	100.0	19.6	6.5	2.2	26.1
Trapezoid	Tr	70	0.0	25.7	10.0	8.6	0.0	0.0	12.9	100.0	25.7	24.3	41.4
Rondel	Ro	24	0.0	25.0	8.3	0.0	0.0	0.0	25.0	62.5	100.0	8.3	45.8
Oblong	Ob	26	0.0	26.9	15.4	26.9	0.0	0.0	0.0	53.8	7.7	100.0	11.5
Reniform	Re	37	2.7	16.2	16.2	0.0	0.0	2.7	27.0	73.0	18.9	5.4	100.0

Table 4. Relative abundance of GSSC-morphotypes based on proportional representation within each category. The frequencies are standardized, so that their sum in each row is equal to 100%. For example, in the Bilobate Variant 1 category (n = 52), the Bilobate Variant 1 morphotype accounts for 73.02%, while the Bilobate Variant 2 represents 14.48% of the total number of GSSC-morphotypes counted.

Morphotype			Lobate%					Saddle%		Trapeziform%			
	1 Abbrev.	2 Species	3 Bilobate Var1	4 Bilobate Var2	5 Bilobate Var3	6 Polylobate	7 Cross	8 Saddle Var1	9 Saddle Var2	10 Trapezoid	11 Rondel	12 Oblong	13 Reniform
Bilobate Var1	B1	52	73.02	14.48	0.77	8.87	1.98	0.65	0.00	0.00	0.00	0.00	0.42
Bilobate Var 2	B2	139	6.01	69.97	4.63	8.03	4.39	0.00	0.52	4.29	0.41	1.20	0.76
Bilobate Var 3	B3	40	2.60	46.02	29.45	3.62	3.77	6.75	0.00	4.31	0.05	0.87	2.27
Polylobate	Po	51	14.53	38.90	3.20	33.57	0.69	0.00	0.00	2.75	0.18	6.31	0.27
Cross	Cr	25	6.00	54.20	3.48	1.80	34.52	0.00	0.00	0.00	0.00	0.00	0.00
Saddle Var 1	S1	49	0.34	0.00	4.06	0.00	0.00	85.75	9.55	0.00	0.00	0.00	0.45
Saddle Var 2	S2	46	0.00	0.80	0.00	0.00	0.00	28.07	50.11	10.59	2.35	0.00	8.13
Trapezoid	Tr	70	0.00	10.45	2.61	1.87	0.00	0.00	3.62	46.54	9.34	10.41	15.20
Rondel	Ro	24	0.00	9.91	0.63	0.29	0.00	0.00	7.29	34.50	40.00	0.79	7.65
Oblong	Ob	26	0.00	8.15	4.12	7.23	0.00	0.00	0.00	18.19	1.27	59.42	1.19
Reniform	Re	37	0.45	8.16	5.13	0.08	0.02	0.91	9.43	38.44	6.89	0.81	29.29

Table 5. Association through rate of recurrence. Association between GSSC-morphotypes based on their occurrence (absence / presence) within the categories subfamily, photosynthesis, rainfall and habitat, expressed in percentage. For example, 31.03% of the species in the Aristidoideae subfamily (n = 29) produces the Bilobate Variant 1 morphotype, whereas the Bilobate Variant 2 morphotype is produced in only 10.34% of the species.

Table 5. Association through rate of recurrence. Association between GSSC-morphotypes based on their occurrence (absence / presence) within the categories subfamily, photosynthesis, rainfall and habitat, expressed in percentage. For example, 31.03% of the species in the Aristidoideae subfamily (n = 29) produces the Bilobate Variant 1 morphotype, whereas the Bilobate Variant 2 morphotype is produced in only 10.34% of the species.

	Subcategories		Lobate %					Saddle%		Trapeziform%				
		1 Species	2 Bilobate Var1	3 Bilobate Var2	4 Bilobate Var3	5 Polylobate	6 Cross	7 Saddle Var1	8 Saddle Var2	9 Trapezoid	10 Rondel	11 Oblong	12 Reniform
Subfamily	Aristidoideae	29	31.03	10.34	3.45	0.00	0.00	13.79	72.41	10.34	6.90	3.45	17.24
	Chloridoideae	62	8.20	16.39	8.20	0.00	3.28	78.69	24.59	0.00	0.00	0.00	1.64
	Danthonioideae	65	4.62	53.85	24.62	15.38	1.54	0.00	9.23	40.00	18.46	6.15	33.85
	Ehrhartoideae	18	5.56	72.22	27.78	5.56	5.56	0.00	0.00	55.56	27.78	22.22	33.33
	Panicoideae	104	31.37	74.51	9.80	31.37	19.61	0.00	0.98	3.92	0.00	1.96	1.96
	Pooideae	31	0.00	22.58	12.90	25.81	3.23	0.00	0.00	54.84	12.90	70.97	6.45
Photosynthetic pathway	C3	127	3.15	28.35	13.39	7.87	0.79	0.00	4.72	21.26	9.45	3.94	17.32
	NAD	42	6.25	20.31	7.81	1.56	3.13	54.69	43.75	4.69	1.56	3.13	7.81
	NADP	28	37.33	69.33	8.00	22.67	16.00	2.67	2.67	2.67	0.00	1.33	2.67
	PCK	16	14.81	29.63	11.11	11.11	11.11	55.56	22.22	3.70	0.00	0.00	3.70
Rainfall	<500mm S	97	10.31	45.36	9.28	14.43	9.28	35.05	23.71	5.15	4.12	4.12	2.06
	>500mm S	176	22.73	49.43	11.36	19.89	10.80	18.18	6.82	13.64	3.98	11.36	7.39
	>40% W	125	7.20	49.60	16.00	14.40	7.20	4.80	16.80	32.80	13.60	16.00	20.00
Habitat	Desert grasses	26	19.20	30.77	3.85	3.85	0.00	23.08	34.62	23.08	7.69	3.85	7.69
	Succulent Karoo grasses	46	4.35	41.30	10.87	10.87	8.70	13.04	32.61	26.09	13.04	21.74	17.39
	Nama-Karoo grasses	85	10.59	45.88	9.41	14.12	12.94	28.24	15.29	8.24	4.71	12.94	1.18
	Savanna grassland	157	22.29	50.32	9.55	17.20	13.38	26.75	9.55	6.37	0.64	5.10	1.27
	Grassland proper	134	23.88	49.25	8.21	22.39	14.18	20.90	6.72	11.19	3.73	12.69	2.99
	Fynbos grasses	104	7.69	50.00	15.38	14.42	10.58	9.62	8.65	32.69	14.42	12.50	20.19
	Forest grasses	15	6.67	60.00	20.00	26.67	6.67	13.33	0.00	20.00	13.33	26.67	0.00
	Montane grassland	70	14.29	34.29	12.86	18.57	4.29	2.86	7.14	42.86	12.86	24.29	30.00
	High altitude grassland	18	22.22	11.11	5.56	5.56	0.00	0.00	5.56	55.56	27.78	16.67	50.00
	Damp soils	82	15.85	51.22	14.63	18.29	10.98	8.54	4.88	23.17	8.54	20.73	7.32
	Swamps / Vlei	21	14.29	57.14	14.29	23.81	19.05	4.76	4.76	14.29	4.76	9.52	4.76
	Shady grasses	43	25.58	48.84	6.98	39.53	4.65	6.98	4.65	25.58	11.63	44.19	25.58

Table 6. Relative abundance of GSSC-morphotypes based on their proportional representation within the categories subfamily, photosynthesis, rainfall and habitat (one hundred GSSC-bodies counted per species, averaged and standardized so that the sum for each row is equal to 100%). For example, the Bilobate Variant 1 morphotype represents 26.83% and the Bilobate Variant 2 morphotype 2.34% of the total number of GSSC-morphotypes counted within the Aristidoideae category (n = 29).

	Subcategories	1 Species	Lobate%					Saddle%		Trapeziform%				
			2 Bilobate Var1	3 Bilobate Var2	4 Bilobate Var3	5 Polylobate	6 Cross	7 Saddle Var1	8 Saddle Var2	9 Trapezoid	10 Rondel	11 Oblong	12 Reniform
Subfamily	Aristidoideae	29	26.83	2.34	0.93	0.00	0.00	2.38	59.97	0.86	1.21	0.00	5.41
	Chloridoideae	62	7.12	11.41	3.46	0.00	0.63	69.43	6.61	0.00	0.00	0.00	0.00
	Danthonioideae	65	2.55	40.60	5.74	4.63	0.00	0.00	0.85	23.91	7.42	1.83	11.33
	Ehrhartoideae	18	5.56	37.56	10.67	1.50	1.33	0.00	0.00	26.50	2.11	3.67	10.17
	Panicoideae	104	21.82	53.71	2.88	11.49	7.00	0.00	0.66	2.12	0.00	0.00	0.52
	Pooideae	31	0.00	7.71	3.57	6.84	0.67	0.00	0.00	22.42	10.58	45.33	4.48
Photosynthetic pathway	C3	127	3.84	30.80	5.91	5.98	1.31	0.00	0.43	23.67	6.68	12.17	8.47
	NAD	42	4.88	7.21	2.93	0.00	0.31	43.00	35.98	0.60	0.05	0.00	2.86
	NADP	28	25.50	55.32	1.43	11.68	6.43	0.00	0.00	0.00	0.00	0.00	0.00
	PCK	16	16.06	20.81	1.88	4.38	6.88	43.00	7.00	0.00	0.00	0.00	0.00
Rainfall	<500mm S	97	6.86	29.31	2.86	6.85	4.43	27.78	15.74	2.32	2.34	0.25	0.34
	>500mm S	176	16.66	35.69	3.10	6.80	3.85	15.96	1.34	6.32	2.32	5.26	2.25
	>40% W	125	3.89	33.50	5.42	4.50	2.88	3.13	10.16	17.42	3.92	7.67	6.67
Habitat	Desert grasses	26	15.58	16.50	1.19	0.88	0.00	18.92	24.35	16.85	3.46	0.00	2.27
	Succulent Karoo grasses	46	3.50	23.41	3.52	3.48	3.80	7.83	24.33	15.09	1.96	9.96	2.93
	Nama-Karoo grasses	85	8.21	30.32	2.62	4.76	5.31	22.60	9.39	7.07	2.80	5.98	0.14
	Savanna grassland	157	17.07	36.59	2.68	6.09	4.13	23.90	4.52	2.24	0.06	2.19	0.21
	Grassland proper	134	15.19	35.40	2.30	7.28	4.86	18.02	1.63	3.52	3.19	6.90	0.96
	Fynbos grasses	104	4.09	35.99	5.49	3.83	3.26	8.64	4.27	16.81	4.21	5.78	6.61
	Forest grasses	15	6.20	36.73	9.20	13.47	1.13	13.33	0.00	6.40	6.53	7.00	0.00
	Montane grassland	70	11.49	24.30	2.21	3.61	0.89	1.67	0.69	24.63	6.31	13.24	11.12
	High altitude grassland	18	21.83	7.56	0.67	0.39	0.00	0.00	0.22	25.56	14.06	15.00	14.72
	Damp soils	82	11.88	36.44	3.93	5.15	5.56	6.60	0.59	10.89	3.15	12.93	3.38
	Swamps / Vleis	21	13.95	40.29	5.05	11.95	5.80	4.76	0.19	7.76	5.86	3.76	1.48
	Shady grasses	43	16.74	31.14	3.49	12.93	0.74	6.02	1.12	11.74	4.28	10.09	1.70

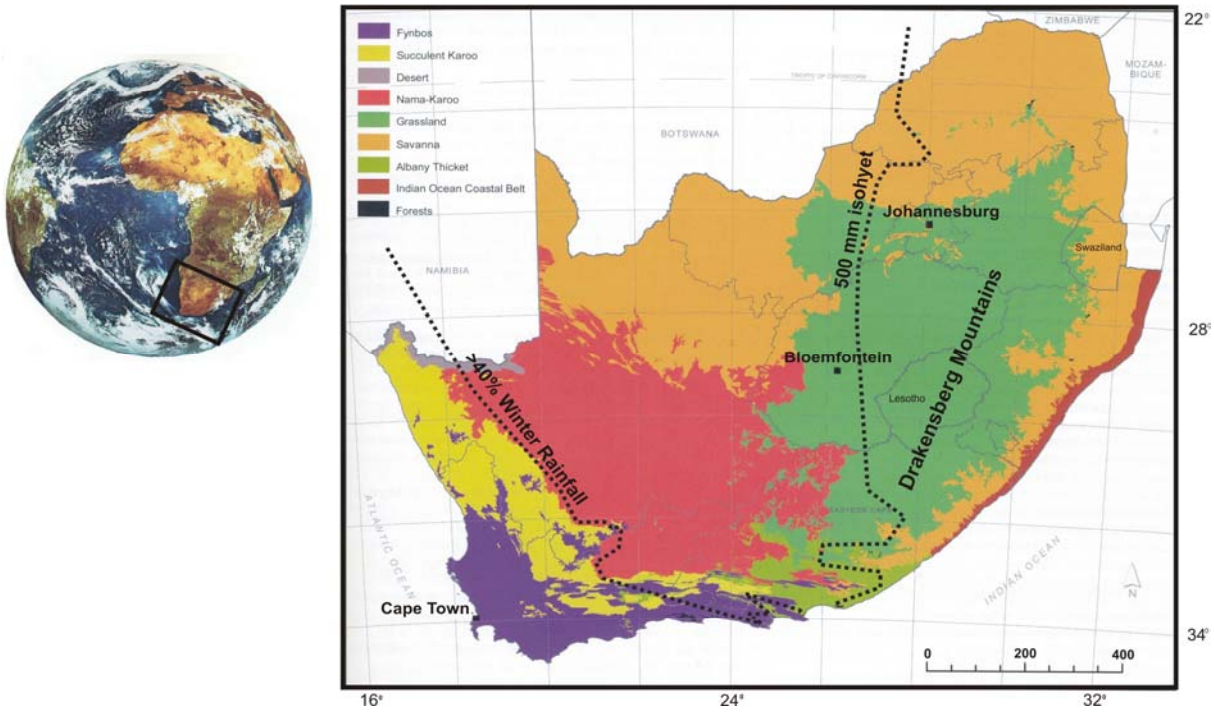

Figure 2. The biomes of South Africa. Map and biome categories after Mucina and Rutherford (2006). Rainfall data after Vogel et al. (1978), Gibbs Russell (1988) and Gibbs Russell *et al.* (1990).

Classification of GSSC-morphotypes

Introduction

Globally, the grass family comprises about one third of the Earth's vegetative cover in terms of grass-dominated ecosystems, savannas and natural grasslands and is ecologically the most dominant and economically the most important plant family in the world (Gould 1968; Chapman 1996; Jacobs 1999; Kellogg 2001; Wooller and Beuning 2002; Piperno and Sues 2005). The grass family is the seventh largest plant family in southern Africa with 194 genera, and 967 species and infraspecific taxa, of which 115 are naturalized and 847 are indigenous, including 329 endemic taxa (Gibbs Russell 1985, 1986, 1987, 1988; Campbell and Kelogg 1987; Gibbs Russell *et al*. 1990). The Grass Phylogeny Working Group (GPWG 2001) recently reclassified the Poaceae into thirteen subfamilies, with eight subfamilies recognized in South Africa, *viz.* Aristidoideae Caro, Arundinoideae Burmeist., Bambusoideae Luerss., Chloridoideae Kunth ex Beilschm., Danthonioideae Barker & H.P.Linder, Ehrhartoideae Link, Panicoideae Link, Pooideae Benth. Classification of subfamilies in the Poaceae is based on a range of cytological and anatomical criteria. A number of anatomical characters indicate photosynthetic pathway with a single pathway that usually predominates in each subfamily (Clayton and Renvoize 1986; Gibbs Russell 1988; GPWG 2001).

Modern grass-dominated ecosystems cover more than fifty percent of southern Africa south of 22°S, a region that is also a transitional zone between tropical and temperate grasslands (Rutherford and Westfall 1994; Scott 2002). The biogeography

of grass communities in South Africa is primarily reflected on a taxonomic level (Gibbs Russell 1988). Of the eight subfamilies recognized by the GPWG (2001), occurring in southern Africa, five contain exclusively C3 species (Bambusoideae, Pooideae, Danthonioideae, Arundinoideae and Ehrhartoideae). The other three subfamilies include C_3, C_4 as well as C_3/C_4 intermediate species (Aristidoideae and Panicoideae), and almost exclusively C_4 species, except for *Eragrostis walterii* Pilg., and the danthonioid species *Merxmuellera rangei* (Pilg.) Conert (Chloridoideae) (Ellis 1984; GPWG 2001). The palaeoclimatic implications are therefore clear for South Africa, where the percentage frequencies of C_3 and C_4 grasses are significantly different in winter, summer and year-round rainfall regions (Vogel et al. 1978; Gibbs Russell 1988).

The Bambusoideae Luerss. is a C_3-subfamily with mostly perennial, tropical species confined to humid forest shade (Gibbs Russell *et al*. 1990; GPWG 2001). The C_3, Ehrhartoideae Link is annual or perennial and found in forests, open hillsides or aquatic habitats (Gibbs Russell *et al*. 1990; GPWG 2001). The C_3 Pooideae Benth. is annual or perennial and of cool temperate regions (GPWG 2001). In South Africa introduced species of the Pooideae are mainly confined to the winter rainfall region of the Fynbos Biome, while indigenous pooids are most abundant in the high Drakensberg mountains on the eastern escarpment (Gibbs Russell *et al.* 1990). Arundinoideae Burmeist. is generally regarded as a diverse, polyphyletic group, lacking reliable diagnostic features, that is mainly distributed throughout the Southern Hemisphere (Gould 1968; Ellis 1986). South African representatives of the Arundinoideae all follow the C_3 photosynthetic pathway and occupy a wide range

of niches, from aquatic species like *Elytrophorus* and *Phragmites,* to montane-adapted species like *Styppeiochloa* (Renvoize 1981; Gibbs Russell *et al*. 1990). The subfamily also has developed several structural adaptations to inhabit and survive in the Fynbos Biome (Linder and Ellis 1990). The Danthonioideae Barker & H.P.Linder, previously included in the Arundinoideae, is exclusively C_3, mostly perennial, and mainly found in mesic to xeric open habitats of the Fynbos, Succulent Karoo and Nama-Karoo Biomes (Ellis and Linder 1992; Gibbs Russell *et al*. 1990; GPWG 2001). The C_4 Aristidoideae Caro represents annual or perennial, mostly xerophytic species, that occur mainly in the Succulent Karoo, but also in the Desert, Nama-Karoo and Savanna Biomes (Gibbs Russell *et al*. 1990; GPWG 2001). The Panicoideae Link can generally be differentiated from other subfamilies by its spikelet characteristics (Ellis 1986). Species are annual or perennial, of the tropics and subtropics, but also diverse in temperate regions (Gibbs Russell *et al*. 1990; GPWG 2001). It is a large subfamily with South African genera incorporated into three tribes, the Andropogoneae Dumort, Arundinelleae Stapf, and Paniceae R. Br. The genus *Panicum* L. includes species exhibiting all five photosynthetic types known in the Poaceae – non-Kranz or C_3, C_3/C_4 intermediate and Kranz or C_4, which is further subdivided into NADP-me, PCK, and NAD-me subtypes (Ellis 1988). With the exception of the C_3 species *Eragrostis walteri* and *Merxmuellera rangei*, the Chloridoideae Kunth ex Beilschm. is regarded as a C_4-subfamily (Ellis 1984, Gibbs Russell 1988; GPWG 2001). Species are annual or perennial, and of dry climates, especially in the subtropical and temperate regions of the Savanna and Grassland Biomes (Gibbs Russell *et al*. 1990; GPWG 2001).

Morphological Description

Background

In a phylogenetic study of grasses Metcalfe (1960) recognized cubical, round, oblong, saddle-shaped, elongated, cross-shaped, dumbbell-shaped, and intermediate phytolith forms. Opal phytoliths from dust and soils were assigned to different grass vegetation types and it was recognized that there is a general difference in the phytolith morphology between short grasses and tall grasses (Suess 1966; Twiss *et al.* 1969). Suess (1966) divided the silica bodies in irregular and regular types in order to classify grassland regions, while Twiss *et al.* (1969) proposed a typological scheme for identifying grass subfamilies by dividing short cell phytoliths into four classes: a chloridoid class (saddle shapes); a panicoid class (dumbbell, cross shapes); a festucoid class (cubical, round, oblong shapes); and an informal "elongate" class. Rovner (1971) made a distinction between panicoid and poacoid phytoliths based on discrete morphological features. He incorporated chloridoid types identified by Twiss *et al*. (1969) into the panicoid class while his “poacoid” class was associated with Twiss’s festucoid class. Rovner (1983) also stated that the elongated type phytoliths are present in all the classes and have therefore no significant diagnostic value. Brown (1984) elaborated on terminology, description and class overlaps, and reiterated Rovner’s view that the correlation between phytoliths and grass taxa are more complex than previously thought. A fundamental concern related to phytolith production in living plants is the production of either a particular phytolith morphotype by many taxa, or a variety of morphotypes by one taxon. These circumstances, known respectively as redundancy and

multiplicity (Rovner 1983), drew attention to the importance of standardized analytical methods as well as the need for modern phytolith reference collections to assist in the interpretation of fossil phytoliths assemblages (Brown 1984; Piperno 1988; Mulholland 1989; Stromberg 2004). Subsequent studies concerning grass phytolith classification validated the basic pattern of short cell phytolith taxonomy initially proposed by Twiss *et al*. (1969) and expanded the framework for grass phytolith classification through modifications to the Twiss *et al.* scheme. Palmer (1976) provided a comparative study of fossil grass cuticles and a reference collection of modern grass epidermises from East Africa, using light microscopy and SEM. Brown (1984) developed a phytolith key based on one hundred and twelve grass species from the USA. Mulholland (1989) looked at phytolith shape frequencies in North Dakota grasses and classified short cell morphotypes into three broad groups. Lobate forms include bilobates and crosses and correspond with Twiss's Panicoid class (Twiss *et al*. 1969; Twiss 1992.) Rectangular and conical bodies were described as sinuates, rectangles and rondels, and correspond with Twiss's Pooid phytoliths (Twiss 1992). The description of Mulholland's saddle type is based on the concavo-convex outline of its cross-section and is equivalent to Twiss's Chloridoid class (Twiss *et al* 1969; Twiss 1992). Fredlund and Tieszen (1994) identified nine diagnostic short cell phytolith types, namely conical, keeled, pyramidal, crenate, S*tipa*-type, simple-lobate, panicoid-type, cross and saddle. They made several comparisons. The conical morphotype correspond with Mulholland's rondel type (Mulholland 1989). The keeled morphotype is also equivalent to Mulholland's rondel type as well as the elliptical and acicular types described by Twiss *et al.* (1969) The

pyramidal type is comparable to the rectangular and oblong types of Twiss *et al.* (1969), and the rectangular form described by Mulholland (1989). The crenate type is similar to Mulholland's sinuate type and the oblong sinuous type defined by Twiss *et al.* (1969). Morphology of the *Stipa*-type bilobate is based on the symmetry of its cross-section, which has been described as distinctly trapezoidal (Brown 1984). The cross, simple lobate, Panicoid type lobate and Other lobate categories are regarded as typically, but not exclusively produced by the Panicoid subfamily (Fredlund and Tieszen 1994). The saddle type is identical to that of Mulholland (1989) and Twiss (1992). In short, the results suggest that bilobate, polylobate and cross morphtypes are generally regarded as common in the Panicoideae subfamily, saddles are mainly produced by the Chloridoid subfamily, while the trapeziform, sinuate and rondel types are generally correlated with the Pooideae subfamily. More recent endeavors included methods to standardize the discipline with regards to identification, description and analytical methods (Madella *et al*. 2005).

GSSC-phytoliths analysed in this study

All phytoliths analysed in this study are the morphologically diagnostic silica bodies found in specialized silica short-cells (GSSC) that are located in both the costal zone and intercostal zones of the leaf epidermis (Metcalfe 1960). In conventional grass-taxonomical studies, silica bodies are normally described as seen in surface (planar) view within the epidermis (Metcalfe 1960; Kok 1972; Ellis 1979). However, for this study, descriptions were made on the basis of three-dimensional shape and two-dimensional outlines (Table 2), according to the guidelines provided by the International Code for Phytolith Nomenclature 1.0 (Madella *et al.* 2005). This included

studying both planar and transverse (side view) aspects of the phytolith types in order to interpret their three-dimensional appearances and distinctive two-dimensional characteristics (Twiss *et al.* 1969; Mulholland 1989; Fredlund and Tieszen 1994) (Figure 3 A). Here the procedure for phytolith description of Mulholland (1989) was followed (Figure 3). Short cell phytoliths were primarily described according to their abaxial / adaxial aspects, defined as the planar (surface) view or top view according to Mulholland (1989). The four sides connecting the planar aspect to the base of the silica body were described as side views for the long opposite faces, compared to end views for the short opposite faces. The figures are presented as composites of several photomicrographs (Figure 3 B, C).

GSSC-phytoliths are geometric variations of cubes, rectangular to cylindrical bodies, truncated cones or beveled pyramids (Mulholland 1989), but according to their most basic outlines in planar view, GSSC-phytoliths can be divided into three fundamental categories: lobate-shaped, saddle-shaped and trapeziform-shaped (Twiss 1992). Because of the effects of multiplicity and redundancy, an effort was made to classify the morphotypes in a simplified system, without considering any taxonomical affiliations. Thus, eleven morphotypes, identified as consistent occurrences in the GSSC-phytolith suite, were divided into a Lobate, Saddle and Trapeziform class. Each class corresponded to morphologically affiliated types that, as a group, form a transitional range of shape variation (Mulholland 1989). It has been suggested that the concavity in the outer surfaces of these morphotypes is not related to specific morphological characteristics, but rather to external factors like dehydration (Ellis 1979).

Lobate Class

The Lobate class is represented by morphotypes with trough-shaped outer surfaces, distinctive central portions and nodular structures, namely Bilobates, Polylobates and Crosses (Figure 4). The Bilobate is perhaps the most diagnostic GSSC-phytolith type. It consists of two lobes separated by a central portion of varying length and thickness, also referred to as a neck, shank, shaft or isthmus (Ellis 1979; Mulholland 1989). The planar surfaces and lateral walls of Bilobates are normally concave. In planar view, the terminal margins of the lobes are mostly rounded but occasionally displayed indentations. Three basic variants were recognized in this study, based on the dimensions of the central portion or neck between the lobes, and the outline symmetry of the planar surface.

Bilobate variant 1

The Variant 1 Bilobate has a comparatively elongated central portion (Figure 4, 1-2). The length of the central portion is defined as more than one third of total length of body. It possesses orbicular lobes that are symmetrical in planar view. It also has a lateral plane of symmetry with the length of central portion or shank equal or greater than one third of total length of body. This morphotype category includes the *Aristida* -type dumbbell described by Mulholland (1989) and Fredlund and Tieszen (1994) and corresponds to types 3c and 3e in Twiss *et al*. (1969) and Twiss (1992).

Bilobate variant 2

The Variant 2 Bilobate has a comparatively short central portion (Figure 4, 3 – 12). The length of the central portion is defined as equal or less than one third of total length of the body. The category includes Bilobates with orbicular to ovate lobes that are symmetrical in planar view. The side view presents a lateral plane of

symmetry. This morphotype is equivalent to the Panicoid and Chloridoid dumbbells in Mulholland (1989) and types 3b, 3d and 3f in Twiss *et al* (1969) and Twiss (1992).

This category also includes the *Stipa*-type Bilobate, a predominantly pooid morphotype, which appear trapezoidal or tabular in side view with generally ovate to scutiform lobes (Mulholland 1989; Fredlund and Tieszen 1994). This type is not exclusive to *Stipa* but is also produced by C_3-taxa, including *Chaetobromus involucratus, Schismus barbatus* and *Pennisetum glaucocladum* (Appendix 1).

Bilobate variant 3

The Variant 3 Bilobate is always asymmetrical in planar view with the length of its central portion less than one third of total length of body (Figure 4, 13 – 16). The side is either tabular or trapezoidal. This type is comparable to the irregular complex dumbbell recognized by Twiss *et al*. (1969) and the 'Other lobate' category in Fredlund and Tieszen (1994).

Polylobate

Polylobates have more than two lobes and distinctive central portions between the lobes to distinguish it from sinuate trapeziform short cells (Figure 4, 17 – 20). They have well-developed lateral planes of symmetry with tabular outlines in side view. It is equivalent to type 3i in Twiss *et al.* (1969).

Cross

Description of the Cross morphotype is follows Mulholland (1989). Crosses are usually equidimensional in planar view and are distinguished by the presence of four lobes that can range from symmetrical to irregular in shape (Figure 4, 21 – 26). Lobes can be rounded or pointy with a moderately defined central portion. This

category corresponds with type 3a in Twiss *et al.* (1969) and Twiss (1992).

Saddle Class

The Saddle class is represented by equidimensional bodies, also with concave outer surfaces, that are distinguished mainly by their planar outlines (Figure 5). Numerous types have been described. Brown (1984) listed eleven types and Thorn (2004a) described three kinds, a narrow base, wide base and tabular variant, based on the proximo-distal dimensions of the silica body. A diagnostic feature distinguishing Saddles from the Trapezoid type in the Trapeziform class, is its comparatively shorter proximo-distal length (Figure 6).

Saddle Variant 1

The body is trapezoidal in side view and exhibits a concave base and plateau that varies from square to rectangular in planar view. The base can widen or taper distally and is rarely vertical, thus including all three variants described by Thorn (2004a, 2004b). The plateau has rounded corners, with two or sometimes only one medially constricted margin (crescent-shaped), and two sides that are always moderately convex (Figure 6).

Saddle Variant 2

The body is trapezoidal in side view and exhibits a concave base and plateau that vary from square to rectangular in planar view. The plateau has rounded corners with no constricted margins (Figure 7). This category includes all three variants described by Thorn (2004).

Trapeziform Class

The Trapeziform class includes more heterogeneous morphotypes that are also

regarded as geometrically uncomplicated (Mulholland 1989) (Figure 8). Except for the Rondel, all the Trapeziform morphotypes exhibit quadrilateral dimensions in planar view. Definition of subcategories is based on constantly recurring morphological occurrences.

Trapezoid

Trapezoids are six-sided, square or rectangular silica bodies with few sides parallel. Planar margins are angular and not medially constricted (Figure 8, 1 – 12). The proximo-distal length of the silica body is generally longer compared to Saddle types. The Trapezoid category is equivalent to types 1b,1d and 1f in Twiss *et al* (1969), the rondel types described by Mulholland (1989), the conical and pyramidal types in Fredlund and Tieszen (1994) and rondel types g, h and i in Thorn (2004a).

Rondel

The Rondel is cylindrical or semi-cylindrical, tapers distally, and resembles a truncated cone (Mulholland 1989). It is circular, elliptical or acicular in planar view (Figure 8, 13 – 18). This morphotype compares to type 1a in Twiss *et al.* (1969) and the conical type in Fredlund and Tieszen (1994).

Oblong

The Oblong category includes six-sided silica bodies that are at least twice as long as broad with parallel or nearly parallel sides (Figure 8, 19 – 27). This category is defined as having smooth, sinuous or crenate planar edges and trapezoidal cross-sections. It corresponds with types 1c, 1g and 1h in Twiss *et al*. (1969), and the "longer forms with more polygonal cross-sections" in Mulholland (1989, p 495). This includes Mulholland's sinuate type which is comparable to the crenate types in

Fredlund and Tieszen (1994).

Reniform

The Reniform type is essentially a crescent-shaped Trapezoid with angular planar margins and one medially constricted edge (Figure 8, 28 – 31). This morpotype is comparable to type 1e in Twiss *et al.* (1969) and the rondel types in Mulholland (1989).

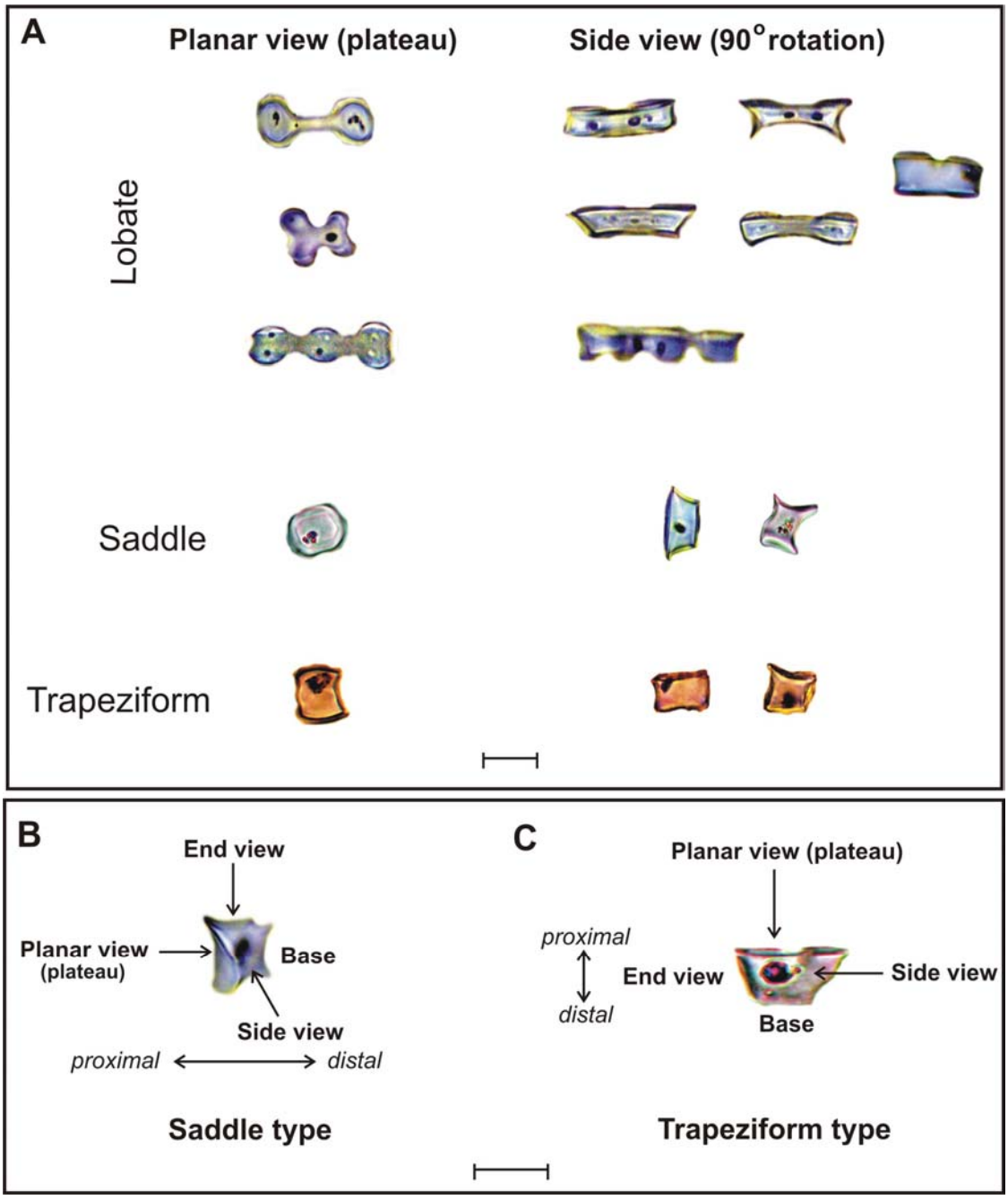

Figure 3. Orientation of short cell phytoliths. Abaxial / adaxial aspects, are defined as the planar view (surface or plateau) or top view (A) according to Mulholland (1989). The four sides connecting the planar aspect to the base of the silica body are described as side views for the long opposite faces, compared to end views for the short opposite faces (B,C).

Figure 4. The Lobate Class. Bilobate variant 1: (1) planar view; (2) side view. Bilobate variant 2: (3-7) planar view; (8-10) oblique view; (11-12) side view. Bilobate variant 3: (13-15) planar view; (16) oblique view. Polylobate: (17-18) planar view; (19-20) oblique view. Cross: (21-24) planar view; (25) side view; (26) oblique view. The so-called *Stipa*-type is represented by 7, 11-12 and 18.

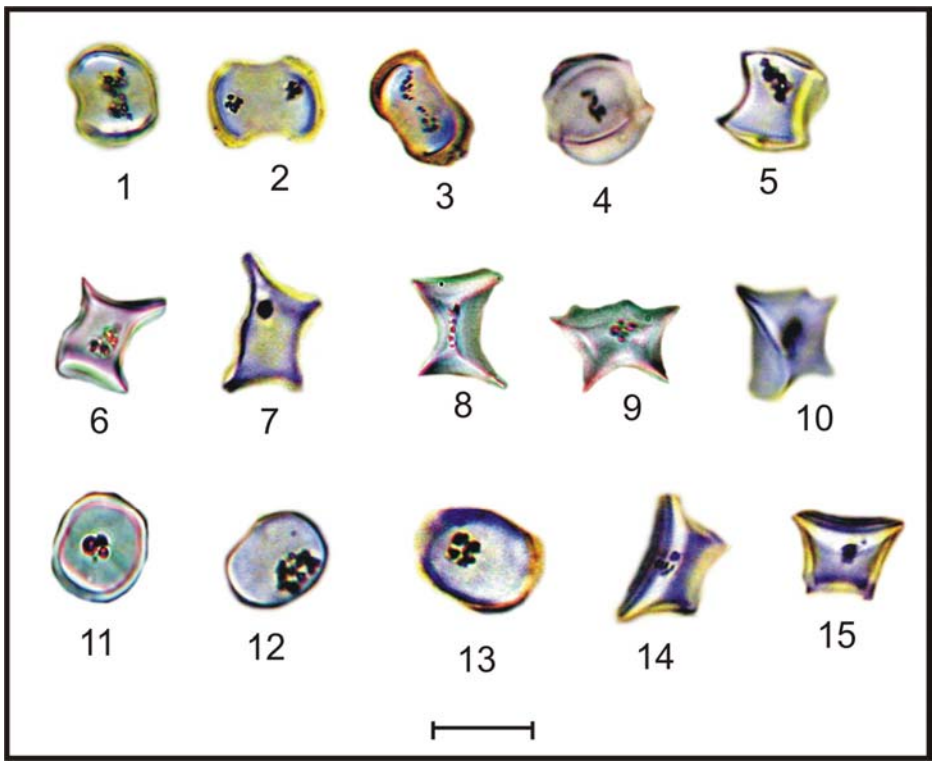

Figure 5. The Saddle Class. Saddle variant 1: (1-5) planar view; (6-8) side view; (9) end view; (10) oblique view. Saddle variant 2: (11-13) planar view; (14-15) side view.

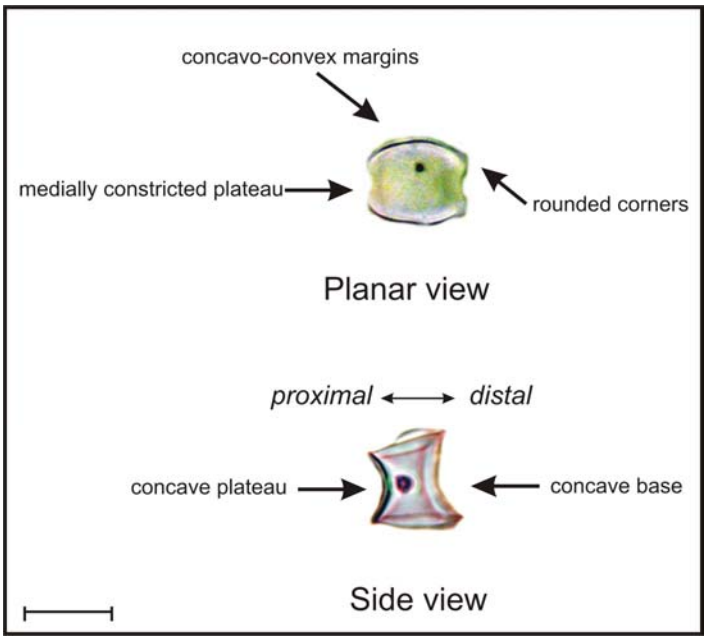

Figure 6. Distinguishing morphological features of the Saddle Variant 1.

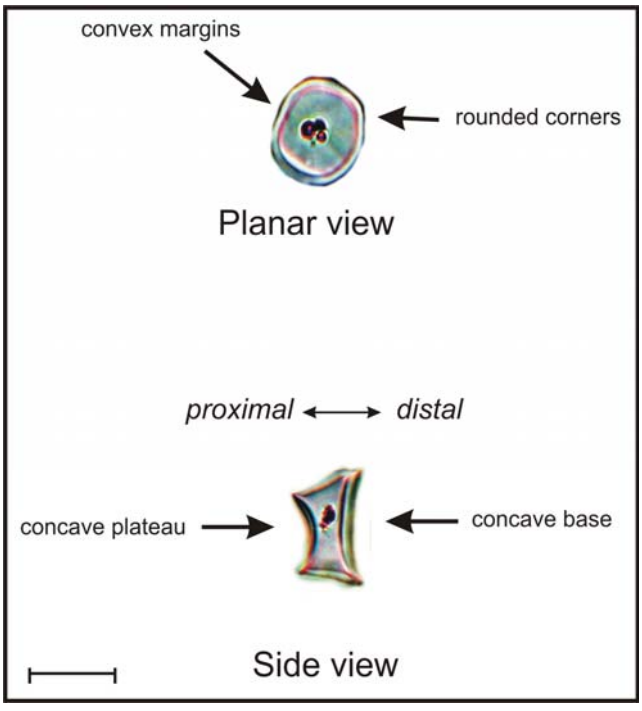

Figure 7. Distinguishing morphological features of the Saddle Variant 2.

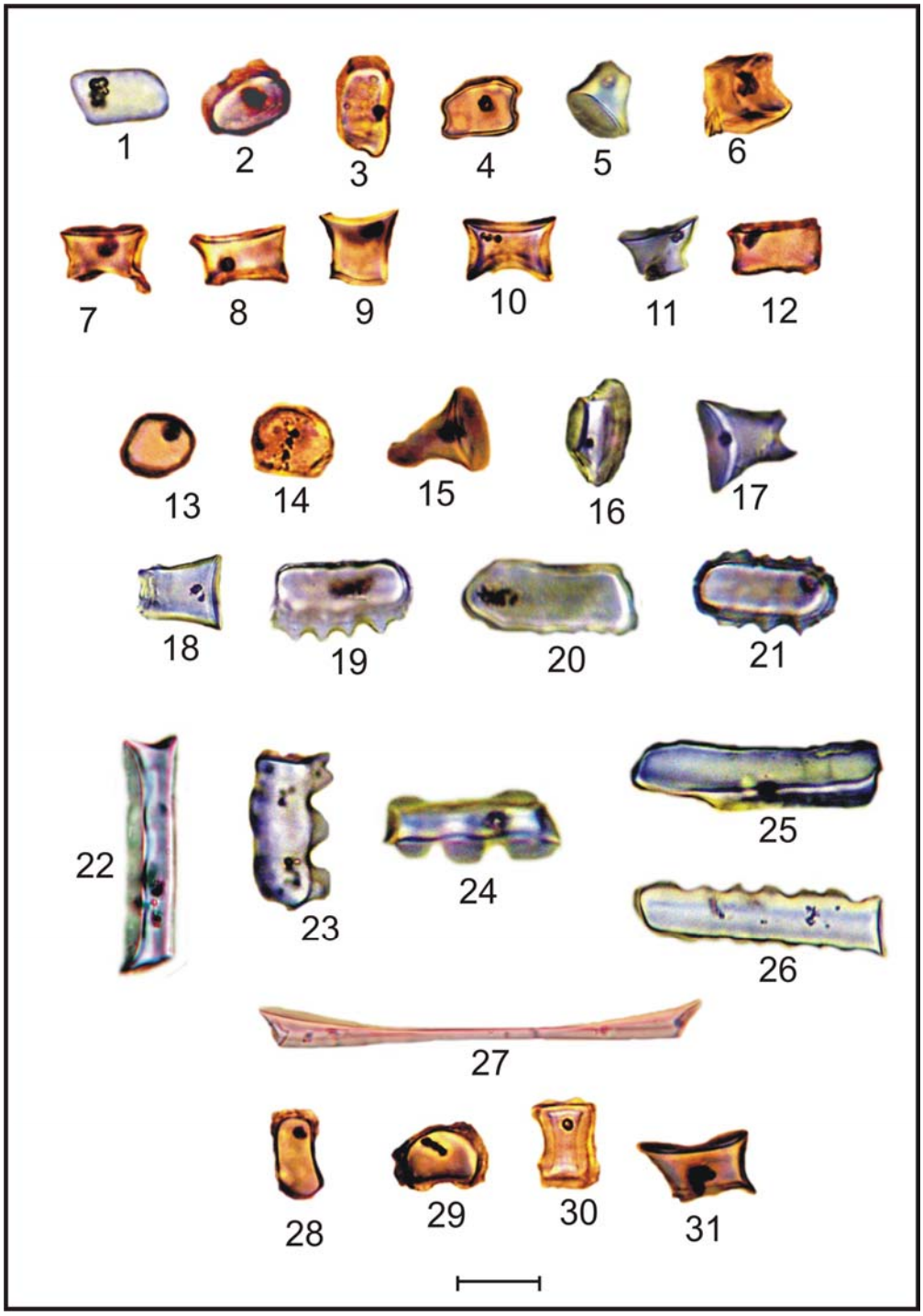

Figure 8. The Trapeziform Class. Trapezoid: (1-4) planar view; (5-6) oblique view; (7-12) side view. Rondel: (13-14) planar view; (15-17) oblique view; (18) side view. Oblong: trapeziform sinuate, (19-21,26) planar view; trapeziform smooth, (22, 25, 27) oblique view; trapeziform polylobate, (23, 24) oblique view; Reniform: (28-30) planar view; (31) side view.

Quantitative analyses

Introduction

The degree of association between eleven GSSC-phytolith morphotypes, according to their association with each other, their association at subfamily level, and their correspondence with ecological adaptations of the grasses that produce them, was evaluated with several statistical techniques in STATISTICA 7.0, using the StatSoft, 2005 software package. Trends in the *association through recurrence* or frequency (Table 3 and 5), and *association based on relative abundance* (Table 4 and 6), between GSSC-morphotypes and between GSSC-morphotypes and subcategories, were recorded and explored with one-way ANOVA tests and ordination using correspondence analysis.

Analysis of variance

Potential significance of differences in the *relative abundance of* GSSC-morphotypes in grass species (Table 4 and 6) was investigated using analyses of variance (one-way ANOVA tests). This was accomplished by comparing the number of GSSC-phytoliths calculated from the grass epidermal slides, in a one-way ANOVA to test significant differences of each morphotype within the categories, subfamily, photosynthesis, rainfall and habitat. Each ANOVA test was further analyzed with Tukey's post hoc Honestly Significantly Different (HSD) test for uneven sample sizes between pairs of subcategories for each morphotype.

Correspondence Analysis

The results were analyzed and illustrated with Correspondence Analysis (CA). Six

sets of CA were performed, one for each category. CA included only the morphotypes identified in the ANOVA and subsequent Tukey's HSD tests, which significantly differentiate between subcategories. The level of significance was restricted by using only those morphotypes found to significantly separate a third or more subcategory pairs in the one-way ANOVA.

CA is a multivariate ordination technique that identifies underlying similarities within specifically constructed datasets, just as principal components account for maximum variance between datasets (Greenacre 1984). CA is a suitable ordination technique in dealing with nonlinear data. For comparison and classification in this study, CA displays different communities along axes, so that communities that resemble each other the most on the basis of phytolith composition are grouped closer together. Presented in table form, the relationships between column and row data are explored simultaneously, with no prior causal relationship inferred between row and column data. For graphical display, two dimensions are used to give a reduced rank approximation to the data, even though it identifies the lines of best fit within a multidimensional cloud of data points (STATISTICA 7.0 Statistics Manual). When plotted on two dimensions, the subcategories that fall closest together are most similar in terms of their morphotype association. Morphotypes are also plotted, with subcategories falling closest to them most affected by their inertia (contribution to variation).

Results

A non-parametric Spearman's rank-order correlation-coefficient, r_S, was used to test the relationship between *GSSC-morphotype association through rate of recurrence*

(Table 3) and *GSSC-morphotype association through relative abundance* (Table 4). This was carried out with the consideration of the null hypothesis that no real association exists between *GSSC-morphotype association through rate of recurrence* and the *relative abundance of GSSC-morphotypes*. Results showed a highly significant linear relationship with positive covariation between the two datasets, which suggests that for each morphotype, frequency values accompany relative abundance values (Table 7, Appendix 4).

Association between Morphotypes

The results of the analysis of association between morphotypes through rate of recurrence are summarized in Table 3. The Variant 1 Bilobate recurred in 23.5% of species that produce the Polylobate (n = 51), but was not found in species that produce the Variant 2 saddle (n = 46), Trapezoid (n = 70), Rondel (n = 24) and Oblong (n = 26) morphotype. The Variant 2 Bilobate recurred in over 70% of species that produce the Variant 3 Bilobate (n = 40), Polylobate (n= 51) and Cross (n = 25) morphotype. Between 20% and 30% of species that generate the Trapezoid (n = 70), Rondel (n= 24) and Oblong (n = 26) morphotypes, also produce the Variant 2 bilobate. Variant 3 Bilobates were not found in species that produce the Variant 2 Saddle (n = 46). The Polylobate was absent in species that produce the Saddle and Rondel morphotypes, but respectively occurred in 26.9% (n = 52), 24.5% (n = 139) and 26.9% (n = 26) of species that generate the Variant 1, Variant 2 Bilobate and Oblong morphotype. The Cross was restricted to Lobate-morphotype producing grasses, and recorded in 15.8% (n = 139) of species that generate the Variant 2 Bilobate and 15% (n = 40) of species that produce the Variant 3 bilobate. The

Saddles were inclined to group together, with the Variant 1 type occurring in 43% (n = 49) of species that produce the Variant 2 Saddle, while the latter was found in 34.7% of species that generate the Variant 1 Saddle. Otherwise, the Variant 1 Saddle was restricted in its association by occurring in only 1.9% of the producers of the Variant 1 Bilobate (n = 52) and in 2.7% (n = 37) of species that produce Reniform morphotypes. The Variant 2 Saddle respectively occurred in 25% and 27% of species that produce the Rondel (n = 24) and Reniform (n = 37) morphotype, but was absent in producers of Cross and Oblong morphotypes. The Trapezoid morphotype was recorded in 62.5% (n = 24) of Rondel-producing species, 53.8% (n = 26) of Oblong producers and 73% (n = 37) of species that generate the Reniform morphotype.

Several trends were observed when the relative abundance of GSSC-phytoliths was calculated for each morphotype and compared with each other in a one-way ANOVA (Table 4, Appendix 6). There is no significant correlation between *relative abundance* and sample size (r = 0.4070, p = 0.2241), indicating that the proportional representation of GSSC-morphotypes were not influenced by differences in sample size (Figure 9). The results showed that the 1st and 2nd Bilobate Variant, as well as the Variant 1 Saddle, was produced in higher quantities compared to the rest of the morphotypes (Figure 10). The Bilobate Variant 1 accounted for 73% of all the morphotypes in the species that produce them (s.e. = 4.37; n = 52), the Variant 2 Bilobate nearly 70% (s.e. =2.51; n = 139), and 85% for the Variant 1 Saddle (s.e. = 3.02; n = 48). Grasses that generate the Variant 3 Bilobate, Polylobate and Cross, tend to produce more quantities of the Variant 2 Bilobates. As a result, representation of the Variant 3 Bilobate, Polylobate and Cross morphotypes by the species that

produce them, were comparatively low (Figure 10). In contrast, the Variant 3 Bilobate, Polylobate and Cross contributed only about 17% of the total number of morphotypes produced by grasses that generate the Variant 2 Bilobate. This suggests a possibly meaningful, but one-way association between the Variant 3 Bilobate, Polylobate and Cross morphotypes and the Variant 2 Bilobate. The Variant 2 Saddle accounted for 50% (n = 46) of all the GSSC-morphotypes by the species that produce them. Variant 2 Saddle producers also generated the Variant 1 Saddle (28%, s.e. = 5.53), and most of the Trapeziform morphotypes (21%), but almost no Lobate morphotypes (0.8%, s.e. = 0.65). The Trapeziform class of morphotypes is produced by grasses that also tend to frequently generate the Variant 2 Bilobate, albeit in comparatively low quantities. The Trapezoid morphotype represented 46% (s.e. = 3.63, n = 70) of the total number of morphotypes in the species that produce them. The rest were mostly made up of the Variant 2 Bilobate (11.76%), Rondel (9.34%), Oblong (10.41%) and the Reniform (15.42%). The Variant 1 Bilobate, Cross and Variant 1 Saddle were not produced by these grasses. Grasses that produce the Rondel (40%, s.e. = 6.86, n = 24), also generated comparatively high amounts of Trapezoid morphotypes (36.5%). The Oblong accounted for 59.0% of all the GSSC-morphotypes in the species that produce them (s.e. = 6.83; n = 26). Cross and Saddle morphotypes were absent in the Oblong producers. The Reniform morphotype accounted for only 29% (s.e. = 3.75, n = 37) of the morphotypes epresentation (quality ≥ 0.767). Almost 27% of the total inertia (Dimension 1) is driven by the difference in association between Lobate and non-Lobate morphotypes and in the species that produce them, with 38% (s.e. = 5.12) made up of Trapezoid

morphotypes.

One-way ANOVA of the relative abundance of GSSC-morphotypes phytoliths in the Morphotype dataset (Table 4) demonstrated that the proportional representation of each phytolith morphotype is significantly different ($p < 0.05$) among the eleven subcategories (Table 8, Appendix 6).

The first CA, which was carried out using the morphotypes found to be significant in the ANOVA, resulted in two dimensions explaining a cumulative 48.94% of inertia with a total of ten dimensions extracted (Table 9, Fig 11). The structure of the relationships indicated clustering of the Lobate, Saddle and Trapeziform morphotype classes, marked by the Variant 1 Saddle and Trapezoid morphotypes and reflecting the highest quality of 22% (Dimension 2) by a difference in association between Trapeziform and non-Trapeziform morphotypes.

Association between Morphotype and Subfamily

The association between GSSC-morphotypes and six different subfamilies based on morphotype rate of recurrence are summarized in Table 5. The Variant 1 Bilobate was recorded in at least 30% of Aristidoid (n = 29) and Panicoid species (n = 104). This concurs with the observation that the long-necked type is prevalent in the C_4, arid-adapted *Aristida* genus (Mulholland 1989; Gibbs Russell *et al.* 1991). The Variant 2 Bilobate is even more common, being recorded in all six subfamilies, but occurring more frequently in the Danthionoideae (53% of species, n = 65), the Ehrhartoideae (72% of species, n = 18) and the Panicoideae (74% of species, n = 104), It occurs less frequently in the Aristidoideae (10% of species, n = 29) and Chloridoideae (16% of species, n = 62). Occurrence of the Variant 3 Bilobate is

highest among the Danthionoideae (24% of species, n = 65) and Ehrhartoideae (27% of species, n = 18). The Polylobate is uncommon in the Aristidoideae and Chloridoideae, but prevalent in the Panicoideae (31% of species, n = 104) and the Pooideae (25%, n = 31). The Cross is primarily produced in the Panicoideae (19%, n = 104). Out of the eleven morphotype categories, the Variant 1 Saddle is probably the most selective morphotype, occurring only in the Aristidoideae (13% of species, n = 29) and Chloridoideae (78% of species, n = 62). This trend is more or less similar for the Variant 2 Saddle, which also occur almost exclusively in the Aristidoideae (72% of species, n = 29) and Chloridoideae (24% of species, n = 62). The Trapezoid is not found in the Chloridoideae, but common in the Danthionoideae (40% of species, n = 65) and Ehrhartoideae (55% of species, n = 18) and Pooideae (54% of species, n = 31). The Rondel is absent in the Chloridoideae and Panicoideae. More than 70% of species belonging to the Pooideae, and 22% of species belonging to the Ehrhartoideae subfamily (n = 31) were found to produce the Oblong morphotype. The Reniform is mainly produced by the Danthionoideae (33% of species, n = 65) and Ehrhartoideae subfamilies (33% of species, n = 18).

The relative abundance of GSSC-phytoliths calculated for each Subfamily subcategory is provided in Appendix 7 and summarized in Table 6. The long-necked Variant 1 Bilobate represented more than 20% of the total number of morphotypes counted in the Aristidoideae (s.e. = 8.08, n = 29) and Panicoideae (s.e. = 3.52, n = 102). The Variant 2 Bilobate represented 40.6%, of the total number of morphotypes counted in the Danthionoideae (s.e. = 5.22, n = 65), 37.5% in the Ehrhartoideae (s.e. = 7.67, n = 18) and 53.7% in the Panicoideae (s.e. = 4.04, n = 102). Despite their low

values, the Variant 3 Bilobate and Polylobate respectively represented the highest count in the Ehrhartoideae (10.6%, s.e = 5.03, n = 18) and Panicoideae (11.4%, s.e = 2.40, n = 104). The Cross morphotype was mainly produced by the Panicoideae (6.8%, s.e. = 1.64, n = 104). The two Saddle variants respectively represent 69.9% and 59.8% of the total number of morphotypes counted in the Chloridoideae (s.e. = 5.03, n = 62) and Aristidoideae (s.e. = 8.12, n = 29). The Trapezoid morphotype was relatively abundant in the Danthionioideae (23.9%, s.e. = 3.97, n = 65), Ehrhartoideae (26.5%, s.e. = 6.52, n = 18) and Pooideae (22.4%, s.e. = 5.17, n = 31), but the Oblong represented 43.8% of the total number of morphotypes counted in the Pooideae (s.e. = 7.55, n = 31).

One-way ANOVA indicated that only the Variant 3 Bilobate (p = 0.2381) was not significantly different between the six subfamilies included in the study (Table 10). The Tukey's HSD tests also showed that the Polylobate was not significantly different among a third or more subcategory pairs (Appendix 8). These two morphotypes were left out of the subsequent CA. The Tukey's HSD tests further indicated that the Aristidoideae subfamily were the most often significantly differentiated in terms of Variant 1 Bilobate, Variant 2 Bilobate and Variant 2 Saddle representation (Appendix 8). The Chloridoideae subfamily was the most often significantly differentiated by the Variant 1 Saddle. The Danthionoideae was most frequently different from other subfamilies in terms of the Variant 2 Bilobate, Rondel and Reniform morphotypes. Trapezoids and Rondels most frequently discriminated between the Ehrhartoideae and the rest of the subfamilies. The Panicoideae subfamily was the most often significantly differentiated by the Cross, the Variant 1 and Variant 2 Bilobate, while

the Pooideae was most frequently differentiated by the Trapezoid and Oblong morphotypes. Overall, the two Saddle variants, the Trapezoid and the Oblong provided the most differences between subcategory pairs.

The second CA, which was carried out using only those morphotypes found to be significant in the ANOVA test for the Subfamily -subcategories, show two dimensions that explain a cumulative 71.71% of inertia, with a maximum of five dimensions that can be extracted to reconstruct the frequency table (Table 11, Eigenvalues). As expected, those variables found to be significantly different between the most subfamilies delivered the highest contribution to total relative inertia, such as the Variant 1 Saddle morphotype (Table 11, Column coordinates). The association between subfamily and morphotype was plotted on the first two dimensions in Figure 12 and confirmed by maximum row percentage values (Table 11, Percentages of row totals). The Variant 1 Bilobate affiliated strongly with Aristidoideae (25.0%), the Variant 2 Bilobate with Panicoideae (62.5%), the Variant 1 Saddle with Chloridoideae (72.9%), the Trapezoid morphotype with Ehrhartoideae (30.4%) and the Oblong morphotype with Pooideae (49.7%). Inertia created by the matrix provided a first dimension that accounted for 48.93%, and a second dimension that accounted for 22.78% of the total inertia (Figure 12). The first dimension correspond to a C_4 / C_3 - gradient , with the two Saddle Variants representing predominantly C_4 subfamilies on the left side of the plot (positive values) and the Rondel, Trapezoid and Oblong morphotypes representing predominantly C_3 subfamilies on the right side of the plot (negative values).

Ecological Categories

Association between Morphotype and Photosynthetic pathway

Association between GSSC-phytoliths through their rate of recurrence (Table 5) indicated that the Variant 1 Bilobate mainly recur in the NADP-subcategory (37% of species, n = 28) and least in the C_3-subcategory (3% of species, n = 127). Recurrence of the Variant 2 Bilobate was comparatively frequent in the C_3- (28% of species, n = 127), NAD- (20% of species, n = 42) and PCK-subcategory (29% of species, n = 16), but very common in the NADP-subcategory (69% of species, n = 28). Recurrence of the Variant 3 Bilobate and Cross morphotype however, was generally low among all the subcategories (≤ 16% of species). The Polylobate persisted mainly in the NADP-subcategory (22% of species, n = 28) compared to the other subcategories (≤ 11% of species). The Variant 1 Saddle was significantly absent from the C_3-subcategory, extremely rare in the NADP-subcategory, and predominant in the NAD- (54% of species, n = 42) and PCK-subcategories (55% of species, n = 16). Recurrence of the Variant 2 Saddle was also very high in the NAD- (43% of species, n = 42) and PCK-subcategories (22% of species, n = 16) and rare in the C3- and NADP-subcategories. The Trapezoid and Reniform morphotype respectively persisted in 22% and 17% of species in the C_3-subcategory (n = 127), but in less than 8% in the rest of the subcategories. Recurrence of the Rondel and Oblong morphotypes was generally low among all the subcategories (≤ 10% of species).

The relative abundance reflected by GSSC-phytoliths in the Photosynthesis-category (Table 6, Appendix 9) showed that the Variant 1 Bilobate and Trapezoid morphotypes

respectively represented 30.8% (s.e. = 3.38, n = 127) and 23.6% (s.e. = 2.78, n = 127) of the total number of morphotypes counted in the C_3-subcategory. The Saddle Variant 1 (43.0%, s.e. = 7.06, n = 42) and Variant 2 (35.9%, s.e. = 2.20, n = 42) made the the biggest contribution to the NAD-subcategory. Trapeziform-class morphotypes were significantly absent in this subcategory. The Variant 2 Bilobate represented 55.3% (s.e. = 8.01, n = 28), and the Variant 1 Bilobate 25.5% (s.e. = 7.31, n = 28) of the total number of morphotypes counted in the NADP-subcategory. All the Saddle- and Variant 1 Saddle represented 43.0% (s.e. = 11.50, n = 16), and Variant 2 Bilobate 20.8% (s.e. = 9.06, n = 16) of the total number of morphotypes counted in the PCK-subcategory. The Trapeziform-class morphotypes were not represented in this subcategory.

A bivariate plot of the relative abundance of morphotypes with mean carbon isotope ratios, shows clear variation in $\delta\ ^{13}C$ values along a morphological gradient ranging from predominantly C_3 Trapeziform class morphotypes to predominantly C_4 Lobate and Saddle morphotypes (Table 12, Figure 13). The one-way ANOVA for the Photosynthetic pathway-category, including both C_3 and C_4 subcategories revealed that the Variant 3 Bilobate ($p = 0.28630$) is not significantly different between subcategories (Table 13). The Tukey's HSD tests also indicated that the Cross and Rondel morphotypes is not significantly different between a third or more subcategory pairs (Appendix 10). The C_3-subcategory was the most frequently differentiated by the Trapezoid and Oblong morphotypes, the NAD-subcategory by the Variant 2 Saddle, the PCK-subcategory by the Variant 1 Saddle, and the NADP-subcategory by Bilobate Variants 1 and 2 (Appendix 10).

By not including the Variant 3 Bilobate, Cross and Rondel morphotype, the third CA resulted in two dimensions explaining a cumulative 96.98% of total inertia, with a maximum of three dimensions extracted, and thus reflecting the use of only significant morphotypes (Table 14, Eigenvalues). The two-dimensional solution represented the row and column points very well (quality for all points ≥ 0.824). Contributions to the highest relative inertia were provided by the morphotypes found to be significantly different between the most subcategories, namely the Variant 1 and 2 Saddle and Trapezoid morphotypes (Table 14, Column coordinates). The association between the Photosynthetic pathway -category and the remaining GSSC-morphotypes was plotted on the first two dimensions (Figure 14). Maximum row percentage values indicated close alliances between the NADP-subcategory and the Variant 1 (27.5%) and Variant 2 Bilobate (59.8%), while the Variant 1 Saddle associated strongly with the NAD- and PCK-subcategories (Table 14, Percentages of row totals). The Variant 2 Saddle and Trapeziform morphotypes were mainly affiliated with the NAD- and C_3-subcategories (37.2% and 27.7%, respectively). The first dimension in the CA accounts for 60.69% of the total inertia and clearly represents a temperature gradient, with mild to cooler growing conditions represented by Bilobate Variant 1 and 2 and the trapeziform morphotype (positive values), and warm to hot growing conditions, represented by the two Saddle Variants (negative values). The second dimension (36.30% of total inertia) reflects differences between photosynthetic pathways, with primarily C_4 grasses represented by the two Bilobate and Saddle Variants (positive values), and predominantly C_3 grasses represented by the Trapeziform, Oblong and Reniform morphotypes (negative values).

One-way ANOVA conducted for the Photosynthetic pathway category using only C_4 subtypes, expectedly revealed that the Variant 3 Bilobate, as well as the morphotypes corresponding with the C_3-subcategory in the preceding CA, are not significantly different between subcategory pairs. In addition, the Tukey's HSD test singled out the Cross morphotype as not significantly different between subcategory pairs (Appendix 11).

As a result the fourth CA offered two dimensions explaining a cumulative 100% of inertia (Table 16, Eigenvalues) and consequently, the two-dimensional solution represented the row and column points very well (quality for all points = 1.0). Contributions to the highest relative inertia (≥ 0.242) were provided by the Variant 1 and 2 Saddle (Table 16, Column coordinates). The first dimension accounts for 95.40% of the inertia and represents a biochemical gradient in grasses between aspartate formers (NAD and PCK), marked by the two Saddle Variants, and malate formers (NADP), marked by the Variant 1 Bilobate (Figure 15).

Association between Morphotype and Rainfall

Association through the rate of recurrence between phytolith morphotypes and Rainfall-subcategories (Table 5) demonstrated that the Variant 1 Bilobate (22%, n = 176) and Polylobate (19%, n = 176) recurred mainly, but moderately in the in the >500mm S – subcategory. The Variant 2 Bilobate (49%, n = 176), recurred strongly in the in the >500mm S – subcategory, as well as in the <500mm S -subcategory (45%, n = 97) and >40% W –subcategory (49%, n = 125). Recurrence of the Variant 1 (35%, n = 97) and Variant 2 Saddle (23%, n = 97) was highest in the <500mm S – subcategory. The Trapezoid (32%, n = 125) and Reniform morphotypes (20%, n =

125) were most common in the >40% W –subcategory. Recurrence of the Variant 3 Bilobate, Cross, Rondel and Oblong morphotypes is generally low in all the subcategories (≤ 16% of species).

Relative abundance of GSSC-morphotypes calculated for the Rainfall-category (Table 6, Appendix 12) showed that the Variant 2 Bilobate was the predominant morphotype in all three of the subcategories (> 29% of total GSSC-morphotypes counted). Other morphotypes with high values were both Saddle Variants in the >500mm S – subcategory (27.7%, s.e. = 4.28 and 15.7%, s.e. = 3.37, n = 97), the Variant 1 Bilobate in the >500mm S – subcategory (16.6%, s.e. = 2.57, n = 176) and the Trapezoid morphotype in the >40% W –subcategory (17.4%, s.e. = 2.62, n = 125).

Altogether five morphotypes were shown not to be significantly different ($p < 0.05$) between subcategory pairs in the one-way ANOVA test for the rainfall category, namely the Variant 2 and 3 Bilobate, Polylobate, Cross as well as the Rondel morphotype (Table 17, Appendix 13). The >500S-subcategory was the most frequently differentiated by the Variant 1 Bilobate and the Variant 1 and 2 Saddle. The <500S-subcategory was most frequently differentiated by the Variant 2 Saddle and the >40%W-subcategory by the Trapezoid and Reniform morphotypes (Appendix 13). The fifth CA was carried out using only those morphotypes found to be significant in the ANOVA test for the Rainfall-subcategories. The first two dimensions of the CA explained a cumulative 100% of inertia, confirming the significance of the morphotypes with high-quality representation of row and column points (quality for all points = 1.0) (Figure 16 and Table 18, Eigenvalues). The Variant 1 Saddle

contributed the most relative inertia (0.337). This was confirmed by maximum row percentage values (Table 18, Percentages of row totals) which suggested a strong affiliation between the Variant 1 Saddle and <500S-subcategory (52.1%). Additional associations were between the Variant 1 Bilobate and >500S-subcategory (34.8%), the Variant 2 Saddle and <500S-subcategory (29.5%) and the Trapezoid morphotype and >40%W-subcategory (35.5%). In the two-dimensional matrix (Figure 16), the first dimension (contributing 77.52% of the total inertia) reflects a seasonal gradient, with cool, winter rainfall conditions represented by the Trapezoid, Oblong and Reniform morphotypes (negative values) and warm summer rainfall conditions represented by the Variant 1 and 2 Saddle morphotypes (positive values) The second dimension (contributing 22.48% of the total inertia) possibly reflects differences in precipitation patterns, with comparatively high rainfall conditions represented by the Variant 1 Bilobate (positive values) and low rainfall conditions represented by the two Saddle Variants (negative values).

Association between Morphotype and Habitat

Recurrence of GSSC-morphotypes amongst Habitat-subcategories (Table 5) revealed that the Variant 1 Bilobate was moderately frequent in the Desert grasses (19% of species, n = 26), Savanna grassland (22% of species, n = 157), Grassland biome (23% of species, n = 134), High altitude grassland (22% of species, n = 18) and Shady habitat –subcategories (25% of species, n = 43). The Variant 2 Bilobate recurred in 50% or more species in the Savanna grassland (n = 157), Fynbos grasses (n = 104), Forest grasses (n = 15), Damp soils (n = 82) and Swamps/Vleis – subcategories (n = 21). Representation of the Variant 3 Bilobate was modest in the

Forest grasses –subcategory (20% of species, n = 15) and comparatively low in the other subcategories (≤ 15%). Frequent occurrences of the Polylobate morphotype was recorded in the Grassland proper (22% of species, n = 134), Forest grasses (26% of species, n = 15), Swamps/Vleis (23% of species, n = 21) and Shady habitat –subcategory (39% of species, n = 43). The Variable 1 Saddle recurred most frequently in the Desert grasses (23% of species, n = 26), Nama-Karoo grasses (28% of species, n = 85), Savanna grassland (26% of species, n = 157), and Grassland biome –subcategory (20% of species, n = 134). Subcategories Desert grasses (34% of species, n = 26) and Succulent Karoo grasses (32% of species, n = 46), presented the highest recurrence of the Variant 2 Saddle, while the occurrence of the Trapezoid morphotype was most noticeable in the Fynbos grasses (32% of species, n = 104), Montane grassland (42% of species, n = 70) and High altitude grassland subcategory (55% of species, n = 18). The Oblong recurred most frequently in the Forest grasses (26% of species, n = 15) and Montane grassland –subcategories (24% of species, n = 70) and the Reniform morphotype in the Montane grassland (30% of species, n = 70) and High altitude grassland subcategories (50% of species, n = 18). The Cross morphotype recurred most often in the Swamps/vleis –subcategory (19% of species, n = 21), but was otherwise comparatively uncommon (< 15% of species).

Association between GSSC-morphotypes and Habitat-subcategories, based on the relative abundance of phytoliths (Table 6), indicated that the Variant 1 (18.9%, s.e. = 7.16, n = 26) and Variant 2 Saddle (24.3%, s.e. = 6.72, n = 26) were most common, while the Variant 3 Bilobate, Polylobate, Rondel and Reniform morphotypes were

rare in the Desert grasses –subcategory. There were no Cross and Oblong morphotypes recorded in the Desert grasses –subcategory. The Succulent Karoo – subcategory was best represented by the Variant 2 Bilobate (23.4%, s.e. = 5.12, n = 46) and Variant 2 Saddle (24.3%, s.e. = 5.72, n = 46) morphotypes. The Variant 2 Bilobate and Variant 1 Saddle respectively provided the highest values in the Nama-Karoo grasses -subcategory (30.3%, s.e. = 4.26 and 22.6%, s.e. = 4.31, n = 85), Savanna grassland -subcategory (36.5%, s.e. = 3.41 and 23.9%, s.e. = 3.28, n = 157) and the Grassland biome subcategory (35.4%, s.e. = 3.59 and 18.0%, s.e. = 3.18, n = 134). The Variant 2 Bilobate was also the most prominent morphotype in the Forest grasses –subcategory (36.7%, s.e. = 10.77, n = 15), whereas the Variant 2 Saddle and Reniform morphotype were absent. The Variant 2 Bilobate and Trapezoid morphotype respectively accounted for the highest values in the Fynbos grasses – subcategory (35.9%, s.e. = 3.92 and 16.8%, s.e. = 2.76 n = 104), and the Montane grassland –subcategory (24.3%, s.e. = 4.36 and 24.6%, s.e. = 3.92, n = 70). The Variant 2 Bilobate respectively accounted for more then 30% of the total number of GSSC-phytoliths counted in the Damp soils (36.4%, s.e. = 4.55, n = 82), Swamps/Vleis (40.2%, s.e. = 9.31, n = 21) and Shady habitat –subcategories (31.1%, s.e. = 5.65, n = 43). Maximum values in the High altitude grassland –subcategory were provided by the Variant 1 Bilobate (21.8%, s.e. = 9.91, n = 18) and Trapezoid morphotypes (25.5%, s.e. = 7.04, n = 18).

The one-way ANOVA indicated that the Variant 3 Bilobate (p = 0.4110) and Cross morphotype (p = 0.1951) was not significantly different between the habitat subcategories included in the study (Table 19). Tukey's HSD tests further

demonstrated that the Variant 1 and 2 Bilobate, Polylobate, Rondel and Oblong morphotypes were significantly different between a third or less, subcategory pairs (Appendix 15) and were left out of the subsequent CA. The Variant 1 Saddle and Trapezoid most often significantly distinguish between the Savanna and Montane grassland subcategories, and the Variant 2 Saddle, between the Succulent Karoo and Desert subcategories. The Reniform morphotype most often significantly differentiate between the High altitude and Montane grassland subcategories.

The sixth CA, carried out using only those morphotypes found to be significant in the ANOVA, resulted in two dimensions that explain a cumulative 94.64%% of inertia (Figure 17 and 18), with a maximum of three dimensions extracted (Table 20, Eigenvalues). The Variant 1 Saddle delivered the highest contribution to total relative inertia (0.400) (Table 20, Column coordinates), which is also reflected in the row percentage values (Table 20, Percentages of row totals). The row frequencies showed close association between the Variant 1 Saddle and the Savanna grassland- (77.4%) and Grassland biome –subcategories (74.6%). High affiliation values were also indicated between the Trapezoid morphotype and the Montane grassland- (64.6%) and High altitude grassland –subcategories (63.1%); and the Variant 2 Saddle and the Desert grasses- (39.0%) and Succulent Karoo grasses –subcategory (48.4%). In the two-dimensional representation, the first dimension accounts for 75.81% of the total inertia and is driv en by a climatic gradient between C_4 grassland and savanna habitats, represented by the Variant 1 Saddle and primarily cool or wet C_3 grassland habitats, represented by the Trapezoid morphotype (Fig 17 and 18). The second dimension accounts for 18.83% of the total inertia and may represent a

surface temperature gradient that is evidently reflected in the percentage row values of the Variant 2 Saddle's association with the Succulent Karoo grasses- (48.4%) and Forest grasses –subcategory (0.00%).

Table 7. Spearman's rank-order correlation between association through the rate of recurrence of GSSC-morphotypes (Table 3) and relative abundance of GSSC-morphotypes (Table 4) in the sample (309 species).

Pair of Variables	Spearman Rank Order Correlations MD pairwise deleted Marked correlations are significant at p <.05000 Valid N	Spearman R	t(N-2)	p-level
Bilobate Var1	11	0.937810	8.10437	0.000020
Bilobate Var2	11	0.956722	9.86303	0.000004
Bilobate Var3	11	0.742621	3.32660	0.008847
Polylobate	11	0.938083	8.12405	0.000020
Cross	11	0.850332	4.84753	0.000911
Saddle Var1	11	0.945941	8.74960	0.000011
Saddle Var2	11	0.963558	10.80636	0.000002
Trapezoid	11	0.983761	16.44339	0.000000
Rondel	11	0.967153	11.41436	0.000001
Oblong	11	0.988070	19.24714	0.000000
Reniform	11	0.915353	6.81994	0.000077

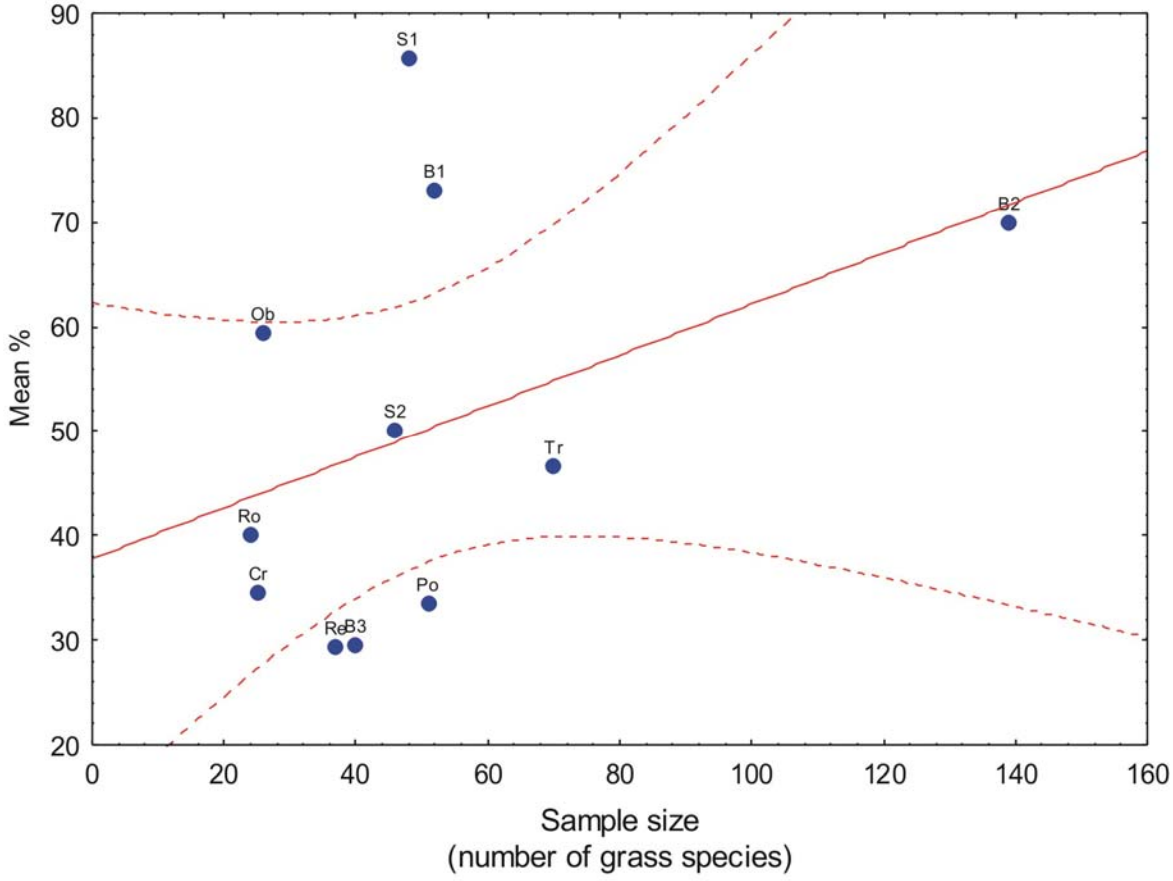

Figure 9. Bivariate plot of the number of morphotypes (mean %) with sample size. Regression line with 0.95 conf. int.; r2 = 0.1657; r = 0.4070, p = 0.2241.

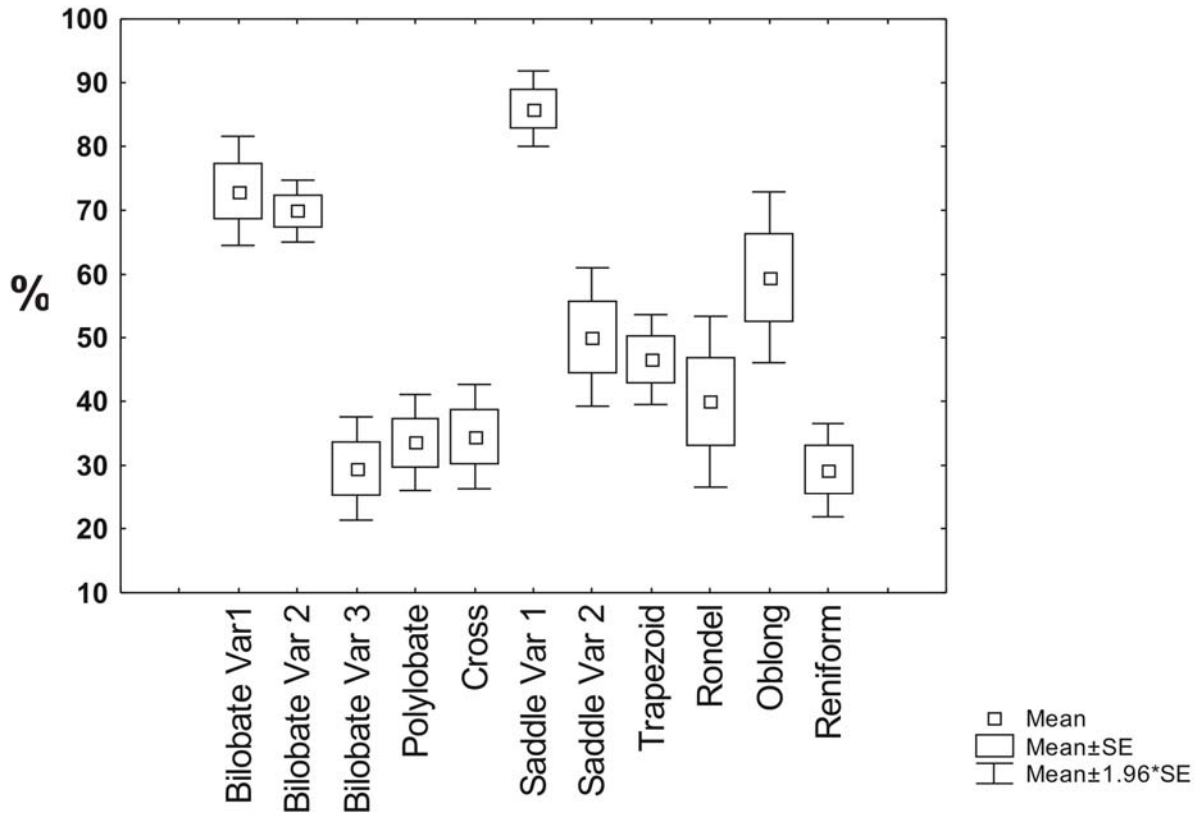

Figure 10. Box plot with whiskers showing relative abundance of GSSC-morphotypes as a proportion of the total number of morphotypes in grasses that produce them.

Table 8. One-way ANOVA of the number of morphotypes as a proportion of the total number of phytoliths produced by dataset of 309 grass species. Marked differences are significant at p < .05000.

	Test of SS Whole Model vs. SS Residual									
	Multiple R	Multiple R^2	Adjusted R^2	SS Model	MS Model	SS Residual	df Residual	MS Residual	F	p
Bilobate Var1	0.780677	0.609456	0.602329	236842.2	23684.22	151770.2	548	276.9530	85.5171	0.00
Bilobate Var 2	0.739785	0.547281	0.539020	413220.9	41322.09	341822.1	548	623.7630	66.2465	0.00
Bilobate Var 3	0.487945	0.238090	0.224187	27169.9	2716.99	86946.1	548	158.6607	17.1245	0.00
Polylobate	0.529881	0.280774	0.267650	46745.8	4674.58	119743.0	548	218.5092	21.3931	0.00
Cross	0.644049	0.414799	0.404121	27705.6	2770.56	39087.2	548	71.3270	38.8431	0.00
Saddle Var 1	0.876994	0.769119	0.764906	337627.2	33762.72	101351.9	548	184.9487	182.5518	0.00
Saddle Var 2	0.678643	0.460557	0.450713	102004.0	10200.40	119475.6	548	218.0212	46.7863	0.00
Trapezoid	0.693931	0.481541	0.472080	159807.8	15980.78	172059.9	548	313.9779	50.8978	0.00
Rondel	0.596335	0.355615	0.343857	39392.0	3939.20	71379.4	548	130.2544	30.2424	0.00
Oblong	0.651899	0.424973	0.414480	85940.9	8594.09	116286.0	548	212.2008	40.4998	0.00
Reniform	0.529369	0.280231	0.267097	47067.2	4706.72	120891.2	548	220.6044	21.3356	0.00

Table 9. Dimension contributions to inertia in CA for GSSC-morphotypes.The eigenvalues are the squared singular values that add up to the Total Inertia which is listed in the header of the Eigenvalue spreadsheet below. Mass represents the row and column totals of the matrix of relative frequencies. Quality reflects the quality of representation of each respective data point in the coordinate system as defined by the respective numbers of dimensions. A low Quality means that the current number of dimensions does not well represent the respective row or column.

Number of Dims.	Eigenvalues and Inertia for all Dimensions Input Table (Rows x Columns): 11 x 11 Total Inertia=2.9293 Chi²=3225.2 df=100 p=0.0000				
	Singular Values	Eigen-Values	Perc. of Inertia	Cumulatv Percent	Chi Squares
1	0.887832	0.788245	26.90878	26.9088	867.8493
2	0.803388	0.645432	22.03350	48.9423	710.6139
3	0.654070	0.427808	14.60432	63.5466	471.0118
4	0.648955	0.421143	14.37681	77.9234	463.6741
5	0.444861	0.197902	6.75589	84.6793	217.8877
6	0.418088	0.174798	5.96717	90.6465	192.4504
7	0.370171	0.137026	4.67775	95.3242	150.8646
8	0.304511	0.092727	3.16547	98.4897	102.0912
9	0.187405	0.035121	1.19894	99.6886	38.6676
10	0.095503	0.009121	0.31136	100.0000	10.0419

Row Name	Row Coordinates and Contributions to Inertia Input Table (Rows x Columns): 11 x 11 Standardization: Row and column profiles				
	Coordin. Dim.1	Coordin. Dim.2	Mass	Quality	Relative Inertia
Bilobate Var1	-1.09288	1.03534	0.091002	0.461409	0.152586
Bilobate Var2	-0.68836	0.27753	0.091010	0.421655	0.040589
Bilobate Var3	-0.35371	0.27902	0.090561	0.120768	0.051955
Polylobate	-0.78206	0.30709	0.091184	0.387641	0.056687
Cross	-0.84178	0.52133	0.090827	0.306576	0.099154
Saddle Var1	1.84799	1.28466	0.090964	0.878711	0.179007
Saddle Var2	1.35486	0.18883	0.090872	0.560632	0.103546
Trapezoid	0.15620	-0.97538	0.090870	0.767872	0.039419
Rondel	0.30891	-1.07558	0.091795	0.437101	0.089779
Oblong	-0.25406	-0.98995	0.090443	0.243060	0.132685
Reniform	0.34386	-0.85346	0.090472	0.478968	0.054593

Column Name	Column Coordinates and Contributions to Inertia Input Table (Rows x Columns): 11 x 11 Standardization: Row and column profiles				
	Coordin. Dim.1	Coordin. Dim.2	Mass	Quality	Relative Inertia
Bilobate Var1	-1.09943	1.03542	0.093503	0.472309	0.154144
Bilobate Var2	-0.64631	0.24658	0.237110	0.509342	0.076047
Bilobate Var3	-0.21428	0.14210	0.052747	0.030004	0.039673
Polylobate	-0.78746	0.27236	0.059359	0.283582	0.049611
Cross	-0.89648	0.61764	0.041204	0.212490	0.078453
Saddle Var1	1.78640	1.19489	0.110931	0.917368	0.190673
Saddle Var2	1.27629	0.03796	0.073136	0.443030	0.091878
Trapezoid	0.24168	-0.99894	0.144959	0.814213	0.064198
Rondel	0.34655	-1.20702	0.054933	0.376094	0.078633
Oblong	-0.26841	-1.06053	0.072494	0.222019	0.133401
Reniform	0.41778	-0.86756	0.059624	0.435953	0.043290

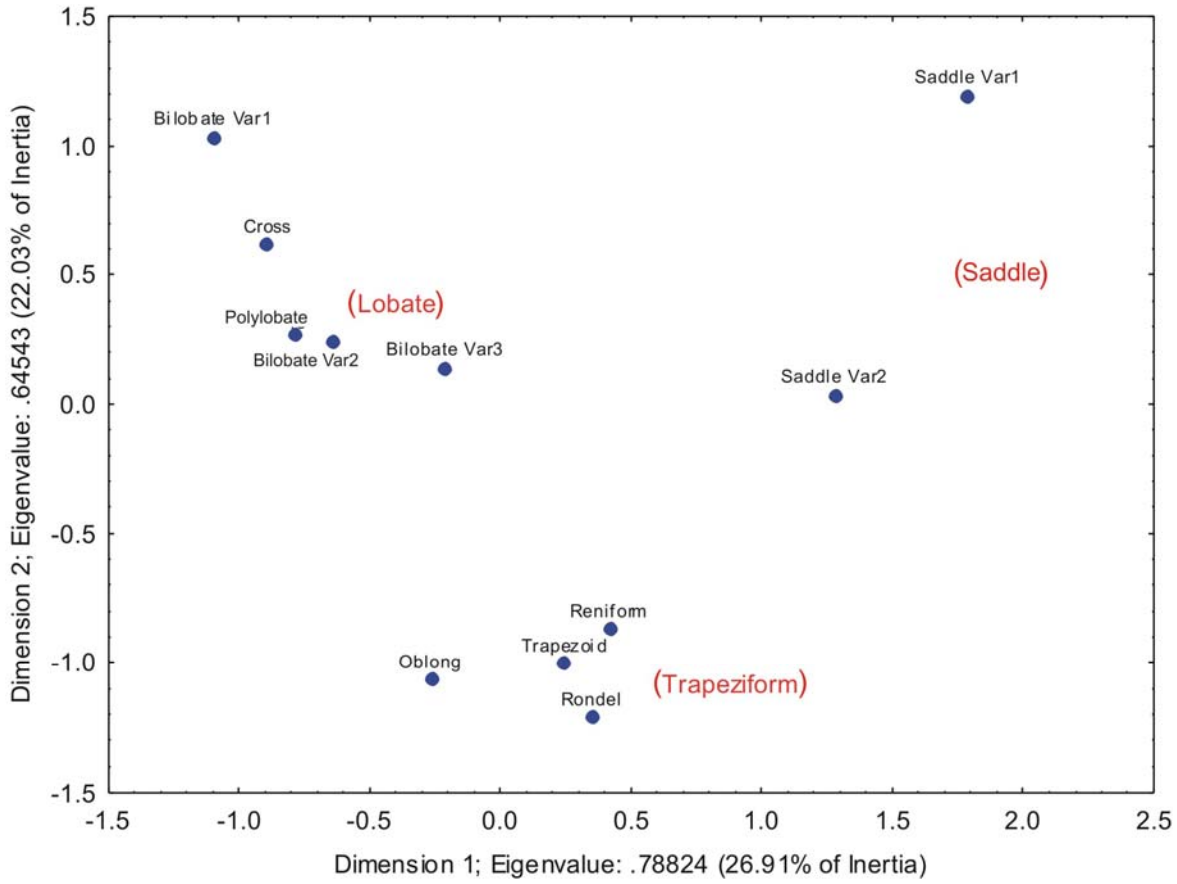

Figure 11. A two-dimensional distribution of CA demonstrating the relationship between GSSC-morphotypes.

Table 10. One-way ANOVA for the Subfamily category. Marked differences are significant at p < .05000.

Dependnt Variable	Test of SS Whole Model vs. SS Residual								
	Multiple R	Multiple R^2	Adjusted R^2	SS Model	MS Model	SS Residual	MS Residual	F	p
Bilobate Var 1	0.322713	0.104144	0.086462	28537.4	4756.23	245481.7	807.506	5.8900	0.000008
Bilobate Var 2	0.505996	0.256032	0.241348	128500.9	21416.82	373393.9	1228.270	17.4366	0.000000
Bilobate Var 3	0.160631	0.025802	0.006575	1482.7	247.12	55982.1	184.152	1.3419	0.238180
Polylobate	0.281708	0.079360	0.061189	6865.3	1144.21	79643.4	261.985	4.3675	0.000300
Cross	0.316255	0.100017	0.082254	3619.3	603.22	32567.5	107.130	5.6307	0.000015
Saddle Var 1	0.840981	0.707250	0.701472	234620.2	39103.37	97115.7	319.460	122.4047	0.000000
Saddle Var 2	0.752747	0.566627	0.558074	90550.8	15091.81	69255.8	227.815	66.2458	0.000000
Trapezoid	0.520393	0.270809	0.256417	46927.6	7821.26	126359.0	415.655	18.8167	0.000000
Rondel	0.288559	0.083267	0.065173	4660.1	776.68	51305.9	168.769	4.6020	0.000172
Oblong	0.676390	0.457503	0.446796	52386.4	8731.06	62118.6	204.338	42.7286	0.000000
Reniform	0.338696	0.114715	0.097242	6366.7	1061.12	49133.7	161.624	6.5654	0.000002

Table 11. Dimension contributions to inertia in CA using only morphotypes found to significantly differentiate between six subfamilies. The eigenvalues are the squared singular values that add up to the Total Inertia which is listed in the header of the Eigenvalue spreadsheet below. Mass represents the row and column totals of the matrix of relative frequencies. Quality reflects the quality of representation of each respective data point in the coordinate system as defined by the respective numbers of dimensions. A low Quality means that the current number of dimensions does not well represent the respective row or column. The row frequencies (percentage of row totals) are standardized, so that their sum in each row is equal to 100%. High row frequencies are marked.

Number of Dims.	Eigenvalues and Inertia for all Dimensions Input Table (Rows x Columns): 6 x 9 Total Inertia=1.2870 Chi²=1278.7 df=40 p=0.0000 Singular Values	Eigen-Values	Perc. of Inertia	Cumulatv Percent	Chi Squares
1	0.793600	0.629800	48.93460	48.9346	625.7066
2	0.541451	0.293170	22.77886	71.7135	291.2639
3	0.482139	0.232458	18.06169	89.7752	230.9474
4	0.360943	0.130280	10.12258	99.8977	129.4333
5	0.036279	0.001316	0.10227	100.0000	1.3076

Row Name	Row Coordinates and Contributions to Inertia Input Table (Rows x Columns): 6 x 9 Standardization: Row and column profiles Coordin. Dim.1	Coordin. Dim.2	Mass	Quality	Relative Inertia
Aristidoideae	-0.70615	0.314178	0.166600	0.408004	0.189522
Chloridoideae	-1.62000	-0.547682	0.133656	0.908874	0.334137
Danthionoideae	0.38848	0.125534	0.168789	0.400042	0.054641
Ehrhartoideae	0.52957	0.001564	0.223676	0.719208	0.067768
Panicoideae	0.11116	0.982280	0.135192	0.633727	0.161980
Pooideae	0.78517	-0.775639	0.172086	0.848501	0.191951

Column Name	Column Coordinates and Contributions to Inertia Input Table (Rows x Columns): 6 x 9 Standardization: Row and column profiles Coordin. Dim.1	Coordin. Dim.2	Mass	Quality	Relative Inertia
Bilobate Var1	-0.42075	0.838353	0.081303	0.786004	0.070715
Bilobate Var2	0.25875	0.419928	0.251532	0.614358	0.077394
Cross	0.11159	0.843426	0.033424	0.392374	0.047907
Saddle Var1	-1.86958	-0.774106	0.093087	0.899891	0.329095
Saddle Var2	-1.02574	0.196463	0.107917	0.501207	0.182477
Trapezoid	0.62099	-0.340130	0.165738	0.944158	0.068376
Rondel	0.51792	-0.153271	0.066471	0.538935	0.027957
Oblong	0.81393	-0.903207	0.105438	0.778906	0.155481
Reniform	0.28348	0.112251	0.095091	0.169183	0.040597

	Percentages of Row Totals Input Table (Rows x Columns): 6 x 9 Total Inertia=1.8859 Chi²=1030.8 df=40 p=0.0000 Bilobate Var1	Bilobate Var2	Cross	Saddle Var1	Saddle Var2	Trapezoid	Rondel	Oblong	Reniform	Total
Pooideae	0.00000	8.45419	0.731046	0.00000	0.00000	24.58437	11.60241	49.71112	4.91687	100.0000
Panicoideae	25.42838	62.57711	8.156271	0.00000	0.76536	2.46744	0.00000	0.00000	0.60544	100.0000
Ehrhartoideae	6.39386	43.22251	1.534527	0.00000	0.00000	30.49872	2.42967	4.21995	11.70077	100.0000
Danthionoideae	2.88629	45.88505	0.000000	0.00000	0.95630	27.01985	8.38067	2.06909	12.80275	100.0000
Chloridoideae	7.47607	11.98605	0.665318	72.93236	6.94020	0.00000	0.00000	0.00000	0.00000	100.0000
Aristidoideae	27.09857	2.36851	0.000000	2.40334	60.57123	0.87078	1.21909	0.00000	5.46848	100.0000

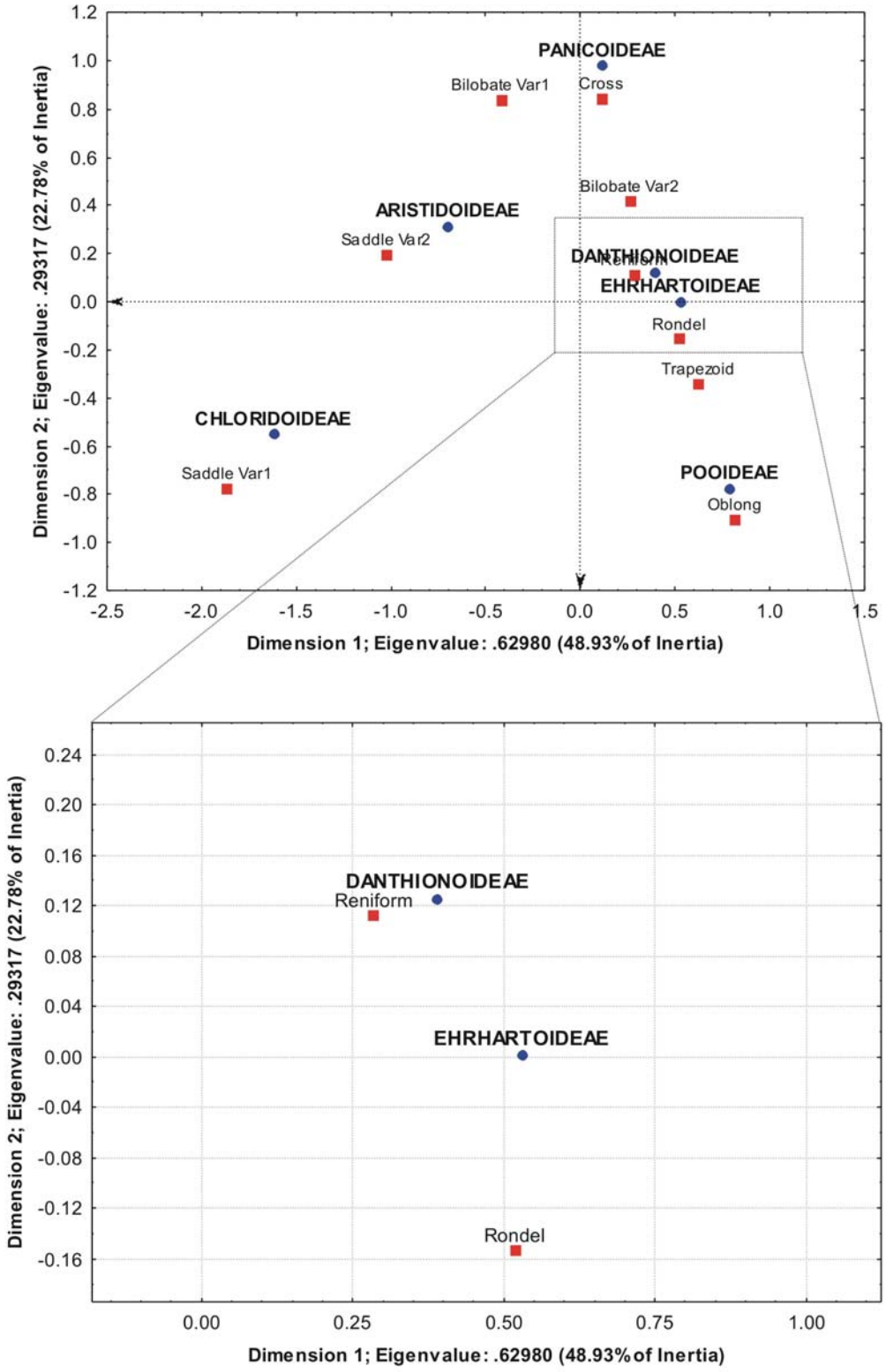

Figure 12. First two dimensions of CA using only morphotypes found to significantly differentiate between six subfamilies.

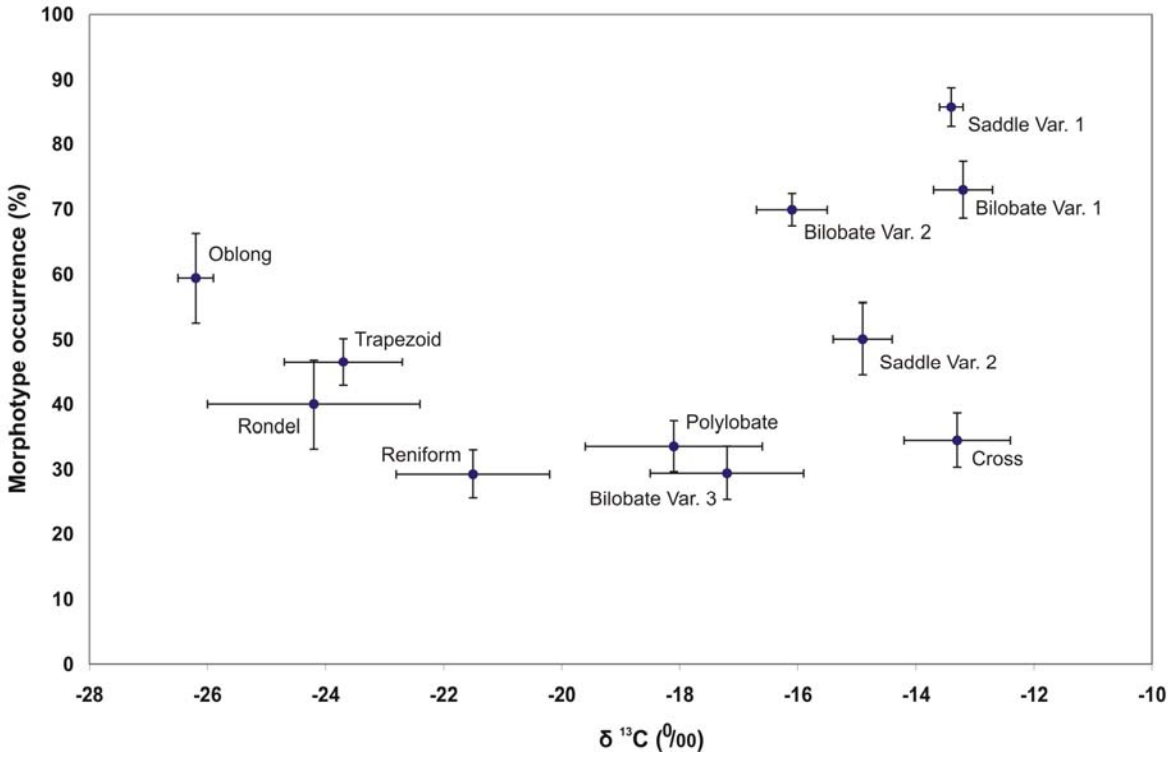

Figure 13. Bivariate plot of relative abundance of morphotypes and average carbon isotope δ 13C ratios in species that produce them. C_3 grasses show an average of -26.5 ‰ (δ< -20‰) and C_4 grasses an average of -12.5 ‰ (δ< -16 ‰) (Vogel *et al*. 1978).

Table 12. Proportional representation of GSSC-morphotypes and their mean carbon isotope δ 13C ratio in ‰. Delta value data from Vogel *et al.* (1978); Ellis *et al.* (1980) and Schulze *et al.* (1996).

	Morphotype Occurrence			Delta Value		
	Species	Mean %	Std. Error	Species	Mean ‰	Std. Error
Bilobate Var1	52	73.0	4.4	18	-13.2	0.5
Bilobate Var2	139	69.9	2.5	40	-15.3	0.7
Bilobate Var3	40	29.5	4.2	12	-17.2	1.3
Polylobate	51	33.6	3.9	13	-18.1	1.5
Cross	25	34.5	4.1	11	-13.3	0.9
Saddle Var1	48	85.8	3.0	28	-13.4	0.1
Saddle Var2	46	50.1	5.6	31	-14.9	0.5
Trapezoid	70	46.5	3.6	14	-23.7	1
Rondel	24	40.0	6.9	5	-24.2	1.8
Oblong	26	59.4	6.8	7	-26.2	0.3
Reniform	37	29.3	3.8	15	-21.5	0.9

Table 13. One-way ANOVA for the Photosynthetic pathway category, including both C_3 and C_4 subcategories. Marked differences are significant at p < .05000.

	Test of SS Whole Model vs. SS Residual									
Dependnt Variable	Multiple R	Multiple R^2	Adjusted R^2	SS Model	MS Model	SS Residual	df Residual	MS Residual	F	p
Bilobate Var1	0.309012	0.095488	0.082505	12211.30	4070.43	115671.2	209	553.451	7.35464	0.000104
Bilobate Var 2	0.361698	0.130826	0.118350	40783.90	13594.63	270958.3	209	1296.451	10.48604	0.000002
Bilobate Var 3	**0.133699**	**0.017875**	**0.003778**	**730.82**	**243.61**	**40153.4**	**209**	**192.122**	**1.26799**	**0.286369**
Polylobate	0.203986	0.041610	0.027853	2388.44	796.15	55011.8	209	263.214	3.02470	0.030598
Cross	0.226187	0.051161	0.037541	1101.71	367.24	20432.6	209	97.764	3.75638	0.011716
Saddle Var 1	0.631488	0.398778	0.390148	78039.95	26013.32	117658.0	209	562.957	46.20836	0.000000
Saddle Var 2	0.593524	0.352271	0.342973	41948.67	13982.89	77132.2	209	369.053	37.88853	0.000000
Trapezoid	0.428722	0.183802	0.172087	28033.50	9344.50	124486.2	209	595.628	15.68849	0.000000
Rondel	0.205059	0.042049	0.028299	2270.31	756.77	51721.7	209	247.472	3.05800	0.029294
Oblong	0.261492	0.068378	0.055006	7588.78	2529.59	103393.5	209	494.706	5.11333	0.001960
Reniform	0.229368	0.052610	0.039011	2692.46	897.49	48485.7	209	231.989	3.86866	0.010106

Table 14. Dimension contributions to inertia in CA using only morphotypes found to significantly differentiate between C_3 and C_4 subcategories. The eigenvalues are the squared singular values that add up to the Total Inertia which is listed in the header of the Eigenvalue spreadsheet below. Mass represents the row and column totals ofthe matrix of relative frequencies. Quality reflects the quality of representation of each respective data point in the coordinate system as defined by the respective numbers of dimensions. A low Quality means that the current number of dimensions does not well represent the respective row or column. The row frequencies (percentage of row totals) are standardized, so that their sum in each row is equal to 100%. High row frequencies are marked.

	Eigenvalues and Inertia for all Dimensions Input Table (Rows x Columns): 4 x 8 Total Inertia=.61500 Chi²=314.19 df=21 p=0.0000				
Number of Dims.	Singular Values	Eigen-Values	Perc. of Inertia	Cumulatv Percent	Chi Squares
1	0.610925	0.373229	60.68717	60.6872	190.6735
2	0.472458	0.223216	36.29511	96.9823	114.0359
3	0.136232	0.018559	3.01772	100.0000	9.4814

	Row Coordinates and Contributions to Inertia Input Table (Rows x Columns): 4 x 8 Standardization: Row and column profiles				
Row Name	Coordin. Dim.1	Coordin. Dim.2	Mass	Quality	Relative Inertia
C3	0.608234	-0.924914	0.169541	0.998871	0.338196
NAD	-0.691246	-0.104643	0.278321	0.954214	0.231808
NADP	0.704020	0.487012	0.276649	0.994356	0.331519
PCK	-0.382949	0.185864	0.275489	0.824216	0.098476

	Column Coordinates and Contributions to Inertia Input Table (Rows x Columns): 4 x 8 Standardization: Row and column profiles				
Column Name	Coordin. Dim.1	Coordin. Dim.2	Mass	Quality	Relative Inertia
Bilobate Var1	0.484175	0.59728	0.120475	0.997299	0.116120
Bilobate Var2	0.450910	0.15671	0.288959	0.994668	0.107642
Polylobate	0.583771	0.27711	0.084589	0.960047	0.059825
Saddle Var1	-0.829235	0.11063	0.221012	0.967080	0.260072
Saddle Var2	-0.758623	-0.10152	0.143603	0.915255	0.149453
Trapezoid	0.514078	-1.18981	0.063259	0.987978	0.174900
Oblong	0.228736	-0.83678	0.016433	0.849232	0.023678
Reniform	0.290687	-0.99781	0.061670	0.999999	0.108311

	Percentages of Row Totals Input Table (Rows x Columns): 4 x 8 Total Inertia=1.0182 Chi²=372.32 df=21 p=0.0000								
	Bilobate Var1	Bilobate Var2	Polylobate	Saddle Var1	Saddle Var2	Trapezoid	Oblong	Reniform	Total
C3	4.5017	36.0778	7.0108	0.0000	0.5074	27.7294	14.2522	9.92087	100.000
NAD	5.0555	7.4723	0.0000	46.6091	37.2873	0.6165	0.0000	2.95931	100.000
NADP	27.5676	59.8069	12.6255	0.0000	0.0000	0.0000	0.0000	0.00000	100.000
PCK	17.6027	22.8082	4.7945	47.1233	7.6712	0.0000	0.0000	0.00000	100.000

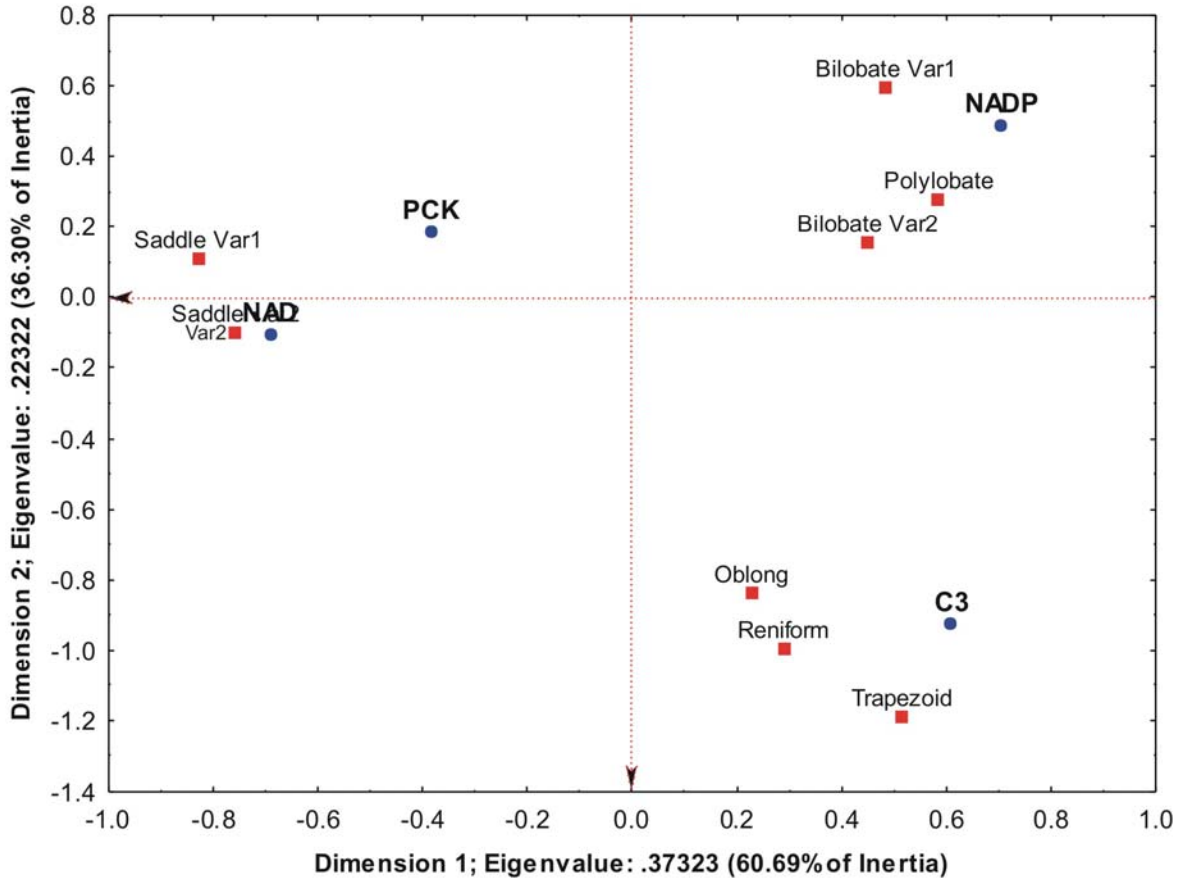

Figure 14. First two dimensions of CA using only morphotypes found to significantly differentiate between C_3 and C_4 photosynthetic types.

Table 15. One-way ANOVA for the Photosynthetic pathway category including only C_4 subtypes. Marked differences are significant at p < .05000.

	Test of SS Whole Model vs. SS Residual									
Dependnt Variable	Multiple R	Multiple R^2	Adjusted R^2	SS Model	MS Model	SS Residual	df Residual	MS Residual	F	p
Bilobate Var1	0.298469	0.089084	0.067134	7254.54	3627.27	74180.3	83	893.739	4.05853	0.020814
Bilobate Var 2	0.555856	0.308976	0.292324	39295.14	19647.57	87883.6	83	1058.839	18.55577	0.000000
Bilobate Var 3	**0.073812**	**0.005448**	**-0.018517**	**40.48**	**20.24**	**7389.4**	**83**	**89.029**	**0.22734**	**0.797146**
Polylobate	0.290837	0.084586	0.062528	2292.48	1146.24	24809.9	83	298.914	3.83468	0.025534
Cross	0.290952	0.084653	0.062596	849.87	424.94	9189.6	83	110.718	3.83800	0.025457
Saddle Var 1	0.478379	0.228846	0.210264	34916.00	17458.00	117658.0	83	1417.566	12.31547	0.000021
Saddle Var 2	0.492184	0.242245	0.223986	24514.62	12257.31	76683.0	83	923.891	13.26705	0.000010
Trapezoid	**0.186142**	**0.034649**	**0.011388**	**7.61**	**3.81**	**212.1**	**83**	**2.556**	**1.48954**	**0.231440**
Rondel	**0.111018**	**0.012325**	**-0.011474**	**0.05**	**0.02**	**3.9**	**83**	**0.047**	**0.51787**	**0.597702**
Reniform	**0.215007**	**0.046228**	**0.023246**	**175.42**	**87.71**	**3619.1**	**83**	**43.604**	**2.01145**	**0.140264**

Table 16. Dimension contributions to inertia in CA using only morphotypes found to significantly differentiate between C_4 subtypes. The eigenvalues are the squared singular values that add up to the Total Inertia which is listed in the header of the Eigenvalue spreadsheet below. Mass represents the row and column totals of the matrix of relative frequencies. Quality reflects the quality of representation of each respective data point in the coordinate system as defined by the respective numbers of dimensions. A low Quality means that the current number of dimensions does not well represent the respective row or column. The row frequencies (percentage of row totals) are standardized, so that their sum in each row is equal to 100%. High row frequencies are marked.

Number of Dims.	Eigenvalues and Inertia for all Dimensions Input Table (Rows x Columns): 3 x 5 Total Inertia=.41705 Chi²=164.55 df=8 p=0.0000 Singular Values	Eigen-Values	Perc. of Inertia	Cumulatv Percent	Chi Squares
1	0.630756	0.397853	95.39796	95.3980	156.9777
2	0.138537	0.019193	4.60204	100.0000	7.5727

Row Name	Row Coordinates and Contributions to Inertia Input Table (Rows x Columns): 3 x 5 Standardization: Row and column profiles Coordin. Dim.1	Coordin. Dim.2	Mass	Quality	Relative Inertia
NAD	0.649983	-0.142339	0.320767	1.000000	0.340528
NADP	-0.844644	-0.051227	0.341306	1.000000	0.586008
PCK	0.236115	0.186850	0.337927	1.000000	0.073463

Column Name	Column Coordinates and Contributions to Inertia Input Table (Rows x Columns): 3 x 5 Standardization: Row and column profiles Coordin. Dim.1	Coordin. Dim.2	Mass	Quality	Relative Inertia
Bilobate Var1	-0.650822	-0.004197	0.148007	1.000000	0.150329
Bilobate Var2	-0.509921	-0.054872	0.302298	1.000000	0.190660
Polylobate	-0.695623	0.141455	0.089568	1.000000	0.108222
Saddle Var1	0.651672	0.157255	0.286164	1.000000	0.308369
Saddle Var2	0.725992	-0.232589	0.173962	1.000000	0.242420

	Percentages of Row Totals Input Table (Rows x Columns): 3 x 5 Total Inertia=.59697 Chi²=165.27 df=8 p=0.0000 Bilobate Var1	Bilobate Var2	Polylobate	Saddle Var1	Saddle Var2	Total
NAD	5.24297	7.74936	0.00000	48.33760	38.67008	100.0000
NADP	27.56757	59.80695	12.62548	0.00000	0.00000	100.0000
PCK	17.60274	22.80822	4.79452	47.12329	7.67123	100.0000

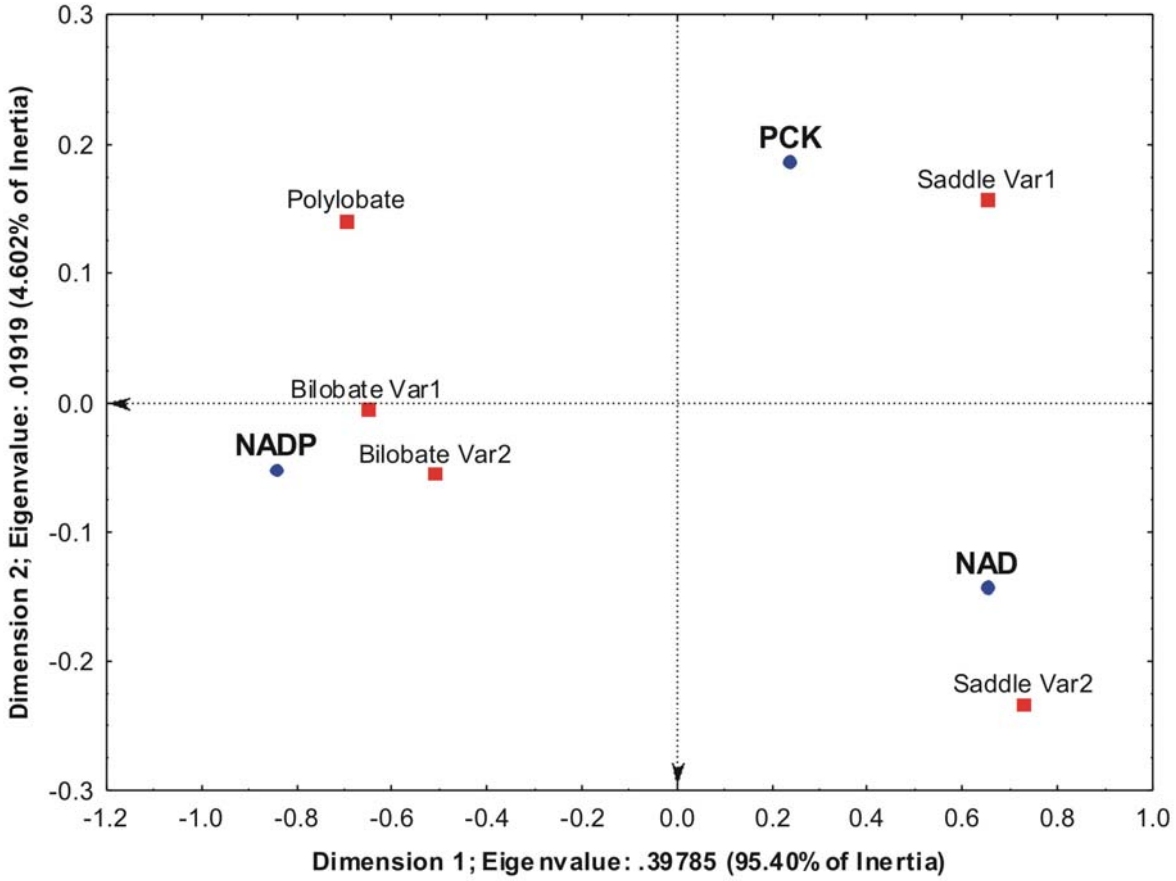

Figure 15. First two dimensions of CA using only morphotypes found to significantly differentiate between C_4 subtypes (aspartate (NAD & PCK) and malate formers (NADP).

Table 17. One-way ANOVA for the Rainfall category. Marked differences are significant at p < .05000.

Dependnt Variable	Test of SS Whole Model vs. SS Residual									
	Multiple R	Multiple R^2	Adjusted R^2	SS Model	MS Model	SS Residual	df Residual	MS Residual	F	p
Bilobate Var1	0.210973	0.044510	0.039672	13419.19	6709.60	288069.6	395	729.290	9.20017	0.000124
Bilobate Var 2	**0.062689**	**0.003930**	**-0.001113**	**2548.99**	**1274.50**	**646065.4**	**395**	**1635.609**	**0.77922**	**0.459469**
Bilobate Var 3	**0.083166**	**0.006917**	**0.001888**	**501.53**	**250.76**	**72008.7**	**395**	**182.300**	**1.37555**	**0.253908**
Polylobate	**0.061346**	**0.003763**	**-0.001281**	**461.95**	**230.98**	**122290.0**	**395**	**309.595**	**0.74606**	**0.474897**
Cross	**0.044655**	**0.001994**	**-0.003059**	**139.87**	**69.93**	**70003.9**	**395**	**177.225**	**0.39461**	**0.674210**
Saddle Var 1	0.273082	0.074574	0.069888	33617.74	16808.87	417179.1	395	1056.150	15.91523	0.000000
Saddle Var 2	0.256265	0.065672	0.060941	14144.81	7072.40	201240.9	395	509.471	13.88187	0.000001
Trapezoid	0.271217	0.073559	0.068868	14448.89	7224.45	181978.2	395	460.704	15.68131	0.000000
Rondel	**0.053424**	**0.002854**	**-0.002195**	**217.88**	**108.94**	**76121.2**	**395**	**192.712**	**0.56531**	**0.568645**
Oblong	0.149278	0.022284	0.017333	3078.00	1539.00	135049.1	395	341.896	4.50136	0.011669
Reniform	0.208577	0.043504	0.038661	2462.42	1231.21	54139.3	395	137.062	8.98290	0.000153

Table 18. Dimension contributions to inertia in CA using only morphotypes found to significantly differentiate between Rainfall subcategories. The eigenvalues are the squared singular values that add up to the Total Inertia which is listed in the header of the Eigenvalue spreadsheet below. Mass represents the row and column totals of the matrix of relative frequencies. Quality reflects the quality of representation of each respective data point in the coordinate system as defined by the respective numbers of dimensions. A low Quality means that the current number of dimensions does not well represent the respective row or column. The row frequencies (percentage of row totals) are standardized, so that their sum in each row is equal to 100%. High row frequencies are marked.

Number of Dims.	Eigenvalues and Inertia for all Dimensions Input Table (Rows x Columns): 3 x 6 Total Inertia=.33618 Chi²=86.776 df=10 p=0.0000 Singular Values	Eigen-Values	Perc. of Inertia	Cumulatv Percent	Chi Squares
1	0.510510	0.260621	77.52449	77.5245	67.27299
2	0.274878	0.075558	22.47551	100.0000	19.50344

Row Name	Row Coordinates and Contributions to Inertia Input Table (Rows x Columns): 3 x 6 Standardization: Row and column profiles Coordin. Dim.1	Coordin. Dim.2	Mass	Quality	Relative Inertia
<500 S	0.656105	-0.205388	0.311524	1.000000	0.437994
>500 S	0.044448	0.409044	0.310366	1.000000	0.156294
>40% W	-0.577048	-0.166540	0.378110	1.000000	0.405712

Column Name	Column Coordinates and Contributions to Inertia Input Table (Rows x Columns): 3 x 6 Standardization: Row and column profiles Coordin. Dim.1	Coordin. Dim.2	Mass	Quality	Relative Inertia
Bilobate Var1	0.176203	0.540677	0.155879	1.000000	0.149945
Saddle Var1	0.710031	-0.035192	0.224826	1.000000	0.337984
Saddle Var2	0.255183	-0.375020	0.183358	1.000000	0.112224
Trapezoid	-0.567212	-0.066520	0.199868	1.000000	0.193908
Oblong	-0.374633	0.131324	0.121984	1.000000	0.057185
Reniform	-0.655854	-0.090545	0.114085	1.000000	0.148755

	Percentages of Row Totals Input Table (Rows x Columns): 3 x 6 Total Inertia=.45090 Chi²=67.650 df=10 p=0.0000 Bilobate Var1	Saddle Var1	Saddle Var2	Trapezoid	Oblong	Reniform	Total
<500S	12.86430	52.13428	29.53953	4.35258	0.46428	0.64503	100.0000
>500s	34.86581	33.39177	2.80543	13.23070	10.99587	4.71041	100.0000
>40%W	7.94377	6.39098	20.75842	35.59987	15.67506	13.63191	100.0000

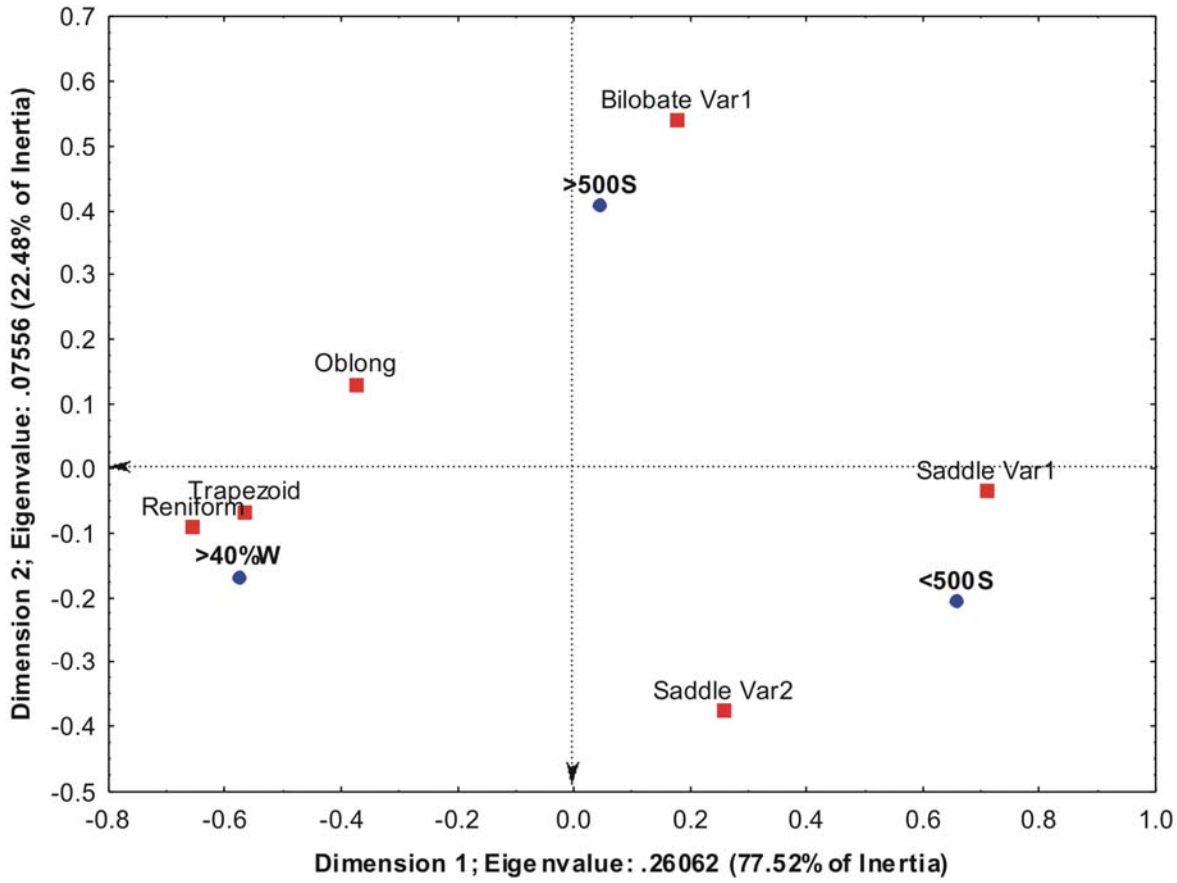

Figure 16. First two dimensions of CA using only morphotypes found to significantly differentiate between Rainfall subcategories.

Table 19. One-way ANOVA for the Habitat category. Marked differences are significant at p < .05000.

	Test of SS Whole Model vs. SS Residual									
Dependnt Variable	Multiple R	Multiple R^2	Adjusted R^2	SS Model	MS Model	SS Residual	df Residual	MS Residual	F	p
Bilobate Var1	0.168418	0.028365	0.014819	19998.40	1818.037	685045	789	868.245	2.09392	0.018662
Bilobate Var 2	0.164112	0.026933	0.013367	34639.97	3149.088	1251521	789	1586.212	1.98529	0.027111
Bilobate Var 3	**0.119387**	**0.014253**	**0.000510**	**1676.13**	**152.376**	**115919**	**789**	**146.919**	**1.03714**	**0.411091**
Polylobate	0.168088	0.028254	0.014706	6308.63	573.512	216977	789	275.002	2.08548	0.019218
Cross	**0.135625**	**0.018394**	**0.004709**	**2394.80**	**217.709**	**127800**	**789**	**161.977**	**1.34408**	**0.195129**
Saddle Var 1	0.246989	0.061004	0.047912	52474.63	4770.420	807713	789	1023.718	4.65990	0.000001
Saddle Var 2	0.349805	0.122364	0.110128	34974.36	3179.488	250849	789	317.932	10.00051	0.000000
Trapezoid	0.311319	0.096920	0.084329	42853.37	3895.761	399301	789	506.085	7.69784	0.000000
Rondel	0.164797	0.027158	0.013595	4899.23	445.384	175498	789	222.431	2.00235	0.025582
Oblong	0.176787	0.031254	0.017748	12930.84	1175.531	400808	789	507.994	2.31406	0.008536
Reniform	0.319507	0.102085	0.089566	11011.96	1001.087	96859	789	122.762	8.15472	0.000000

Table 20. Dimension contributions to inertia in CA using only morphotypes found to significantly differentiate between Habitat-subcategories. The eigenvalues are the squared singular values that add up to the Total Inertia which is listed in the header of the Eigenvalue spreadsheet below. Mass represents the row and column totals of the matrix of relative frequencies. Quality reflects the quality of representation of each respective data point in the coordinate system as defined by the respective numbers of dimensions. A low Quality means that the current number of dimensions does not well represent the respective row or column. The row frequencies (percentage of row totals) are standardized, so that their sum in each row is equal to 100%. High row frequencies are marked.

	Eigenvalues and Inertia for all Dimensions Input Table (Rows x Columns): 12 x 4 Total Inertia=.41663 Chi²=312.47 df=33 p=0.0000				
Number of Dims.	Singular Values	Eigen-Values	Perc. of Inertia	Cumulatv Percent	Chi Squares
1	0.562019	0.315865	75.81442	75.8144	236.8993
2	0.280076	0.078442	18.82787	94.6423	58.8319
3	0.149405	0.022322	5.35771	100.0000	16.7414

	Row Coordinates and Contributions to Inertia Input Table (Rows x Columns): 12 x 4 Standardization: Row and column profiles				
Row Name	Coordin. Dim.1	Coordin. Dim.2	Mass	Quality	Relative Inertia
Desert grasses	-0.477907	-0.387159	0.117948	0.976684	0.109650
Succulent Karoo grasses	-0.144078	-0.466527	0.118840	0.992758	0.068500
Nama-Karoo grasses	-0.926230	0.065431	0.070588	0.979683	0.149106
Savanna grassland	-0.975533	0.277789	0.058599	0.952882	0.151860
Grassland Biome	-0.653020	0.319868	0.055721	0.980928	0.072092
Fynbos grasses	0.268338	0.053293	0.094872	0.990952	0.017199
Forest grasses	-0.279200	0.691080	0.044444	0.801656	0.073926
Montane grassland	0.568742	0.025796	0.110476	0.997043	0.086204
High altitude grassland	0.743648	0.033838	0.148160	0.981867	0.200706
Damp soils	0.088534	0.191234	0.058536	0.469475	0.013290
Swamps/Vleis	0.068488	0.041400	0.038095	0.108491	0.005398
Shady grasses	0.460722	0.071449	0.083721	0.838884	0.052069

	Column Coordinates and Contributions to Inertia Input Table (Rows x Columns): 12 x 4 Standardization: Row and column profiles				
Column Name	Coordin. Dim.1	Coordin. Dim.2	Mass	Quality	Relative Inertia
Saddle Var1	-0.833169	0.295235	0.210778	0.987712	0.400204
Saddle Var2	-0.472407	-0.544866	0.179248	0.996252	0.224584
Trapezoid	0.293920	0.125768	0.385479	0.803604	0.117676
Reniform	0.654767	-0.058102	0.224495	0.904066	0.257535

	Percentages of Row Totals Input Table (Rows x Columns): 12 x 4 Total Inertia=.57417 Chi²=228.32 df=33 p=0.0000				
	Saddle Var1	Saddle Var2	Trapezoid	Reniform	Total
Desert grasses	30.33292	39.02589	27.00370	3.63748	100.0000
Succulent Karoo grasses	15.59792	48.48354	30.06932	5.84922	100.0000
Nama-Karoo grasses	57.65306	23.94958	18.03721	0.36014	100.0000
Savanna grassland	77.44532	14.63062	7.24309	0.68097	100.0000
Grassland Biome	74.67532	6.77180	14.59493	3.95795	100.0000
Fynbos grasses	23.79566	11.75225	46.26787	18.18422	100.0000
Forest grasses	67.56757	0.00000	32.43243	0.00000	100.0000
Montane grassland	4.38676	1.79970	64.63911	29.17443	100.0000
High altitude grassland	0.00000	0.54870	63.10014	36.35117	100.0000
Damp soils	30.76955	2.76063	50.73294	15.73687	100.0000
Swamps/Vleis	33.55705	1.34228	54.69799	10.40268	100.0000
Shady grasses	29.26554	5.42373	57.06215	8.24859	100.0000

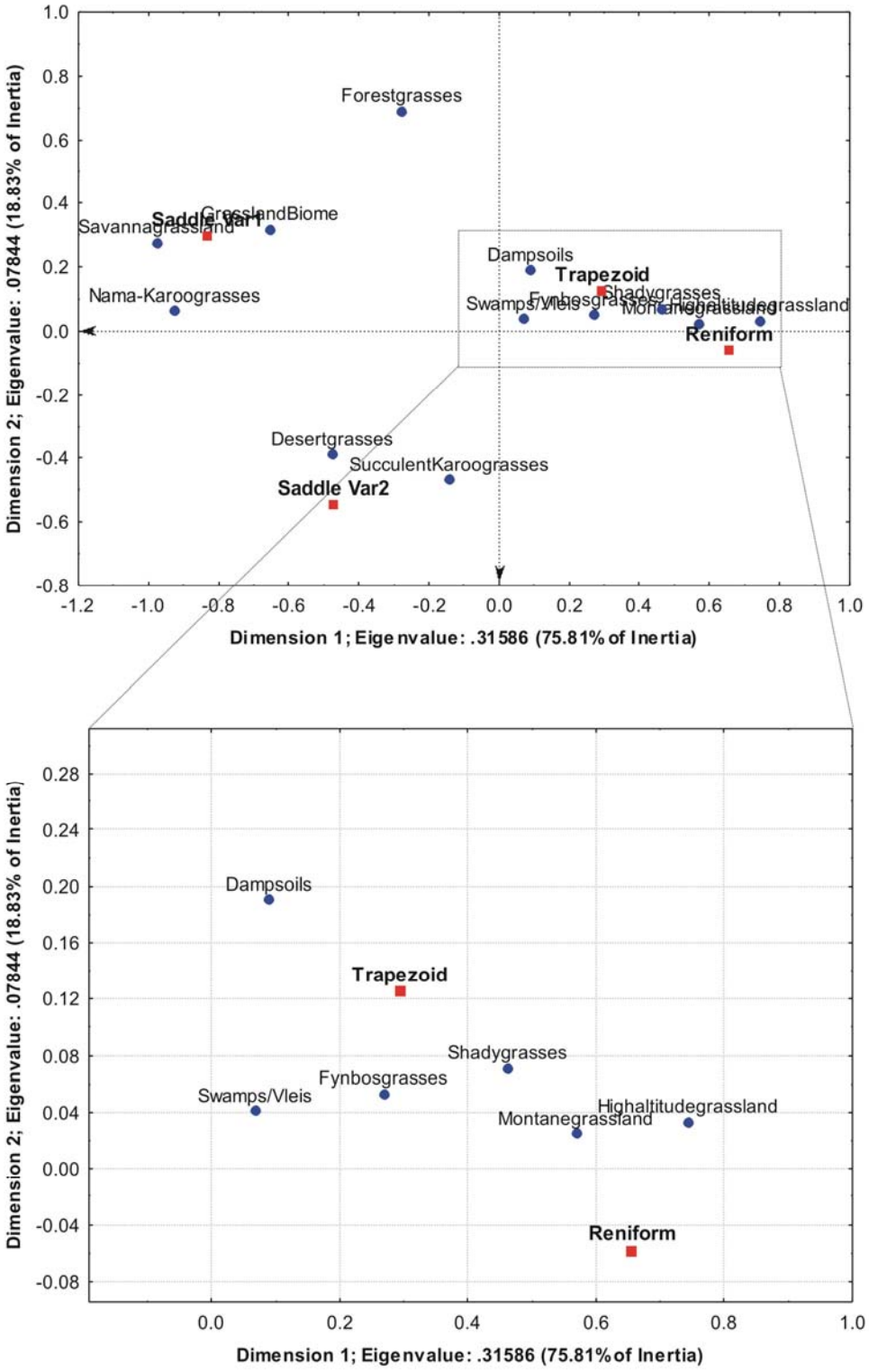

Figure 17. First two dimensions of CA using only morphotypes found to significantly differentiate between Habitat subcategories (Trapezoid and Reniform associations enlarged).

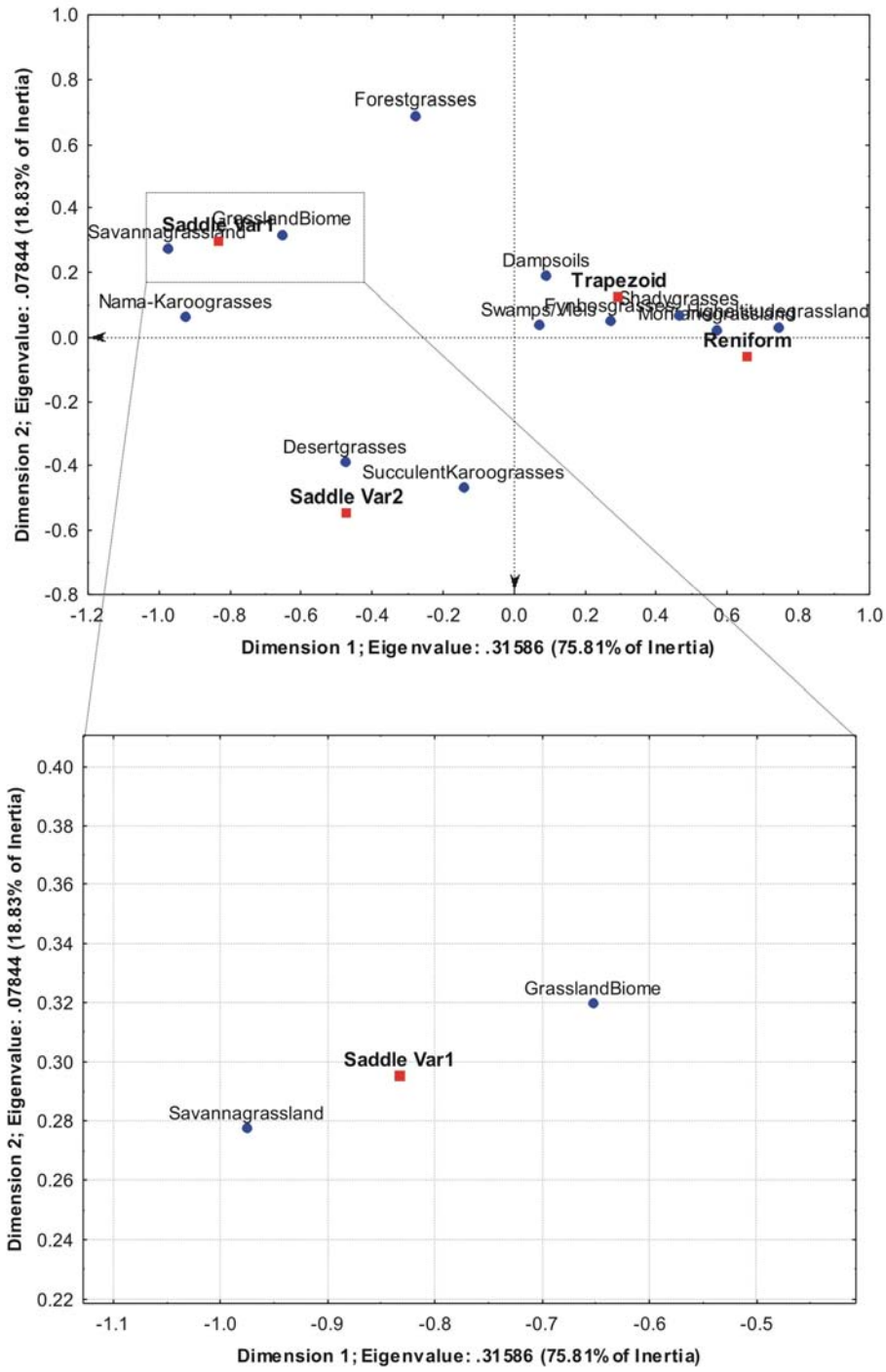

Figure 18. First two dimensions of CA using only morphotypes found to significantly differentiate between Habitat subcategories (Saddle Var1 associations enlarged).

Discussion and Conclusion

Production and affiliation between GSSC- phytoliths

Rates of morphotype production appear to be variable. Relative abundance values indicate that the 1st and 2nd Bilobate Variant, Variant 1 Saddle as well as the Oblong morphotype, are produced in comparably higher quantities, while the Variant 3 Bilobate, Polylobate and Cross, are produced in lower amounts by the species that produce them (Figure 10). However, the potential for bias as a result of variable production of GSSC-phytoliths in species is mitigated by the fact that positive covariation is demonstrated between *relative abundance* and the *rate of recurrence* of the GSSC-morphotypes. Strong morphological affilation has been expressed by clustering of the Lobate, Saddle and Trapeziform morphotype classes in the first correspondence analysis (Figure 11), alluding to genetic control, which also suggests that association between GSSC-phytoliths is not completely random, as implied by the complexities of multiplicity and redundancy (Rovner 1983).

The effects of multiplicity and redundancy are more noticeable at subfamily-level, because the hierarchal position of subfamily, as a taxonomic unit in biological classification, is based on inherent, homologous characters other than phytolith morphology. The original classification scheme by Twiss *et al.* (1969) has shown that several GSSC-phytolith morphotypes associate well with particular North American subfamilies, and mainly according to photosynthetic pathway. This trend is corroborated by the study, which also indicates that as a result of multiplicity and redundancy, comparatively few morphotypes appear to be really meaningful indicators at subfamily level (Appendix 8), namely the Variant 1 Saddle

(Chloridoideae), Variant 2 Saddle (Aristidoideae), Variant 2 Bilobate (Panicoideae), the Trapezoid morphotype (Ehrhartoideae and Danthionoideae) and the Oblong morphotype (Pooideae).

GSSC-phytoliths and the environment

Inter-relationships based on GSSC-morphotype assemblages amongst the habitat-, rainfall- and photosynthetic pathway - categories, are illustrated in Figure 19. Dimension contributions to total inertia and the degree of separation shown by the two-dimensional plots in the six sets of CA, suggest that the GSSC-morphotypes selected to describe the different subcategories are ecologically appropriate, (cumulative percent inertia > 90% and number of dimensions extracted ≤ 3, Table 21). It is evident that short cell phytolith association in grasses is primarily driven by a temperature gradient, marked by cool growing temperatures (as pointed out by the C_3 photosynthetic pathway -category, versus warm growing temperatures (i.e. C_4 photosynthetic pathway) (Figure 19, Dimension 1). Rainfall seasonality and relative moisture, to a lesser extent, also contribute to the general pattern (Figure 19, Dimension 2). This observation is by and large supported by significant positive correlation between C_4 -species abundance and the <500mm summer rainfall niche ($r^2 = 0.6521$; $r = 0.8075$, $p = 0.0008$), and significant negative correlation between C_3-species abundance and <500mm summer rainfall niche ($r^2 = 0.6427$; $r = -0.8017$, $p = 0.0010$) (Figure 20). One possible example of the influence of relative moisture is exemplified in the Chloridoideae where the marsh grass species, *Sporobolus ludwiggi* show Bilobate morphology, while *Sporobolus panicoides*, which do not occur in wet environments, essentially exhibit saddle-shaped GSSC-morphotypes

(Appendix 2).

The Variant 2 Bilobate, Variant 1 Saddle, Variant 2 Saddle, Trapezoid and Reniform morphotypes affiliate with several subcategories, as opposed to the Variant 3 Bilobate, Polylobate, Cross and Rondel morphotypes (Table 22). The Variant 1 Bilobate appears to be a suitable indicator of mesic and warm-season, growing conditions, while the Variant 2 Bilobate seems to indicate towards a gradient between C_4 aspartate formers and C_3 grasses. The Variant 3 Bilobate bears no significance to any of the subcategories whereas the Cross and Rondel morphotypes contributes only on subfamily level with their association to the Panicoideae and Pooideae, respectively. The Variant 1 Saddle is a meaningful predictor of the Chloridoideae subfamily, warm and locally mesic to regionally dry summer rainfall conditions and environments related to Nama-Karoo and Savanna grass communities as well as the Grassland Biome. The Variant 2 Saddle is well-associated with the Aristidoideae subfamily, dry to arid summer rainfall conditions, as well as conditions related to Desert and Succulent-Karoo grass communities. The Trapezoid and Reniform morphotypes strongly associates with the Pooideae subfamily, C_3, winter rainfall conditions, and environments relating to relatively moist, edaphic grasslands, forest habitats and montane grasslands. The Oblong morphotype is an appropriate indicator of the Pooideae subfamily and C3, winter rainfall conditions in general.

Applicability to fossil phytolith assemblages

It was demonstrated that grass short-cell phytoliths consistently follows meaningful environmental traits that are rooted in the relationship between phytolith shape and the ecological niche of grasses. The thesis examined the predictive power of GSSC-

phytoliths within a quantitative model that successfully assigned ecological meaning to them, irrespective of taxonomic affiliation.

The model allowed for comparison of geographically diverse grass phytolith assemblages from indigenous and endemic species, by converting them into one homogenous group represented by ecological categories. Consequently, this also applies to temporally diverse fossil assemblages, making it a potentially useful method for acquiring palaeoenvironmental data through GSSC-phytolith analysis. This implies the use of interpretive techniques to work backwards in time from the known present to the unknown past. To make extrapolations about the past, we must assume that the principles underlying the structure of natural systems in the past were the same as those of the present. Thus, inferences can be made about the palaeontological record with the knowledge of present processes (Sampson 1970).

It is recognized that the effects of post-depositional processes on the preservation of fossil phytolith assemblages, are potential obstacles to refining scale in terms of localized conditions or longer term regional changes (Fredlund and Tieszen 1994). The ecological significance of modern GSSC-morphotypes provides a means to reconstruct palaeoenvironmental scenarios from fossil phytolith assemblages, albeit on a relatively wider scale, but using modern soil assemblages as a point of reference may also pose a problem. Environmental signals provided by modern soil assemblages affected by widespread human impacts on vegetation, may be skewed by underrepresentation (vegetation degradation, afforestation) or misrepresentation (deforestation, crop cereals). For example, overgrazing by domestic animals is seen as the main cause for vegetation degradation in the South African region, while

replacement of mostly fynbos and grassland by alien timber species comprises a combined area of over fourteen thousand square kilometers (Hoffman 1997) In addition, crop cultivation, including several kinds of cereals, make up close to fifteen percent of total potential arable land in South Africa (Hoffman 1997). In the end, interpretation of the scale represented by fossil phytolith assemblages is contingent on understanding the context of a fossil locality. In light of this, the model was briefly assessed against several palaeoenvironmental interpretations provided by three fossil faunal assemblages (Appendix 16).

Conclusion

Knowledge about the ecological significance of modern GSSC-morphotypes and other morphologically diagnostic phytolith morphotypes remain critically under-researched. The investigations carried out in this study have increased our understanding of the ecological paprameters in which GSSC-morphotypes operate. The central hypothesis, namely that the morphology of South African grass short-cell phytoliths consistently follows meaningful environmental traits that are rooted in the relationship between phytolith shape and the ecological niche of grasses, have been validated. Several meaningful ecological trends were demonstrated by the GSSC-morphotypes in this study, which underscores the advantage of investigating phytolith systematics with the aid of adequate comparative reference collections. Standardization of grass phytolith assemblages using short cell sums have yielded a proxy for regional environmental conditions. The challenge for future research will be to refine the methodology further by testing it through wide-ranging actualistic studies.

Table 21. Number of dimensions that explain 100% of the variability and the sum total of inertia for the first two dimensions that were extracted from each of the six sets of CA carried out in the study.

Category	No. of Dimensions Extracted	Cumulative % Inertia of Dim 1 and 2
Morphotype	10	48.9%
Subfamily	5	71.7%
Photosynthetic pathway (C3 and C4 subtypes)	3	96.9%
Photosynthetic pathway (C4 subtypes)	2	100.0%
Rainfall	2	100.0%
Habitat	3	94.6%

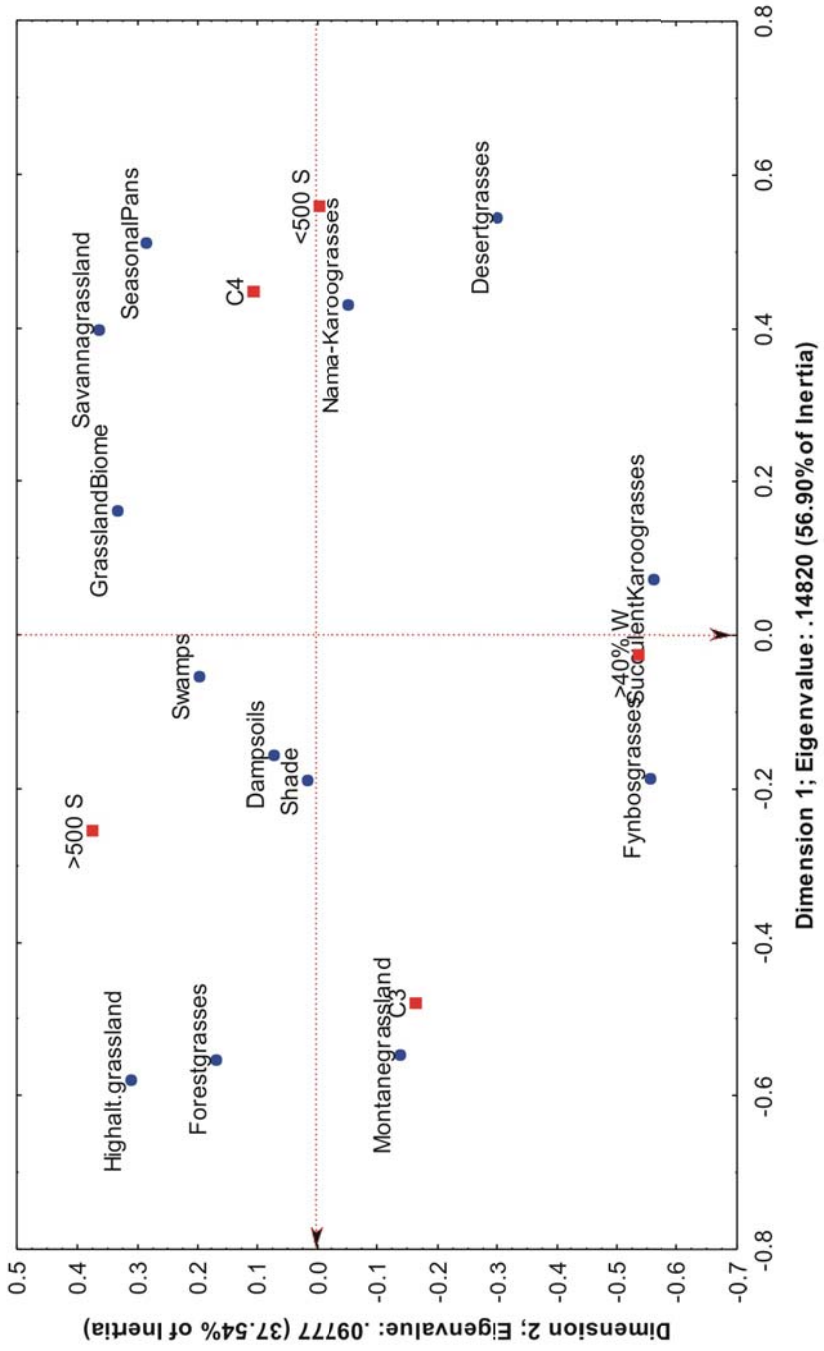

Figure 19. A two-dimensional distribution of CA demonstrating the relationship between the categories habitat, rainfall and photosynthesis, based on the occurrence of eleven GSSC-morphotypes in 309 grass species.

Table 22. Meaningful association between GSSC-morphotypes and subcategories highlighted by the univariate (ANOVA) and multivariate analyses (CA).

	SUBFAMILY							PHOTOSYNTHESIS			RAINFALL		HABITAT											
	Pooideae	Panicoideae	Ehrhartoideae	Danthonioideae	Chloridoideae	Aristidoideae	C3	NADP	NAD	PCK	>500 mm S	<500 mm S	>40%W	Damp soils	Swamps/Vleis	Shady grasses	Forest grasses	Montane grassland	High alt.grassland	Desert grasses	Succulent Karoo grasses	Nama-Karoo grasses	Savanna grassland	Grassland Biome	Fynbos grassland
Bilobate Var1		*						*			*														
Bilobate Var 2		*	*	*				*																	
Bilobate Var 3																									
Polylobate								*																	
Cross		*																							
Saddle Var 1					*					*		*										*	*		
Saddle Var 2						*			*			*								*	*				
Trapezoid	*						*						*	*	*	*		*	*						*
Rondel	*																								
Oblong	*						*						*												
Reniform							*						*	*	*	*		*							*

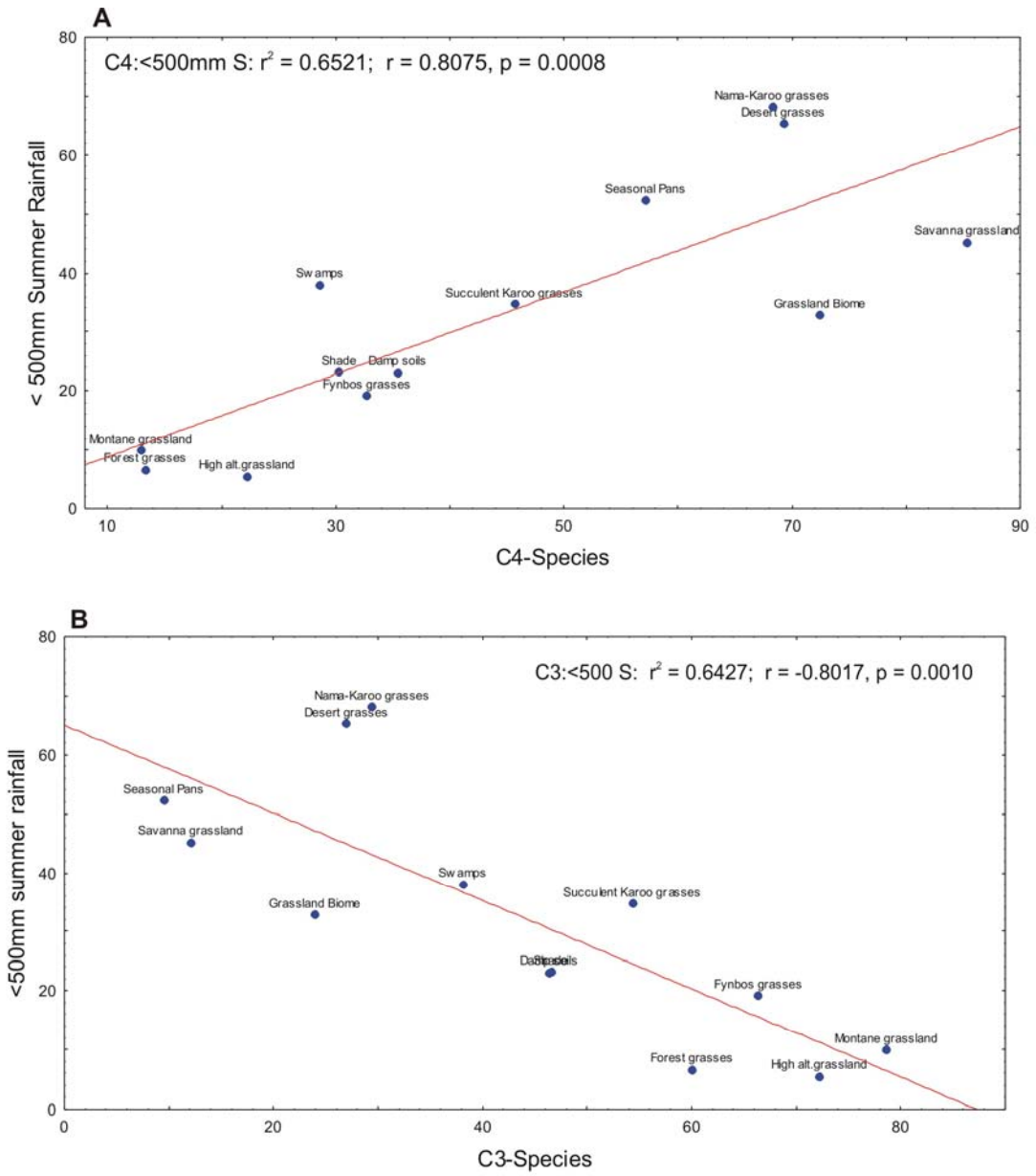

Figure 20. Bivariate plot of the number of C_4- (A) and C_3-grass species (B) with <500mm summer rainfall areas. Regression line with 0.95 confidence interval.

References

Abrantes, F. 2003. A 340 000 year continental climate record from tropical Africa - news from opal phytoliths from the equatorial Atlantic. *Earth and Planetary Science Letters* 209: 165 - 179.

Acocks, J.H.P., 1988. Veld types of South Africa. *Memoirs of the Botanical Survey of South Africa* 40: 1 – 130.

Akersten W.A. 1988. Extraction of dental boluses from the teeth of Pleistocene herbivores to indicate palaeodiet preferences. *Quaternary Research* 30: 92 - 97.

Albert, R.M., Bar-Yosef, O, Meignen, L. and Weiner, S. 2003. Quantitave phytolith study of hearths from the Natufian and Middle Palaeolithic levels of Hyonim Cave (Galilee, Israel). *Journal of Archaeological Science* 30: 461 - 480.

Albert, R.M., Bamford, M.K. and Cabanes, D. 2006. Taphonomy of phytoliths and macroplants in different soils from Olduvai Gorge (Tanzania) and the application to Plio-Pleistocene palaeoanthropological samples. *Quaternary International* 148: 78 – 94.

Alexandre, A., Meunier, J.D., Lezine, A.M. Vincens, A. and Schwarz, D. 1997. Phytoliths: indicators of grassland dynamics during the late Holocene in intertropical Africa. *Palaeogeography, Paleoclimatology, Palaeoecology* 136: 213 - 229.

Andrews, P. 1989. Palaeoecology of Laetoli. *Journal of Human Evolution* 18: 173 – 181.

Andrews, P.J.M. and Nesbitt–Evans, E.M. 1979. Patterns of ecological diversity in

fossil and modern mammalian faunas. *Biological Journal of the Linnean Society* 11: 177 – 205.

Armitage. P.L. 1975. The extraction and identification of opal phytoliths from the teeth of ungulates. *Journal of Archaeological Science* 2: 187 - 197.

Baker, G. 1959. Opal phytoliths in some Victorian soils and “Red Rain” residues. *Australian Journal of Botany* 7:64 – 87.

Bamford, M.K., Albert, R.M and Cabanes, D. 2006. Plio-Pleistocene macroplant fossil remains and phytoliths from Lowermost Bed II in the eastern palaeolake margin of Olduvai Gorge, Tanzania. *Quaternary International* 148: 95 – 112.

Barboni, D., Bonnefille, R., Alexandre, A., Meunier, J.D. 1999. Phytoliths as palaeoenvironmental indicators, West Side Middle Awash Valley, Ethiopia. *Palaeogeography, Palaeoclimatology, Palaeoecology* 152: 87 – 100.

Barboni, D., Bremond, L. Bonnefille, R. 2007. Comparative study of modern phytolith assemblages from inter-tropical Africa. *Palaeogeography, Palaeoclimatology, Palaeoecology* 246: 454 – 470.

Barrable, A., Meadows, M. E. and Hewitson, B. C. 2002. Environmental reconstruction and climate modelling of the late Quaternary in the winter rainfall region of the Western Cape, South Africa. *South African Journal of Science* 98: 611.

Bartoli, F. and Wilding, L.P. 1980. Dissolution of biogenic opal as a function of its physical and chemical properties. Soil Science Society of America Proceedings 44: 873 – 878.

Beavers, A.H and Stephan, I. 1958. Some features of the distribution of plant opal in Illinois soils. Soil Science. 86: 1 – 5.

Bobe, R. and Behrensmeyer, A.K. 2004. The expansion of grassland ecosystems in Africa in relation to mammalian evolution and the origin of the genus *Homo*. *Palaeogeography, Palaeoclimatology, Palaeoecology* 207: 399 – 420.

Boyd, M. 2005. Phytoliths as palaeoenvironmental indicators in a dune field on the northern Great Plains. *Journal of Arid Environments* 61: 357 - 375.

Bremond, L., Alexandre, A., Peyron, O. and Guiot, J. 2005. Grass water stress estimated from phytoliths in West Africa. *Journal of Biogeography* 32: 311 – 327.

Bremond, L., Alexandre, A., Wooller, M.J., Hely, C., Williamson, D., Schafer, P.A., Majule, A. and Guiot, J. 2008. Phytolith indices as proxies of grass subfamilies on East African tropical Mountains. *Global and Planetary Change* 61: 209 – 224.

Brink, J.S. 1987. The Archaeozoology of Florisbad, Orange Free State. *Memoirs van die Nasionale Museum Bloemfontein* 24: 1 – 151.

Brink, J.S. 1988. The taphonomy and palaeoecology of the Florisbad spring fauna. *Palaeoecology of Africa* 19: 169 – 179.

Brink, J.S. and Rossouw, L. 2000. New trial excavations at the Cornelia – Uitzoek type locality. *Navorsinge van die Nasionale Museum, Bloemfontein* 16 (6): 141 – 156.

Brown, R.H. 1978. A difference in N use in C3 and C4 plants and its implications in adaptation and evolution. *Crop Science* 18: 93 – 98.

Brown, D.A. 1984. Prospects and limits of a phytolith key for grasses in the central

United States. *Journal of Archaeological Science* 11: 345 – 368.

Bryant, V.M. 1993. Phytolith research: a look towards the future. In: D.M. Pearsall & D.R. Piperno (eds). Current research in phytolith analysis: applications in archaeology and paleoecology. MASCA, Research Papers in Science and Archaeology 10, pp. .. University of Pennsylvania, Philidelphia.

Campbell, C.S. and Kelogg, E.A. 1987. Sister group relationships in the Poaceae. In: T.R. Soderstrom, K.W. Hilu, C.S. Campbell and M.E. Barkworth (eds.) *Grass Systematics and Evolution,* pp. 217 – 225. Washington DC. Smithsonian Institute Press.

Carnelli, A.L. Madella, M., Theurillat, J. and Amman, B. 2002. Aluminium in the opal silica reticule of phytoliths: a new tool in palaeoecological studies. American Journal of Botany 89(2): 346-351.

Cerling, T.U., Harris, J.M. et al 1997. Global vegetation change through the Miocene / Pliocene boundary. *Nature.* 389: 153 – 158.

Chapman, G.P. 1996. *The biology of grasses*. Wallingford. CAB International.

Chase, B. M. and Meadows, M.E. 2007. Late Quaternary dynamics of southern Africa's winter rainfall zone. *Earth Science Reviews* 84: 103-138.

Chippendall, L.K.A. and Crook, A.O. 1976. *Two hundred and forty grasses of southern Africa.* Edinburgh Press, Salisbury.

Ciochon, R.L. et al. 1990. Opal phytoliths found on the teeth of the extinct ape Giganthropus blacki: Implications for paleodiatary studies. *Proceedings of the*

National Academy of Sciences, USA 87: 8120 - 8124.

Clayton, W.D. and Renvoize S.A. 1986. *Genera Graminum*. Kew Bulletin Additional Series 13: 1 – 389.

Coetzee, J. A. 1967. Pollen analytical studies in east and southern Africa. *Palaeoecology of Africa* 3: 1-146.

Cowling, R.M. and Hilton-Taylor, C. 1994. Patterns of plant diversity and endemism in southern Africa. In: Huntley, B.J. (ed) *Botanical diversity in Southern Africa.* Strelitzia 1: 31 – 52. National Botanical Institute, Pretoria.

Deacon, J. and Lancaster, N. 1988. *Late Quaternary palaeoenvironments of Southern Africa*. Clarendon Press. Oxford.

DeMenocal, P.B. 1995. Plio-Pleistocene African climate. *Science*. 270: 53-59.

Dugas, D.P. and Retallack, G.J. 1993. Middle Miocene fossil grasses from Fort Ternan, Kenya. *Journal of Paleontology* 67 (1): 113 - 129.

Ehleringer, J.R., Sage, R.F., Flanagan, L.B. and Pearcy, R.W. 1991. Climate change and the evolution of climate change. *Trends in Ecological Evolution* 6: 95 – 99.

Ehleringer, J.R. and Monson, R.K. 1993. Evolutionary and ecological aspects of photosynthetic pathway variation. *Annual Review of Ecological Systematics*. 24: 411-439.

Ehleringer, J.R., Cerling, T.E. and Helliker, B.R. 1997. C4 photosynthesis, atmospheric CO2, and climate. *Oecologia* 112: 285 – 299.

Elbaum, R., Weiner, S., Albert, R.M. and Elbuam, M. 2003. Detection of burning of

plant materials in the archaeological record by changes in the refractive indices of silaceous phytoliths. *Journal of Archaeological Science* 30: 217 – 226.

Ellis, R.P. 1979. A procedure for standardizing comparitive leaf anatomy in the Poaceae.II. The epidermis as seen in surface view. *Bothalia* 12 (4): 641 – 671.

Ellis, R. P., Vogel J C & Fuls, A. 1980. Photosynthetic pathways and the geographical distribution of grasses in southwest Africa / Namibia. *South African Journal of Science* 76: 307-314.

Ellis, R.P. 1984. Eragrostis walteri – a first record of non–Kranz leaf anatomy in the sub-family Choloridoideae (Poaceae). *South African Journal of Botany* 3: 380 – 386.

Ellis, R.P. 1986. A review of comparative leaf blade anatomy in the systematics of the Poaceae: the past twenty-five years. In: Grass systematics and Evolution. T.R. Soderstrom, K.W. Hilu, C.S. Campbell and M.E. Barkworth (eds), pp 3 – 11. Smithsonian Institution Press. Washington D.C.

Ellis, R.P. 1988. Leaf anatomy and systematics of *Panicum* (Poaceae: Panicoideae) in southern Africa. *Monographs in Systematic Botany. Missouri Botanical Gardens* 25: 129 – 156.

Ficken, K.J., Wooller, M.J., Swain, D.L., Street-Perrott F.A. and Eglinton, G. 2002. CO_2 and temperature controlled altitudinal shifts of C_4- and C_3-dominated grasslands aloe reconstruction of palaeoatmospheric pCO2. *Palaeogeography, Palaeoclimatology, Palaeoecology* 177: 137 – 150.

Fox, L. C. Perez Perez, A. and Juan, J. 1994. Dietary information through the

examinatyion of plant phytoliths on the enamel surface of human dentition. *Journal of Archaeological Science* 21: 29 – 34.

Fredlund, G.G., Johnson, W.C. and Dort W. 1985. A preliminary analysis of opal phytoliths from the Eustis Ash Pit, Frontier County, Nebraska. *Inst. Ter-Qua.Stud.Symposium* 1: 147 – 162.

Fredlund, G.G. and Tieszen L.T. 1994. Modern phytolith assemblages from the North American Great Plains. *Journal of Biogeography* 21: 321 – 335.

Fredlund, G.G. and Tieszen L.T. 1997. Calibrating grass phytolith assemblages in climatic terms: Application to late Pleistocene assemblages from Kansas and Nebraska. *Palaeogeography, Palaeoclimatology, Palaeoecology* 136: 199 – 211.

Gibbs Russell, G.E. 1985. PRECIS: The National Herbarium's computerized information system. *South African Journal of Science* 81: 62 – 65.

Gibbs Russell, G.E. 1986. Significance of different centres of diversity in subfamilies of Poaceae in southern Africa. *Palaeoecology of Africa* 17: 183 – 192.

Gibbs Russell, G.E. 1987. Preliminary floristic analysis of the major biomes in southern Africa. *Bothalia* 17 (2): 213 – 227.

Gibbs Russell, G.E. 1988. Distribution of subfamilies and tribes of Poaceae in southern Africa. *Monographs in Systematic Botany, Missouri Botanical Gardens* 25: 555 – 566.

Gibss Russell, G. E., Watson, L., Koekemoer, M., Smook, L., Barker, N. P., Anderson, H. M. and Dallwitz, M. J. (eds) 1990. Grasses of Southern Africa. *Memoirs*

of the Botanical Survey of South Africa 58. National Botanical Institute.

Gill, E.D. Stability of biogenic opal. *Science* 158: 810

Gobetz, K.E. and Bozarth, S.R. 2001. Implications for Late Pleistocene Mastodon Diet from Opal Phytoliths in Tooth Calculus. *Quaternary Research* 55(2): 115 – 122.

Gould, F.W. 1968. *Grass Systematics*. 1 – 382. Texas. Texas A&M University.

GPWG: Grass Phylogeny Working Group 2001. Phylogeny and subfamilial classification of the Grasses (Poaceae). *Annals of the Missouri Botanical Garden* 88: 373 – 357.

Greenacre, M. J. (1984). *Theory and applications of correspondence analysis.* New York: Academic Press.

Hansen, B.T. Plew, M.G. and Schimpf, M. 1998. Elucidation of size patterning in phytolith assemblages by field-flow fractionation. *Journal of Archaeological Science* 25: 349 - 357.

Harvey, E.L. and Fuller, D.Q. 2005. Investigating crop processing using phytolith analysis: the example of rice and millets. *Journal of Archaeological Science* 32: 739 – 752.

Hoffman, M.T. 1997. Human impacts on vegetation. In: R.M. Cowling, D.M. Richardson and S.M. Pierce (eds), *Vegetation of southern Africa*, pp 507 – 531. Cambridge University Press. Cambridge.

Hopley, P.J., Weedon, G.P., Marshall. J.D., Herries, A.I.R. and Latham, A.G. 2007. High and low latitude orbital forcing of early hominin habitats in South Africa. *Earth*

and Planetary Science Letters 256: 419 – 432.

Iriarte, J. 2003. Assessing the feasibility of identifying maize through the analysis of cross-shaped size and three-dimensional morphology of phytoliths in the grasslands of southeastern South America. *Journal of Archaeological Science* 30: 1085 – 1094.

Jacobs, B.F., Kingston, J.D. and Jacobs, L.L. 1999. The origin of grass-dominated ecosystems. *Annals of the Missouri Botanical Gardens* 86: 590–643.

Jones, R.L. 1964. Note on the occurrence of opal phytoliths in some Cenozoic sedimentary rocks. *Journal of Paleontology* 38: 773-775.

Jones, R.L. and Beavers, A.H. 1963. Some mineralogical and chemical properties of plant opal. Soil Science 96 (3) 375 – 379.

Jones, R.L. and Handreck, K.A. 1963. Effects of iron and aluminium oxides on silica in solution in soils. *Nature* 198: 852 – 853.

Jurgens, N., Burke, A., Seely, M.K., and Jacobsen, K.M. 1997. Desert. In: R.M. Cowling, D.M. Richardson and S.M. Pierce (eds), *Vegetation of southern Africa*, pp 91 – 98. Cambridge University Press. Cambridge.

Jurgens, N. 2006. Desert Biome. In: L. Mucina and M.C. Rutherford (eds.) 2006. The vegetation of South Africa, Lesotho and Swaziland. *Strelitzia* 19: 1 – 807. National Botanical Institute, Pretoria.

Kaelhofer, L. and Piperno, D.R. 1994. Early agriculture in southeast Asia: phytolith evidence from the Bang Pakong Valley, Thailand. *Antiquity* 68: 564 – 572.

Kellogg, E.A. 2001. Evolutionary history of the grasses. *Plant Physiology* 125: 1198 -

1205

Klein, R.G. 1984. The large mammals of southern Africa: Late Pliocene to Recent. In: R.G. Klein (ed.) *Southern African prehistory and palaeoenvironments*. Balkema. Rotterdam, pp 107 – 146.

Kok, P.D.F. 1972. Die epidermis van grasse met spesiale verwysing na die terminologie. *Tydskrif vir Natuurwetenskappe* 12 (2): 77 – 87.

Low, A.B. and Rebelo, A.T.G. (eds) 1996. *Vegetation of South Africa, Lesotho and Swaziland.* Department of Environmental Affairs and Tourism, Pretoria.

Krull, E.S., Skjemstad, J.O., Graetz, D, Grice, K., Dunning, W., Cook, G. and Parr, J.F. 2003. $^{13}\delta$-Depleted charcoal from C4 grasses and the role of occluded carbon in phytoliths. *Organic Geochemistry* 34: 1337 – 1352.

Lee Thorp, J.A. and Talma, A.S. 2000. Stable light isotopes and past environments in the southern African Quaternary. In: Partridge, T.C. and Maud, R.R. (Eds.) *The Cenozoic of Southern Africa.* Oxford University Press, New York pp 236 – 251.

Linder, H.P. and Ellis, 1990. Vegetative morphology and interfire survival strategies in the Cape Fynbos grasses. *Bothalia* 20 (1): 91 – 103.

Madella, M., Jones, M.K., Goldberg, P. Goren, Y., Hovers, E. 2002. The exploitation of plant resources by Neanderthals in Amud Cave (Israel): the evidence from phytolith studies. *Journal of Archaeological Science* 29: 703 – 719.

Madella, M., Alexandre, A. and Ball, T. 2005. International Code for Phytolith Nomenclature 1.0 *Annals of Botany* 96: 253 – 260.

McClaren, M.P. and Umlauf, M. 2000. Desert grassland dynamics estimated from carbon isotopes in grass phytoliths and soil organic matter. *Journal of Vegetation Science*. 11: 71 – 76.

McLean, B. and Scott, L. 1999. Phytoliths in sediments of the Pretoria Saltpan and their potential as indicators of environmental history at the site. In: Partridge, T.C. (Ed.), *Tswaing-investigations into the origin, age and palaeoenvironments of the Pretoria Saltpan.* Council for Geosciences, Pretoria, pp 167 – 171.

Meadows, M.E. and Linder, H.P. 1993. A palaeoecological perspective on the origin of Afromontane grasslands. *Journal of Biogeography* 20: 345 – 355.

Mercader, J., Runge, F., Vrydaghs, L., Doutrelpont, H. Ewango, C.E.N. and Juan-Tresseras, J. 2000. Phytoliths from archaeological sites in the tropical forest of Ituri, Democratic Republic of the Congo. *Quaternary Research* 54: 102 – 112.

Metcalfe, C.R. 1960. *Anatomy of the monocotyledons*. I. Graminar. London. Oxford University Press pp 1 – 731.

Middleton, W.D. and Rovner, I. 1994. Extraction of opal phytoliths from herbivore dental calculus. *Journal of Archaeological Science* 21: 469 – 473.

Milton, S.J., Yeaton, R.I., Dean, W.R.J. and Vlok, J.H.J. 1997. Succulent Karoo. In: R.M. Cowling, D.M. Richardson and S.M. Pierce (eds), *Vegetation of southern Africa*, pp 91 – 98. Cambridge University Press. Cambridge.

Mucina, L. and Geldenhuys, C.J. 2006. Afrotemperate, Subtropical and Azonal Forests. In: L. Mucina and M.C. Rutherford (eds.) 2006. The vegetation of South Africa, Lesotho and Swaziland. *Strelitzia* 19: 584 - 615. National Botanical Institute,

Pretoria.

Mucina, L. and Rutherford, M.C. (eds.) 2006. The vegetation of South Africa, Lesotho and Swaziland. *Strelitzia* 19: 1 – 807. National Botanical Institute, Pretoria.

Mucina, L., Hoare, D.B., Lotter, M. du Preez, J.P., Rutherford, M.C., Scott-Shaw, C.R. *et al*. 2006a. Grassland Biome. In: L. Mucina and M.C. Rutherford (eds.) 2006. The vegetation of South Africa, Lesotho and Swaziland. *Strelitzia* 19: 348 - 437. National Botanical Institute, Pretoria.

Mucina, L., Rutherford, M.C., Palmer, A.R., Milton, S.J., Scott, L. *et al*. 2006b. Nama-Karoo Biome. In: L. Mucina and M.C. Rutherford (eds.) 2006. The vegetation of South Africa, Lesotho and Swaziland. *Strelitzia* 19: 324 - 347. National Botanical Institute, Pretoria.

Mucina, L., Rutherford, M.C and Powrie, L.W. 2006c. Inland Azonal Vegetation. In: L. Mucina and M.C. Rutherford (eds.) 2006. The vegetation of South Africa, Lesotho and Swaziland. *Strelitzia* 19: 615 - 657. National Botanical Institute, Pretoria.

Mulder, C. and Ellis, R.P. 2000. Ecological significance of South-Wet African grass leaf phytoliths: a climatic response of vegetation biomes to modern aridification trends. In: S.W.L Jacobs and J. Everett (eds). *Grasses: Systematics and Evolution*, pp 248 – 258.

Mulholland, S.C. 1989. Phytolith shape frequencies in North Dakota grasses: a comparison to general patterns. *Journal of Archaeological Science* 16: 489 – 511.

Mulholland, S.C. and Rapp, G.J. 1992. A morphological classification of grass silica-bodies**.** In: G.J. Rapp and S.C. Mulholland (eds). *Phytolith Sustematics. Emerging*

Issues. Advances in Archaeological and Museum Science 1. Plenum Press. New York, pp 65 – 81.

Oberholster, R.E. 1968. Opal phytoliths in two soil profiles on the Springbok Flats. *South African Journal of Agricultural Science* 11: 743 – 748.

O'Connor, T.G. and Bredenkamp, G.J. 1997. Grassland. In: R.M. Cowling, D.M. Richardson and S.M. Pierce (eds), *Vegetation of southern Africa*, pp 215 – 257. Cambridge University Press. Cambridge.

Oldfield, F. and Thompson, R. 2004. Archives and proxies along the PEP III transect. In: R.W. Battarbee, F. Gasse and C.E. Stickley (eds). *Past Climate Variability through Europe and Africa*. Springer. Dordrecht, The Netherlands, pp 7-23.

Ollendorf, A.L. 1987. Archaeological implications of a phytolith study at Tel Miqne (Ekron), Israel. *Journal of Field Archaeology* 14: 453 – 463.

Palmer, P.G., 1976. Grass cuticles: a new palaeoecological tool for East African lake sediments. *Canadian Journal of Botany* 54 (15): 1725 – 1734.

Parr, J.F., Lentfer, C.J. and Boyd, W.E. 2001. A comparative analysis of wet and dry ashing techniques for the extraction of phytoliths from plant material. *Journal of Archaeological Science* 28: 875 – 886.

Partridge, T. C., deMenocal, P. B., Lorentz, S. A., Paiker, M. J. & Vogel, J. C. 1997. Orbital forcing of climate over South Africa: a 200,000-year rainfall record from the Pretoria Saltpan. *Quaternary Science Reviews* 16, 1125-1133.

Partridge, T. C., Scott, L. and Schneider, R. 2004. Between Agulhas and Benguela: responses of South African climates of the Late Pleistocene to current fluxes,

orbital precession and the extent of the Circum-Antarctic vortex. In: R.W. Battarbee, F. Gasse and C.E. Stickley (eds). *Past Climate Variability through Europe and Africa*. Springer. Dordrecht, The Netherlands, pp 45-64.

Pearsall, D.M. 1982. Phytoliths analysis: Applications of a new palaeoethnobotanical technique in archaeology. *American Anthropologist* 84: 862 – 871.

Pearsall, D.M. and Trimble, M.K. 1984. Identifying past agricultural activity through soil phytolith analysis: a case study from the Hawaiian Islands. *Journal of Archaeological Science* 11: 119 – 133.

Pearsall, D.M., Chandler-Ezell, K., Chandler-Ezell, A. 2003. Identifying maize in neotropical sediements and soils using cob phytoliths. *Journal of Archaeological Science* 30: 611- 627.

Pearsall, D.M., Chandler-Ezell, K. Zeidler, J.A. 2004. Maize in ancient Ecuador: results of residue analysis of stone tools from the Real Alto site. *Journal of Archaeological Science* 31: 423 – 442.

Piperno, D. R., 1984. A comparison and differentiation of phytoliths from maize and wild grasses: use of morphological criteria. *American Antiquity* 49 (2): 361 – 383.

Piperno, D. R. 1988. Phytolith analysis: an archaeological and geological perspective. Academic Press. London.

Piperno, D. R. (2006). Phytoliths: a comprehensive guide for archaeologists and paleoecologists. Altamira Press, New York.

Piperno, D. R. 1989. The occurrence of phytoliths in the reproductive structures of selected tropical angiosperms and their significance in tropical paleoecology,

paleoethnobotany and systematics. *Review of Palaeobotany and Palinology* 61: 147 – 173.

Piperno, D. R., 2003. A few kernels short of a cob: on the Staller and Thompson late entry scenario for the introduction of maize into northern South America. *Journal of Archaeological Science* 30: 831 – 836.

Piperno, D. R. and Pearsall D.M. 1993. Phytolith structures in the reproductive structures of maize and teosinte: implications for the study of maize evolution. *Journal of Archaeological Science* 20: 337 – 362.

Piperno, D. R. and Sues, H. 2005. Dinosaurs dined on grass. *Science* 310: 1126 – 1128.

Powers, A.H., Padmore, J. and Gilbertson, D.D. 1989. Studies of Late Prehistoric and modern opal phytoliths from coastal sand dunes and machair in northwest Britain. *Journal of Archaeological Science* 16: 27 - 45.

Powers-Jones, A.H. & Padmore, J. 1993. The use of quantitative methods and statistical analyses in the study of opal phytoliths. In: D.M. Pearsall & D.R. Piperno (eds). *Current research in phytolith analysis: applications in archaeology and paleoecology. MASCA, Research Papers in Science and Archaeology Vol. 10.* University of Pennsylvania, Philidelphia.

Prasad, V., Stromberg, C.A.E., Alimohammadian, H. and Sahni, A. 2005. Dinosaur coprolites and the early evolution of grasses and grazers. *Science* 310: 1177 – 1180.

Rebelo, A.G., Boucher, C., Helme, N. Mucina, L. and Rutherford, M.C. 2006. Fynbos Biome. In: L. Mucina and M.C. Rutherford (eds.) 2006. The vegetation of South

Africa, Lesotho and Swaziland. *Strelitzia* 19: 1 – 807. National Botanical Institute, Pretoria.

Reed, K.E. 1997. Early hominid evolution and ecological change through the African Plio-Pleistocene. *Journal of Human Evolution* 32: 289 – 322.

Reed, K.E. 1998. Using large mammal communities to examine ecological and taconomic structure and predict vegetation in extant and extinct assemblages. *Paleobiology* 24: 384 – 408.

Reinhard, K.J. and Danielson, D.R. 2005. Pervasivenes of phytoliths in prehistoric southwestern diet and implications for regional and temporal trends for dental microwear. *Journal of Archaeological Science* 32: 981 – 988.

Renvoize, S.A. 1981. The subfamily Arundinoideae and its position in relation to the general classification of the Gramineae. *Kew Bulletin* 36: 85 – 102.

Retallack, G.J. 1992. Middle Miocene fossil plants from Fort Ternan (Kenya) and evolution of African grasslands. *Paleobiology* 18 (4): 383 – 400.

Retallack, G.J. 2001. Cenozoic expansion of grasslands and climate cooling. *Journal of Geology* 109: 407 – 426.

Retallack, G.J., Dugas, D.P. and Bestland, E.A. 1990. Fossil soils and grasses of a Middle Miocene East African grassland. *Science* 247: 1325 – 1328.

Rossouw, L. 2006. Florisian mammal fauna from dongas in the Modder River drainage, central Free State, South Africa. *Navorsinge van die Nasionale Museum, Bloemfontein.*

Rovner, I. 1971. Potential of opal phytoliths for use in palaoecological reconstruction. *Quaternary Research* 1: 343 – 359.

Rovner, I. 1983. Plant phytolith analysis: major advances in archaeobotanical research. *Advances in Archaeological Method and Theory* 6: 225 – 266.

Rovner, I. 1988. Macro- and micro-ecological reconstruction using plant opal phytolith data from archaeological sediments. *Geoarchaeology* 3 (2): 155 – 163.

Rovner, I. 1994. Floral history by the back door: A test of phytolith analysis in residential yards at Harpers Ferry. *Historical Archaeology* 28 (4): 37 – 48.

Runge, F. 1999. The opal phytolith inventory of soils in central Africa – quantities, shapes, classification, and spectra. *Review of Palaeobotany and Palynology* 107: 23 – 53.

Russ, J.C. and Rovner, I. 1989. Stereological identification of opal phytolith populations from wild and cultivated *Zea. American Antiquity* 54 (4): 784 – 792.

Rutherford, M.C. 1997. Categorization of biomes. In: R.M. Cowling, D.M. Richardson and S.M. Pierce (eds), *Vegetation of southern Africa*, pp 91 – 98. Cambridge University Press. Cambridge.

Rutherford, M.C. and Westphall, R.H. 1994. Biomes of Southern Africa: an objective categorization. *Memoirs of the Botanical Survey of South Africa, 63*. National Botanical Institute.

Rutherford, M.C., Mucina, L. and Powrie, L.W. 2006a. Biomes and Bioregions of Southern Africa. In L. Mucina and M.C. Rutherford (eds.) The vegetation of South

Africa, Lesotho and Swaziland. *Strelitzia* 19: 1 – 807. National Botanical Institute, Pretoria.

Rutherford, M.C., Mucina, L., Lotter, M., Bredenkamp, G.J., Smit, J.H.L.,Scott-Shaw, C.R. *et al*. 2006b. Savanna Biome. In: L. Mucina and M.C. Rutherford (eds). The vegetation of South Africa, Lesotho and Swaziland. *Strelitzia* 19: 1 – 807. National Botanical Institute, Pretoria.

Sage, R.F. 2004. The evolution of C4 photosynthesis. *New Phytologist* 161: 341 – 370.

Sage, R.F. and Monson, R.K. 1999. The taxonomic distribution of C_4-photosynthesis. In R.F. Sage and R.K. Monson (eds.) *C_4 Plant Biology* Academic Press. San Diego, USA.

Simpson, G.G. 1970. Uniformitarianism: an inquiry into principle, theory, and method in geohistory and biohistory. In: M.K. Hecht and W.C. Steere (eds.) *Essays in evolution and genetics in honour of Theodosius Dobzhansky.* Pp 43 – 96. New York.

Scholtz, A. 1985. Palynology of the Upper Cretaceous lacustrine sediments of the Arnot pipe, Banke, Namaqualand. *Annals of the South African Museum*, 95: 1-109.

Schultz, R.E. 1997. Climate. In: R.M. Cowling, D.M. Richardson and S.M. Pierce (eds.) *Vegetation of Southern Africa*. Cambridge University Press. Cambridge. Pp. 21 - 42

Schultz, E.D., Ellis R., Schultz, W, Trimborn, P. and Ziegler, H. 1996. Diversity, metabolic types and δ ^{13}C carbon isotope ratios in the grass flora of Namibia in

relation to growth form, precipitation and habitat conditions. *Oecologia* 106: 352 – 369.

Scott, L., 1995. Pollen evidence for vegetational and climate change during the Neogene and Quaternary in Southern Africa. In: Vrba E., Denton, G., Partridge, T.C., and Burckle, L.H., (eds)., *Paleoclimate and Evolution with Emphasis on Human Origins*. Yale University Press. Yale. Pp. 65-76.

Scott, L. 1999a. Palynological analysis of the Pretoria Saltpan (Twaing Crater) sediments and vegetation history of the Bushveld Savanna Biome, South Africa. In: Partridge (ed.) *Tswaing – Investigations into the origin, age and palaeoenvironments of the Pretoria Saltpan*. Council for Geosciences, Pretoria, pp 143 – 166.

Scott, L. 1999b. The vegetation history and climate in the Savanna Biome, South Africa, since 190000 KA: A comparison of pollen data from the Tswaing Crater (the Pretoria Saltpan) and Wonderkrater. *Quaternary International* 57-58: 215-223.

Scott, L. 2002. Grassland development under glacial and interglacial conditions in southern Africa: review of pollen, phytolith and isotope evidence. *Palaeogeography, Palaeoclimatology, Palaeoecology* 177 (1-2): 47 – 58.

Scott, L. & Lee-Thorp, J. A. 2004. Holocene climatic trends and rhythms in Southern Africa. In**:** Battarbee R.W., Gasse F., and Stickley C.E. (eds). *Past Climate Variability through Europe and Africa.* Springer. Dordrecht, The Netherlands, pp 69-87.

Scott, L, Steenkamp M and Beaumont P B 1995. Palaeoenvironmental conditions in South Africa at the Pleistocene-Holocene transition. *Quaternary Science Reviews* (Global Younger Dryas Issue) 14 (9): 937-947.

Shaw, P. A. and Thomas, D. S. G. 1996. The Quaternary palaeoenvironmental history of the Kalahari, Southern Africa. *Journal of Arid Environments* 32: 9-22. Smithson, F. 1958. Grass opal in British soils. *Journal of soil science*. 9: 148.

Stromberg, C. A. E. 2002. The origin and spread of grassland-dominated ecosystems in the late Tertiary of North America: preliminary results concerning the evolution of hypsodonty. *Palaeogeography, Palaeoclimatology, Palaeoecology* 177 (1-2): 59 – 76.

Stromberg, C. A. E. 2004. Using phytolith assemblages to reconstruct the origin and spread if grass-dominated habitats in the great plains of North America during the late Eocene to early Miocene. *Palaeogeography, Palaeoclimatology, Palaeoecology* 207: 239 – 275.

Stromberg, C. A. E. 2005. Decoupled taxonomic radiation and ecological expansion of open-habitat grasses in the Cenozoic of North America. *Proceedings of the National Academy of Science* 102 (34): 11980 – 11984.

Suess, E. 1966. *Opal phytoliths*. Kansas State University M.S. thesis, 74p.

Thorn, V.C. 2004a. Phytolith evidence for C_4-dominated grassland since the early Holocene at Long Pocket, northeast Queensland, Australia. *Quaternary Research* 61: 168 – 180.

Thorn, V.C. 2004b. An annotated bibliography of phytolith analysis and atlas of selected New Zealand Subantarctic and Subalpine phytoliths. *Antarctic Data Series* 29: 1 – 67.

Tsartsidou, G., Lev-Yadun, S., Albert, R.M., Miller-Rosen, A., Efstratiou, N. and Weiner, S. 2006. The phytolith archaeological record: strengths and weaknesses

evaluated based on a quantitive modern reference collection from Greece. *Journal of Archaeological Science* 34, 1262-1275.

Twiss, P.C.1992. Predicted world distribution of C_3 and C_4 grass phytoliths. In: G.Rapp Jr. and S.C. Mulholland (eds). Phytolith Systematics. Emerging Issues. Advances in Archaeological and Museum Science 1: 113 – 128. Plenum Press.

Twiss, P.C., Suess, E. and Smith, R.M. 1969. Morphological classification of grass phytoliths. *Proceedings of the Soil Science Society of America* 33: 109 – 115.

Vogel, J.C., Fuls, A and Ellis, R.P. 1978. The geographical distribution of Krantz grasses in South Africa. *South African Journal of Science* 74: 209 – 215.

Van Couvering, J.A.H. 1980. Community evolution in Africa during the Cenozoic. Pp 272 – 298. In A.K. Behrensmeyer and A. Hill (eds.) *Fossils in the making*. University of Chicago Press, Chicago.

Vrba, E.S. 1995. The fossil record of African antelopes (Mammalia, Bovidae) in relation to human evolution and paleoclimate. In**:** E.S. Vrba (ed.). *Paleoclimate and evolution, with emphasis on human origins.* Yale University Press. New Haven, Yale University, pp. 385-424.

Wallis, L.A. 2001. Environmental history of northwest Australia based on phytolith analysis at Carpenter's Gap 1. *Quaternary International* 83-85: 103 – 117

Webb, E.A and Longstaff, F.J. 2006. Identifying the δ18O signature of precipitation in grass cellulose and phytoliths: refining the paleoclimate model. *Geochemica et Cosmochimica Acta* 70: 2417 – 2426.

White, F. 1983. The Vegetation of Africa: A descriptive memoir to accompany UNESCO/AETFAT/UNSO vegetation maps of Africa. Paris: UNESCO.

Wooller, M.J. and Beuning, K.R. 2002. Introduction to the reconstruction and modelling of grass-dominated ecosystems. *Palaeogeography, Palaeoclimatology, Palaeoecology* 177 (1-2): 1-3.

Wynn Parry, D. and Smithson, F. 1958. Silicification of bulliform cells in grasses. *Nature* 181: 1549 – 1550.

Wynn Parry, D. and Smithson, F. 1964. Types of opaline silica depositions in the leaves of British Grasses. *Annals of Botany* 28 (109): 169 – 185.

Zinderen Bakker, E.M., van, 1984. Palynological evidence for Late Cenozoic arid conditions along the Namib coast from Holes 532 and 530A, Leg 75, Deep Sea Drilling Project. *Initial Reports of the Deep Sea Dilling Project* 75: 763 – 768.

Zinderen Bakker, E.M., van, 1989. Middle Stone Age palaeoenvironments at Florisbad (South Africa), *Palaeoecology of Africa* 20: 133-154.

Zinderen Bakker, E. M., van, 1995. Archaeology and palynology. *South African Archaeological Bulletin* 162: 98-105.

APPENDICES

Appendix 1: Atlas of GSSC-phytoliths extracted from grass leaves.

Appendix 2: Atlas of 227 grass leaf epidermis slide vouchers.

Appendix 3: Indicator matrix of GSSC-morphotypes recorded in 309 grass species.

Appendix 4: Spearman's rank-order correlation between association through rate of recurrence of morphotypes and relative abundance of morphotypes.

Appendix 5: Basic statistics of the number of GSSC-morphotypes counted for each GSSC-morphotype subcategory.

Appendix 6: GSSC-phytolith abundance as a proportion of all morphotypes per category.

Appendix 7: Basic statistics of the number of GSSC-morphotypes counted for each subfamily subcategory.

Appendix 8: Subfamily: Tukey's HSD test for unequal sample sizes.

Appendix 9: Basic statistics of the number of GSSC-morphotypes counted for each photosynthetic pathway subcategory, including C_4 subtypes.

Appendix 10: Tukey's HSD test for unequal sample sizes in the Photosynthetic pathway-category (including C_3 and C_4).

Appendix 11: Tukey's HSD test for unequal sample sizes in the photosynthetic pathway - category (C_4 only).

Appendix 12: Basic statistics of the number of GSSC-morphotypes counted for each Rainfall subcategory.

Appendix 13: Tukey's HSD test for unequal sample sizes in the Rainfall-category

Appendix 14: Basic statistics of the number of GSSC-morphotypes counted for each habitat subcategory.

Appendix 15: Tukey's HSD test for unequal sample sizes in the Habitat-category.

Appendix 16: Comparison of GSSC-phytoliths against three Palaeoenvironmental Scenarios.

Appendix 1: Atlas of GSSC-phytoliths extracted from grass leaves.

Five-centimeter leaf sections were removed from voucher specimens of mature individuals housed at the herbarium of the Department of Botany at the National Museum in Bloemfontein, the National Herbarium of Pretoria and the Bolus Herbarium at the University of Cape Town. Standard dry-ashing procedures were followed to extract phytoliths from the five-centimeter leaf sections (Piperno 1988; Parr *et al.* 2001). Parr *et al*. (2001) has demonstrated that the dry ashing technique produces less residual plant matter than the wet-ashing technique with no detectible evidence of morphological impact caused by the former method. The leaf sections were rinsed with distilled water, transferred to crucibles and burnt in a furnace at 500°C for 6 h. The burnt residue was treated with 10%HCl and centrifuged (@ 2500 rpm for 5 minutes), re-suspended in distilled water and centrifuged again. The supernatant was discarded and the silica residue placed on microslides, mounted in silicon oil for rotation and finally in a rigid medium (DPX Mountant) for permanent storage. Photographs were taken at X400 and X1000 magnification with a digital camera mounted on a 50i Nikon polarizing light microscope. GSSC-phytoliths are presented as composites of several photomicrographs. Scale bar = 10 micron.

List of subfamilies and genera illustrated in Appendix 1.

Subfamily	Tribe
Aristidoideae	Aristideae
Arundinoideae	Arundineae
Bambusoideae	Bambuseae
Chloridoideae	Cynodonteae Eragrostideae Pappophoreae
Danthionioideae	Danthonieae
Ehrhartoideae	Ehrharteae Oryzeae
Panicoideae	Andropogoneae Arundinelleae Paniceae
Pooideae	Aveneae Brachypodieae Bromeae Meliceae Poeae Stipeae Triticeae

Aristidoideae
Tribe: Aristideae

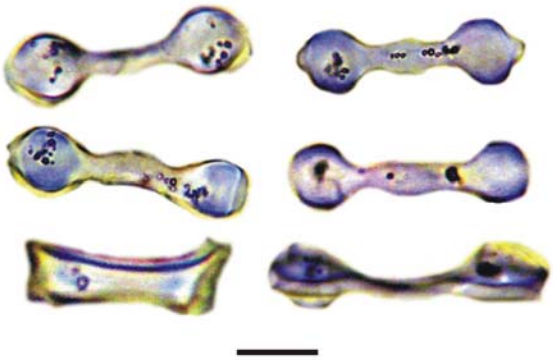

Aristida adscensionis

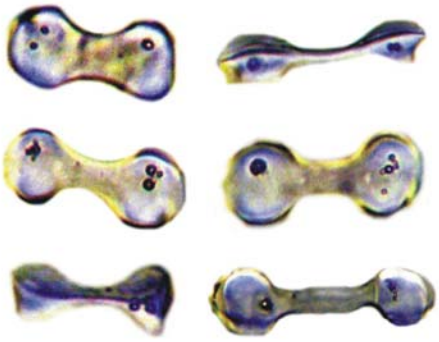

Aristida congesta

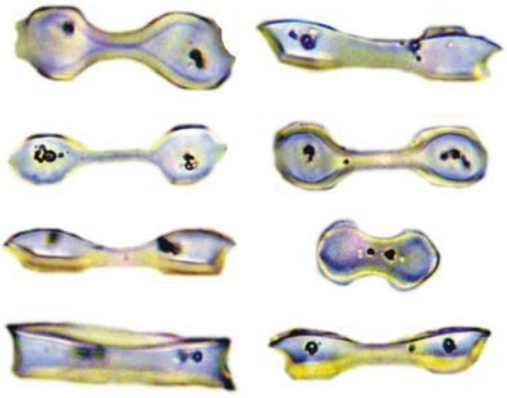

Aristida diffusa

Aristida junciformis

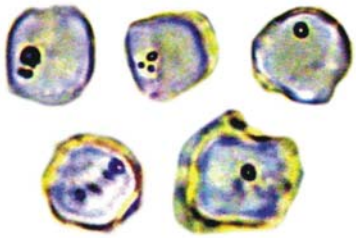

Stipagrostis obtusa

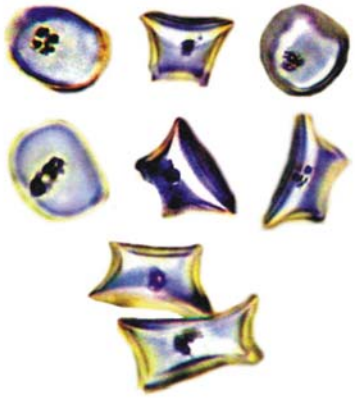

Stipagrostis namaquensis

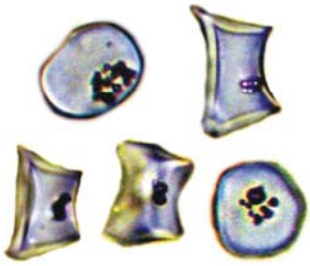

Stipagrostis uniplumis

Arundinoideae
Tribe: Arundineae

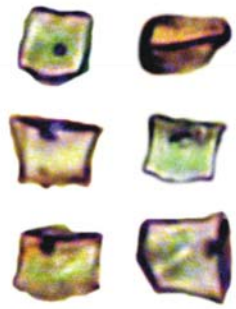

Dregechloa calviniensis

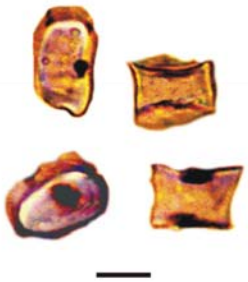

Dregechloa pumila

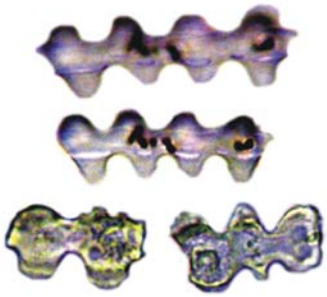

Elytrophorus globularis

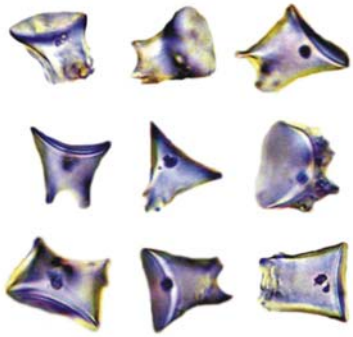

Phragmites australis

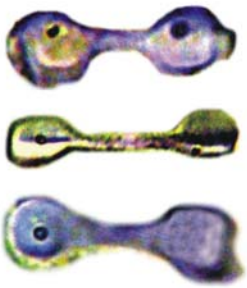

Styppeiochloa gynoglossa

Bambusoideae
Tribe: Bambuseae

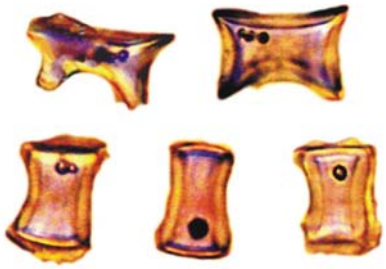

Bambusa vulgaris

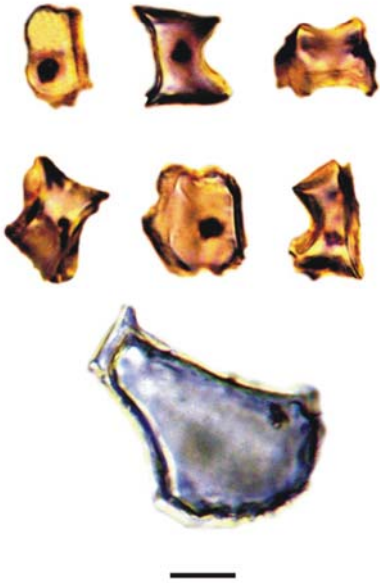

Thamnocalamus tessellatus

Olyra latifolia

Chloridoideae
Tribe: Cynodonteae

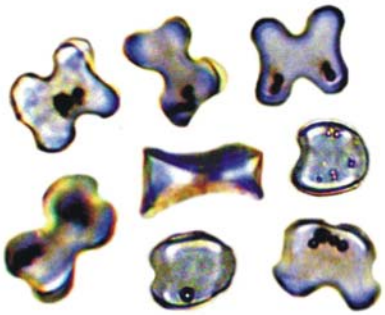

Catalepis gracilis

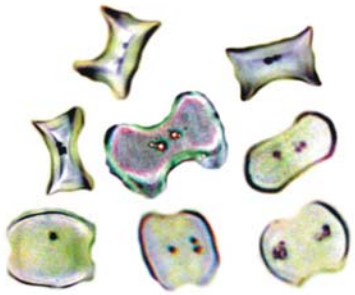

Chloris gayana

Chloris pycnothrix

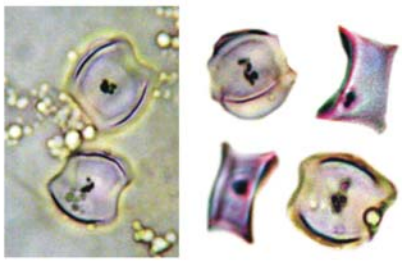

Chloris virgata

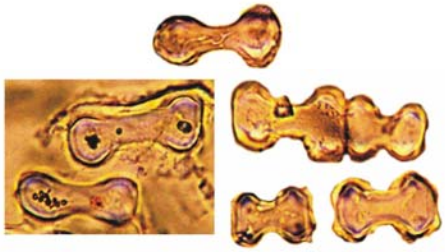

Ctenium concinnum

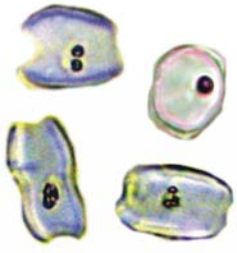

Cynodon dactylon

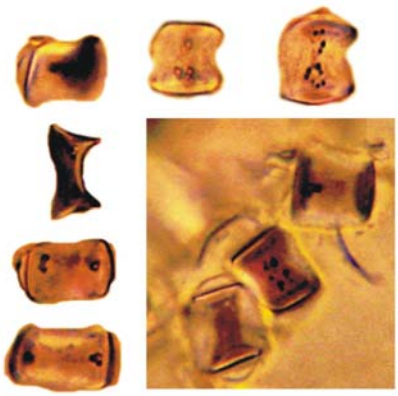

Enteropogon machrostachys

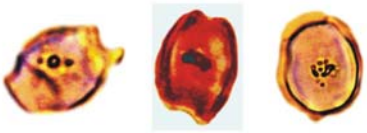

Eustachys mutica

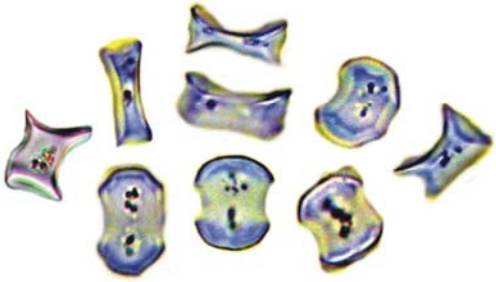

Eustachys paspaloides

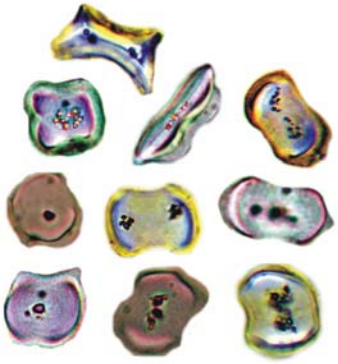

Harpochloa falx

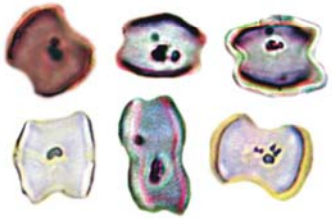

Michrochloa caffra

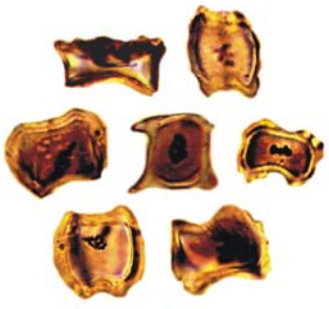

Michrochloa kunthii

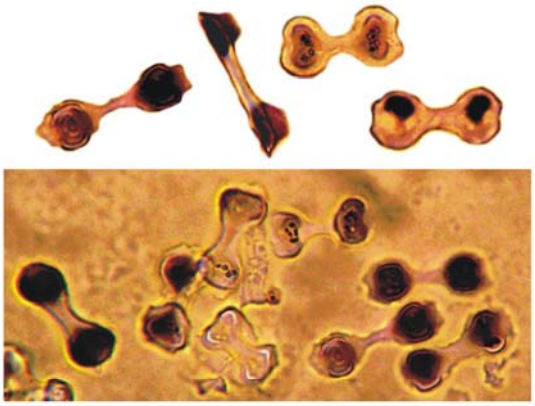

Perotis indica

Perotis patens

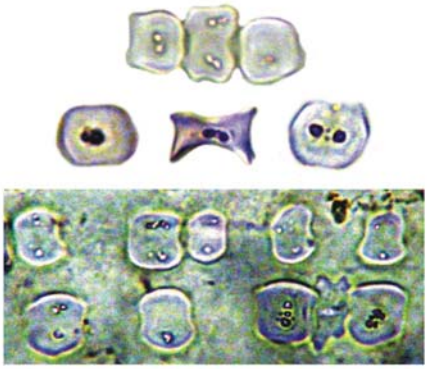

Polevansia rigida

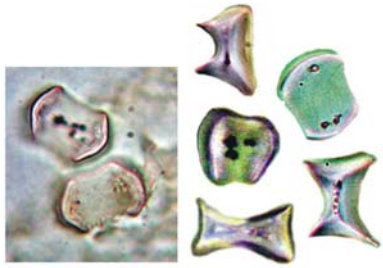

Rendlia altera

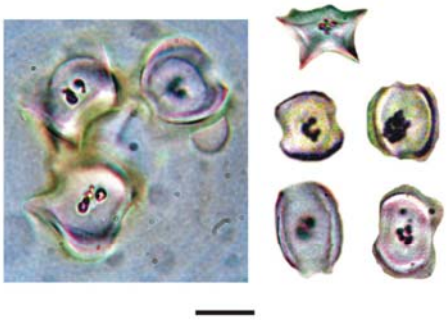

Tragus berteronianus

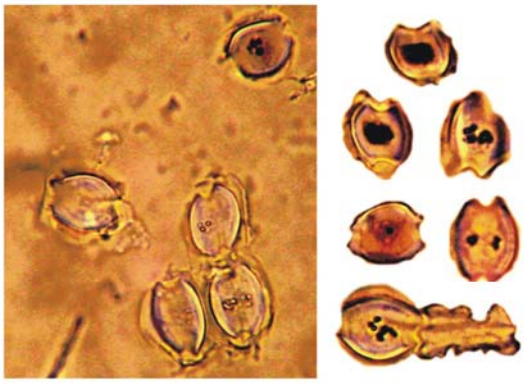

Tragus koeleroides

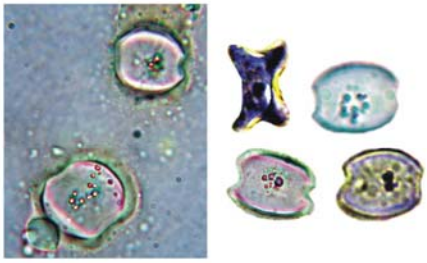

Tragus racemosus

Chloridoideae
Tribe: Eragrostideae

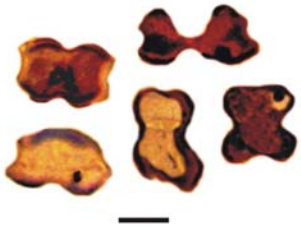

Acrachne racemosa

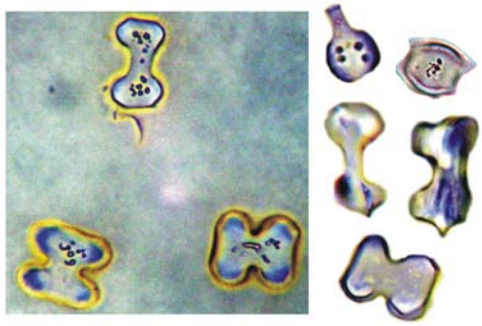

Bewsia biflora

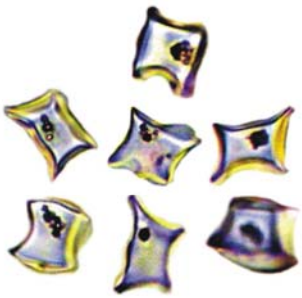

Cladoraphis spinosa

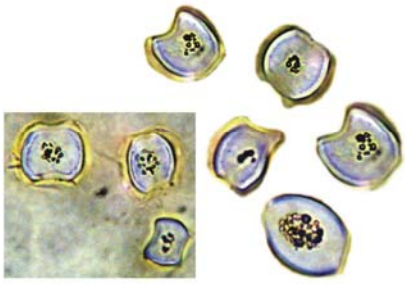

Coelachyrum yemenicum

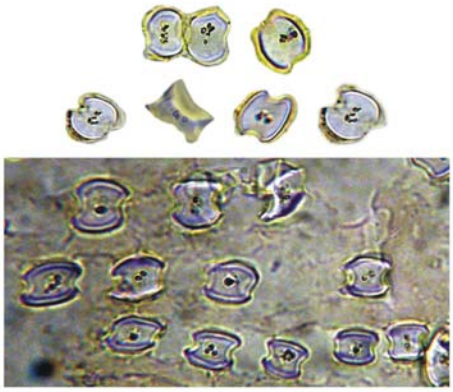

Dactyloctenium australe

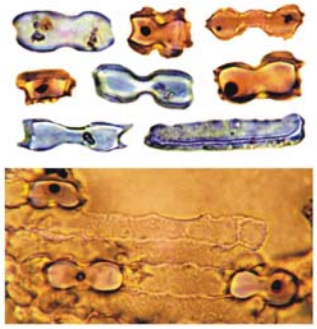

Diandrochloa namaquensis

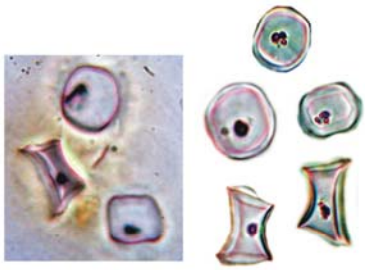

Dinebra retroflexa

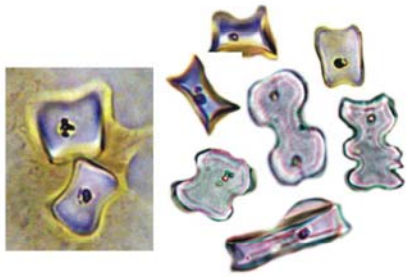

Diplachne fusca

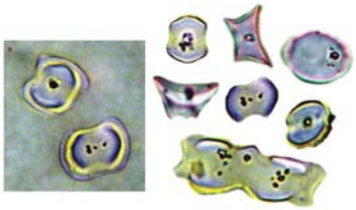

Eleusine coracana

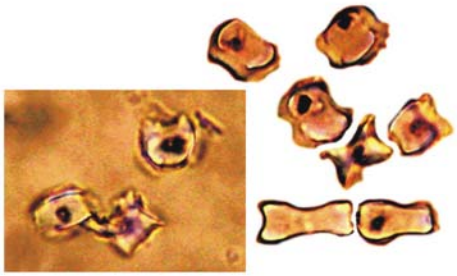

Eragrostis bicolor

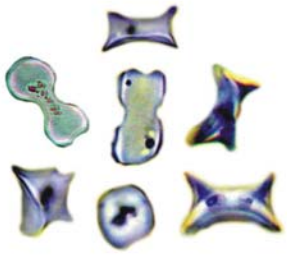

Eragrostis capensis

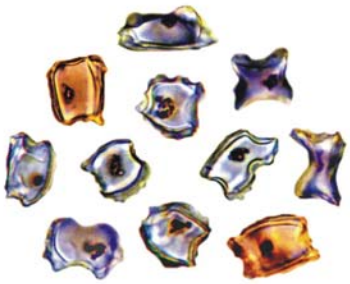

Eragrostis chloromelas

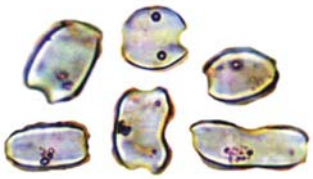

Eragrostis denudata

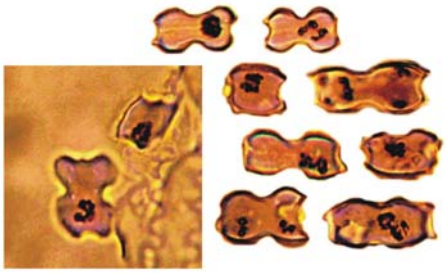

Eragrostis macrochlamys (138)

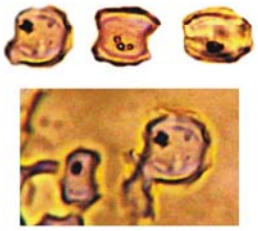

Eragrostis micrantha

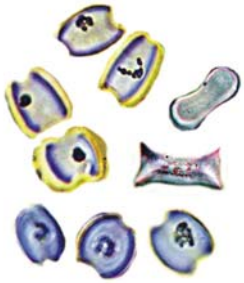

Eragrostis obtusa

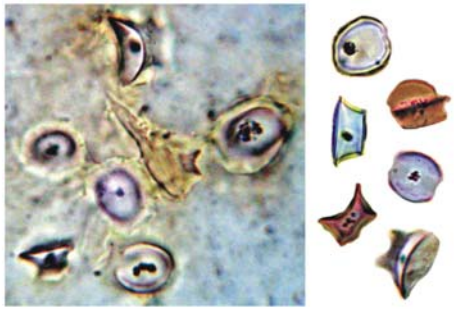

Fingerhuthia africana

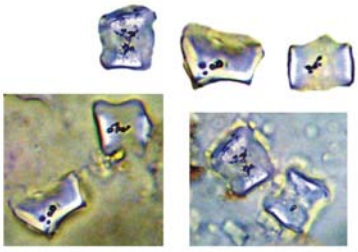

Oropetium capense

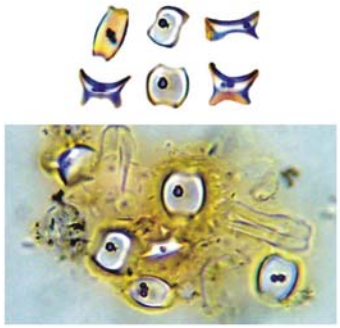

Pogonarthria squarrosa

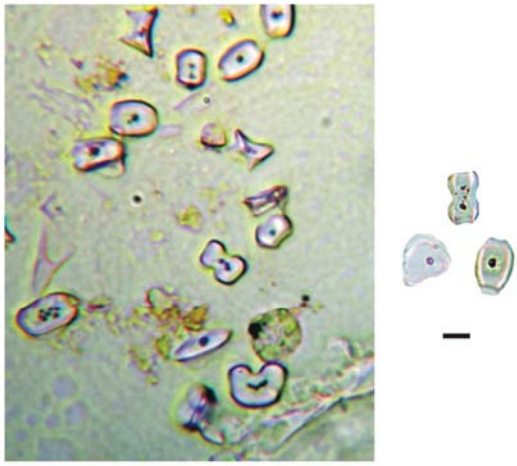

Sporobolus africanus

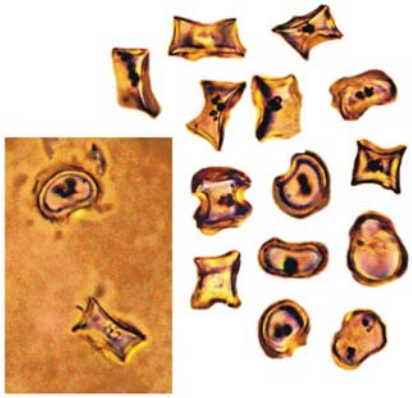

Sporobolus filifolius

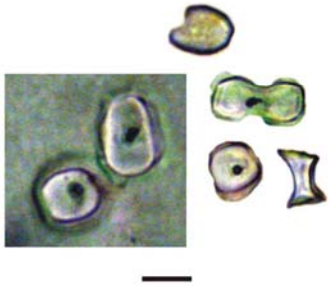

Sporobolus fimbriatus

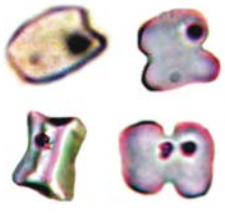

Stiburus alopecuroides

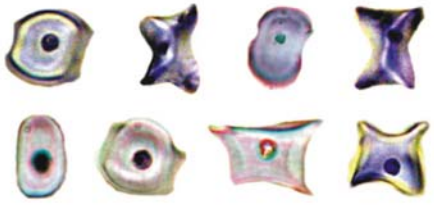

Tetrachne dregei

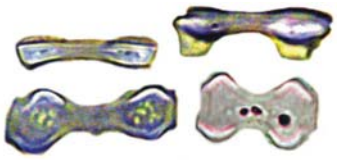

Trichoneura grandiglumis

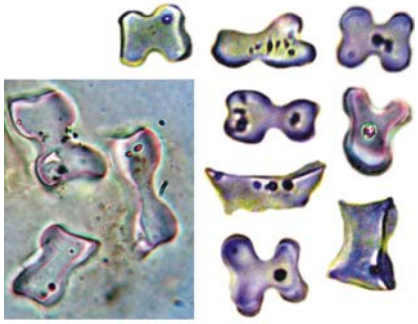

Triraphis andropogonoides

Chloridoideae
Tribe: Pappophoreae

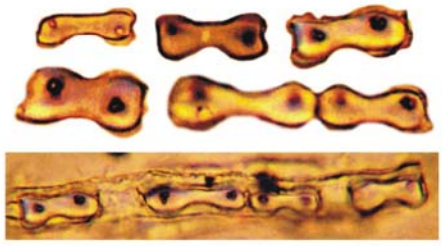

Enneapogon desvauxi

Enneapogon scaber

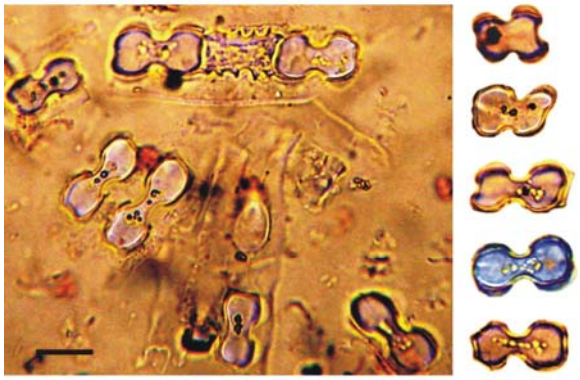

Schmidtia bulbosa

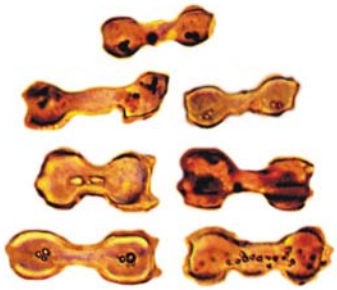

Schmidtia kalahariensis

Schmidtia pappophoroides

Danthionioideae

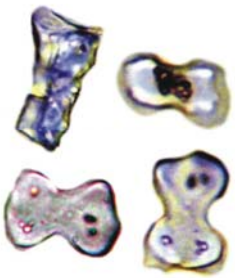

Centropodia glauca

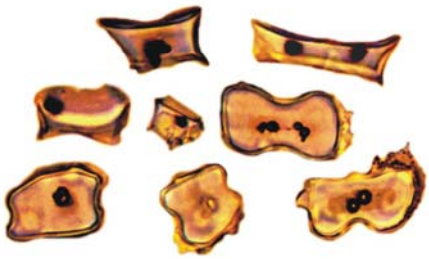

Chaetobromus dregeanus

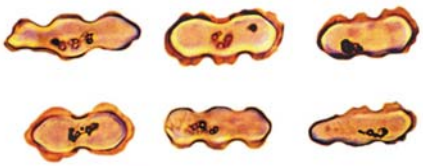

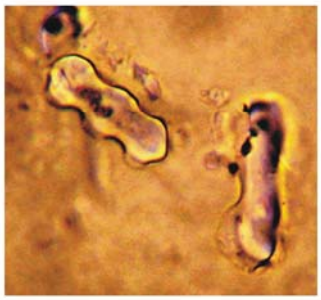

Chaetobromus involucratus

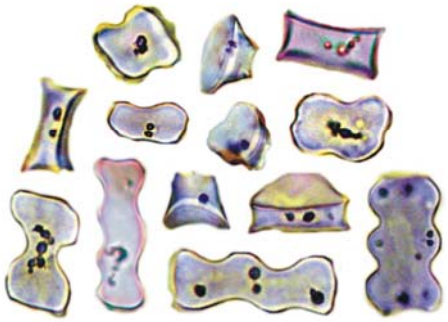

Karroochloa curva

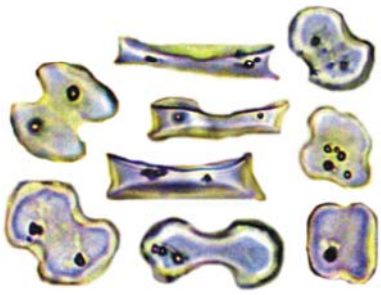

Karoochloa purpurea

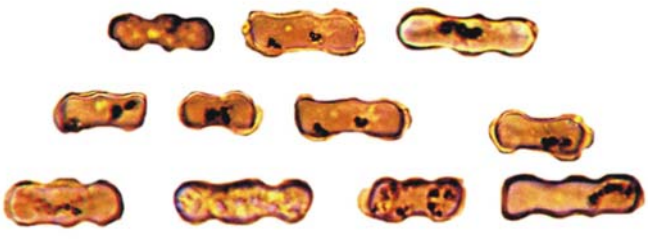

Karroochloa schismoides

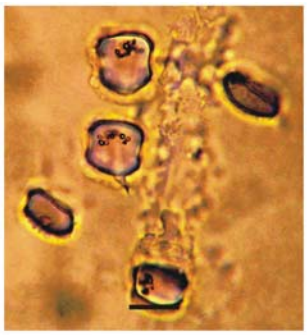

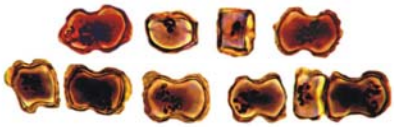

Karroochloa tenella

Merxmuellera lupulina

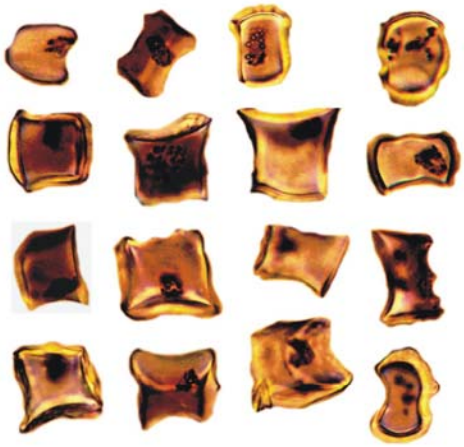

Merxmuellera rufa

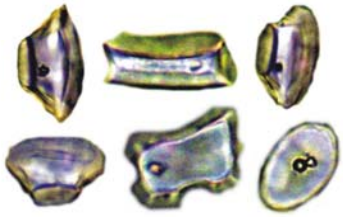

Merxmuellera stricta

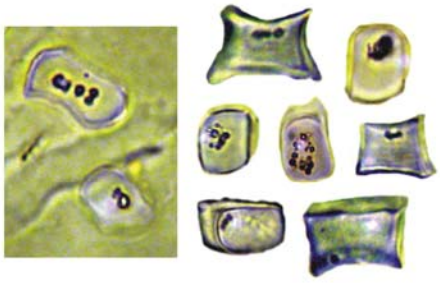

Pentaschistis ancifolia

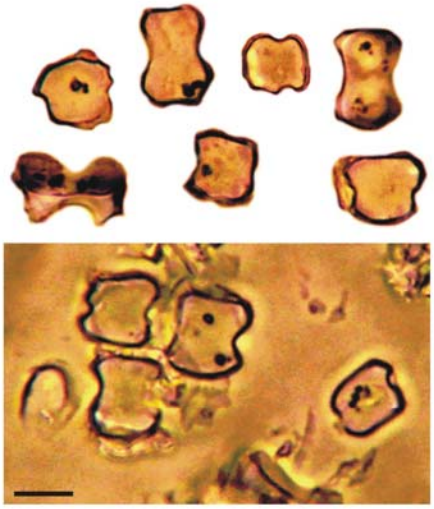

Pentaschistis colerata

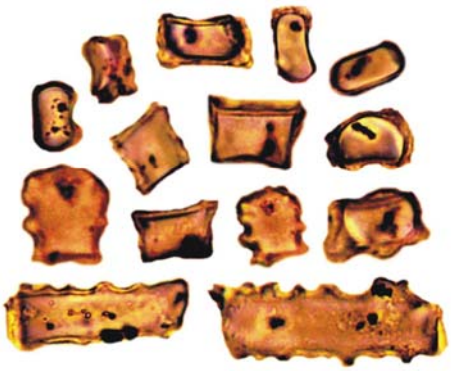

Pentaschistis curvifolia

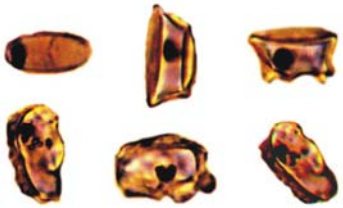

Pentameris longiglumis

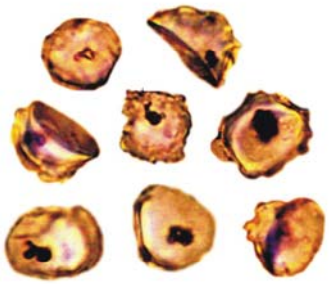

Pentameris macrocalycina

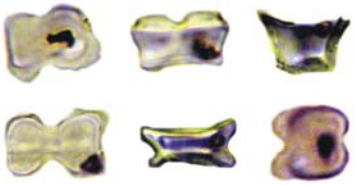

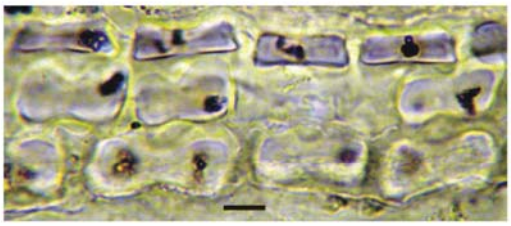

Pseudopentameris brachyphylla

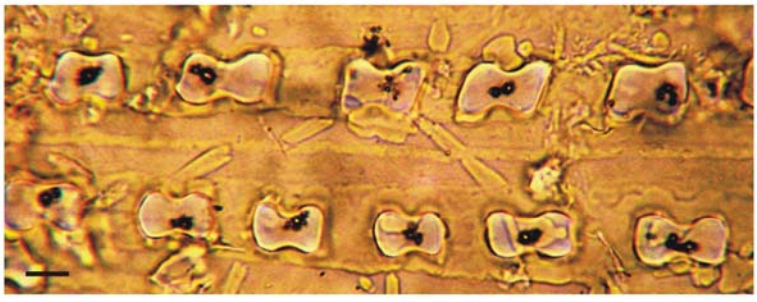

Pseudopentameris macrantha

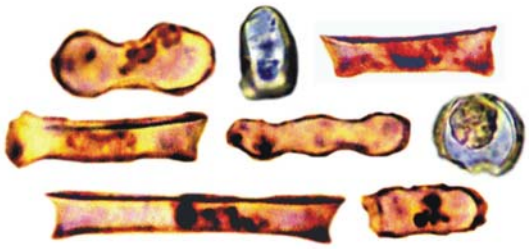

Schismus barbatus

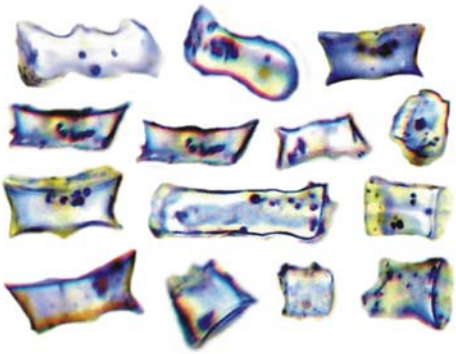

Schismis inermus

Tribolium uniolae

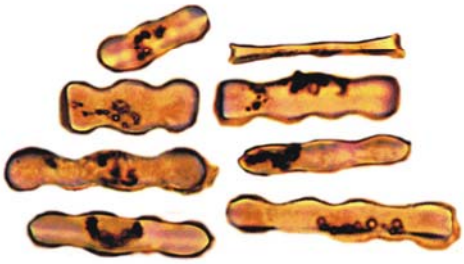

Urochlaena pussilla

Ehrhartoideae
Tribe: Ehrharteae

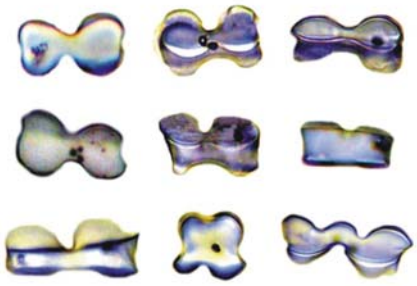

Ehrharta bulbosa

Ehrharta calycina

Ehrharta delicutula

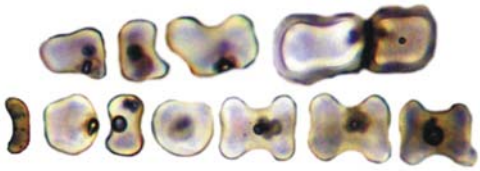

Ehrharta longiflora

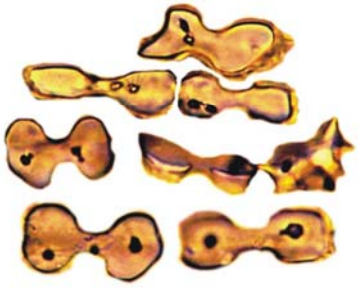

Ehrharta microlaena

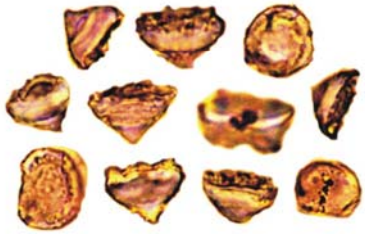

Ehrharta ramosa

Ehrharta rehmanni

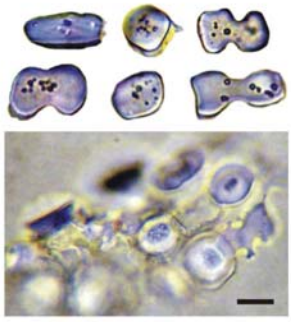

Ehrharta thunbergi

Ehrhartoideae
Tribe: Oryzeae

Leersia hexandra

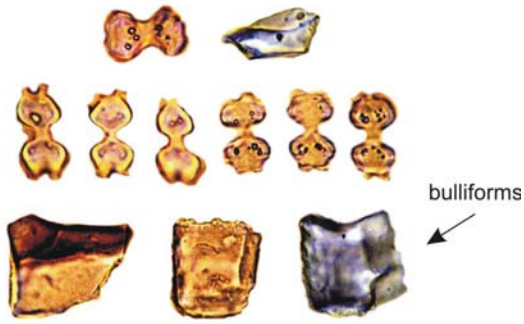

Oryza longistaminata

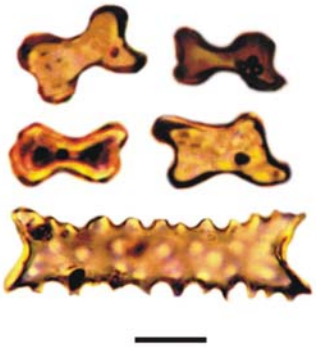

Prosphytochloa prehensilis

Panicoideae
Tribe: Andropogoneae

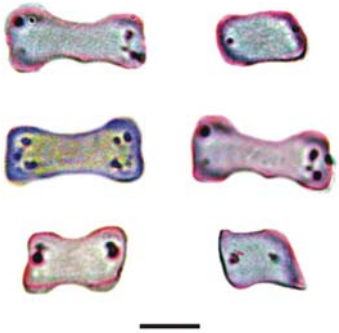

Andropogon appendiculatus

Andropogon eucomis

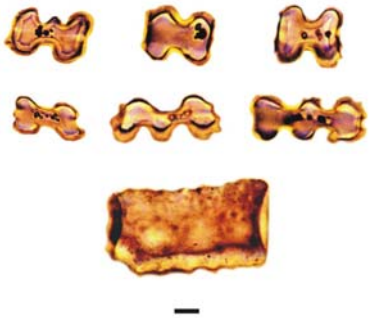

Bothriochloa insculpta

Bothriochloa bladhii

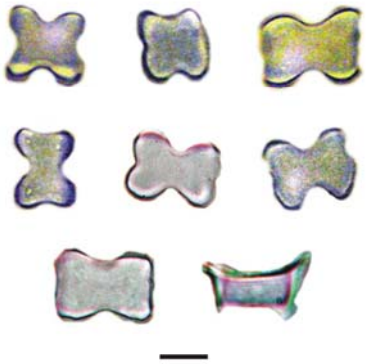

Cymbopogon plurinoides

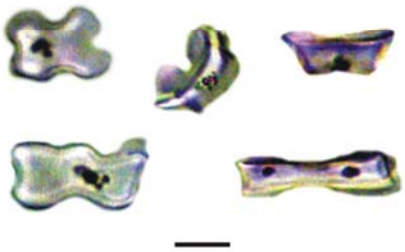

Eulalia villosa

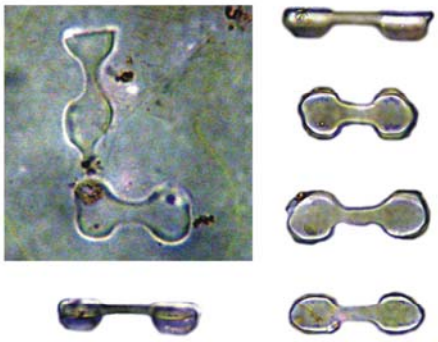

Heteropogon contortus

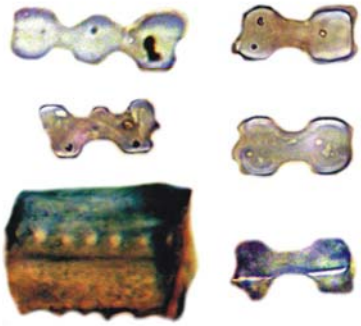

Hyperhenia hirta

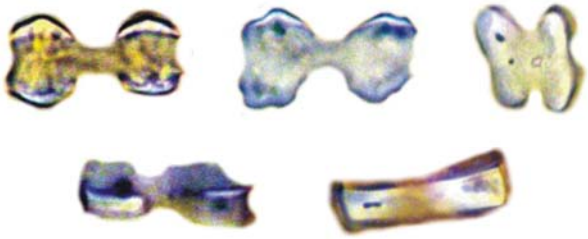

Imperata cylindrica

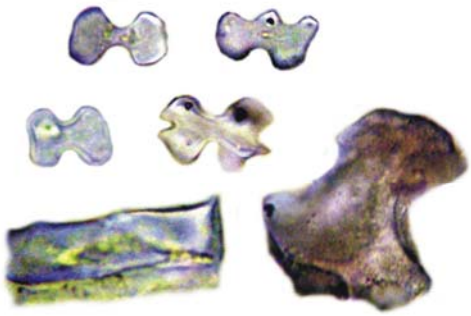

Sorghum bicolor

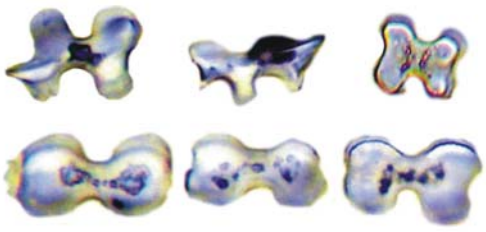

Sorghum caffrorum

Themeda triandra

Trachypogon spicatus

Panicoideae
Tribe: Arundinelleae

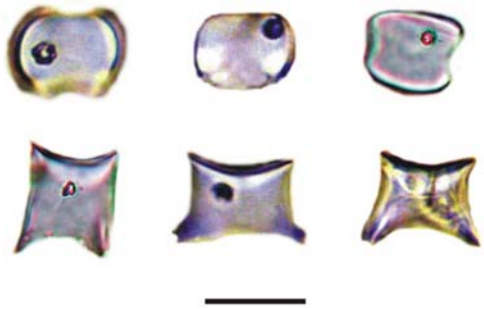

Arundinella nepalensis

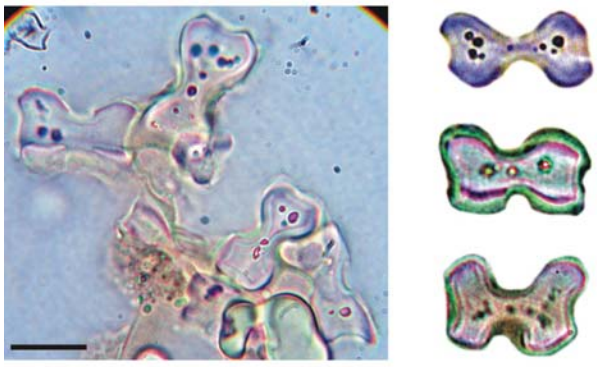

Tristachya leucothrix

Panicoideae
Tribe: Paniceae

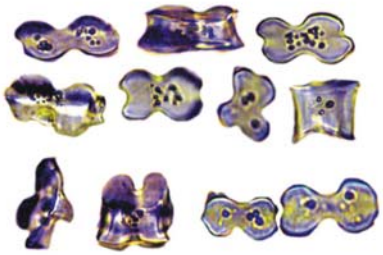

Acroceras macrum

Anthephora pubescens

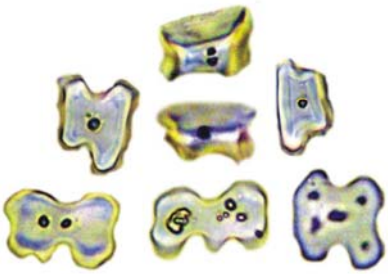

Brachiaria serrata

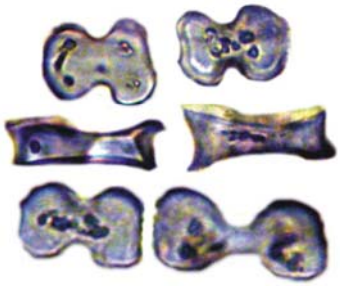

Cenchrus ciliaris

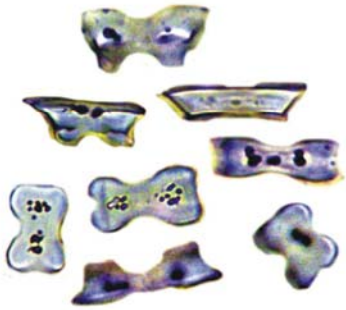

Digitaria eriantha

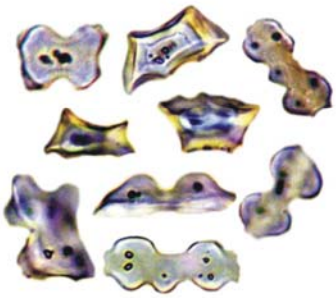

Echinochloa crus-galli

Melenis repens

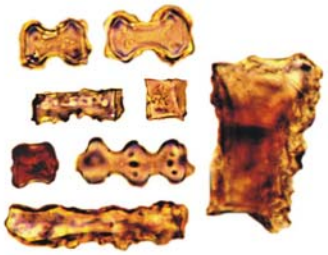

Oplismenus hirtellus

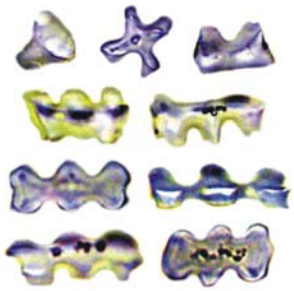

Oplismenus undulatifolius

Panicum coloratum

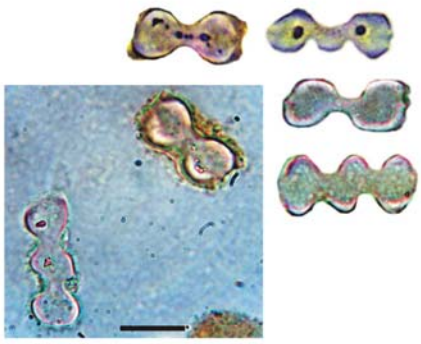

Panicum maximum

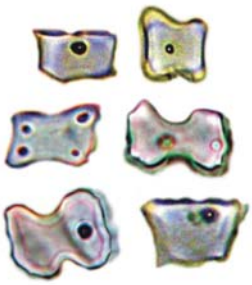

Panicum stapfianum

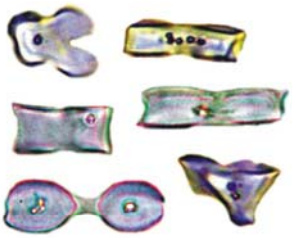

Paspalum dilatatum

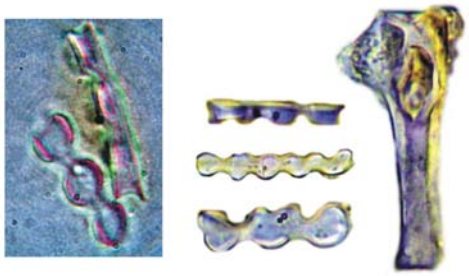

Paspalum distichum

Pooideae
Tribe: Aveneae

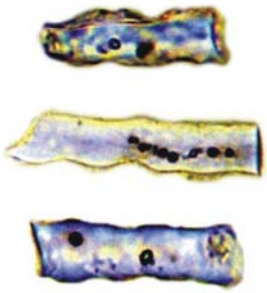

Agrostis holgateana

Agrostis lachnanta

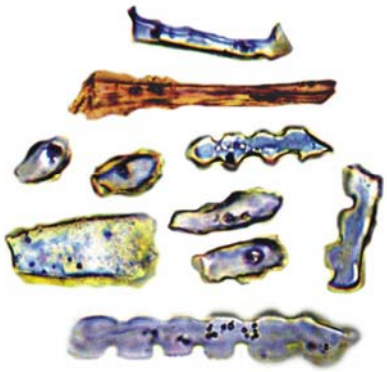

Agrostis media

Ammophila arenaria

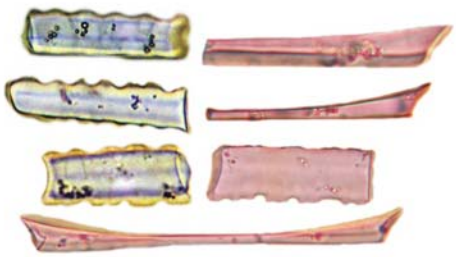

Anthoxanthum ecklonii

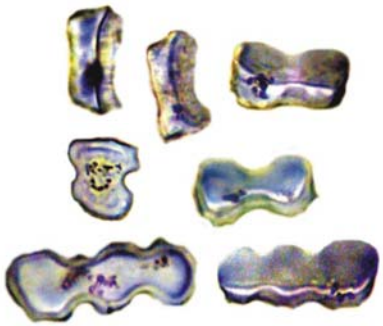

Calamagrostis epigeios

Gastridium phleiodes

Helictotrichon capense

Helictotrichon hirtulum

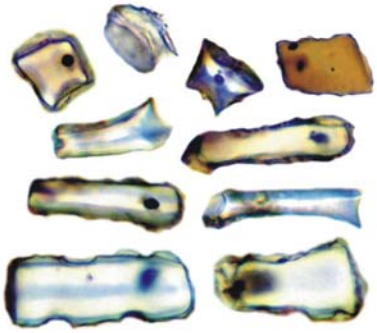

Helictotrichon longum

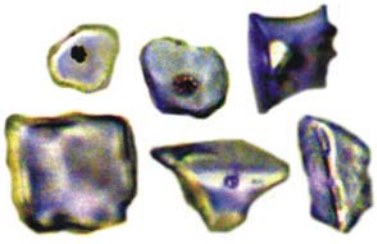

Holcus setiger

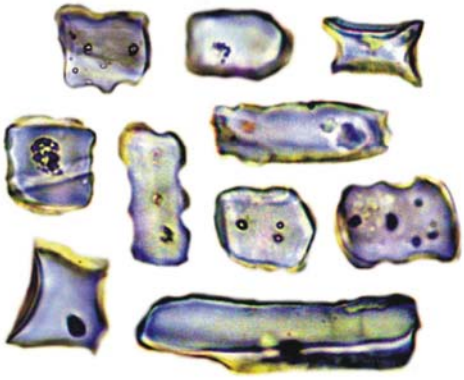

Koeleria capensis

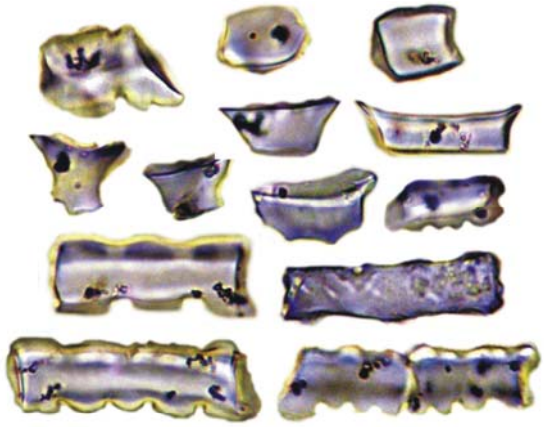

Polypogon strictus

Pooideae
Tribe: Brachypodieae

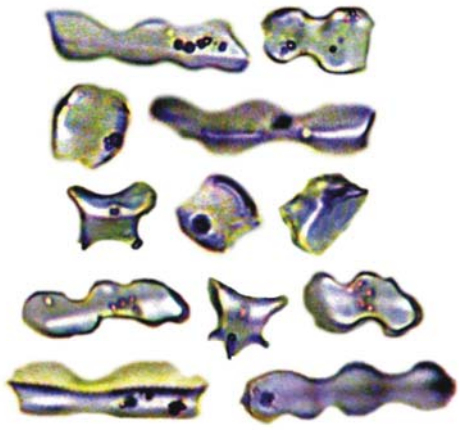

Brachypodium flexum

Pooideae
Tribe: Bromeae

Bromus commutatus

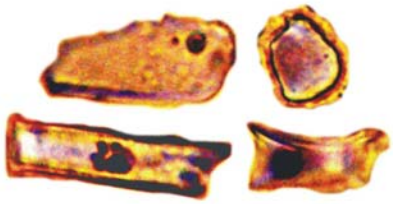

Bromus pectinatus

Bromus rigidus

Pooideae
Tribe: Meliceae

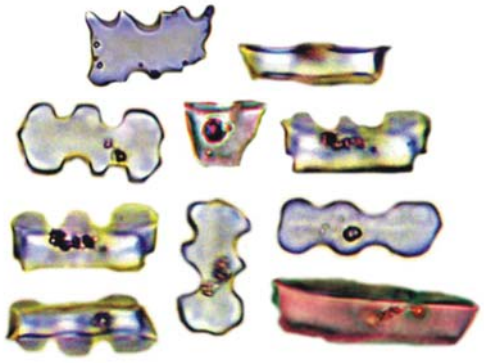

Melica racemosa

Pooideae
Tribe: Poeae

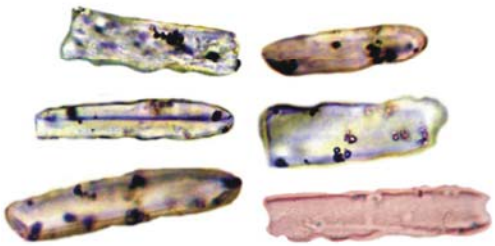

Briza maxima

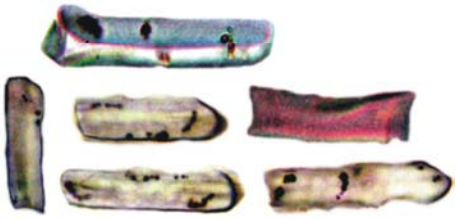

Briza minor

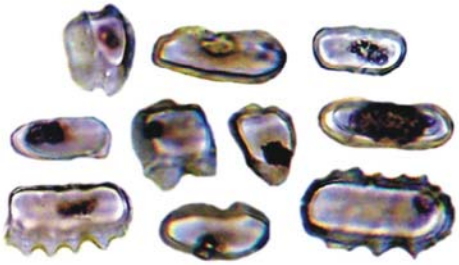

Festuca eliator

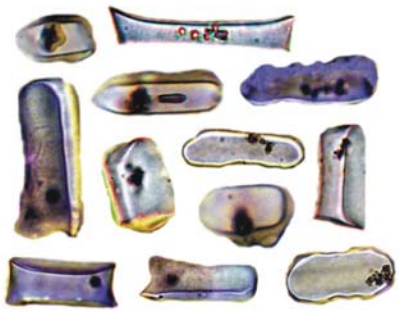

Festuca scabra

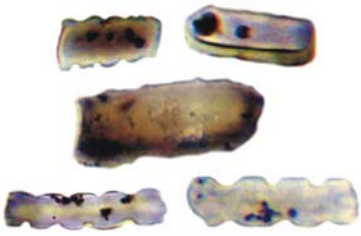

Poa annua

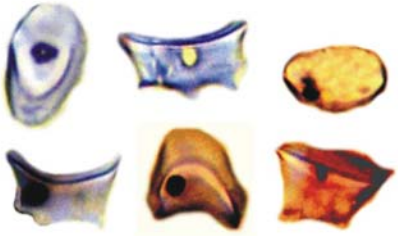

Puccinellia acroxantha

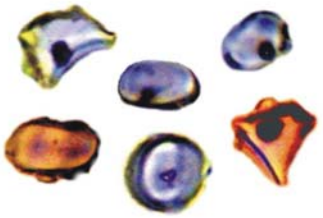

Puccinellia fasciculata

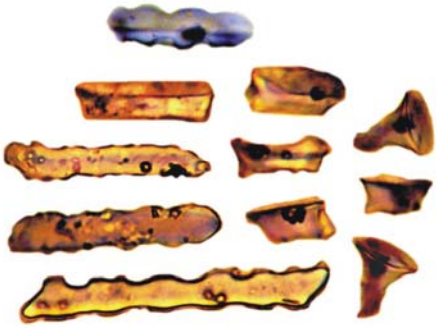

Vulpia bromoides

Pooideae
Tribe: Stipeae

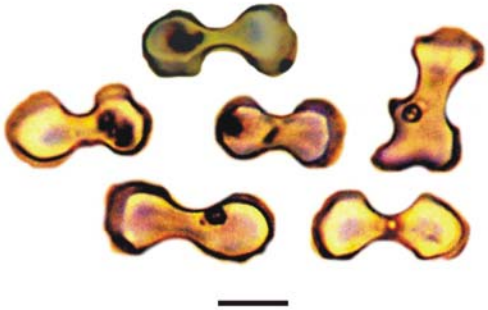

Stipa capensis

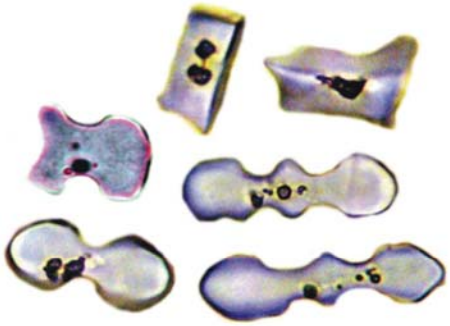

Stipa dregeana

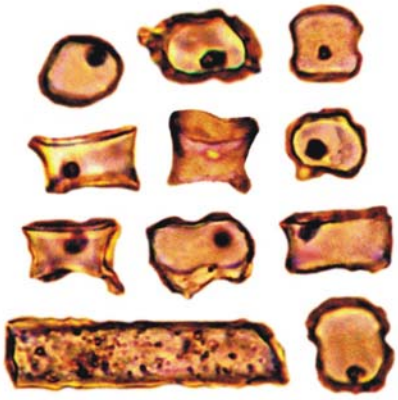

Stipa papposa

Pooideae
Tribe: Triticeae

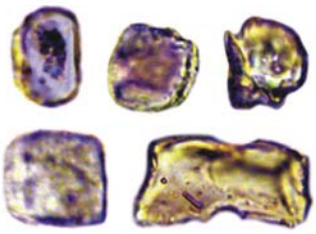

Secale africanum

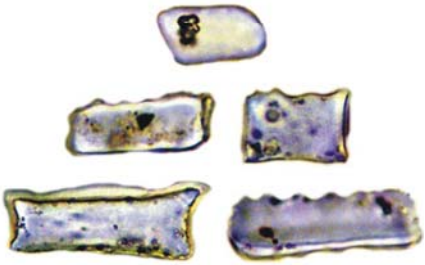

Hordeum capense

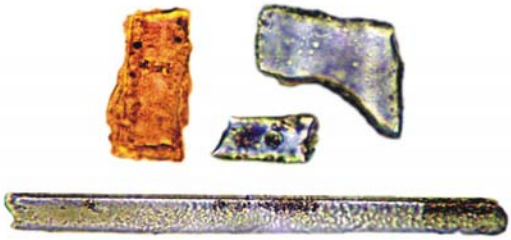

Thinopyrum distichum

Appendix 2: Atlas of 227 grass leaf epidermis slide vouchers.

The collection consists of prepared slide vouchers of fully articulated grass leaf epidermis sections from the Roger Ellis collection housed at the National Herbarium of Pretoria. Photographs were taken with a digital camera mounted on a polarizing light microscope (x160 and x400 magnification). The photomicrographs are listed in alphabetical order with the species name, followed by the name of the collector, collection number, reference number in parenthesis and details regarding habitat-requirements of each species.

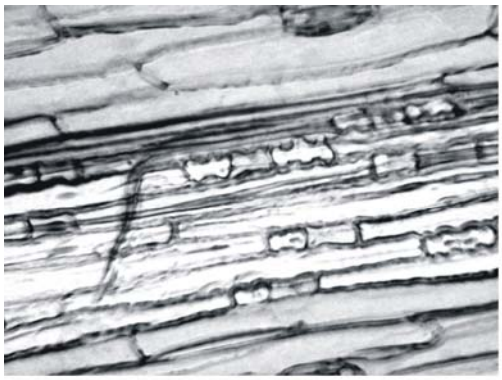

Agrostis barbuligera Ellis 5710 (7786)
Mountain grassland

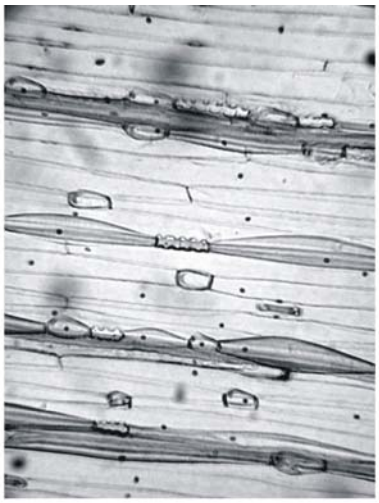

Agrostis bergiana Ellis 5698 (7788)
Mountain grassland, wet places

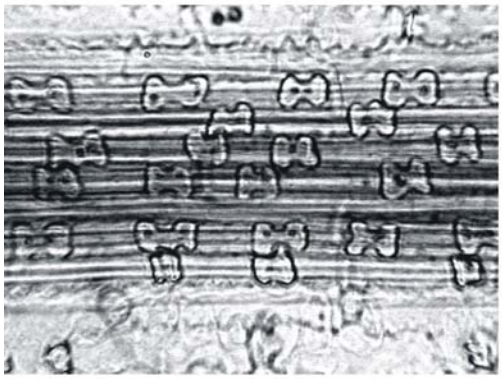

Alloteropsis semialata Saayman
24 (8191) Grassland, bushveld

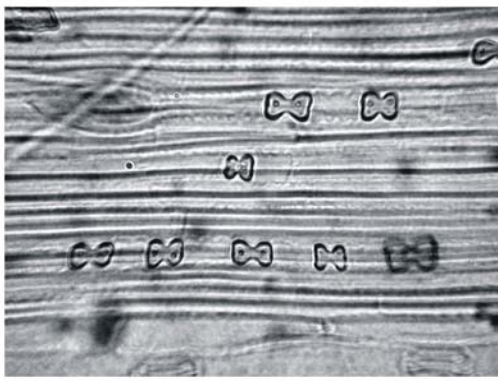

Andropogon appendiculatus Ellis 94
(8195) Wet, shady places

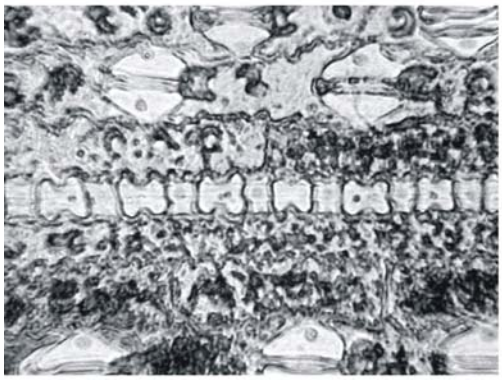

Andropogon gayanus Ellis 3690
(8197) Bushveld

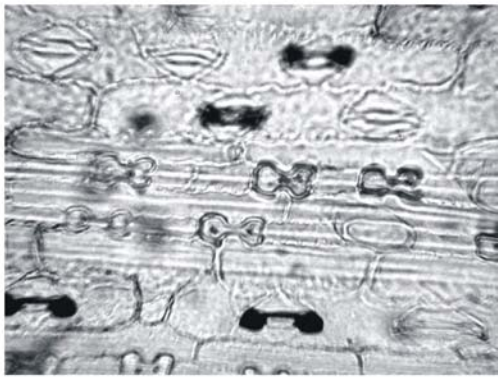

Andropogon huillensis De Wet 967
(8200) Wet places, sand

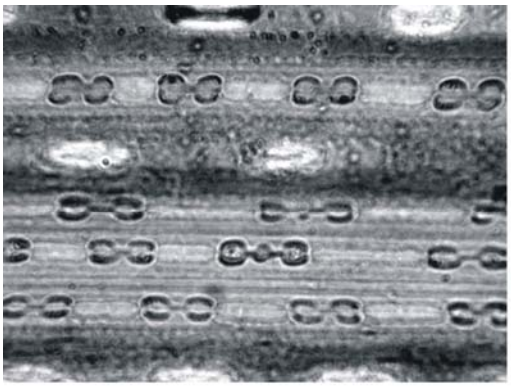

Andropogon laconosus Ellis 2814
(8201) Swampy places, high alt.

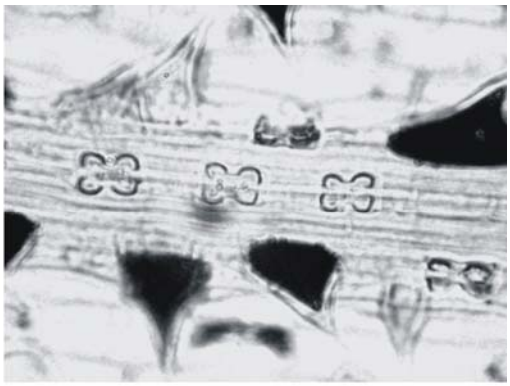

Anthephora argentea Ellis 877
(8207) Sandy soil, Kalahari.

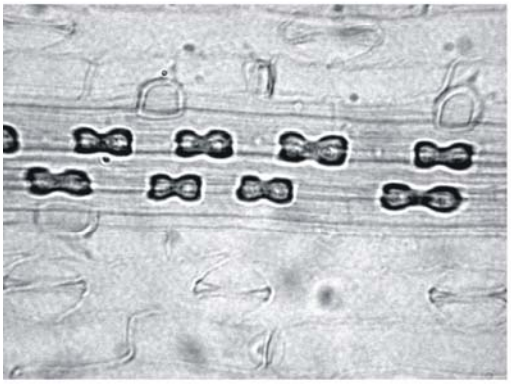

Anthephora pubescens Ellis 1758 (8209)
Acid, sandy soils, hillsides.

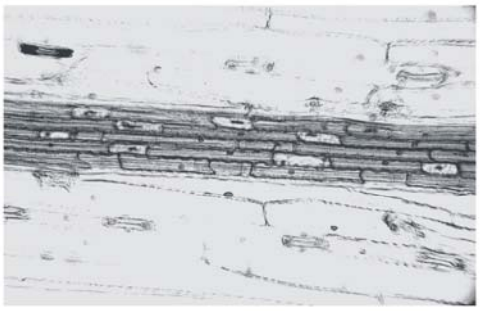

Anthoxanthum dregeanum Ellis 5494
(7795) Moist mountainslopes.

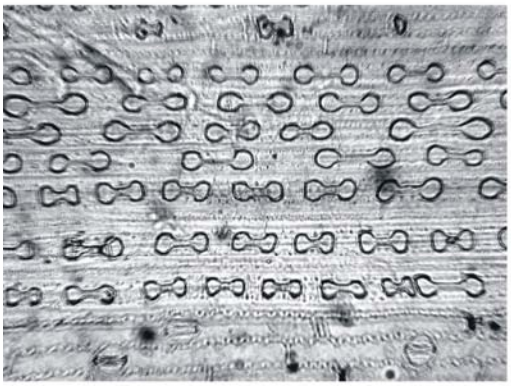

Aristida bipartita Ellis 285 (8036)
Moist areas, vleis.

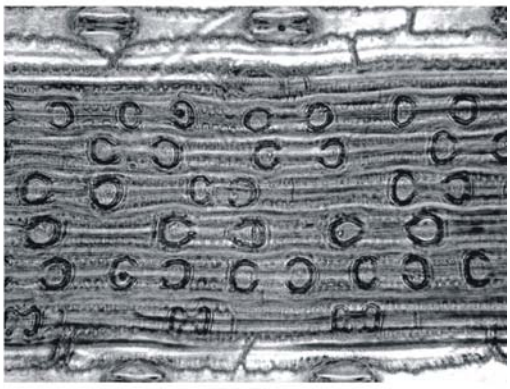

Aristida canescens subs. canescens Acocks
11424 (8038) Stony soils, rocky ridges.

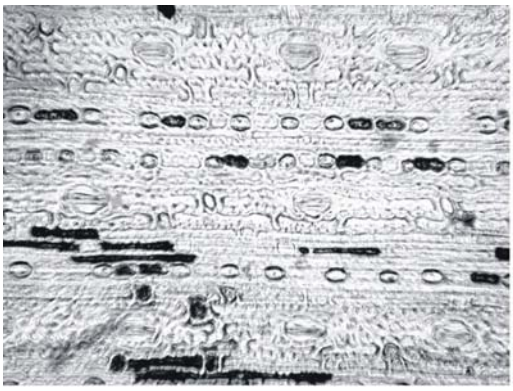

Aristida dasydesimis Pearson De Winter 3487 (8040) Granite slopes, arid areas.

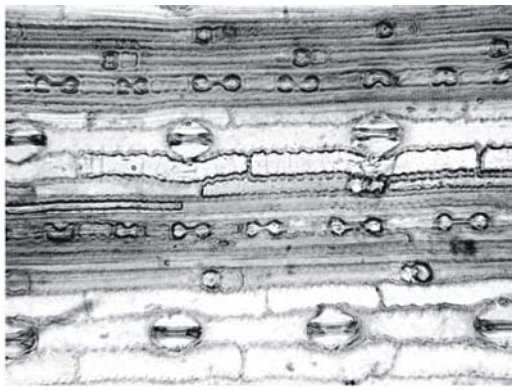

Aristida engleri Polevans De Winter 80 (8044) Rocky outcrops.

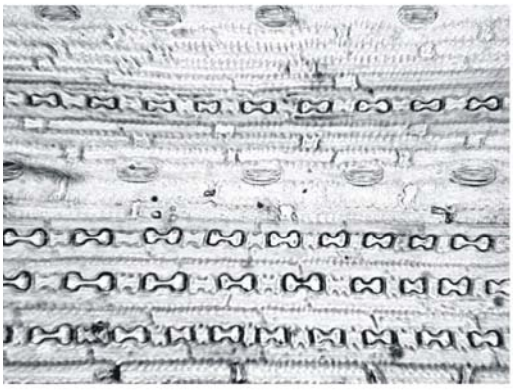

Aristida junciformis subs. galpinii Galpin De Winter 6900 (8046) High mountain terrain.

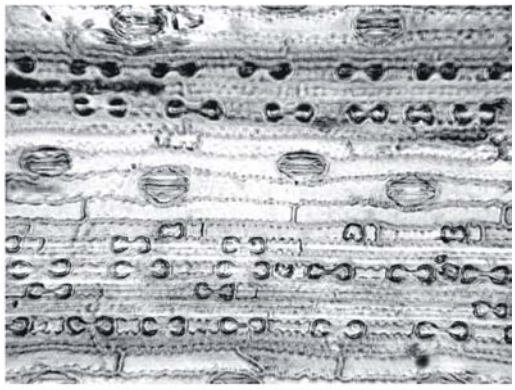

Aristida monticola Mogg De Winter 120634 (8048) Stream banks, mountain slopes.

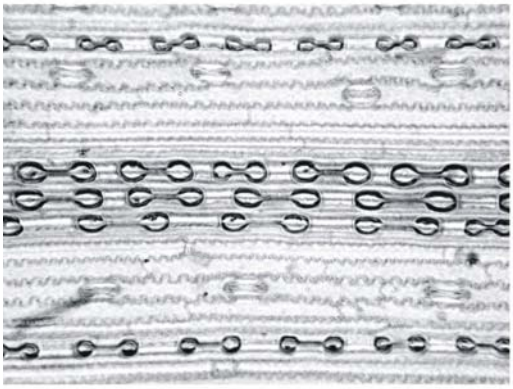

Aristida parvula De Winter 3474 (8050) Plains, along water courses.

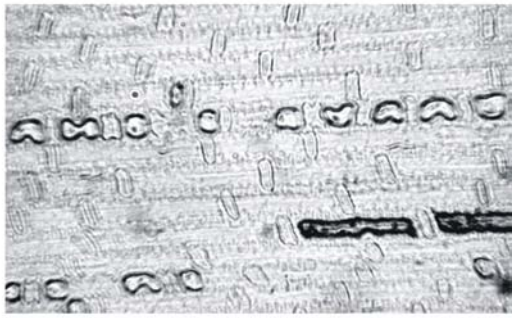

Aristida scuirus Pentz Acocks 10314 (8052) Moist sandy soils, mountain sourveld.

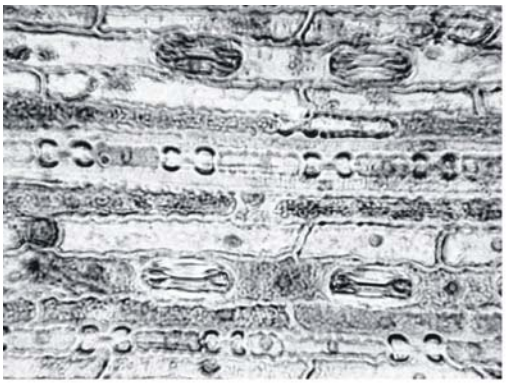

Bothriochloa bladhii Ellis 4473 (8214)
Riverbanks, vleis.

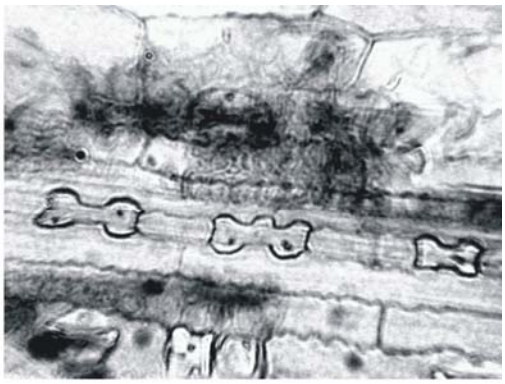

Bothriochloa insculpta Ellis 497 (8211)
Grassland, hillsides.

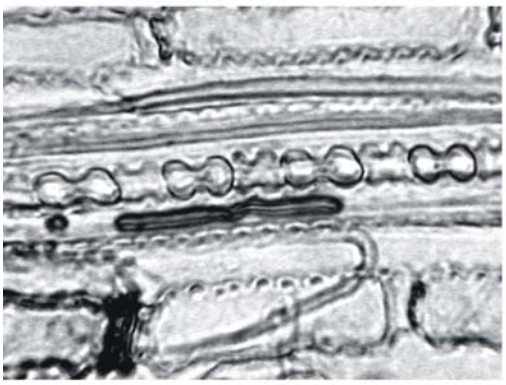

Brachiaria arrecta Ellis 3381 (8216) Vleis,
river floodplains, shallow water.

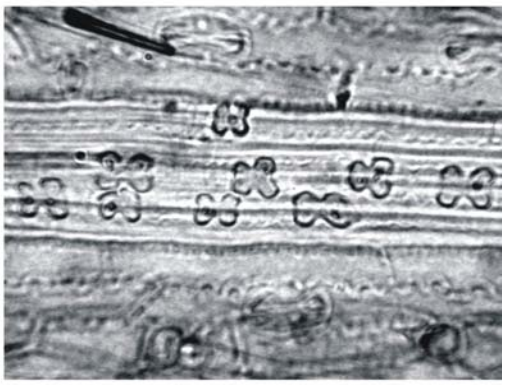

Brachiaria eruciformis Ellis 526 (8218)
Moist places.

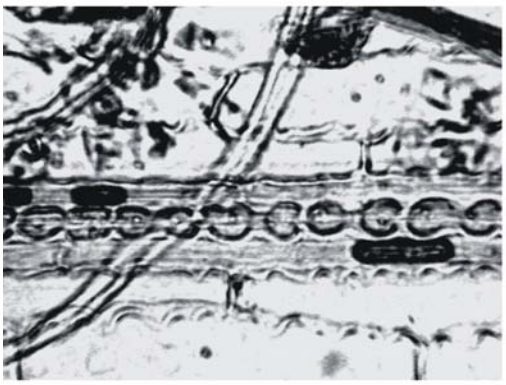

Brachiaria glomerata Ellis 3599 (8221)
Sandy soils, dunes, dry areas.

Brachiaria marlothi Ellis 3607 (8223)
Seasonally moist spots.

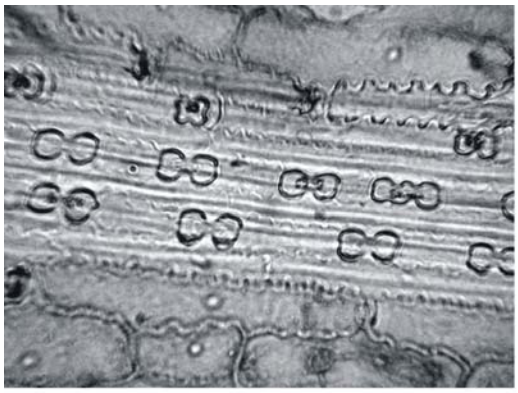

Brachiaria serrata Ellis 293 (8225)
Mountain slopes, grassland, vleis.

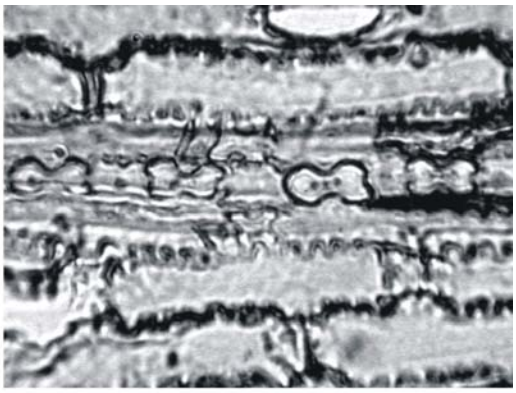

Brachiaria subulifolia Ellis 3535 (8228)
Damp, seepage areas.

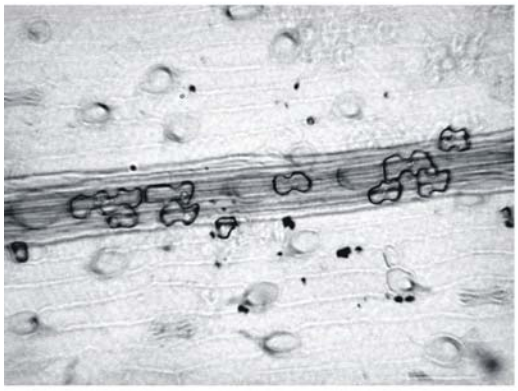

Brachypodium bolussi Ellis 2385 (7801)
Mountain grassland.

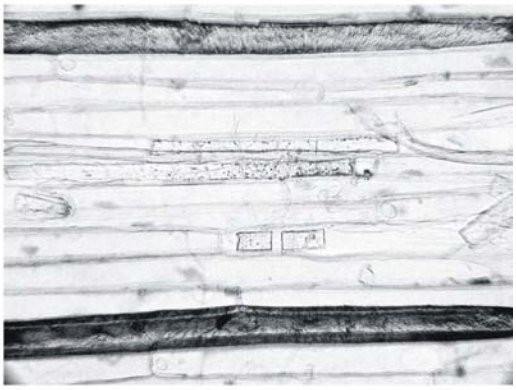

Bromus firmior Ellis 5702 (7803)
High alt., moist grassy mountain slopes.

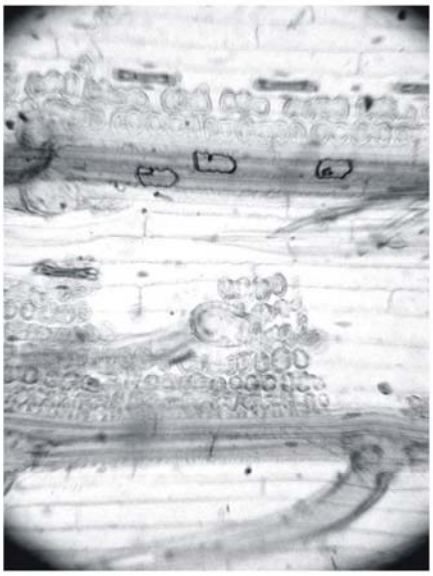

Bromus speciosus Ellis 2381 (7808)
Moist mountain slopes, shade,
along streams.

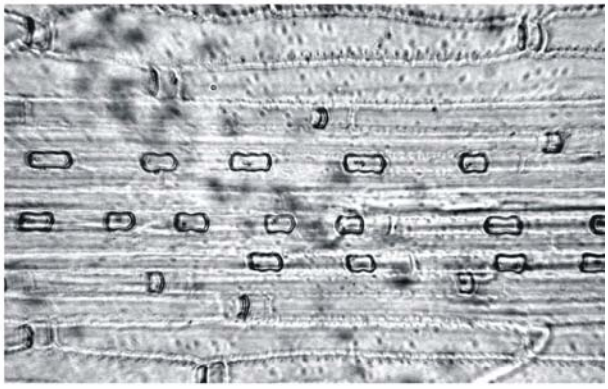

Chaetobromus dregeanus Ellis 2450 (8065)
Sandy, rocky, dry areas.

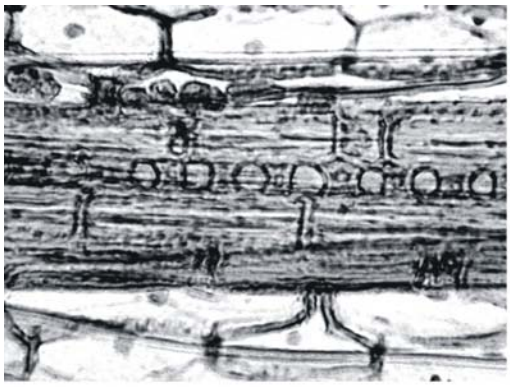

Chaetobromus involucratus Ellis 5345 (8063) Coastal areas, west coast.

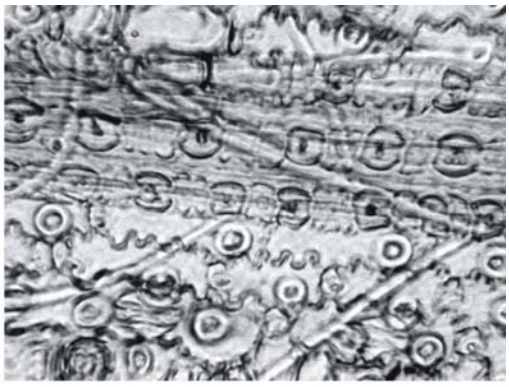

Chloris flabellata Ellis 4355 (8090) Coastal areas, saline marshes, flats.

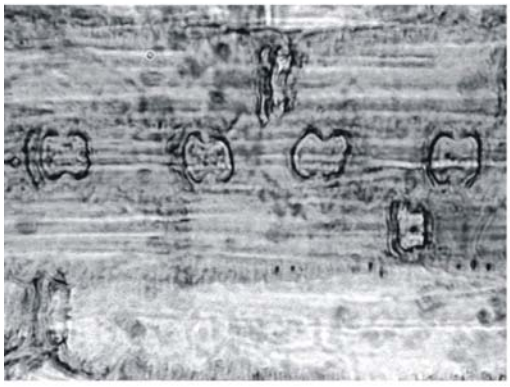

Coelarachis capensis Ellis 5194 (8488) Grassveld.

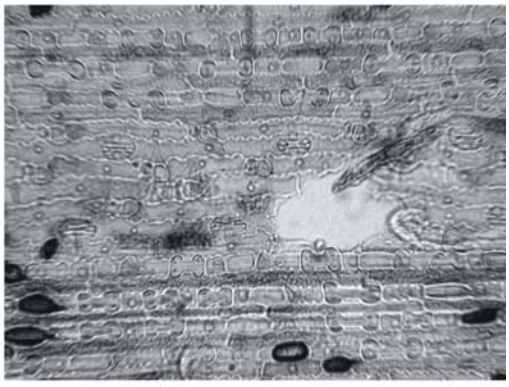

Ctenium concinnum Ellis 380 (8088) Open veld, moist soils.

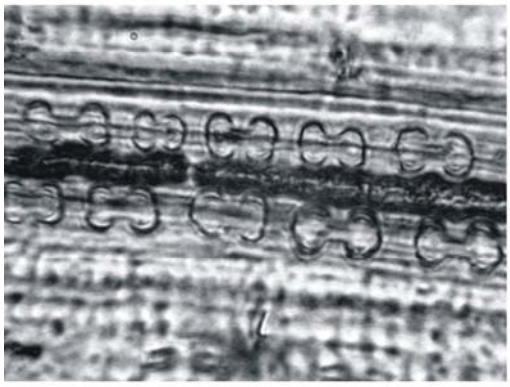

Cymbopogon excavatus Ellis 2047 (8237) Open veld, hillsides.

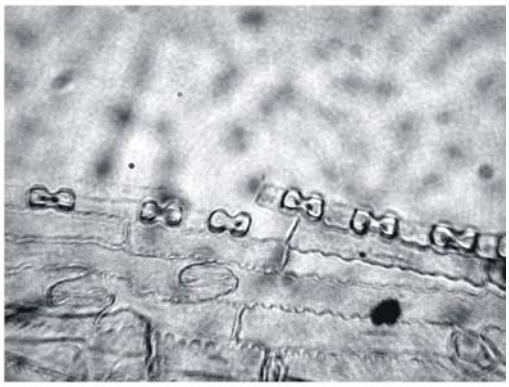

Cymbopogon marginatus van Heerden 29 (8234) Rocky hillsides, winter rainfall areas.

Cymbopogon plurinoides Ellis 3613
(8231) Grassveld.

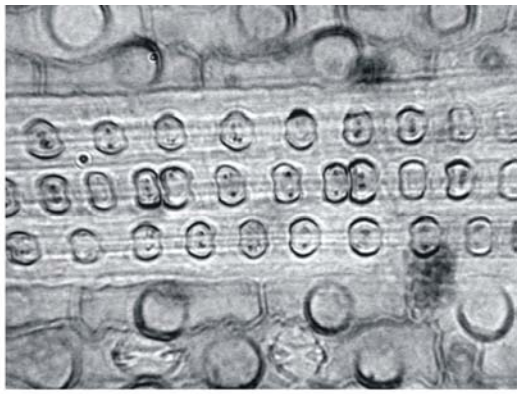

Dactyloctenium giganteum Ellis 529 (8096)
Oprnd veld, river banks, near water.

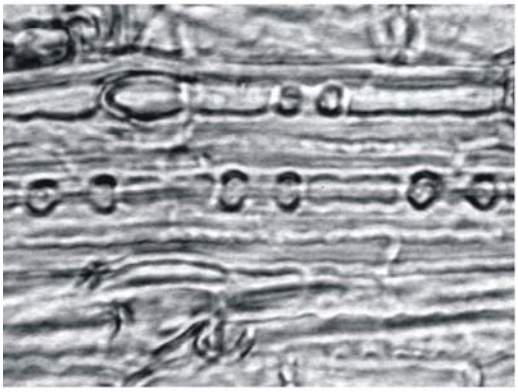

Dianthionopsis parva Ellis 1936
(8239) Rock crevices, cliffs.

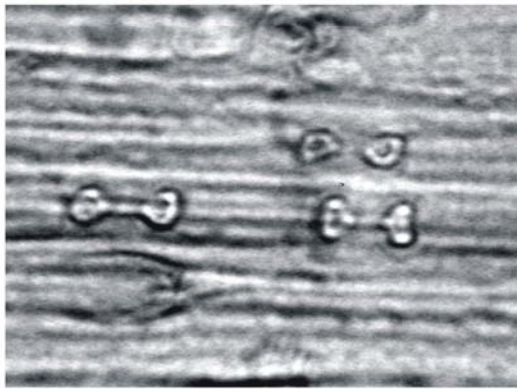

Diantionopsis pruinosa Ellis 1570 (8243)
Rock crevices on mountains.

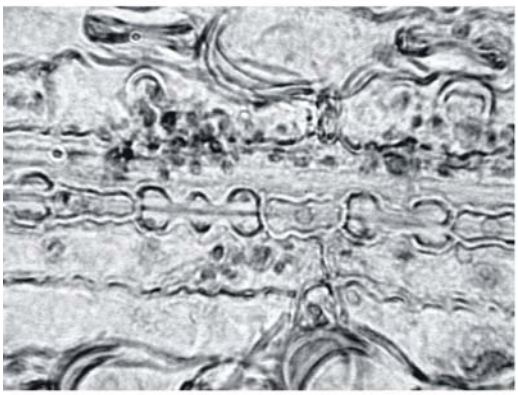

Dichantium annulatum Ellis 5251
(8248) Riverbanks, wet places.

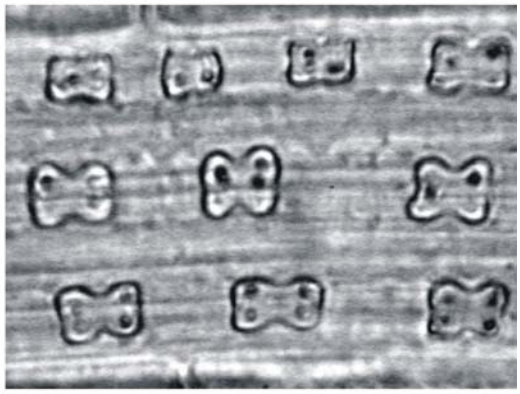

Digitaria brazzae de Wet 996
(8251) Grassland, hillsides.

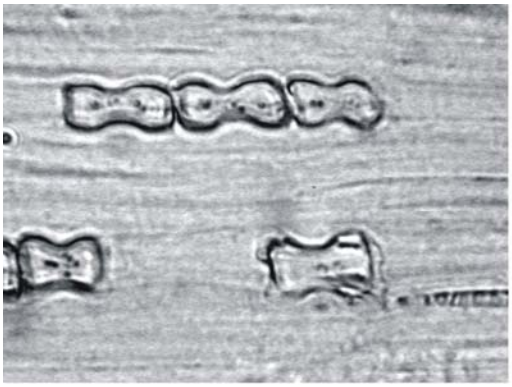

Digitaria diagonalis Ellis 246 (8253)open, sourveld grassland, damp places.

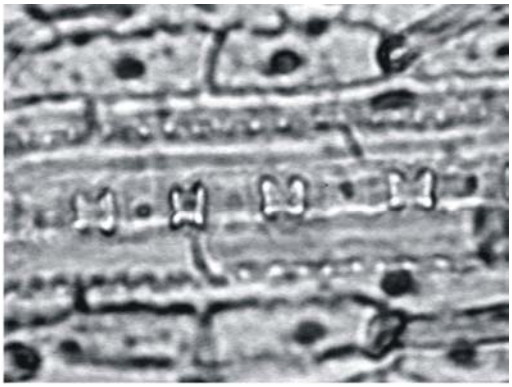

Digitaria diversinervis Ellis 4486 (8256) Sandy, coastal areas.

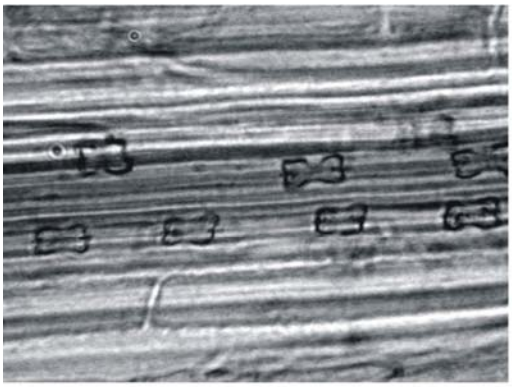

Digitaria monodactyla Ellis 147 (8258) Open grassland, highland sourveld.

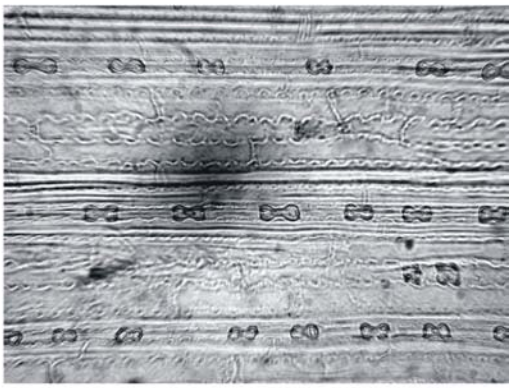

Digitaria setifolia Ellis 56 (8260) Mountain sourveld, damp places, vleis.

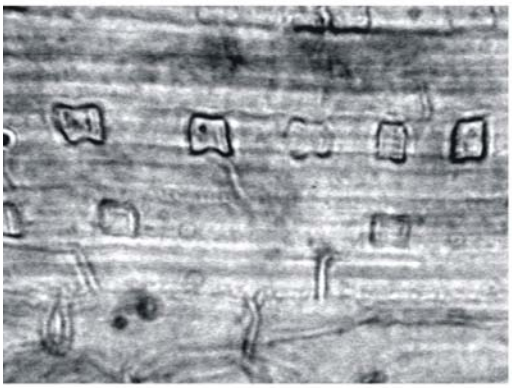

Digitaria ternata Ellis 39 (8263) Damp places.

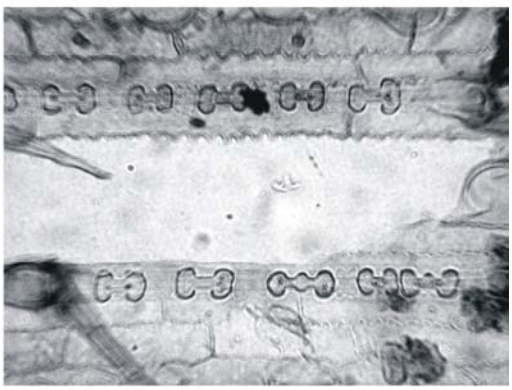

Diheteropogon amplectens Ellis 352 (8266) Stony slopes, woodland.

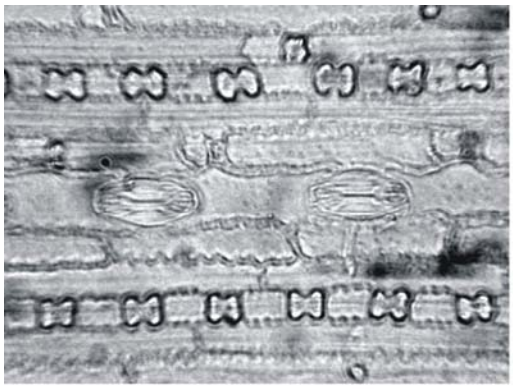

Diheteropogon filifolius Ellis 55 (8269)
Sour open grassveld, hilsides.

Dinebra retroflexa Ellis 3864 (8095)
Moist waterlogged soils, shade.

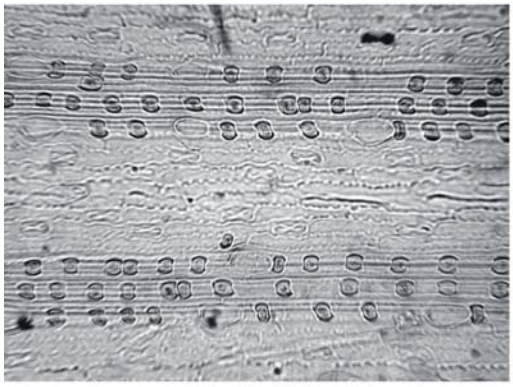

Diplachne eleusine de Wet 993 (8092)
Sandy soils, rocky slopes, shade.

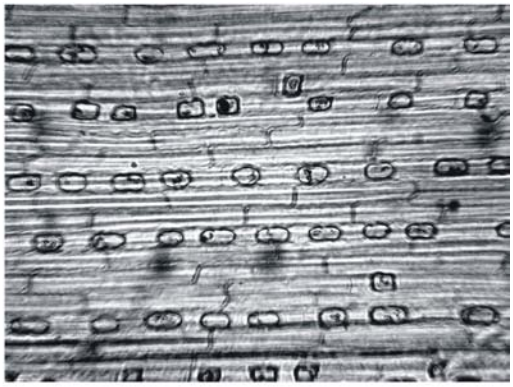

Dregechloa pumila Giess van Vuuren 653
(8058) Rocky areas, loose sand, arid areas.

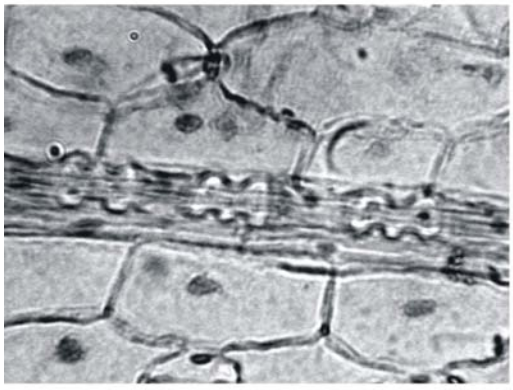

Echinochloa colona Ellis 3896 (8272)
Muddy, swampy places.

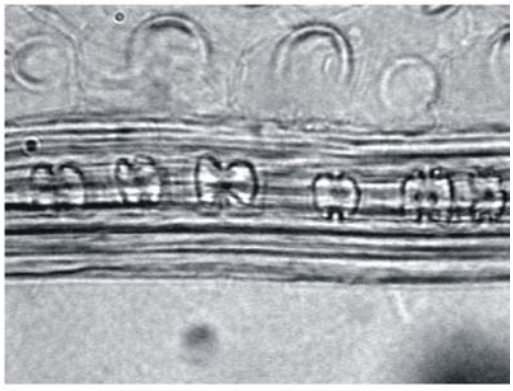

Echinochloa holubii de Wet 1005 (8276)
Swamps, vleis, pans.

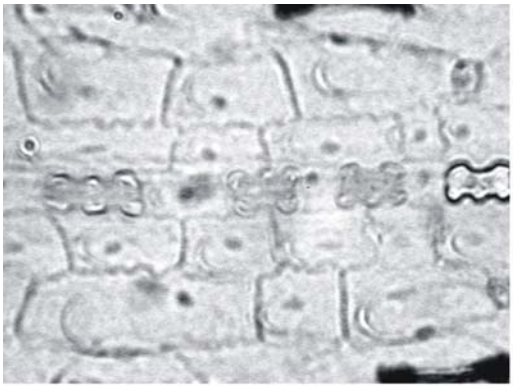

Echinochloa stagnina Ellis 2910 (8278) standing water.

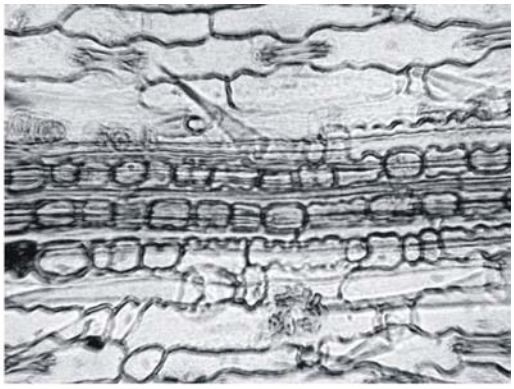

Ehrharta barbinoides Ellis 5409 (8154) Rocky hillsides, west coast.

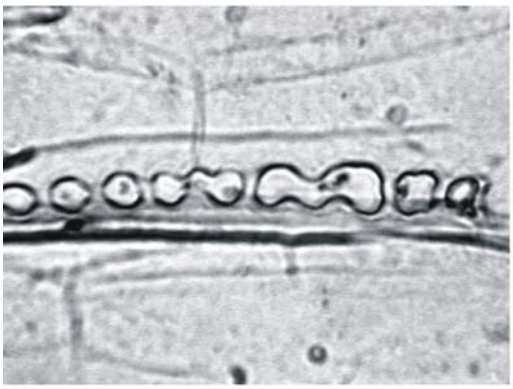

Ehrharta brevifolia subs. brevifolia Ellis 4641 (8159) Sandy soil, west coast.

Ehrharta capensis subs. capensis Ellis 4691 (8160) Mountains, streamsides.

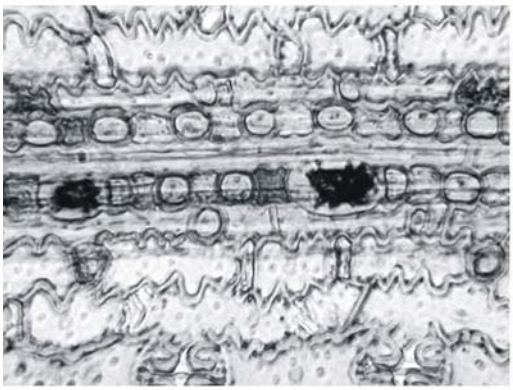

Ehrharta delicatula Ellis 4647 (8164) Mesic microhabitats in arid regions.

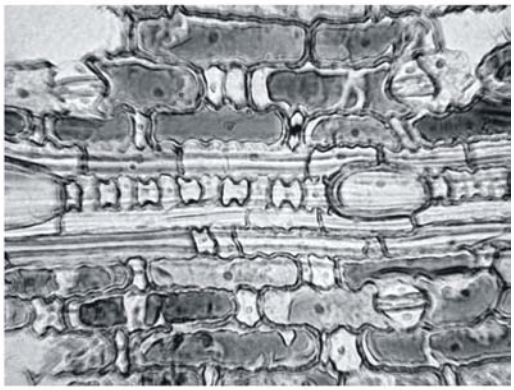

Ehrharta dura Ellis 5457 (8166) Mountain fynbos, seasonally moist open habitats.

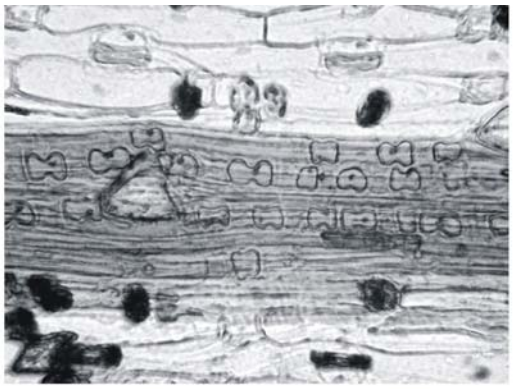

Ehrharta eburnea Ellis 5413 (8167)
Mountainsides, Rhenosterbosveld.

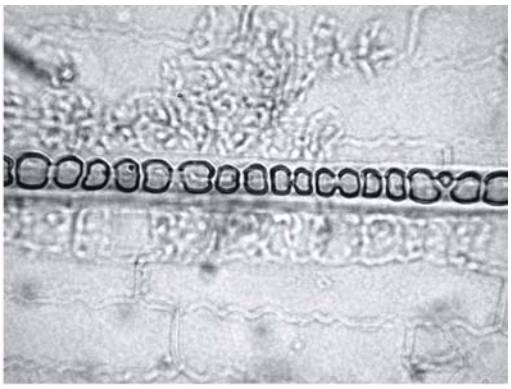

Ehrharta longiflora Ellis 1154 (8179)
Hillsides, shade, wet places.

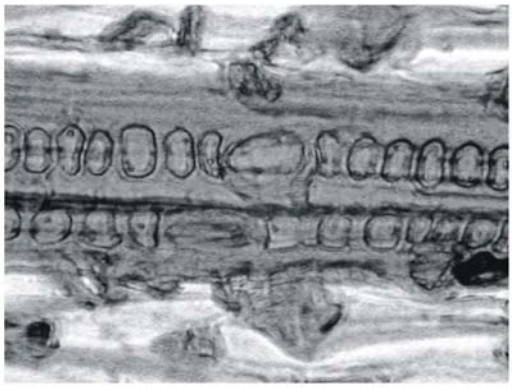

Ehrharta longigluma Ellis 5681
(8176) Mountain grassland.

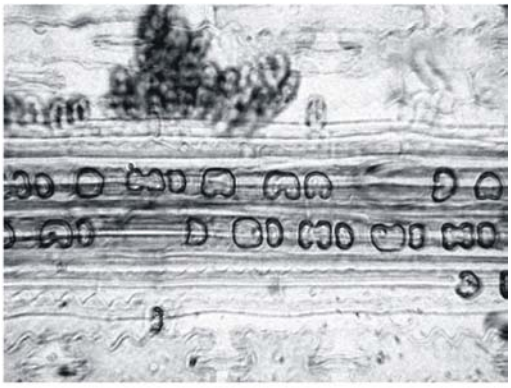

Ehrharta villosa 1700
(8187) Seaside dunes.

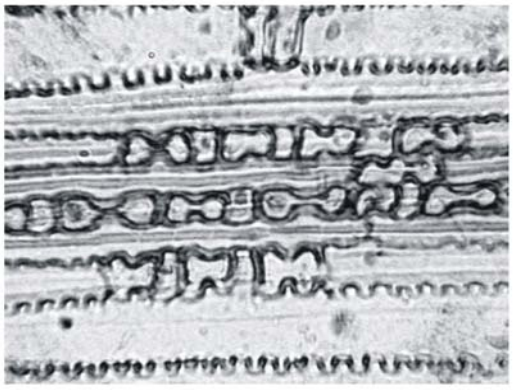

Elionurus muticus Ellis 5172 (8490)
Open grassland, sourveld.

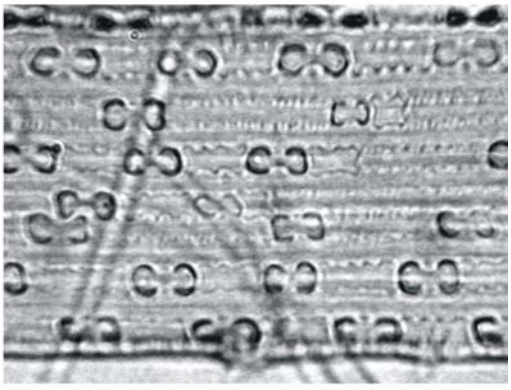

Enneapogon pretoriensis Ellis 1228
(8144) Rocky hillsides, grassveld.

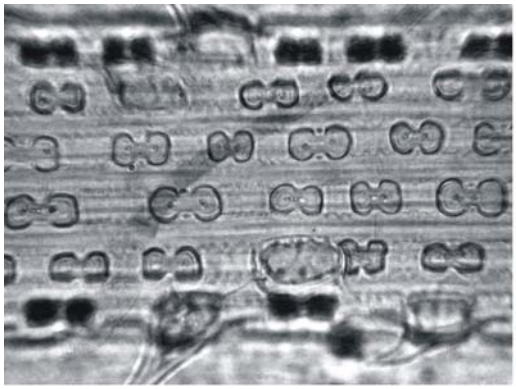

Enneapogon scaber Ellis 1625 (8143) Rock crevices, plains, dry sandy riverbeds.

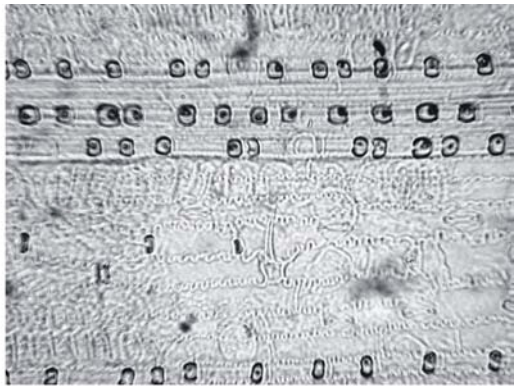

Entolasia imbricata PA Smith 1876 (8282) Floodplains, seasonally flooded to 1m.

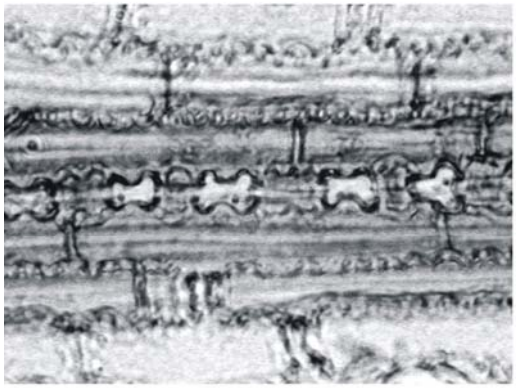

Entoplacamia aristulata de Wet 964 (8097) Rocky outcrops, open plains.

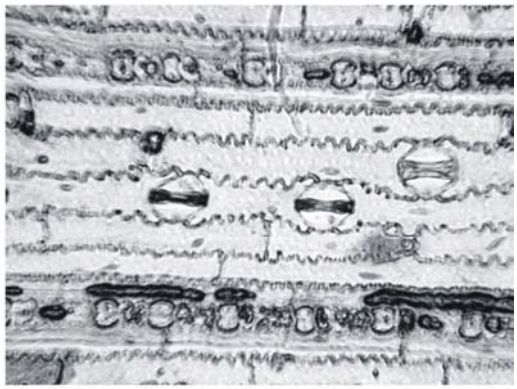

Eragrostis bicolor Ellis 3652 (8100) Wet places, in water, seasonal pans.

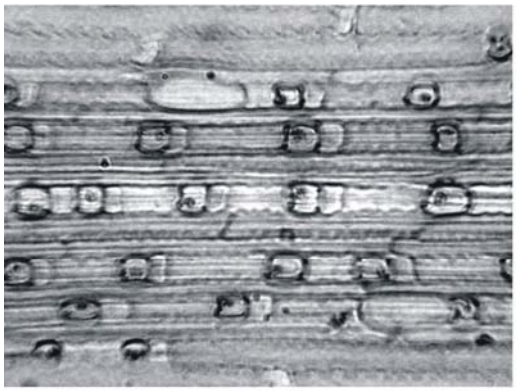

Eragrostis biflora Ellis 1610 (8102) Moist areas, under trees.

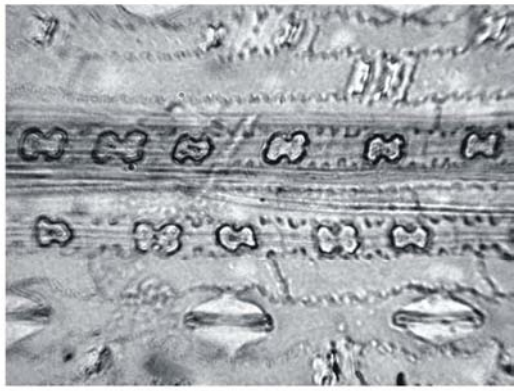

Eragrostis brizantha Ellis 1349 (8104) Sandy, calcareous soils around rivers.

Eragrostis chloromelas Ellis 752
(8106) Hillslopes, rocky ridges.

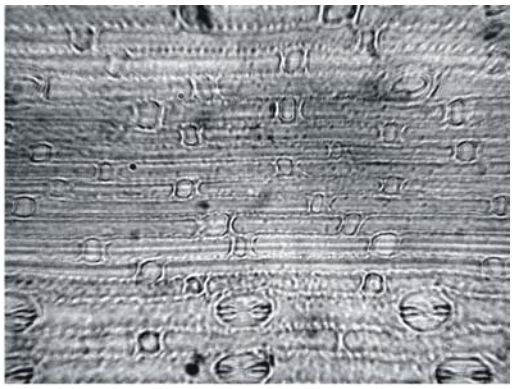

Eragrostis eliator van Heerden 71 (8109)
Riverbanks, periodically inundated areas.

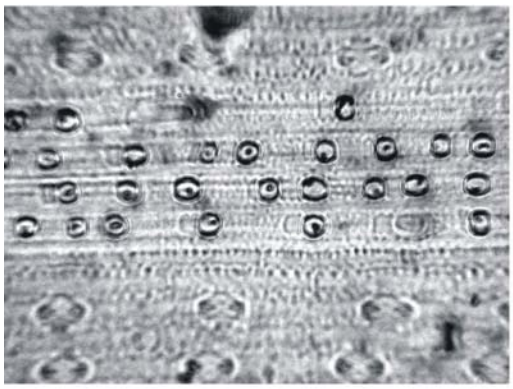

Eragrostis kingesii de Wet Hardy
7872 (8111) Arid regions.

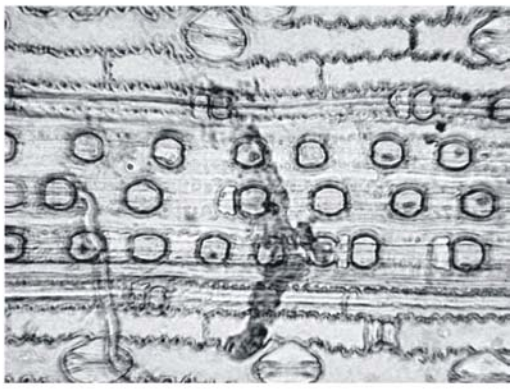

Eragrostis macrochlamys Gibbs Russel
Smook 5436 (8113) Arid areas.

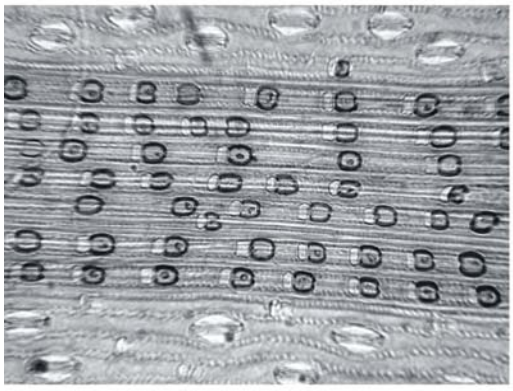

Eragrostis obtusa Ellis 2093
(8114) Open veld.

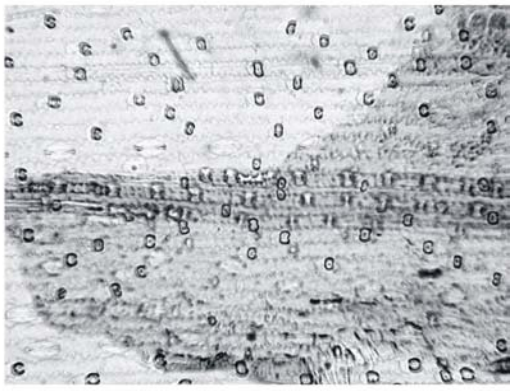

Eragrostis pilgeriana De Wet 2464 (8117)
Calcareous soils with high moisture content.

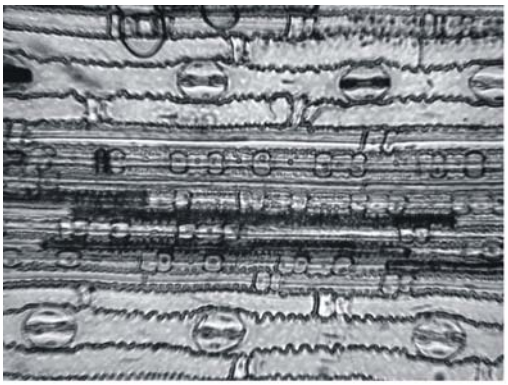

Eragrostis planiculmis Ellis 3330 (8118) Depressions, vlei margins.

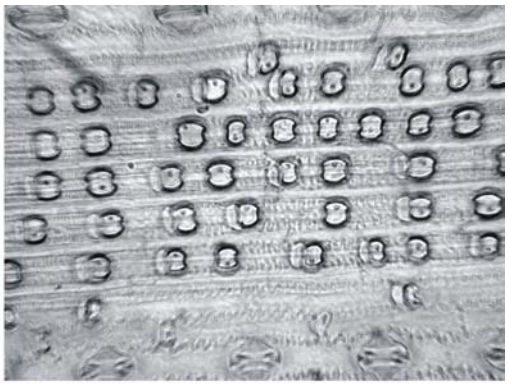

Eragrostis pseudo-obtusa Ellis 838 (8120) Moist areas, along streambeds.

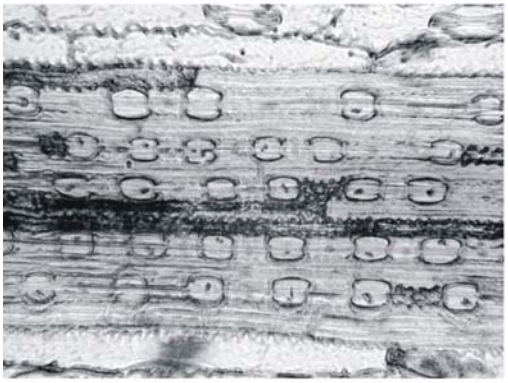

Eragrostis remotiflora Ellis 3666 (8121) Damp, wet places, pans, vleis.

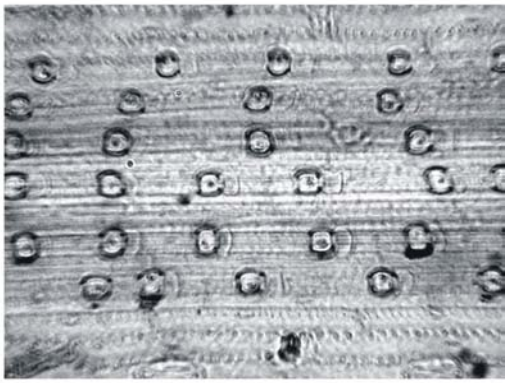

Eragrostis truncata Ellis 3647 (8124) Limestone soils, pans.

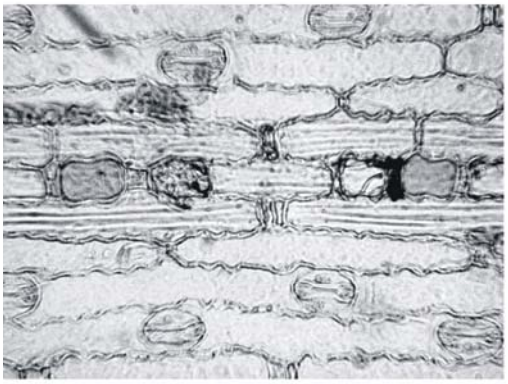

Eragrostis walteri Ellis 4345 (8127) Damp brackish soils, seepage areas, running water, arid regions.

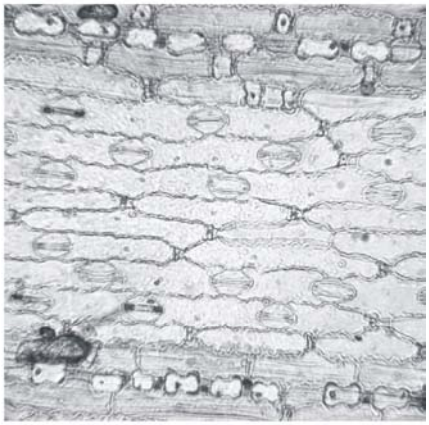

Eragrostis walteri Ellis 4352 (8126) Damp brackish soils, seepage areas, running water, arid regions.

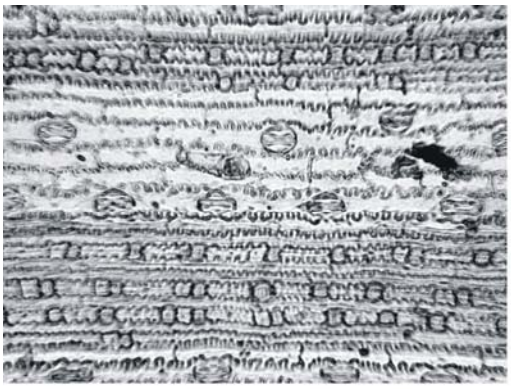

Eragrostis walteri Ellis 4759 (8125) Damp brackish soils, seepage areas, running water, arid regions.

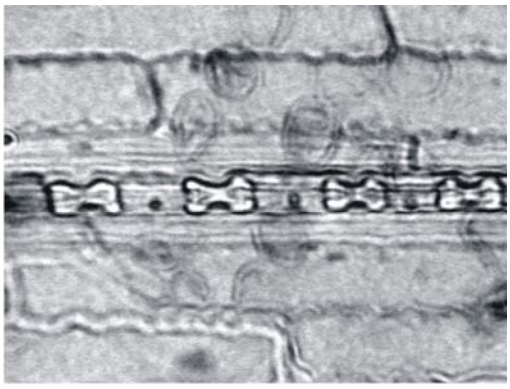

Eriochloa meyeriana Ellis 536 (8285) Riverbanks, wet places.

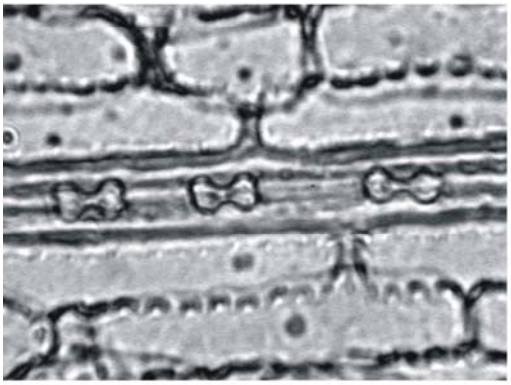

Eriochloa stapfiana Ellis 5248 (8289) Riverbanks, wet places.

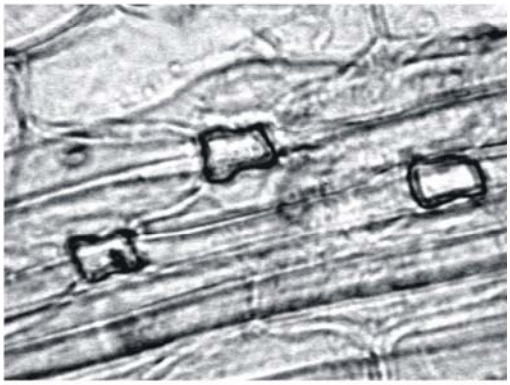

Eriochrysis pallida Ellis 5198 (8293) Vleis, riverbanks.

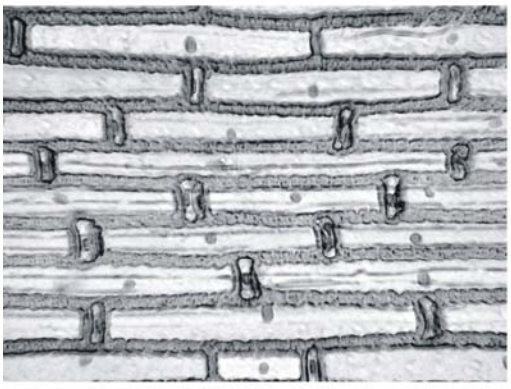

Festuca killicki Ellis 5717 (7817) High alt. subalpine grassveld.

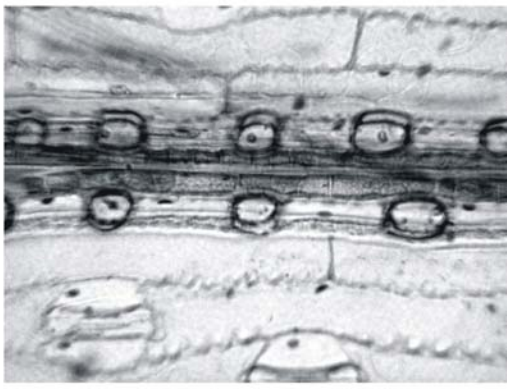

Festuca longipes Ellis 2608 (7821) Steep grassy mountain slopes.

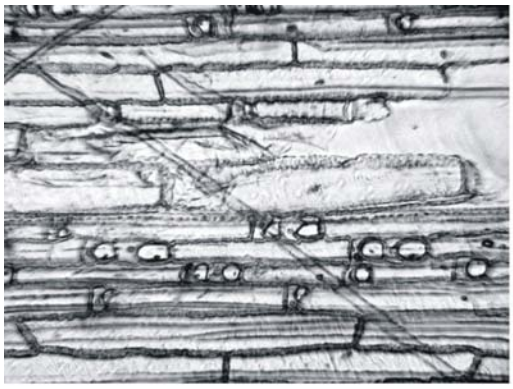

Helictotrichon longifolium Ellis 5676 (7832)
Moist, rocky mountain slopes.

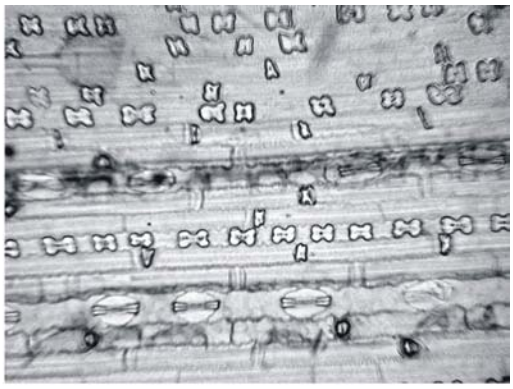

Helictotrichon turgidulum Ellis 71 (7838)
Wet places on mountain slopes, vleis.

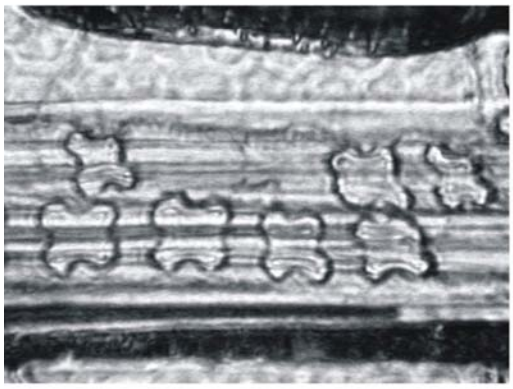

Hemarthria altissima de Wet 1020
(8493) Vleis, river margins.

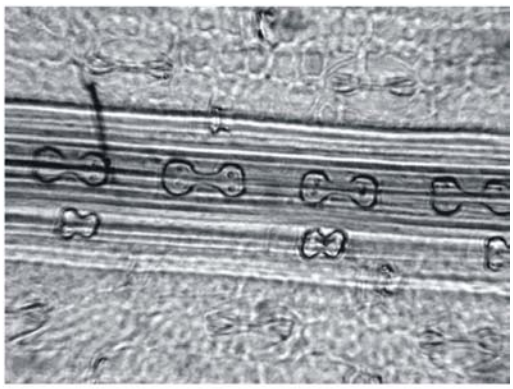

Heteropogon contortus Ellis 1169 (8299)
Open veld, hilsides, rocky places

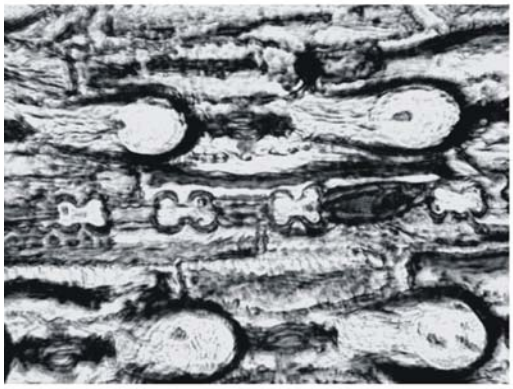

Hyperhenia anamesa Ellis 1649
(8301) Dry soils, open veld.

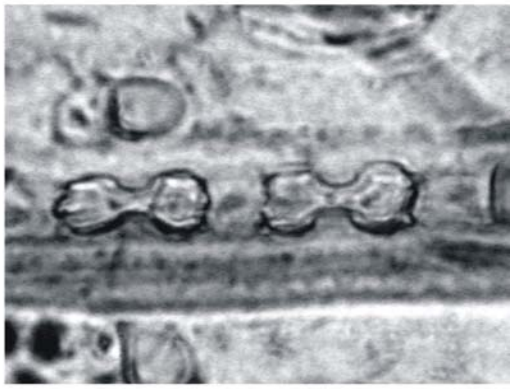

Hyperhenia dregeana R Manders no
nr (8304) Dry soils around vleis.

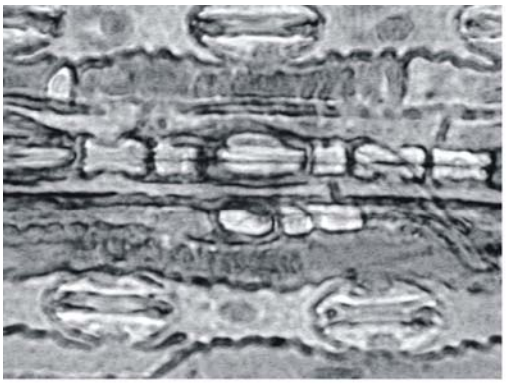

Hyperhenia tamba Ellis 784
(8309) Streamsides.

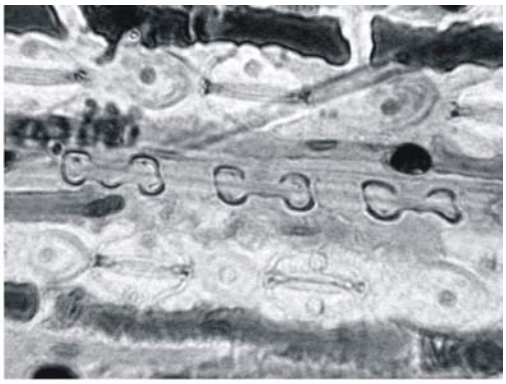

Hyperthelia dissolata Ellis 1513
(8312) Open veld.

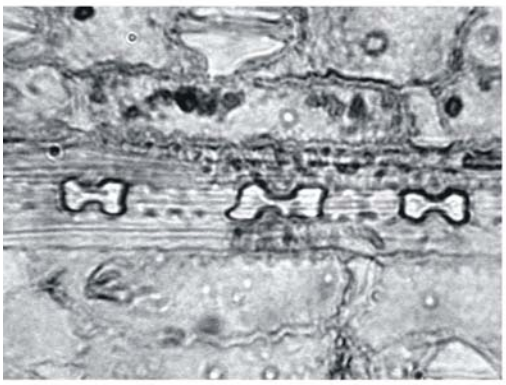

Imperata cylindrica Ellis 1336 (8315)
Riverbanks, vleis, seasonally wet places.

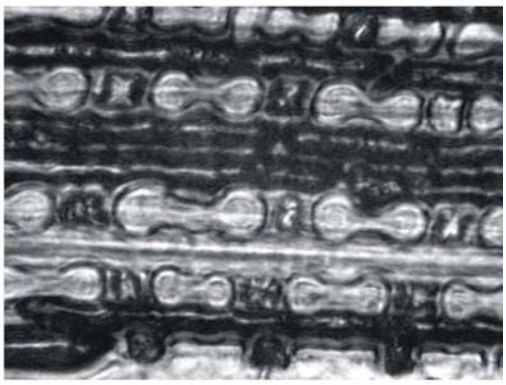

Ischaemum afrum Ellis 505 (8319)
Black turf soil, usually near water.

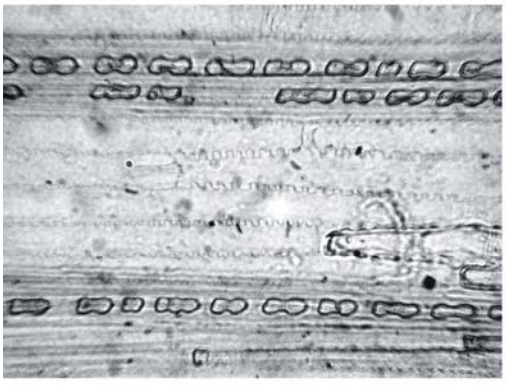

Karroochloa curva Ellis 2570 (8071)
Damp shady habitats.

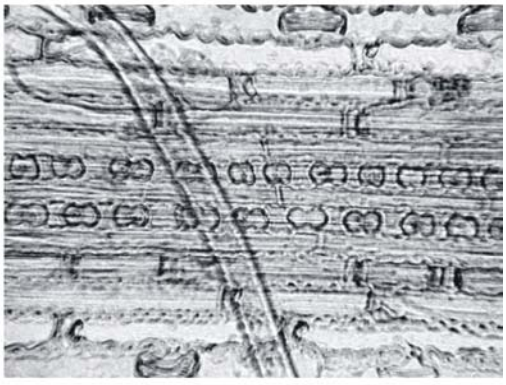

Karroochloa purpurea Ellis 5703 (8073)
Mountainous areas, short grasslands.

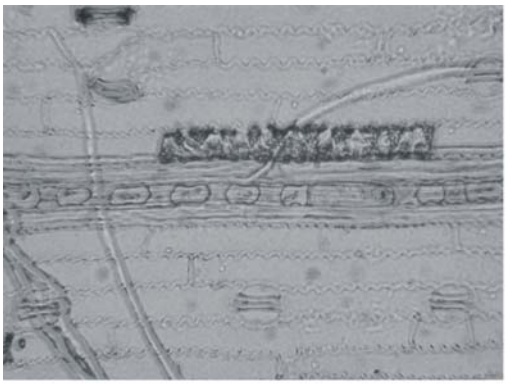

Karroochloa schismoides Ellis 5068 (8069) Dry mountains.

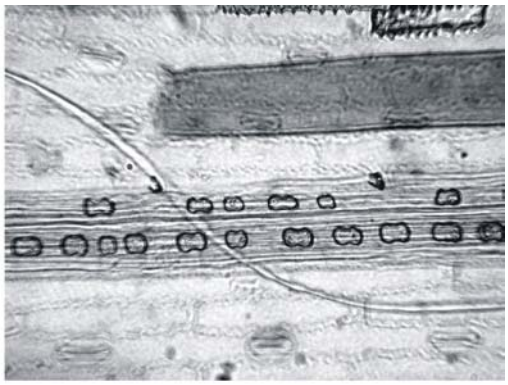

Karroochloa tenella Leistner 470 (8067) Sandy soils, dry regions.

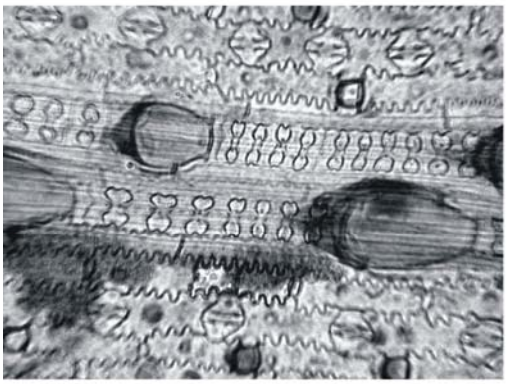

Leersia hexandra Ellis 228 (8150) Floodplains, vleis, pans.

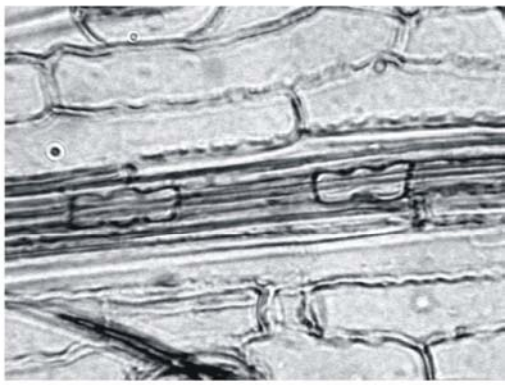

Leucophrys mesocoma Ellis 892 (8322) Sandy riverbeds.

Loudetia flavida Ellis 978 (8327) Rocky soils, vlei margins.

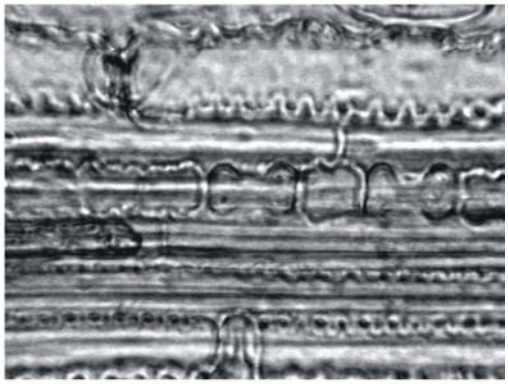

Loudetia simplex Ellis 3376 (8329) Open grassland, hillsides.

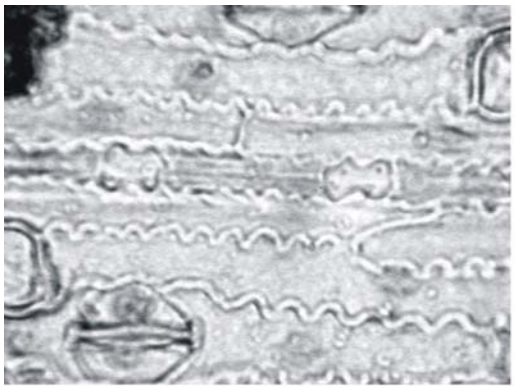

Melenis minutiflora Ellis 3798 (8334) Moist, shady areas, sand or near rocks.

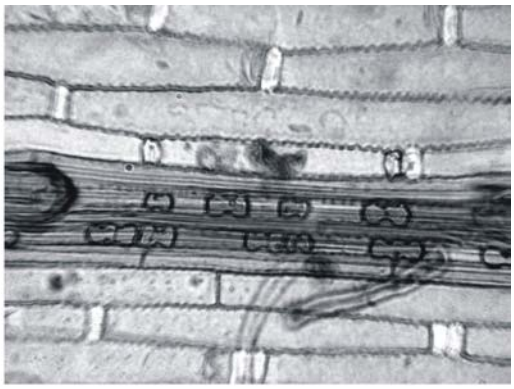

Melica decumbens van Heerden 86 (7848) Hillsides, mountainsides, shade under trees.

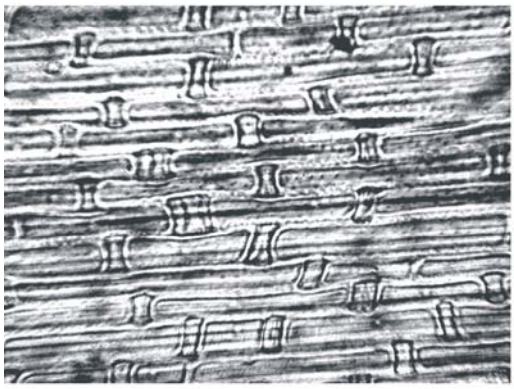

Merxmuellera arundinaceae Ellis 1149 (7910) Xeric areas, Cape fold mountains.

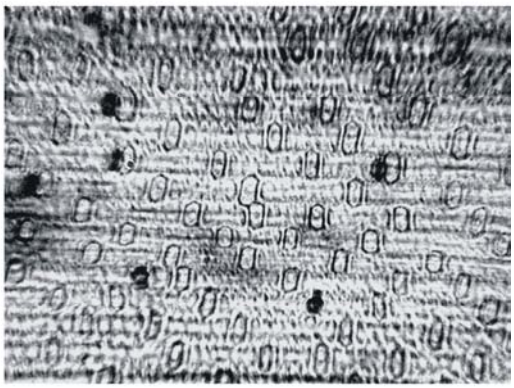

Merxmuellera aureocephala Ellis 3137 (7911) High alt. xeric areas, Drakensberg mountains.

Merxmuellera cincta Ellis 2332 (7913) Moist areas, mountain slopes.

Merxmuellera decora Ellis 657 (7916) Sandy soils, Cape mountain slopes.

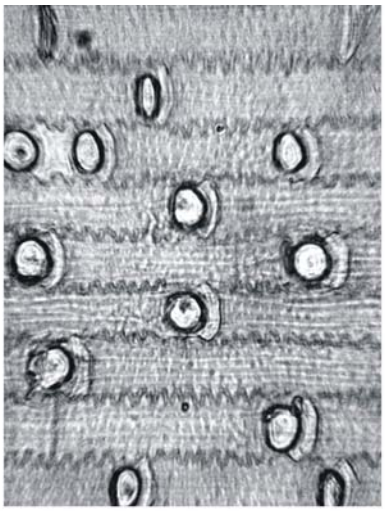

Merxmuellera disticha Loxton 246 (7918) Coastal regions, high alt. mountain regions.

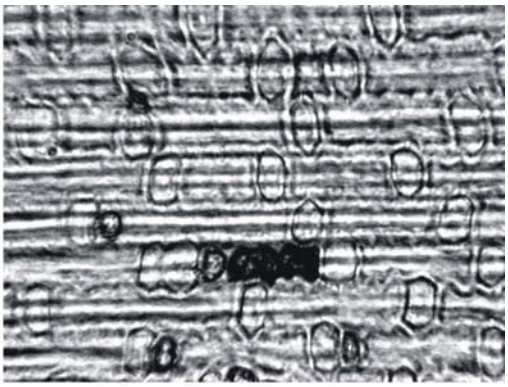

Merxmuellera drakensbergensis Ellis 997 (7920) Mesic sites, streamsides, alpine belt.

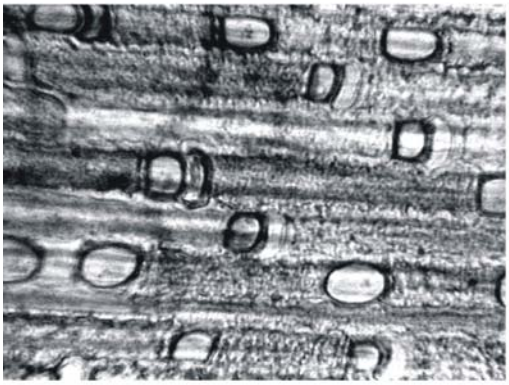

Merxmuellera dura Ellis 2455 (7924) Stony, sandy soils, arid areas.

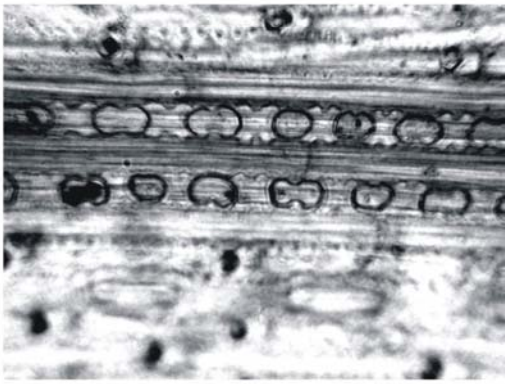

Merxmuellera guillarmodiae Killick 110 (7927) Alpine grassland, moist places.

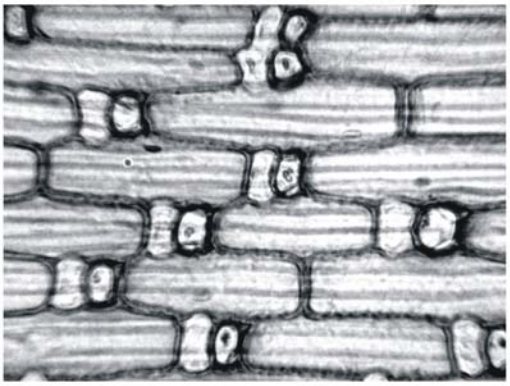

Merxmuellera lupulina Ellis 2255 (7935) Sandy mountain slopes, southwestern Cape mountains.

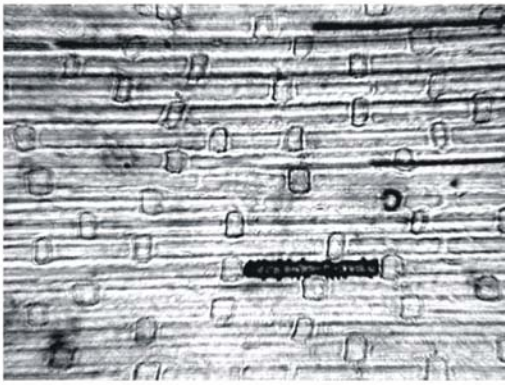

Merxmuellera macowanii Edwards 2673 (7930) Montane, subalpine regions.

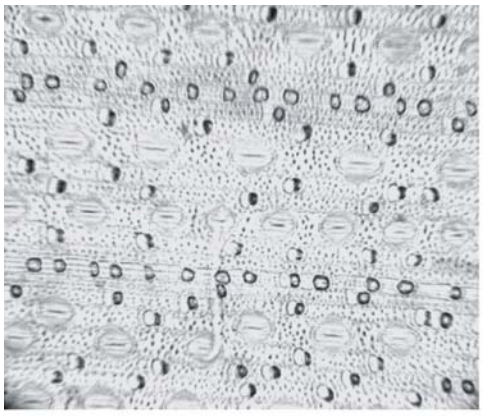

Merxmuellera rangei Schlieben 11599 (7932) Dry sandy ares between hills and koppies.

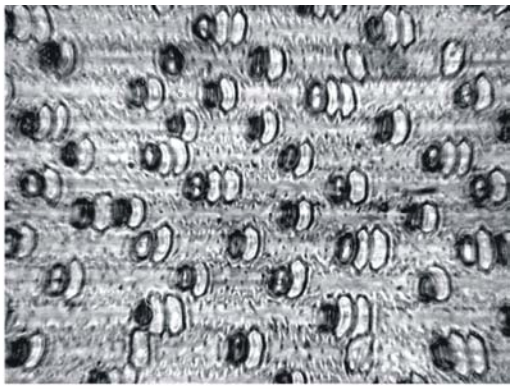

Merxmuellera stereophylla Ellis 3139 (7939) Xeric alpine graaslands, Drakensberg range.

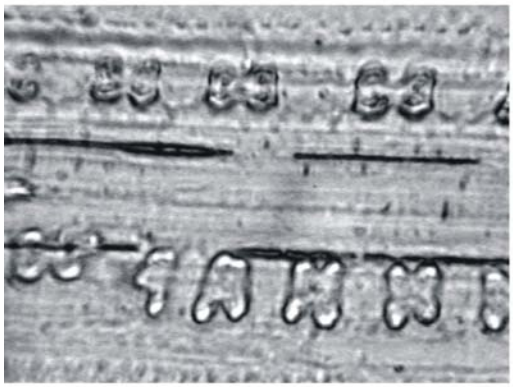

Monocymbium ceresiiforme de Wet 1036 (8340) Open grasslands, hillsides.

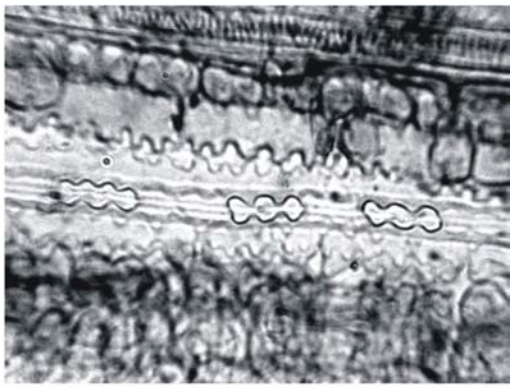

Oplismenus hirtellus Ellis 282 (8345) Forest shade.

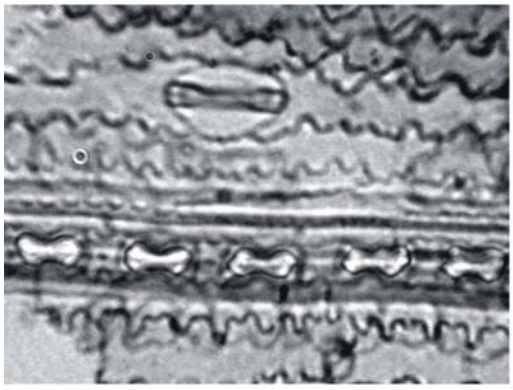

Oplismenus hirtellus Ellis 282 (8349) Forest shade.

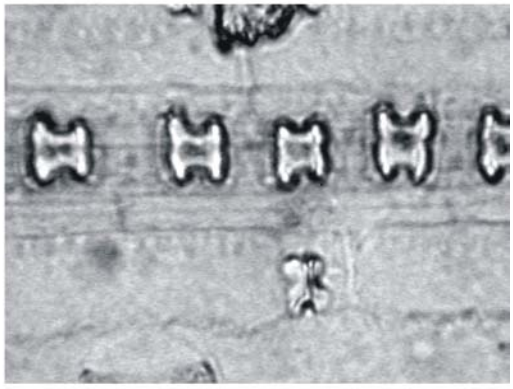

Panicum coloratum Ellis 1783 (8357) Riverbeds, drainages, pans.

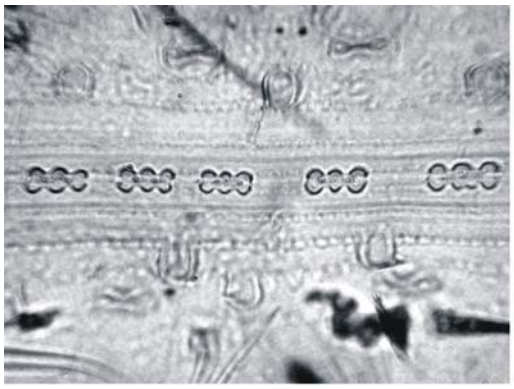

Panicum deustum Ellis 1547 (8360)
Moist soils, shade, rocky hillsides.

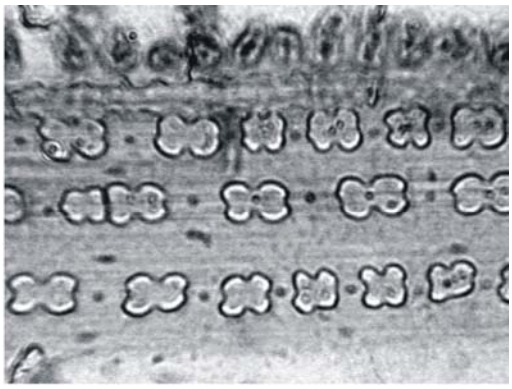

Panicum ecklonii Ellis 1421 (8366)
Moist areas in mountainous regions.

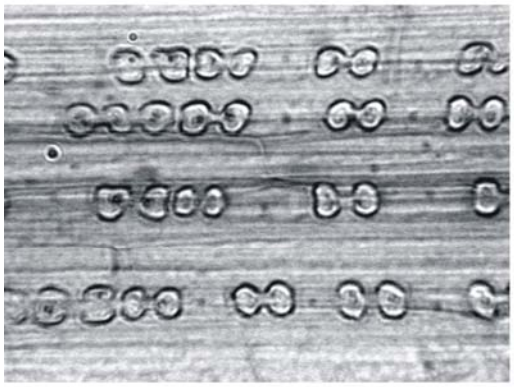

Panicum heterostachyum Ellis 1923 (8367)
Sandy soils in wooded grassland,
seasonally flooded pans.jpg

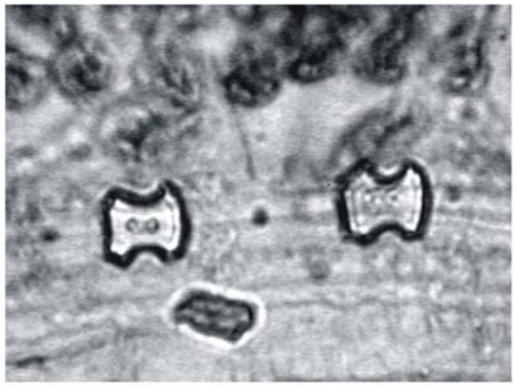

Panicum hymeniochilum Ellis 1560 (8369) Moist,
organically rich soils, river margins, swamps.jpg

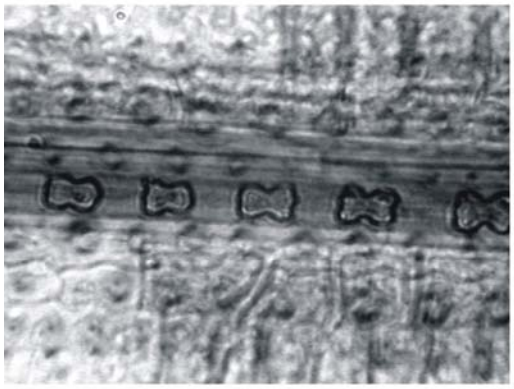

Panicum impeditum Ellis 2918
(8373) Vleis, pans.

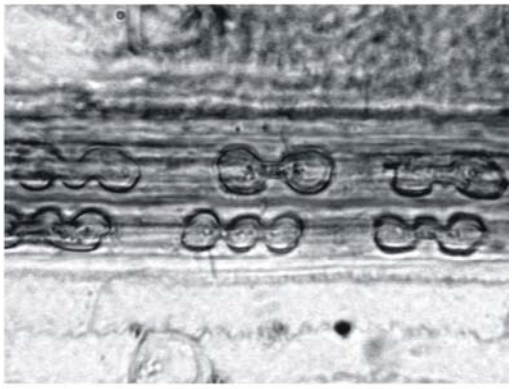

Panicum infestum Ellis 1308 (8375)
Seasonally damp places, hillsides.

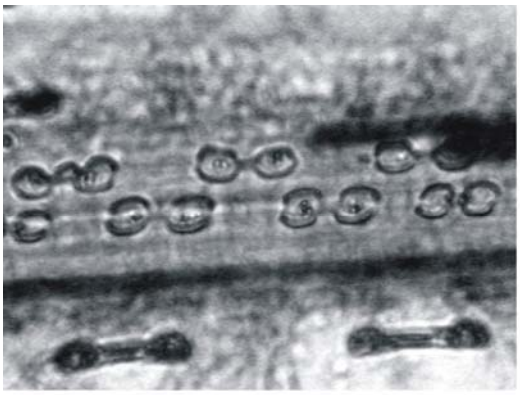

Panicum laticomum Ellis 3231 (8387)
Sandy soils in forests.

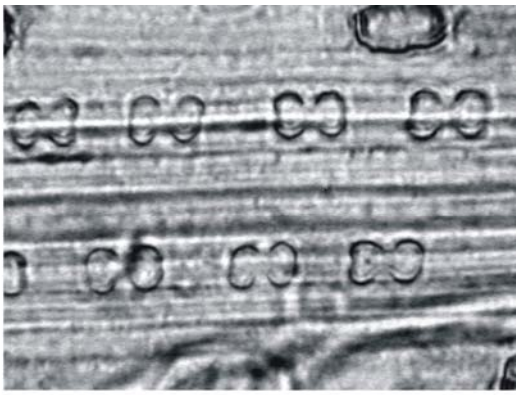

Panicum maximum Ellis 67 (8388)
Shady places, river margins.

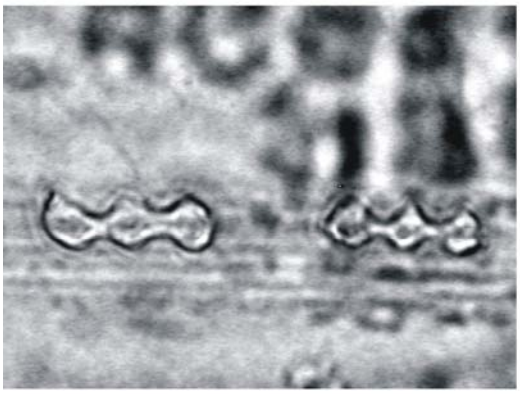

Panicum monticola Ellis 1869 (8390)
Forest, shade.

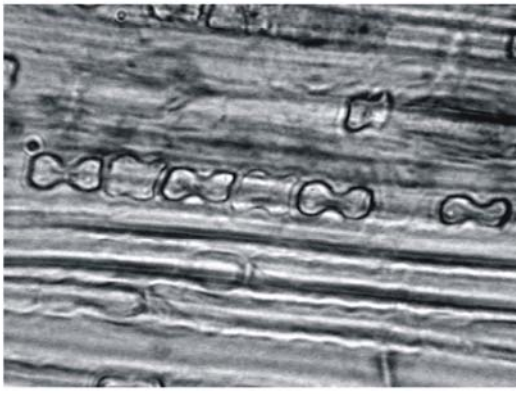

Panicum natalense Ellis 453 (8391) Open
veld, shallow soils in rocky areas.

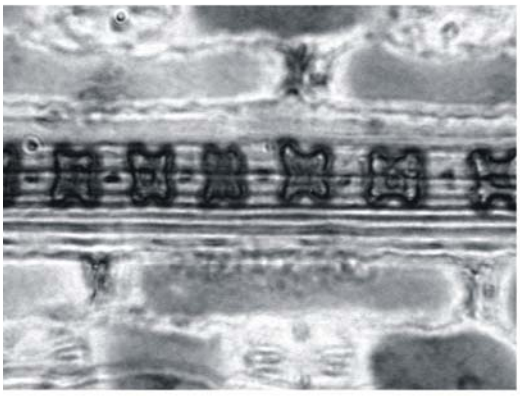

Panicum repens Ellis 2912
(8396) Wet sandy soils.

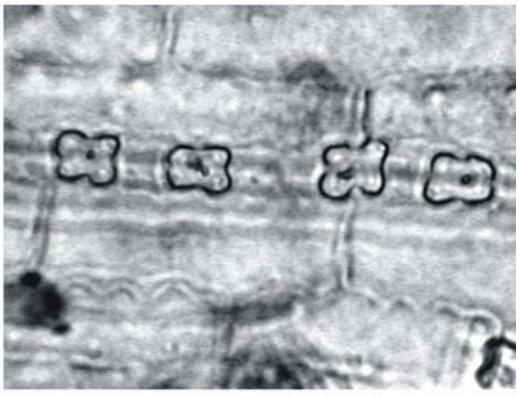

Panicum stapfianum van Heerden
90 (8400) Damp or dry areas.

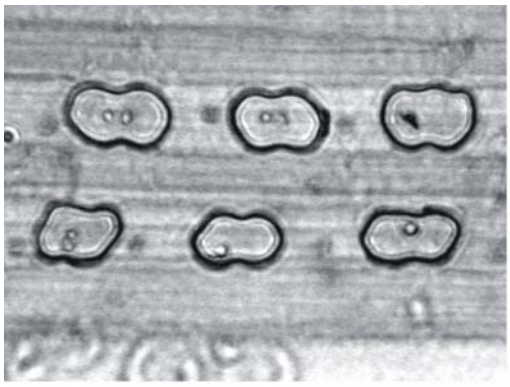

Pennisetum glaucocladum Ellis 2922 (8406) Riverbanks, wet areas.

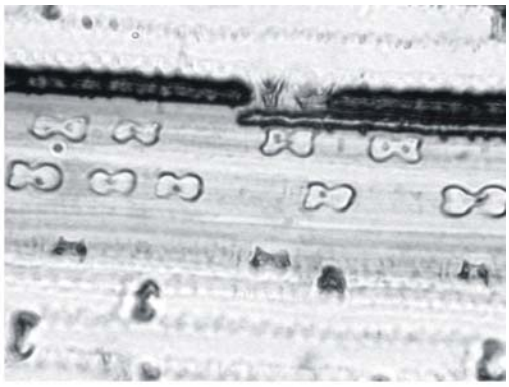

Pennisetum sphacelatum de Wet 8687 (8413) Wet areas, vleis.

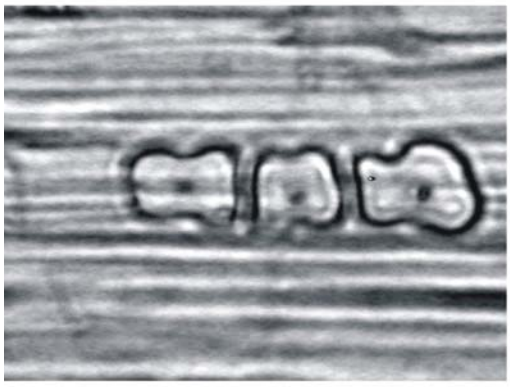

Pennisetum thunbergi Ellis 227 (8416) Wet places, vleis, river banks.

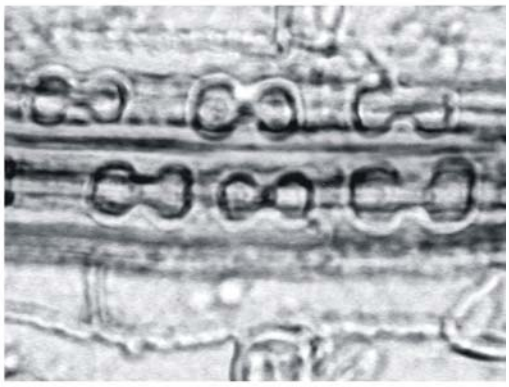

Pennisetum unisetum Ellis 4976 (8418) Near water, shade.

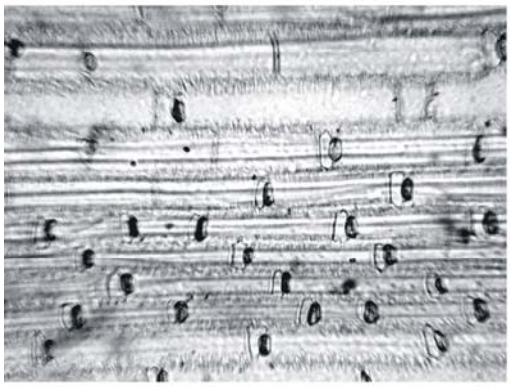

Pentameris dregeana Ellis 2495 (8027) Rock crevices, Cape fold mountains.

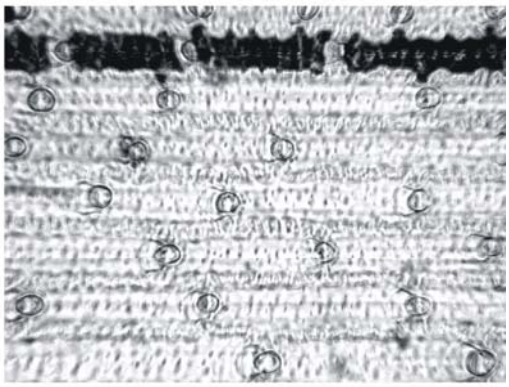

Pentameris macrocalycina Ellis 2500 (8029) Rock crevices, Cape fold mountains.

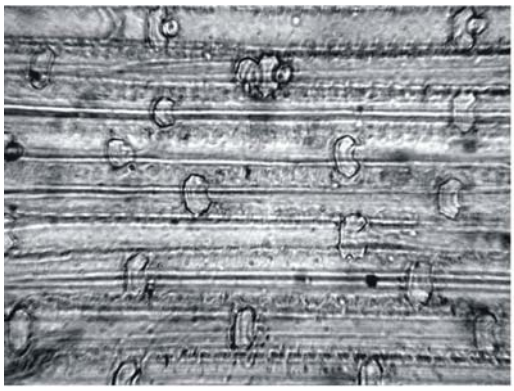

Pentameris obtusifolia Esterhuysen 27442 (8031) Mountain slopes, Hottentots Holland Mountains.

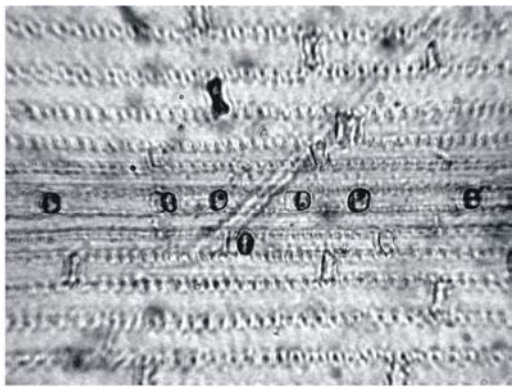

Pentameris thuari Barker 7653 (8033) Seeps, river banks.

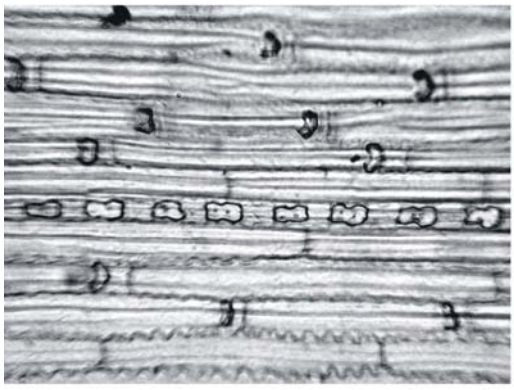

Pentaschistis acinosa Ellis 2267 (7941) Sandstone rock crevices Cape.

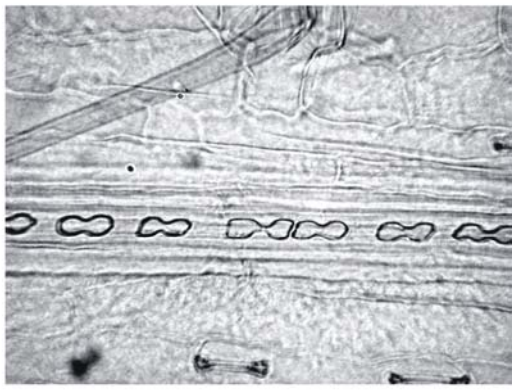

Pentaschistis airoides Ellis 2555 (7944) Rich soils, fynbos.

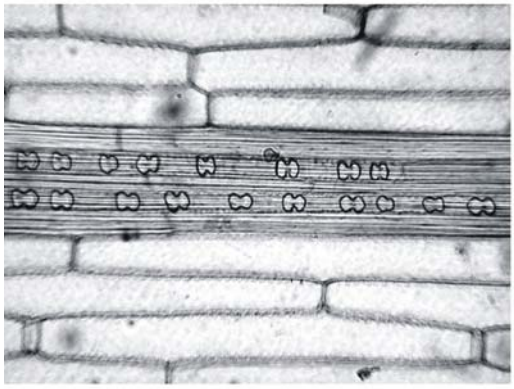

Pentaschistis ampla Esterhuysen 28112 (7946) Low to mid-altitudes on sandstone-derived soils.

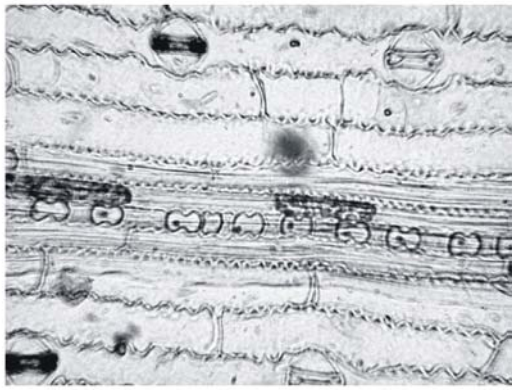

Pentaschistis aristifolia Ellis 5781 (7951) Dry Karoo sediments.

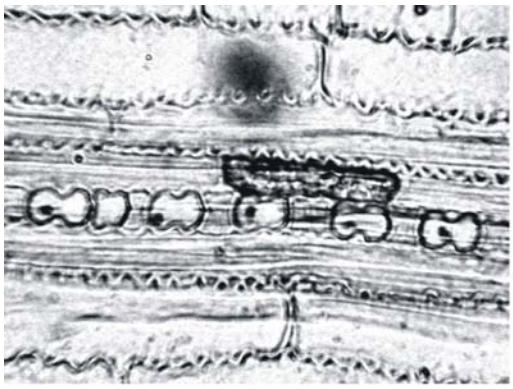

Pentaschistis aristifolia Ellis 5781
(7952) Dry Karoo sediments.

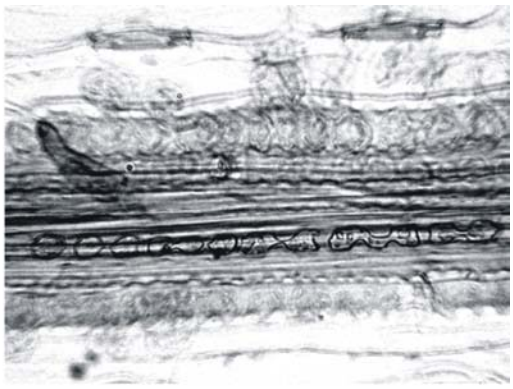

Pentaschistis aspera Ellis 2305
(7954) Stony slopes, fynbos.

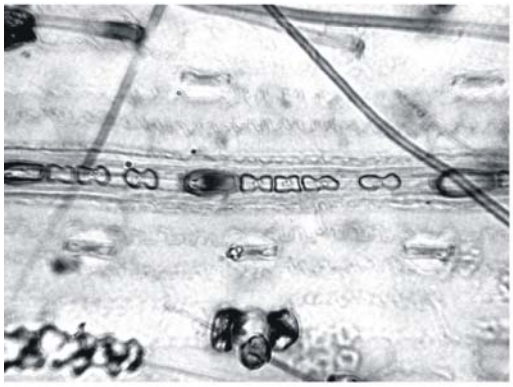

Pentaschistis aurea Acocks 24150
(7956) Marshy areas, fynbos.

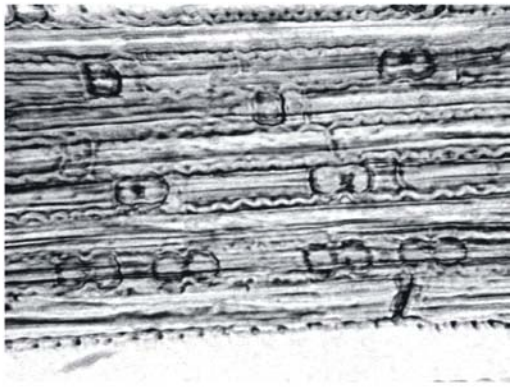

Pentaschistis barbata Ellis 5580
(7957) Coastal sands, fynbos.

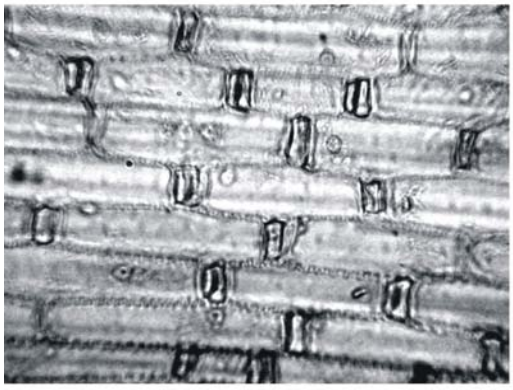

Pentaschistis basutorum Ellis 3292
(7960) Drakensberg slopes.

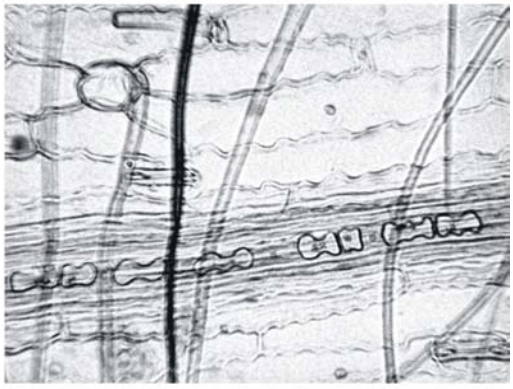

Pentaschistis capillaris Spies 4312 (7967)
Coastal sands, fynbos, west coast.

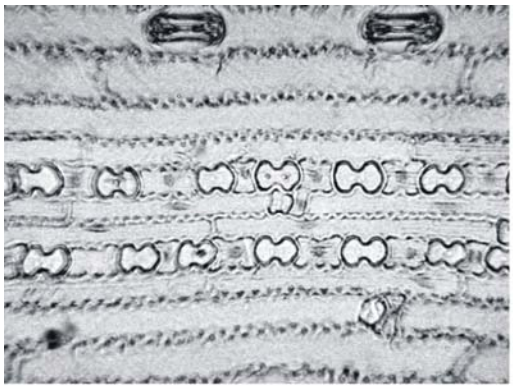

Pentaschistis cederbergensis Ellis 5586 (7968).

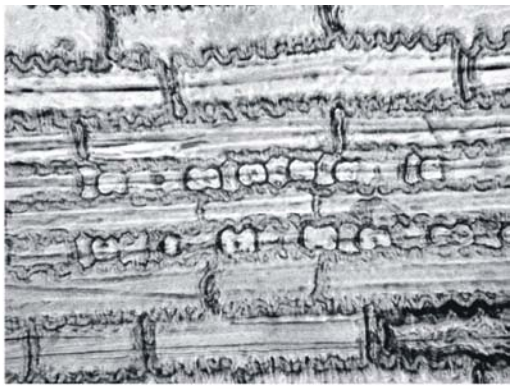

Pentaschistis chippendalliae Ellis 5734 (7971) Sour grassland, afromontane.

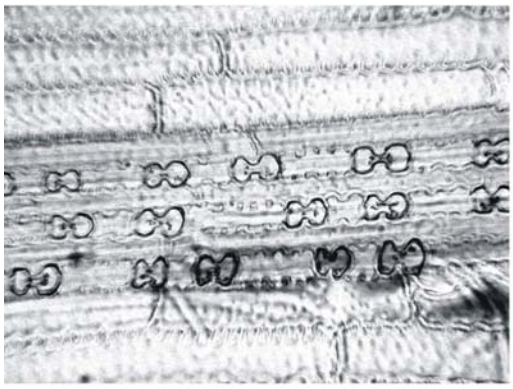

Pentaschistis colorata Ellis 5536 (7976) Stony slopes, sanstone derived soils, fynbos.

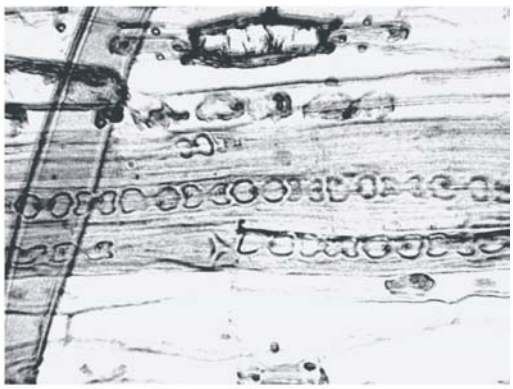

Pentaschistis densifolia Ellis 5584 (7980) Rock crevices, mountain slopes.

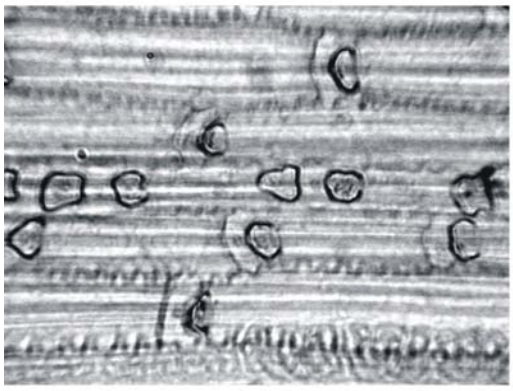

Pentaschistis elegans Ellis 2278 (7983) Coastal sands, fynbos.

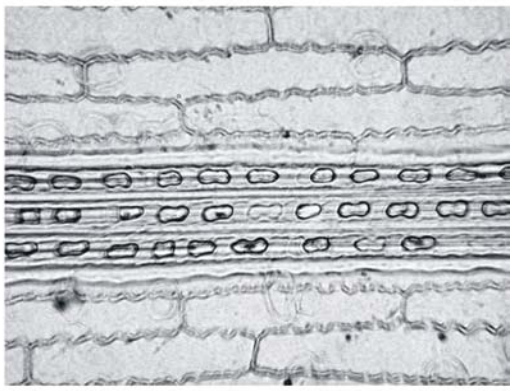

Pentaschistis galpinii Ellis 2398 (7987) Alpine grassland.

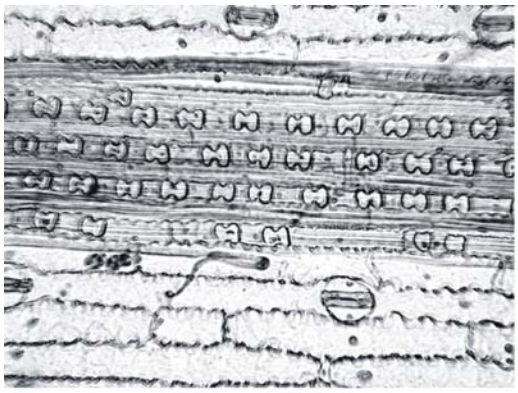

Pentaschistis glandulosa Ellis 5579 (7990)
Granite-derived soils, fynbos.

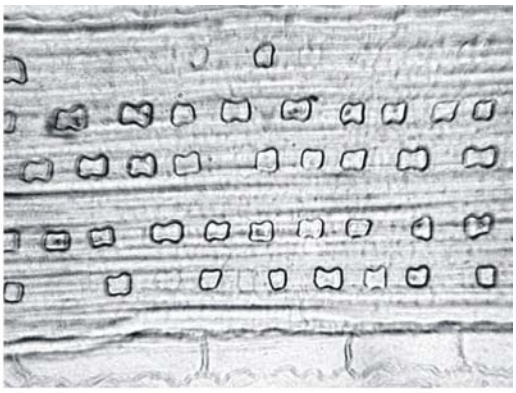

Pentaschistis microphylla Ellis 2592 (8004)
Arid montane grassland, Stormberg.

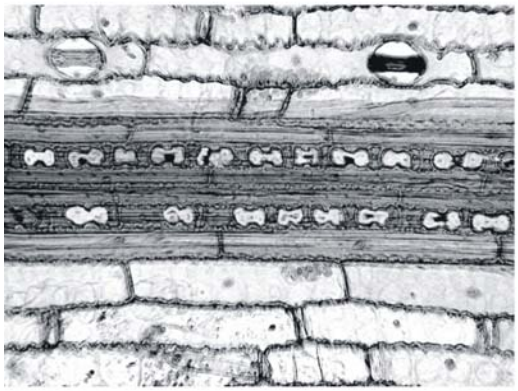

Pentaschistis natalensis Ellis 5735 (7992) Sour grassland, forest margins in afromontane belt.

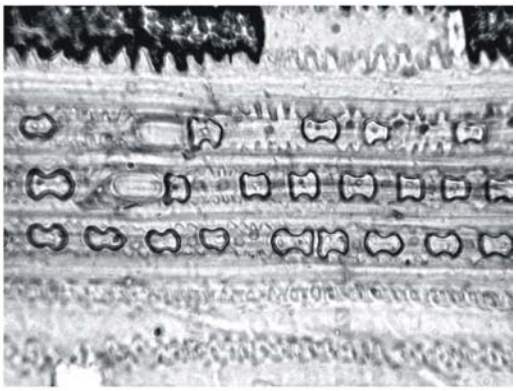

Pentaschistis oreodoxa Ellis 2291 (7994)
Sour grassland, afromontane.

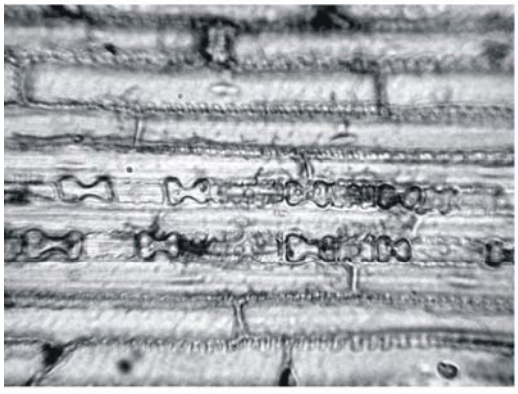

Pentaschistis pallescens Ellis 2226 (8006)
Lower slopes, sandstone mountains, fynbos.

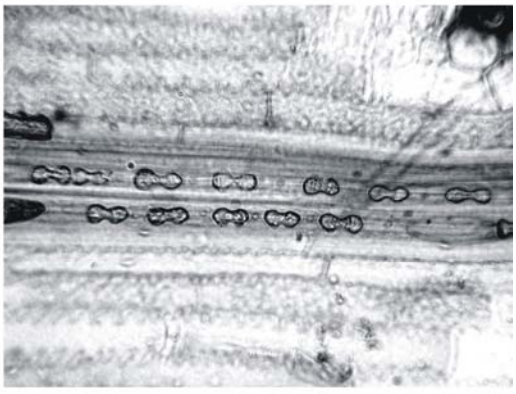

Pentaschistis patula Ellis 2306 (8008)
Sandy soils, arid margins, fynbos.

Pentaschistis pseudopallescens Ellis 5523 (8010) Seeps, streams, in sand, Cape fold mountains.

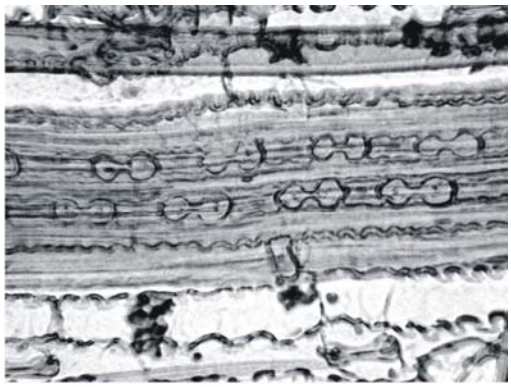

Pentaschistis rupestris Ellis 5596 (8014) Sandstone derived soils, fynbos.

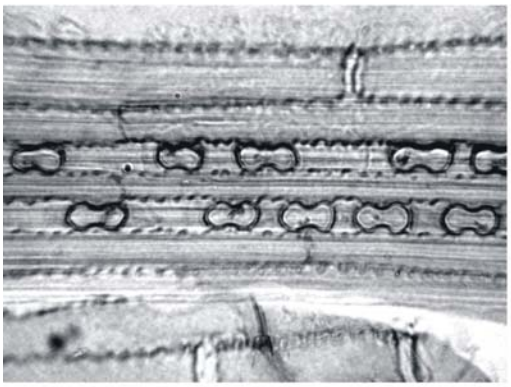

Pentaschistis setifolia Ellis 985 (8016) Sour grasslands, afromontane.

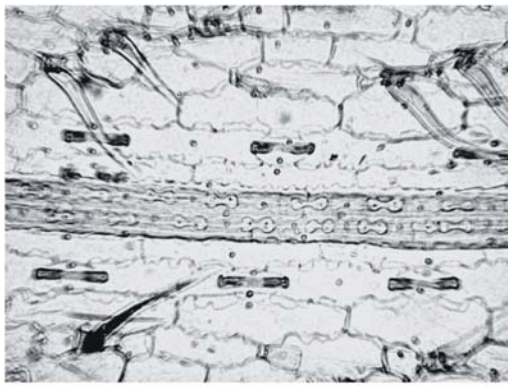

Pentaschistis tomentella Ellis 5420 (8018) Arid regions of Namaqualand.

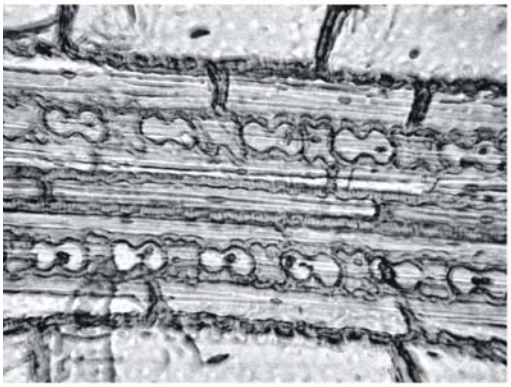

Pentaschistis tortuosa Ellis 5603 (8020) Damp places, sandstone derived soils, fynbos.

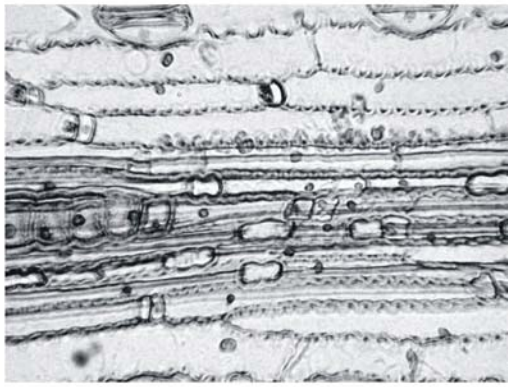

Pentaschistis triseta Ellis 5421 (8023) Sandy soils below 600m, fynbos.

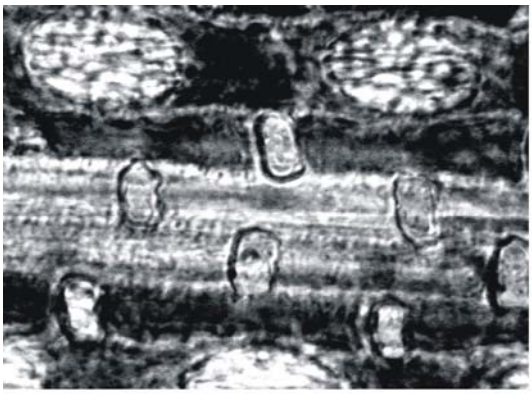

Phacelaris franksae Ellis 3283 (8499) Mountain grassland.

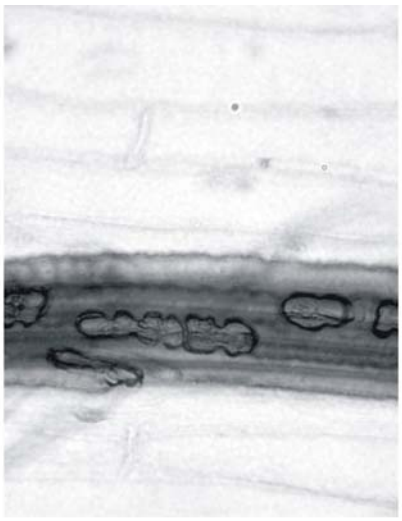

Poa binata Ellis 2852 (7851) Mountain slopes, moist areas.

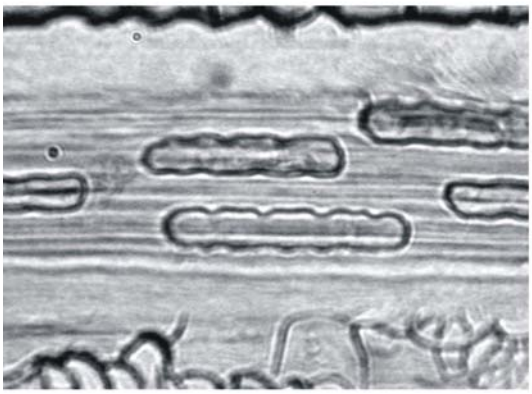

Poa bulbosa Ellis 2471 (7850) Seasonal pans, streamsides.

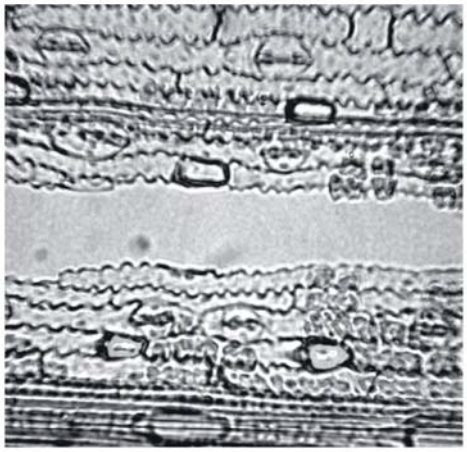

Prosphytochloa prehensilis Ellis 3783 (8148) Moist forests.

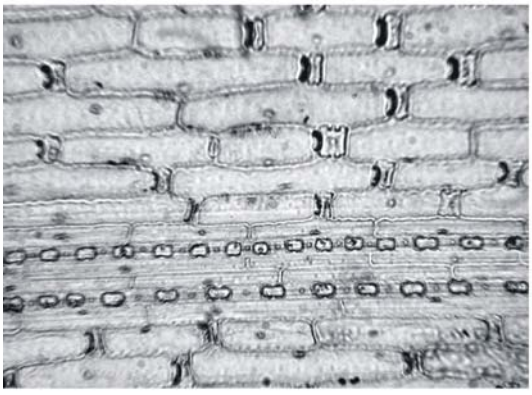

Pseudopentameris macrantha Ellis 2327 (8074) Mountain slopes, fynbos.

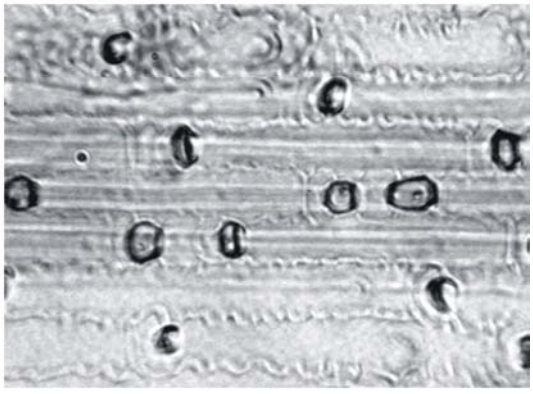

Puccinellia acroxantha Ellis 1674 (7860) Periodically flooded depressions.

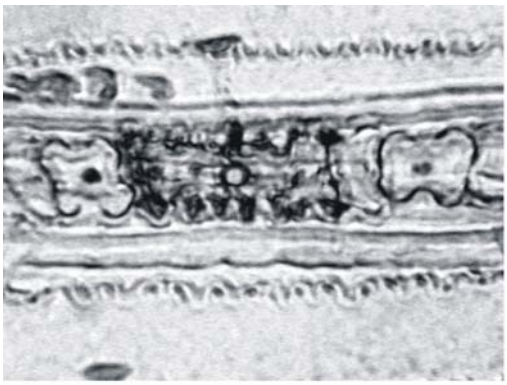

Rhytachne latifolia Ellis 4536 (8501)
Shades streamsides, woodland pans.

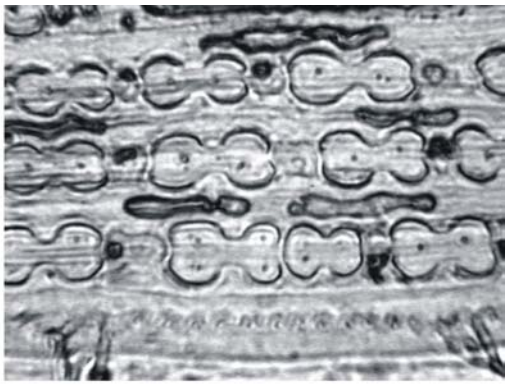

Rottboelia cochinchiniensis Ellis
3852 (8507) Wet places.

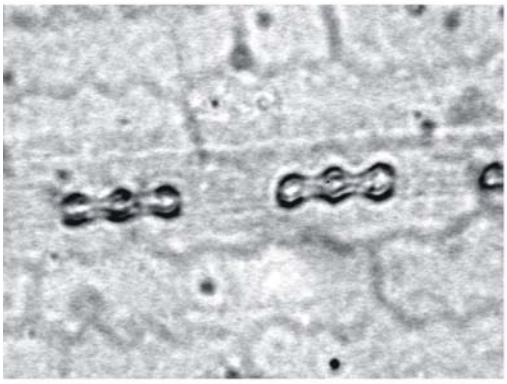

Sacciolepis curvata Ellis 3232 (8420) Damp,
shady places, forest undergrowth.

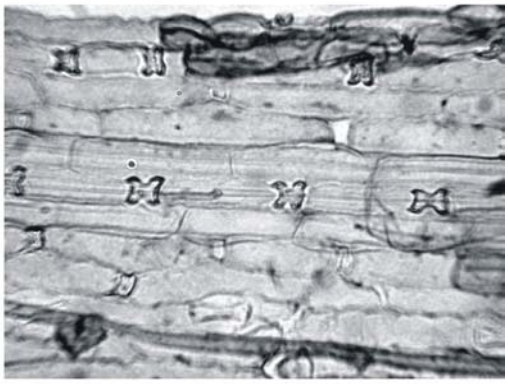

Sacciolepis typhura var. glaucescens Ellis
92 (8426), Swamps, marshy places.

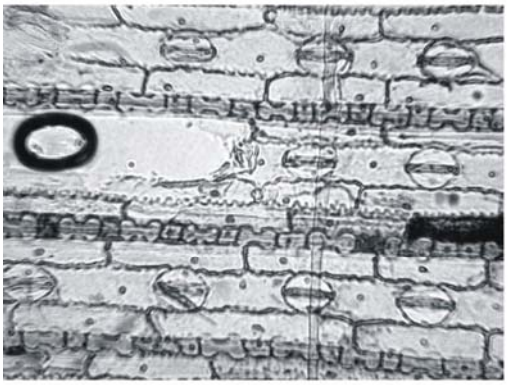

Schizachyrum sanguineum Ellis
4500 (8428) Open veld.

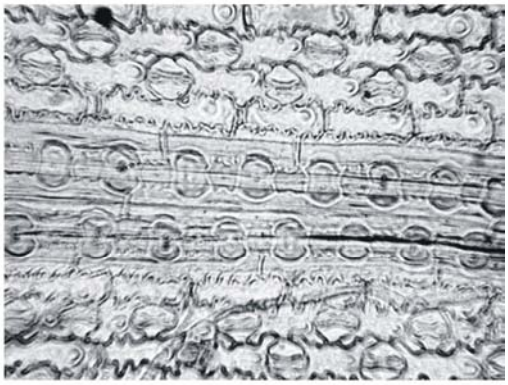

Schoenefeldia transiens Ellis 3867 (8133)
Open veld, seasonally flodded flats.

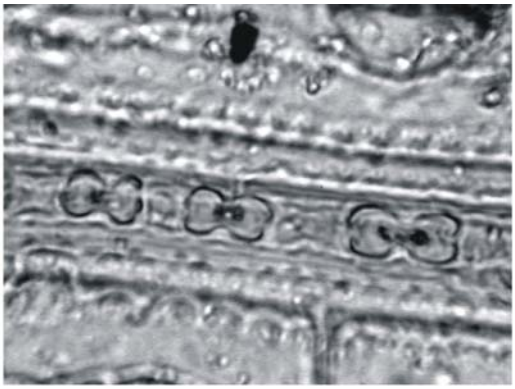

Setaria appendiculata Ellis 905 (8431) Rocky outcrops, among bushes, dry riverbeds

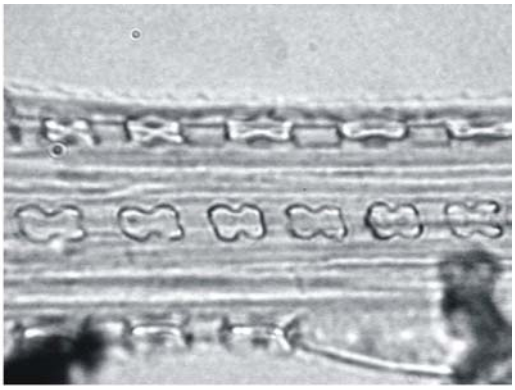

Setaria lindenbergiania de Wet 1066 (8435) Open woodland, forests, rocky hillsides

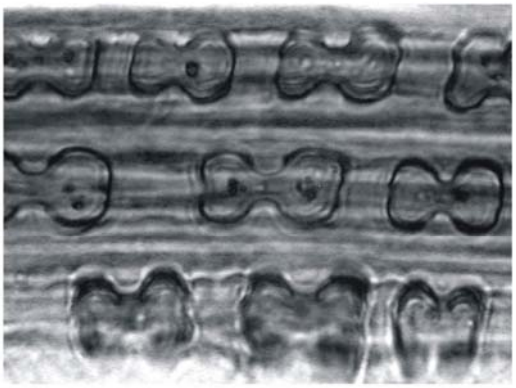

Setaria sphacelata Ellis 149 (8438) Moist places, hillsides

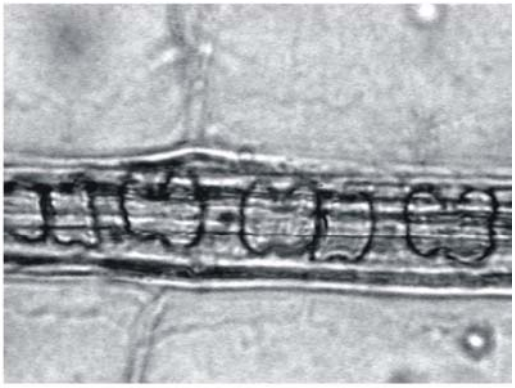

Setaria ustilata Ellis 2890 (8440) Dry bushveld regions, shade of trees, bushes

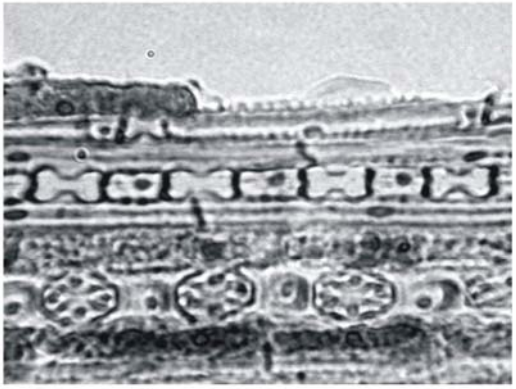

Sorghastrum friesii Ellis 3695 (8443) Wet places

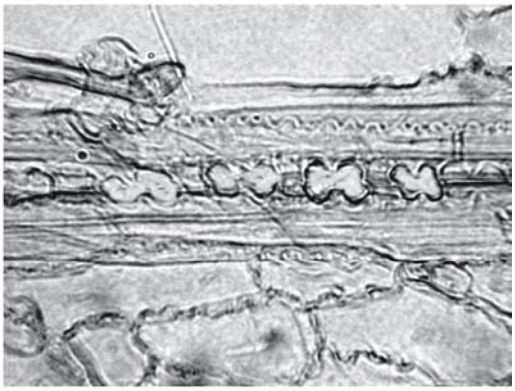

Sorghum bicolor Ellis 4429 (8445)

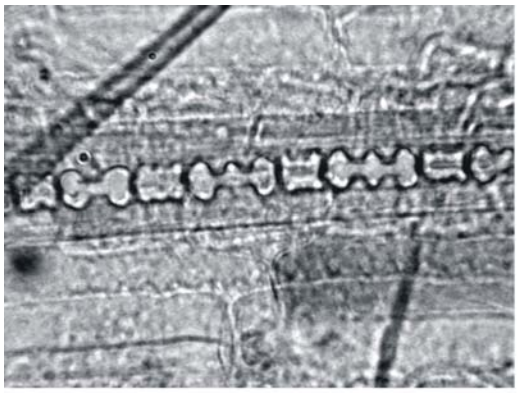

Sorghum versicolor Ellis 133 (8450)

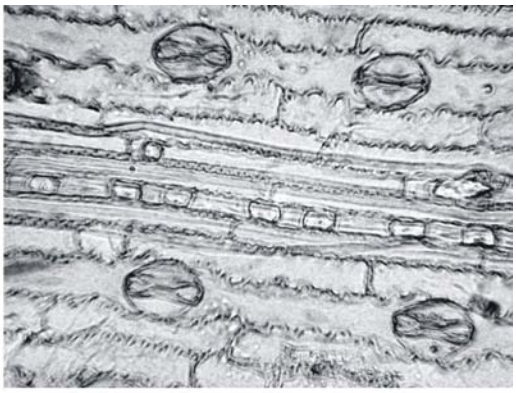

Sporobolus albicans Ellis 3658 (8134)
Limestone pans, dry depressions

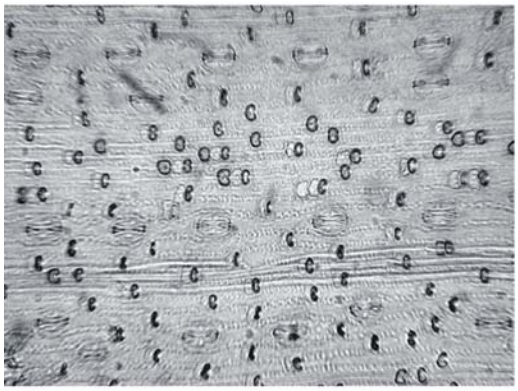

Sporobolus centrifugus Ellis 3658
(8135) High mountainveld

Sporobolus ludwiggi Ellis 850 (8136)
Damp calcareous soils, pans, vleis

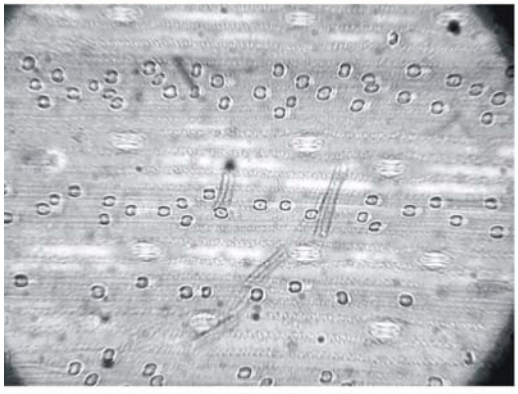

Sporobolus panicoides Ellis 1929 (8138)
Sandy, stony soils, hillsides

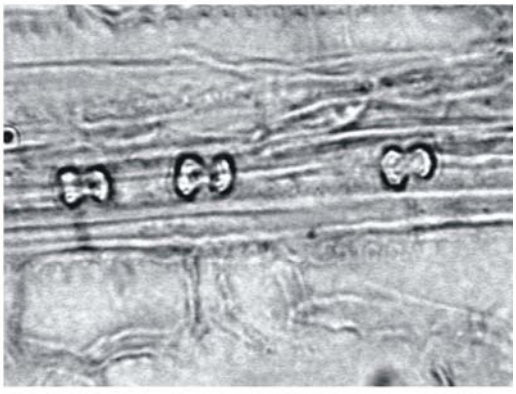

Stenotaphrum secundatum Ellis 267
(8454) Coastal beaches. marshes

Stenotaphrum secundatum Ellis 267 (8454)
Coastal beaches. marshes

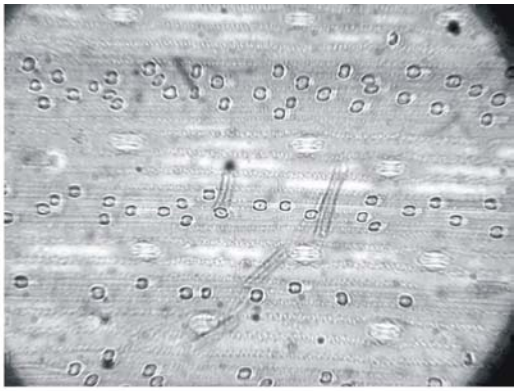

Stipa dregeana Ellis 2099 (8525) Forest

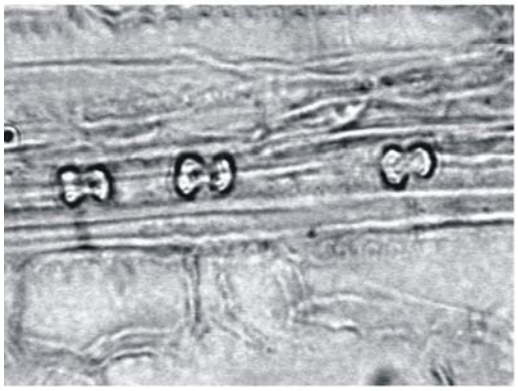

Stipagrostis anomala De Winter 3409 (7866)
Shallow sandy soils, open plains, arid regions

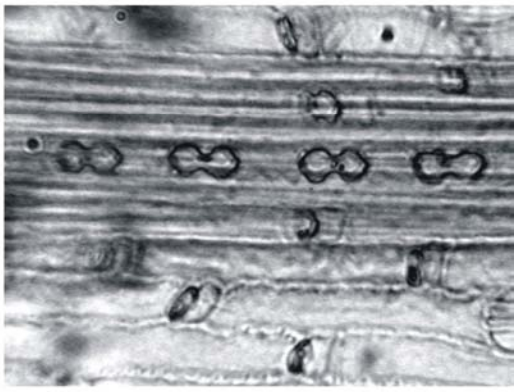

Stipagrostis brevifolia De Winter 3266
(7870) Open plians, arid regions

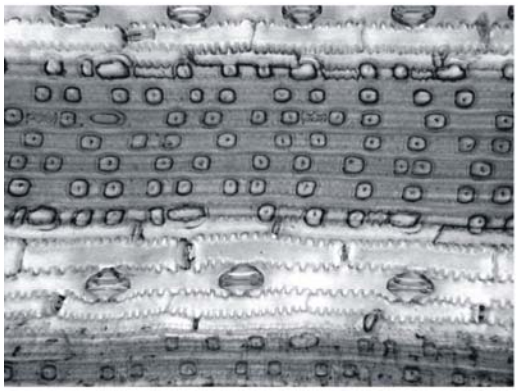

Stipagrostis damarensis De Winter
17837 (7872) Riverbeds, drainage
lines, arid regions

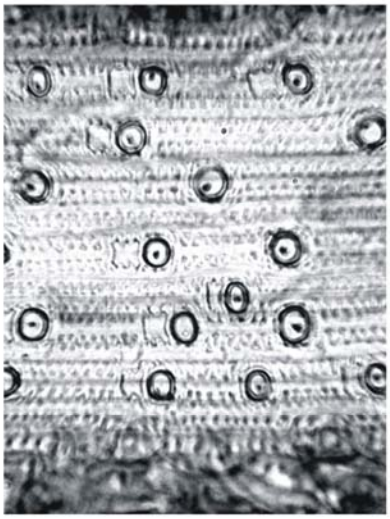

Stipagrostis dregeana De Winter
2572 (7874) Coarse sandy,
shallow soils, arid regions

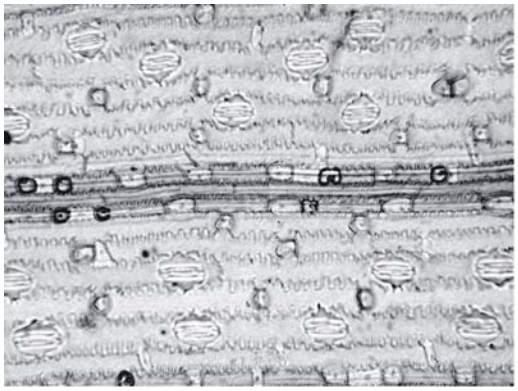

Stipagrostis fastigiata De Winter 3573 (7875) Sandy alkaline soils, arid regions

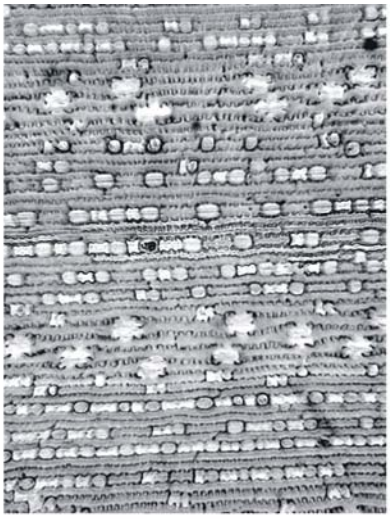

Stipagrostis garubensis De Winter 2289 (7877) Hillslopes, riverbeds, arid regions

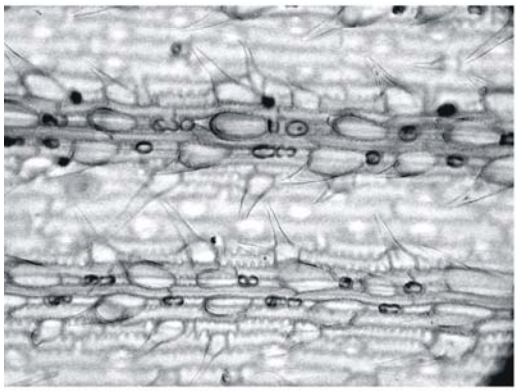

Stipagrostis hermanii De Winter Kinges 2634 (7881) Hills, open plains, arid regions

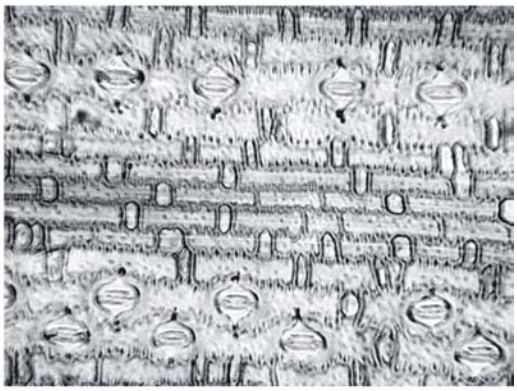

Stipagrostis lutescens De Winter Kinges 2445 (7888) Sandy soils, arid regions

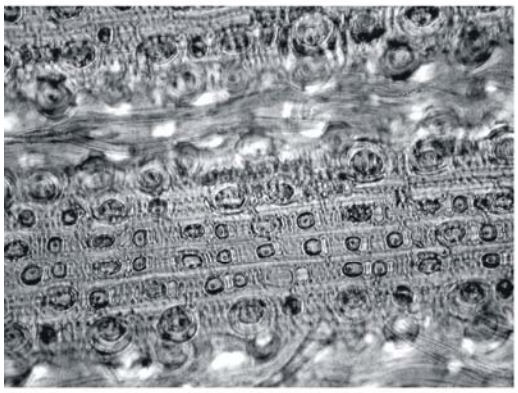

Stipagrostis proxima Flanagan 1657 (7891) Sandy soils, arid regions

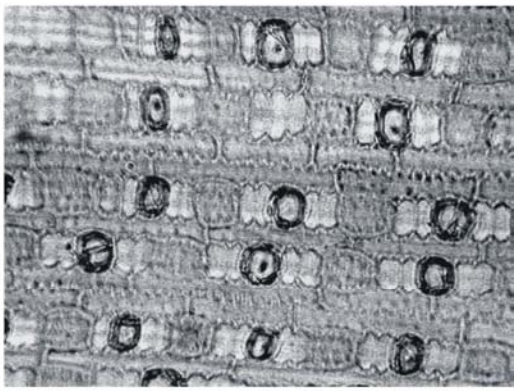

Stipagrostis sabulicola Keet 1612 (7894) Dunetops, sandy gullies, riverbeds, arid regions

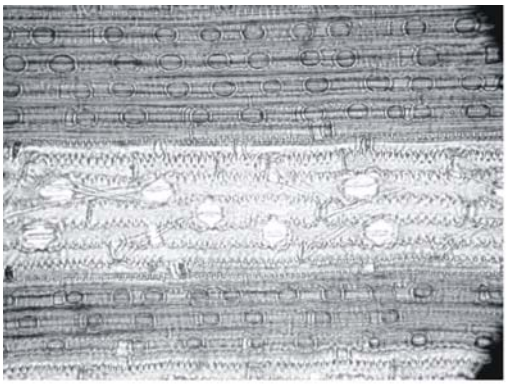

Stipagrostis schaeferii Kinges & De Winter 2586 (7896) Gravel plains, dry watercourses, arid regions

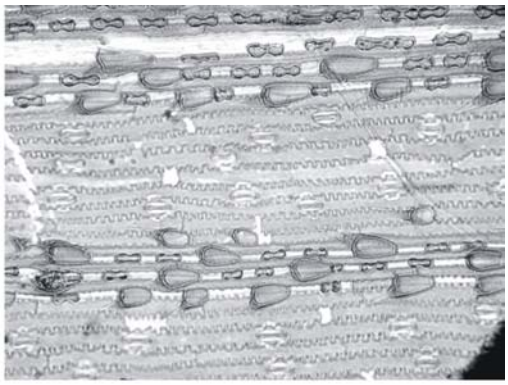

Stipagrostis subacaulis Schweick De Winter 2241 (7897) Coarse sandy soils, hillsides, arid regions

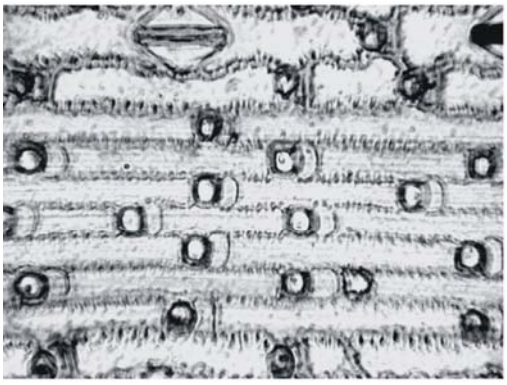

Stipagrostis zeyheri Bolus 12910 (7906) Sandy slopes, limestone hills, fynbos

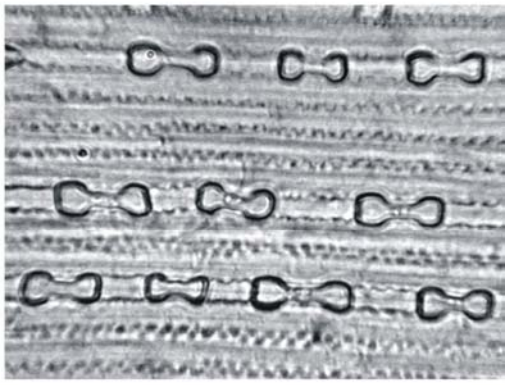

Styppeiochloa gynoglossa Ellis 3293 (8522) Rock crevices, seeps, rainfall above 800mm, high alt.

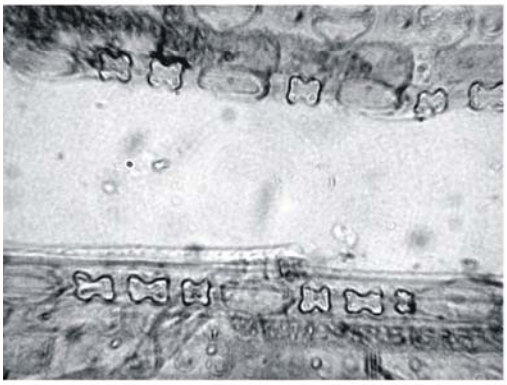

Themeda triandra Ellis 1670 (8458) Open veld

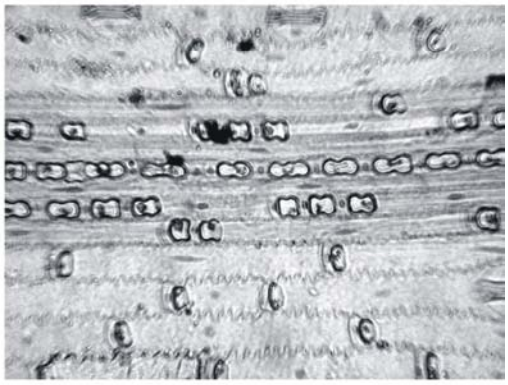

Tribolium acutiflorum Ellis 685 (8076) Sandy soils, fynbos

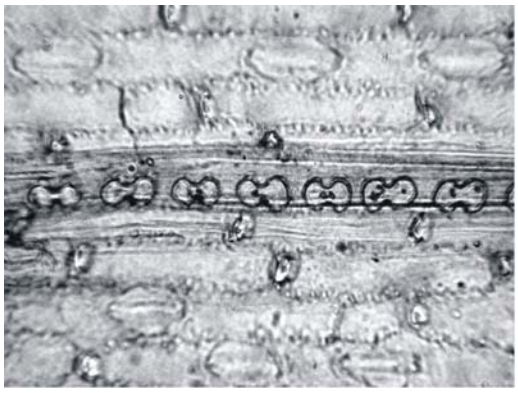

Tribolium alternans (Ellis 1210 (8082)
River flats, sandy soil, fynbos

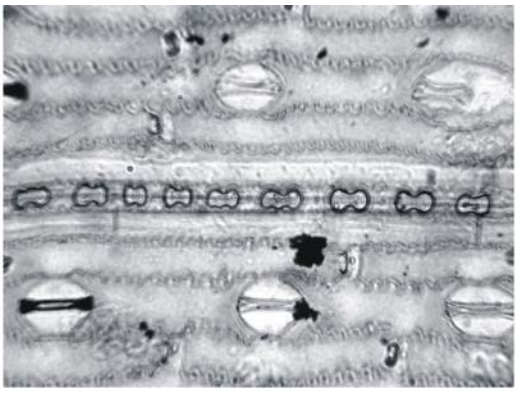

Tribolium brachystachyum Ellis 2213
(8080) Mountainous terrain, fynbos

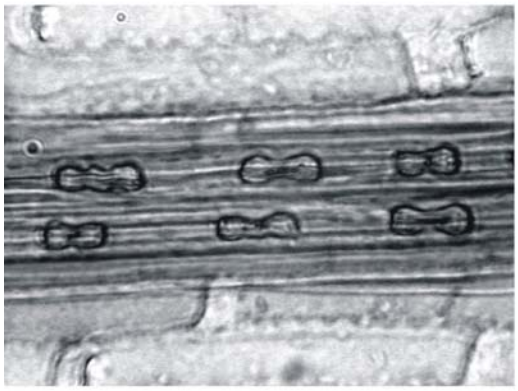

Tricholaena monachne Ellis 1935
(8463) Sandy soil, open veld

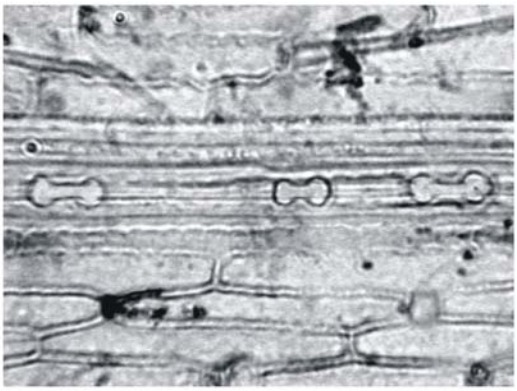

Trichopteryx dregeana Ellis 454 (8460)
Vleis, wet places, shady crevices

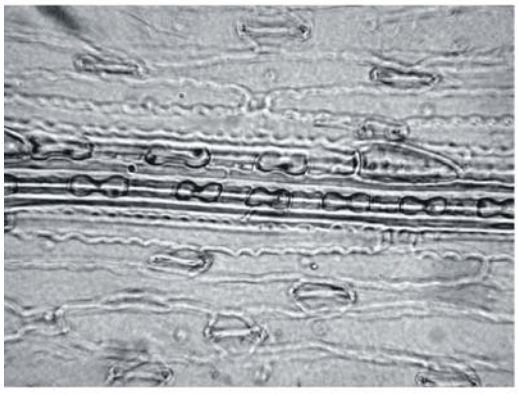

Triraphis purpurea Ellis 4367 (8141) Moist
places, shade, calcareous soils

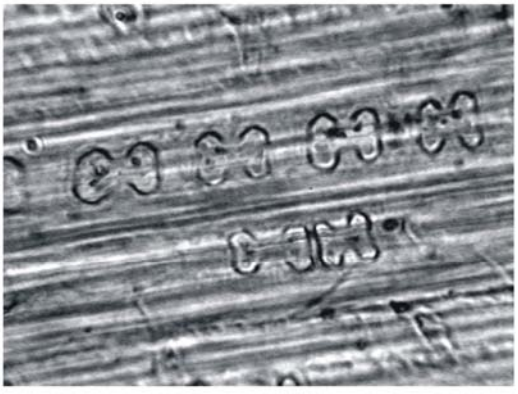

Tristachya biseriata Ellis 1333
(8467) Hillsides, rocky outcrops

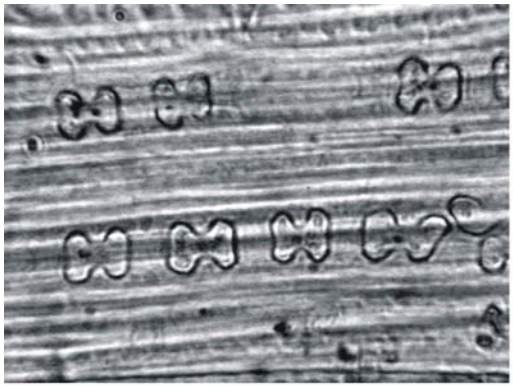

Tristachya leucothrix Ellis 297 (8468)
Marshy grassland, mountain sourveld

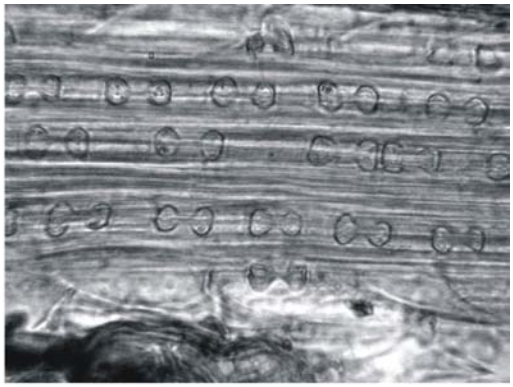

Tristachya rehmannii Ellis 1382
(8471) Open veld

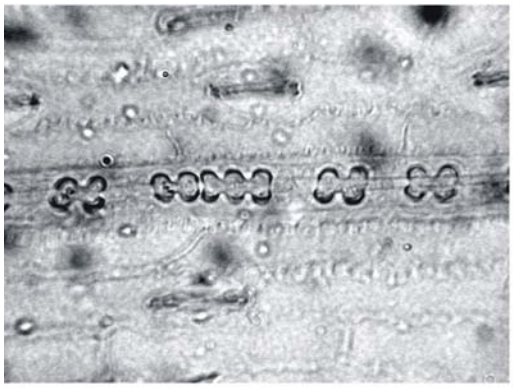

Urochloa brachyura Ellis 407
(8475) Woodland, shade

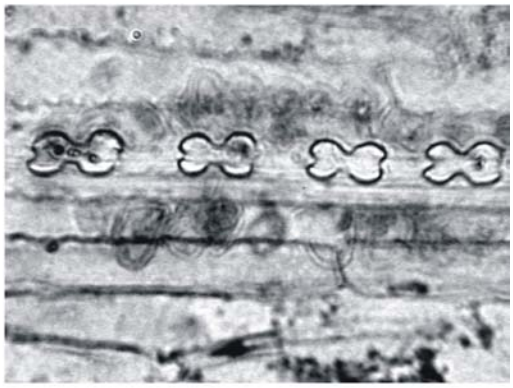

Urochloa mosambicensis Ellis 503
(8478) Sheltered places

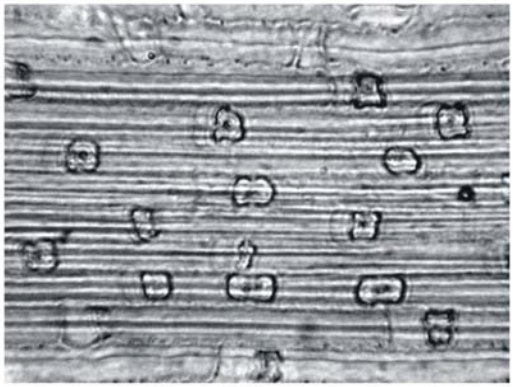

Vetiveria nigritana Ellis 579 (8481)
Wet places

Appendix 3: Indicator matrix of GSSC-morphotypes recorded in 309 grass species.

BINARY INDICATOR MATRIX
(Table 3: Association through Rate of Recurrence)

Genus	Species	Bilobate Var1	Bilobate Var 2	Bilobate Var 3	Polylobate	Cross	Saddle Var 1	Saddle Var 2	Trapezoid	Rondel	Oblong	Reniform
Agrostis	barbuligera	0	0	0	1	0	0	0	1	0	1	0
Agrostis	bergiana	0	0	0	1	0	0	0	1	0	1	0
Agrostis	eriantha	0	0	0	0	0	0	0	1	0	1	0
Agrostis	lachnanta	0	0	0	1	0	0	0	1	0	1	0
Alloteropsis	semialata	0	1	0	0	0	0	0	0	0	0	0
Andropogon	appendiculatus	0	1	0	0	0	0	0	0	0	0	0
Andropogon	festuciformis	1	1	0	0	0	0	0	0	0	0	0
Andropogon	gayanus	0	1	0	0	1	0	0	0	0	0	0
Andropogon	huillensis	1	1	0	0	0	0	0	0	0	0	0
Andropogon	laconosus	1	0	0	1	0	0	0	0	0	0	0
Andropogon	ravus	1	0	0	0	0	0	0	0	0	0	0
Andropogon	schirensis	0	1	0	0	0	0	0	0	0	0	0
Anthephora	argentea	0	1	0	0	1	0	0	0	0	0	0
Anthephora	pubescens	1	1	0	0	0	0	0	0	0	0	0
Anthoxantum	dregeanum	0	0	0	0	0	0	0	0	0	1	0
Anthoxantum	ecklonii	0	0	0	0	0	0	0	1	0	1	0
Anthoxantum	tongo	0	0	0	0	0	0	0	1	0	1	0
Aristida	bipartita	1	0	0	0	0	0	0	0	0	0	0
Aristida	canescens	1	0	0	0	0	0	0	0	0	0	0
Aristida	dasydesmis	0	0	0	0	0	1	1	0	0	0	0
Aristida	difusa	1	0	0	0	0	0	0	0	0	0	0
Aristida	junciformis	1	0	0	0	0	0	0	0	0	0	0
Aristida	monticola	1	0	0	0	0	0	0	0	0	0	0
Aristida	parvula	1	0	0	0	0	0	0	0	0	0	0
Aristida	scuirius	1	0	1	0	0	1	0	0	0	0	1
Aristida	transvaalensis	1	0	0	0	0	0	0	0	0	0	0
Bothriochloa	insculpta	0	1	0	1	0	0	0	0	0	0	0
Bothriochloa	bladhii	1	0	0	0	0	0	0	0	0	0	0
Brachiaria	arrecta	0	1	0	0	0	0	0	0	0	0	0
Brachiaria	ericuformis	0	1	1	0	1	0	0	0	0	0	0
Brachiaria	glomerata	1	0	0	0	0	0	0	0	0	0	0
Brachiaria	marlothii	1	0	0	0	1	0	0	0	0	0	0

NUMBER OF PHYTOLITHS (OUT OF A HUNDRED)
(Table 4: Relative Abundance)

Bilobate Var. 1	Bilobate Var. 2	Bilobate Var. 3	Polylobate	Cross	Saddle Var. 1	Saddle Var. 2	Trapezoid	Rondel	Oblong	Reniform
0	0	0	18	0	0	0	12	0	70	0
0	0	0	4	0	0	0	7	0	89	0
0	0	0	0	0	0	0	24	0	76	0
0	0	0	13	0	0	0	14	0	73	0
0	100	0	0	0	0	0	0	0	0	0
0	100	0	0	0	0	0	0	0	0	0
94	6	0	0	0	0	0	0	0	0	0
0	100	0	0	0	0	0	0	0	0	0
86	14	0	0	0	0	0	0	0	0	0
93	0	0	7	0	0	0	0	0	0	0
100	0	0	0	0	0	0	0	0	0	0
0	100	0	0	0	0	0	0	0	0	0
0	78	0	0	22	0	0	0	0	0	0
17	83	0	0	0	0	0	0	0	0	0
0	0	0	0	0	0	0	0	0	100	0
0	0	0	0	0	0	0	41	0	59	0
0	0	0	0	0	0	0	32	0	68	0
100	0	0	0	0	0	0	0	0	0	0
100	0	0	0	0	0	0	0	0	0	0
0	0	0	0	0	35	65	0	0	0	0
100	0	0	0	0	0	0	0	0	0	0
100	0	0	0	0	0	0	0	0	0	0
100	0	0	0	0	0	0	0	0	0	0
100	0	0	0	0	0	0	0	0	0	0
17	0	27	0	0	34	0	0	0	0	22
100	0	0	0	0	0	0	0	0	0	0
0	84	0	16	0	0	0	0	0	0	0
100	0	0	0	0	0	0	0	0	0	0
0	100	0	0	0	0	0	0	0	0	0
0	33	13	0	54	0	0	0	0	0	0
100	0	0	0	0	0	0	0	0	0	0
57	0	0	0	43	0	0	0	0	0	0

Genus	Species	Bilobate Var1	Bilobate Var 2	Bilobate Var 3	Polylobate	Cross	Saddle Var 1	Saddle Var 2	Trapezoid	Rondel	Oblong	Reniform
Brachiaria	serrata	0	1	0	1	1	0	0	0	0	0	0
Brachiaria	subulifolia	0	1	1	1	0	0	0	0	0	0	0
Brachychloa	schiemanniana	0	0	0	0	0	1	0	0	0	0	0
Brachypodium	bolussii	0	1	1	1	0	0	0	0	0	0	0
Brachypodium	flexum	0	1	1	0	0	0	0	0	0	0	0
Bromus	firmior	0	0	0	0	0	0	0	1	0	1	0
Bromus	speciosus	0	0	0	0	0	0	0	1	0	1	0
Chaetobromus	involucratus	0	0	0	0	0	0	0	1	0	0	0
Chaetobromus	dregeanus	0	1	0	0	0	0	1	1	0	0	0
Chloris	gayana	0	0	0	0	0	1	0	0	0	0	0
Chloris	virgata	0	0	0	0	0	1	0	0	0	0	0
Chloris	flabellata	0	0	0	0	0	1	0	0	0	0	0
Cladoraphis	spinosa	0	0	0	0	0	1	1	0	0	0	0
Coelachyrum	yemenicum	0	0	0	0	0	1	0	0	0	0	0
Colpodium	hedbergii	0	0	0	0	0	0	0	1	0	1	0
Ctenium	concinnum	1	1	0	0	0	0	0	0	0	0	0
Cymbopogon	plurinoides	0	1	0	0	1	0	0	0	0	0	0
Cymbopogon	marginatus	0	1	0	0	0	0	0	0	0	0	0
Cymbopogon	excavatus	0	1	0	0	0	0	0	0	0	0	0
Cynodon	dactylon	0	0	0	0	0	1	0	0	0	0	0
Cynodon	hirsutus	0	0	0	0	0	1	0	0	0	0	0
Dactyloctenium	giganteum	0	0	0	0	0	1	0	0	0	0	0
Dactyloctenium	australe	0	0	0	0	0	1	0	0	0	0	0
Danthoniopsis	parva	1	0	0	0	0	0	0	0	0	0	0
Danthoniopsis	pruinosa	1	0	0	0	0	0	0	0	0	0	0
Dichantium	annulatum	0	1	0	1	0	0	0	0	0	0	0
Digitaria	brazzae	0	1	0	0	0	0	0	0	0	0	0
Digitaria	diagonalis	0	1	0	0	0	0	0	0	0	0	0
Digitaria	diversinervis	0	1	0	0	1	0	0	0	0	0	0
Digitaria	monodactyla	0	1	0	0	0	0	0	0	0	0	0
Digitaria	setifolia	0	1	0	0	0	0	0	0	0	0	0
Diheteropogon	amplectens	1	0	0	1	0	0	0	0	0	0	0
Diheteropogon	filifolius	0	1	0	0	0	0	0	0	0	0	0
Dinebra	retroflexa	0	1	0	0	0	0	0	0	0	0	0
Diplachne	eleusine	0	0	0	0	0	1	0	0	0	0	0
Diplachne	fusca	0	0	0	0	0	1	0	0	0	0	0
Dregechloa	pumila	0	0	0	0	0	0	0	1	0	1	0

Genus	Species	Bilobate Var. 1	Bilobate Var. 2	Bilobate Var. 3	Polylobate	Cross	Saddle Var. 1	Saddle Var. 2	Trapezoid	Rondel	Oblong	Reniform
Brachiaria	serrata	0	67	0	20	13	0	0	0	0	0	0
Brachiaria	subulifolia	0	87	2	11	0	0	0	0	0	0	0
Brachychloa	schiemanniana	0	0	0	0	0	100	0	0	0	0	0
Brachypodium	bolussii	0	18	39	43	0	0	0	0	0	0	0
Brachypodium	flexum	0	0	56	22	0	0	0	0	0	22	0
Bromus	firmior	0	0	0	0	0	0	0	9	0	91	0
Bromus	speciosus	0	0	0	0	0	0	0	0	0	100	0
Chaetobromus	involucratus	0	0	0	0	0	0	0	100	0	0	0
Chaetobromus	dregeanus	0	8	0	0	0	0	13	79	0	0	0
Chloris	gayana	0	0	0	0	0	100	0	0	0	0	0
Chloris	virgata	0	0	0	0	0	100	0	0	0	0	0
Chloris	flabellata	0	0	0	0	0	100	0	0	0	0	0
Cladoraphis	spinosa	0	0	0	0	0	48	52	0	0	0	0
Coelachyrum	yemenicum	0	0	0	0	0	100	0	0	0	0	0
Colpodium	hedbergii	0	0	0	0	0	0	0	21	0	79	0
Ctenium	concinnum	83	17	0	0	0	0	0	0	0	0	0
Cymbopogon	plurinoides	0	67	0	0	33	0	0	0	0	0	0
Cymbopogon	marginatus	0	100	0	0	0	0	0	0	0	0	0
Cymbopogon	excavatus	0	100	0	0	0	0	0	0	0	0	0
Cynodon	dactylon	0	0	0	0	0	100	0	0	0	0	0
Cynodon	hirsutus	0	0	0	0	0	100	0	0	0	0	0
Dactyloctenium	giganteum	0	0	0	0	0	100	0	0	0	0	0
Dactyloctenium	australe	0	0	0	0	0	100	0	0	0	0	0
Danthoniopsis	parva	100	0	0	0	0	0	0	0	0	0	0
Danthoniopsis	pruinosa	100	0	0	0	0	0	0	0	0	0	0
Dichantium	annulatum	0	20	0	80	0	0	0	0	0	0	0
Digitaria	brazzae	0	100	0	0	0	0	0	0	0	0	0
Digitaria	diagonalis	0	100	0	0	0	0	0	0	0	0	0
Digitaria	diversinervis	0	63	0	0	37	0	0	0	0	0	0
Digitaria	monodactyla	0	100	0	0	0	0	0	0	0	0	0
Digitaria	setifolia	0	100	0	0	0	0	0	0	0	0	0
Diheteropogon	amplectens	82	0	0	18	0	0	0	0	0	0	0
Diheteropogon	filifolius	0	100	0	0	0	0	0	0	0	0	0
Dinebra	retroflexa	0	100	0	0	0	0	0	0	0	0	0
Diplachne	eleusine	0	0	0	0	0	100	0	0	0	0	0
Diplachne	fusca	0	0	0	0	0	100	0	0	0	0	0
Dregechloa	pumila	0	0	0	0	0	0	0	73	0	27	0

Genus	Species	Bilobate Var1	Bilobate Var 2	Bilobate Var 3	Polylobate	Cross	Saddle Var 1	Saddle Var 2	Trapezoid	Rondel	Oblong	Reniform	Bilobate Var. 1	Bilobate Var. 2	Bilobate Var. 3	Polylobate	Cross	Saddle Var. 1	Saddle Var. 2	Trapezoid	Rondel	Oblong	Reniform
Dregechloa	calviniensis	0	0	0	0	0	0	0	1	0	0	0	0	0	0	0	0	0	0	100	0	0	0
Echinochloa	colona	0	0	0	1	0	0	0	0	0	0	0	0	0	0	100	0	0	0	0	0	0	0
Echinochloa	holubii	0	1	1	0	1	0	0	0	0	0	0	0	31	27	0	42	0	0	0	0	0	0
Echinochloa	stagnina	0	1	0	1	0	0	0	0	0	0	0	0	7	0	93	0	0	0	0	0	0	0
Ehrharta	barbinodus	0	0	1	0	0	0	0	1	0	1	1	0	0	36	0	0	0	0	29	0	7	17
Ehrharta	brevifolia subs. brevifolia	0	1	1	0	0	0	0	1	0	0	0	0	57	23	0	0	0	0	20	0	0	0
Ehrharta	capensis subs. capensis	0	1	1	0	0	0	0	0	0	0	0	0	61	39	0	0	0	0	0	0	0	0
Ehrharta	delicatula	0	1	0	1	0	0	0	1	0	0	0	0	28	0	23	0	0	0	49	0	0	0
Ehrharta	dura	0	1	0	0	1	0	0	0	0	0	0	0	76	0	0	24	0	0	0	0	0	0
Ehrharta	eburnea	0	1	0	0	0	0	0	1	1	0	1	0	47	0	0	0	0	0	35	5	0	7
Ehrharta	erecta	0	1	0	1	0	0	0	1	1	0	0	0	43	0	4	0	0	0	44	9	0	0
Ehrharta	longiflora	0	1	1	0	0	0	0	1	1	1	1	0	37	15	0	0	0	0	30	2	6	10
Ehrharta	longigluma	0	0	0	0	0	0	0	1	1	0	1	0	0	0	0	0	0	0	69	7	0	24
Ehrharta	melicoides	0	0	0	0	0	0	0	1	1	0	1	0	0	0	0	0	0	0	88	3	0	9
Ehrharta	ramosa	0	1	0	0	0	0	0	1	0	0	0	0	35	0	0	0	0	0	65	0	0	0
Ehrharta	setacea	0	0	0	0	0	0	0	1	0	0	1	0	0	0	0	0	0	0	17	0	0	83
Ehrharta	villosa	0	1	0	0	0	0	0	1	1	0	1	0	24	0	0	0	0	0	31	12	0	33
Ehrharta	thunbergii	0	1	0	0	0	0	0	0	0	1	0	0	47	0	0	0	0	0	0	0	53	0
Elionurus	muticus (argenteus)	1	1	0	0	0	0	0	0	0	0	0	23	77	0	0	0	0	0	0	0	0	0
Enneapogon	scaber	0	1	0	0	0	0	0	0	0	0	0	0	100	0	0	0	0	0	0	0	0	0
Enneapogon	pretoriensis	0	1	0	0	0	0	0	0	0	0	0	0	100	0	0	0	0	0	0	0	0	0
Enteropogon	monostachys	0	0	0	0	0	1	0	0	0	0	0	0	0	0	0	0	0	100	0	0	0	0
Entolasia	imbricata	0	1	1	0	0	0	0	0	0	0	0	0	79	21	0	0	0	0	0	0	0	0
Entoplacamia	aristulata	0	0	0	0	0	1	0	0	0	0	0	0	0	0	0	0	0	100	0	0	0	0
Eragrostis	bicolor	0	0	1	0	0	1	0	0	0	0	0	0	0	3	0	0	0	97	0	0	0	0
Eragrostis	biflora	0	0	0	0	0	1	0	0	0	0	0	0	0	0	0	0	0	100	0	0	0	0
Eragrostis	brizantha	0	1	1	0	1	0	0	0	0	0	0	0	79	8	0	13	0	0	0	0	0	0
Eragrostis	chloromelas	0	0	0	0	0	1	1	0	0	0	0	0	0	0	0	0	0	91	9	0	0	0
Eragrostis	echinochloidea	0	0	0	0	0	1	1	0	0	0	0	0	0	0	0	0	0	97	3	0	0	0
Eragrostis	eliator	0	0	0	0	0	1	1	0	0	0	0	0	0	0	0	0	0	88	12	0	0	0
Eragrostis	homomalla	0	0	1	0	0	1	0	0	0	0	0	0	0	65	0	0	0	45	0	0	0	0
Eragrostis	kingesii	0	0	0	0	0	1	1	0	0	0	0	0	0	0	0	0	0	67	33	0	0	0
Eragrostis	lehmanniana	0	0	0	0	0	1	0	0	0	0	0	0	0	0	0	0	0	100	0	0	0	0
Eragrostis	macrochlamys	0	0	0	0	0	1	1	0	0	0	0	0	0	0	0	0	0	55	45	0	0	0
Eragrostis	obtusa	0	0	0	0	0	1	0	0	0	0	0	0	0	0	0	0	0	100	0	0	0	0

Genus	Species	Bilobate Var1	Bilobate Var 2	Bilobate Var 3	Polylobate	Cross	Saddle Var 1	Saddle Var 2	Trapezoid	Rondel	Oblong	Reniform	Bilobate Var. 1	Bilobate Var. 2	Bilobate Var. 3	Polylobate	Cross	Saddle Var. 1	Saddle Var. 2	Trapezoid	Rondel	Oblong	Reniform
Eragrostis	omahekensis	0	0	0	0	0	1	0	0	0	0	0	0	0	0	0	0	100	0	0	0	0	0
Eragrostis	patentissima	0	0	0	0	0	1	1	0	0	0	0	0	0	0	0	0	70	30	0	0	0	0
Eragrostis	pilgeriana	0	0	0	0	0	1	1	0	0	0	0	0	0	0	0	0	74	26	0	0	0	0
Eragrostis	planiculmis	0	0	0	0	0	1	0	0	0	0	0	0	0	0	0	0	100	0	0	0	0	0
Eragrostis	procumbens	0	0	1	0	0	1	0	0	0	0	0	0	0	47	0	0	53	0	0	0	0	0
Eragrostis	pseudo-obtusa	0	0	0	0	0	1	0	0	0	0	0	0	0	0	0	0	100	0	0	0	0	0
Eragrostis	remotiflora	0	0	0	0	0	1	0	0	0	0	0	0	0	0	0	0	100	0	0	0	0	0
Eragrostis	sabulosa	0	0	1	0	0	0	1	0	0	0	0	0	0	57	0	0	43	0	0	0	0	0
Eragrostis	tef	0	0	0	0	0	1	0	0	0	0	0	0	0	0	0	0	100	0	0	0	0	0
Eragrostis	truncata	0	0	0	0	0	1	1	0	0	0	0	0	0	0	0	0	93	7	0	0	0	0
Eragrostis	walteri	0	1	1	0	0	0	0	0	0	0	0	0	69	31	0	0	0	0	0	0	0	0
Eriochloa	meyeriana	0	1	0	0	0	0	0	0	0	0	0	0	100	0	0	0	0	0	0	0	0	0
Eriochloa	stapfiania	1	1	0	0	0	0	0	0	0	0	0	85	15	0	0	0	0	0	0	0	0	0
Eriochrysis	pallida	0	1	0	0	0	0	0	1	0	0	0	0	17	0	0	0	0	0	93	0	0	0
Eustachys	paspaloides	0	0	0	0	0	1	0	0	0	0	0	0	0	0	0	0	100	0	0	0	0	0
Festuca	costata	0	0	0	0	0	0	0	1	0	0	1	0	0	0	0	0	0	0	67	0	0	33
Festuca	caprina	0	0	0	0	0	0	0	1	0	0	0	0	0	0	0	0	0	0	57	0	0	43
Festuca	killikii	0	0	0	0	0	0	0	1	0	0	1	0	0	0	0	0	0	0	41	0	0	59
Festuca	longipes	0	0	0	0	0	0	0	1	1	0	0	0	0	0	0	0	0	0	11	89	0	0
Festuca	scabra	0	0	0	0	0	0	0	0	0	1	0	0	0	0	0	0	0	0	0	0	100	0
Fingerhuthia	africana	0	0	0	0	0	1	1	0	0	0	0	0	0	0	0	0	77	23	0	0	0	0
Harpochloa	falx	0	0	0	0	0	1	0	0	0	0	0	0	0	0	0	0	100	0	0	0	0	0
Helictotrichon	hirtulum	0	0	0	0	0	0	0	1	0	1	0	0	0	0	0	0	0	0	86	0	14	0
Helictotrichon	leoninum	0	0	0	0	0	0	0	1	0	0	0	0	0	0	0	0	0	0	100	0	0	0
Helictotrichon	longifolium	0	0	0	0	0	0	0	1	1	0	0	0	0	0	0	0	0	0	43	57	0	0
Helictotrichon	longum	0	0	0	0	0	0	0	1	0	1	0	0	0	0	0	0	0	0	33	0	67	0
Helictotrichon	namaquense	0	0	0	0	0	0	0	0	0	1	0	0	0	0	0	0	0	0	0	0	100	0
Helictotrichon	turgidulum	0	1	1	0	1	0	0	0	0	0	0	0	68	12	0	20	0	0	0	0	0	0
Hemarthria	altissima	0	0	0	0	1	0	0	0	0	0	0	0	0	0	0	100	0	0	0	0	0	0
Heteropogon	contortus	1	1	0	0	1	0	0	0	0	0	0	36	47	0	0	17	0	0	0	0	0	0
Hyparrhenia	anamesia	0	1	0	1	0	0	0	0	0	0	0	0	55	0	45	0	0	0	0	0	0	0
Hyparrhenia	dregeana	1	1	0	1	0	0	0	0	0	0	0	28	43	0	29	0	0	0	0	0	0	0
Hyparrhenia	tamba	0	1	0	0	0	0	0	1	0	0	0	0	91	0	0	0	0	0	9	0	0	0
Hyperthelia	dissoluta	1	0	0	1	0	0	0	0	0	0	0	89	0	0	21	0	0	0	0	0	0	0
Imperata	cylindrica	1	0	1	0	0	0	0	0	0	0	0	87	0	13	0	0	0	0	0	0	0	0

Genus	Species	Bilobate Var1	Bilobate Var 2	Bilobate Var 3	Polylobate	Cross	Saddle Var 1	Saddle Var 2	Trapezoid	Rondel	Oblong	Reniform	Bilobate Var. 1	Bilobate Var. 2	Bilobate Var. 3	Polylobate	Cross	Saddle Var. 1	Saddle Var. 2	Trapezoid	Rondel	Oblong	Reniform
Ischaemum	afrum	1	1	0	1	0	0	0	0	0	0	0	19	64	0	17	0	0	0	0	0	0	0
Karroochloa	tenella	0	1	0	0	0	0	0	1	0	0	0	0	57	0	0	0	0	0	43	0	0	0
Karroochloa	schismoides	0	1	0	0	0	0	0	0	0	1	0	0	27	0	0	0	0	0	0	0	73	0
Karroochloa	curva	0	1	0	1	0	0	0	0	0	0	0	0	79	0	21	0	0	0	0	0	0	0
Karroochloa	purpurea	0	1	0	0	0	0	0	0	0	0	0	0	100	0	0	0	0	0	0	0	0	0
Koeleria	capensis	0	0	0	0	0	0	0	1	0	1	1	0	0	0	0	0	0	0	79	0	17	4
Leersia	hexandra	0	1	0	0	0	0	0	0	0	0	0	0	100	0	0	0	0	0	0	0	0	0
Leucophrys	mesocoma	0	1	1	1	0	0	0	0	0	0	0	0	33	17	50	0	0	0	0	0	0	0
Lophacne	digitata	1	0	0	0	0	0	0	0	0	0	0	100	0	0	0	0	0	0	0	0	0	0
Loudetia	flavida	1	0	0	0	0	0	0	0	0	0	0	100	0	0	0	0	0	0	0	0	0	0
Loudetia	simplex	0	1	0	0	0	0	0	0	0	0	0	0	100	0	0	0	0	0	0	0	0	0
Megastachya	mucronata	0	1	0	0	0	0	0	0	0	0	0	0	100	0	0	0	0	0	0	0	0	0
Melenis	minutiflora	0	1	0	1	0	0	0	0	0	0	0	0	13	0	87	0	0	0	0	0	0	0
Melica	racemosa	0	1	0	1	0	0	0	0	0	1	0	0	41	0	35	0	0	0	0	0	24	0
Melica	decumbens	0	1	0	1	0	0	0	0	0	1	0	0	60	0	29	0	0	0	0	0	11	0
Merxmuellera	arundinaceae	0	0	0	0	0	0	0	1	0	0	1	0	0	0	0	0	0	0	61	0	0	39
Merxmuellera	aureocephala	0	0	0	0	0	0	1	1	0	0	1	0	0	0	0	0	0	7	81	0	0	12
Merxmuellera	cincta	0	0	0	0	0	0	1	1	0	0	1	0	0	0	0	0	0	7	39	0	0	54
Merxmuellera	decora	0	0	0	0	0	0	1	1	0	0	1	0	0	0	0	0	0	2	27	0	0	71
Merxmuellera	disticha	0	0	0	0	0	0	0	0	1	0	0	0	0	0	0	0	0	0	0	100	0	0
Merxmuellera	drakensbergensis	0	0	0	0	0	0	0	1	0	0	1	0	0	0	0	0	0	0	63	0	0	37
Merxmuellera	dura	0	0	0	0	0	0	1	1	1	0	1	0	0	0	0	0	0	4	67	21	0	12
Merxmuellera	guillarmodiae	0	1	0	0	0	0	0	1	1	0	1	0	48	0	0	0	0	0	11	27	0	14
Merxmuellera	macowanii	0	0	0	0	0	0	1	1	1	0	1	0	0	0	0	0	0	4	42	23	0	31
Merxmuellera	rangei	0	0	0	0	0	0	1	1	1	0	0	0	0	0	0	0	0	7	64	29	0	0
Merxmuellera	lupulina	0	0	0	0	0	0	0	1	0	0	1	0	0	0	0	0	0	11	63	0	0	26
Merxmuellera	rufa	0	0	0	0	0	0	0	1	0	0	1	0	0	0	0	0	0	0	92	0	0	8
Merxmuellera	stereophylla	0	0	0	0	0	0	0	0	1	0	1	0	0	0	0	0	0	0	0	96	0	4
Microchloa	caffra	0	0	0	0	0	1	1	0	0	0	0	0	0	0	0	0	0	97	3	0	0	0
Monocymbium	ceresiiforme	1	0	0	0	1	0	0	0	0	0	0	57	0	0	0	43	0	0	0	0	0	0
Oplismenus	hirtellus	1	0	0	1	0	0	0	0	0	1	0	33	0	0	67	0	0	0	0	0	0	0
Orepetium	capense	0	0	0	0	0	1	0	0	0	0	0	0	0	0	0	0	100	0	0	0	0	0
Oryza	longistaminata	1	0	0	0	0	0	0	0	0	0	0	100	0	0	0	0	0	0	0	0	0	0
Panicum	aequinerve	1	1	0	1	0	0	0	0	0	0	0	27	28	0	45	0	0	0	0	0	0	0
Panicum	deustum	0	1	0	1	0	0	0	0	0	0	0	0	11	0	89	0	0	0	0	0	0	0

Genus	Species	Bilobate Var1	Bilobate Var 2	Bilobate Var 3	Polylobate	Cross	Saddle Var 1	Saddle Var 2	Trapezoid	Rondel	Oblong	Reniform
Panicum	kalaharense	0	0	0	0	0	0	1	0	0	0	1
Panicum	arbusculum	0	1	0	0	0	0	0	0	0	0	0
Panicum	coloratum	0	1	0	0	1	0	0	0	0	0	0
Panicum	ecklonii	0	1	0	0	1	0	0	0	0	0	0
Panicum	heterostachyum	1	0	0	1	0	0	0	0	0	0	0
Panicum	hymeniochilum	0	1	0	0	1	0	0	0	0	0	0
Panicum	impeditum	0	1	0	0	0	0	0	0	0	0	0
Panicum	infestum	1	0	0	1	0	0	0	0	0	0	0
Panicum	lanipes	0	1	0	1	0	0	0	0	0	0	0
Panicum	laticomum	1	0	0	1	0	0	0	0	0	0	0
Panicum	maximum	1	1	0	1	0	0	0	0	0	0	0
Panicum	monticola	0	0	0	1	0	0	0	0	0	0	0
Panicum	natalense	1	1	0	0	0	0	0	0	0	0	0
Panicum	repens	0	1	0	0	0	0	0	0	0	0	0
Panicum	schinzii	0	1	0	0	0	0	0	0	0	0	0
Panicum	stapfianum	0	1	0	0	1	0	0	0	0	0	0
Panicum	subalbidum	0	1	0	0	0	0	0	0	0	0	0
Pennisetum	glaucocladum	0	1	1	0	0	0	0	0	0	0	0
Pennisetum	natalense	0	1	0	1	0	0	0	0	0	0	0
Pennisetum	sphacelatum	1	1	0	0	0	0	0	0	0	0	0
Pennisetum	thunbergii	0	1	1	0	0	0	0	0	0	0	0
Pennisetum	unisetum	1	1	0	0	0	0	0	0	0	0	0
Pentameris	dregeana	0	0	0	0	0	0	0	1	1	0	1
Pentameris	macrocalycina	0	0	0	0	0	0	0	1	1	0	0
Pentameris	obtusifolia	0	0	0	0	0	0	0	1	0	0	1
Pentameris	thuarii	0	0	0	0	0	0	0	1	1	0	0
Pentaschistis	acinosa	0	0	1	0	0	0	0	0	0	0	1
Pentaschistis	airoides subs airoides	0	1	0	0	0	0	0	0	0	0	0
Pentaschistis	ampla	0	1	0	0	0	0	0	0	0	0	0
Pentaschistis	aristidoides	0	0	0	0	0	0	0	1	0	0	1
Pentaschistis	aristifolia	0	1	1	0	0	0	0	0	0	0	0
Pentaschistis	aspera	0	0	1	0	0	0	0	0	0	0	0
Pentaschistis	aurea	0	1	1	0	0	0	0	0	0	0	0
Pentaschistis	barbata	0	1	1	0	0	0	0	1	0	0	0
Pentaschistis	basutorium	0	0	0	0	0	0	0	1	0	0	1

Genus	Species	Bilobate Var. 1	Bilobate Var. 2	Bilobate Var. 3	Polylobate	Cross	Saddle Var. 1	Saddle Var. 2	Trapezoid	Rondel	Oblong	Reniform
Panicum	kalaharense	0	0	0	0	0	0	67	0	0	0	33
Panicum	arbusculum	0	100	0	0	0	0	0	0	0	0	0
Panicum	coloratum	0	56	0	0	44	0	0	0	0	0	0
Panicum	ecklonii	0	71	0	0	29	0	0	0	0	0	0
Panicum	heterostachyum	89	0	0	11	0	0	0	0	0	0	0
Panicum	hymeniochilum	0	65	0	0	35	0	0	0	0	0	0
Panicum	impeditum	0	100	0	0	0	0	0	0	0	0	0
Panicum	infestum	46	0	0	54	0	0	0	0	0	0	0
Panicum	lanipes	0	81	0	19	0	0	0	0	0	0	0
Panicum	laticomum	93	0	0	7	0	0	0	0	0	0	0
Panicum	maximum	36	40	0	24	0	0	0	0	0	0	0
Panicum	monticola	0	0	0	100	0	0	0	0	0	0	0
Panicum	natalense	32	68	0	0	0	0	0	0	0	0	0
Panicum	repens	0	29	0	0	71	0	0	0	0	0	0
Panicum	schinzii	0	100	0	0	0	0	0	0	0	0	0
Panicum	stapfianum	0	70	0	0	30	0	0	0	0	0	0
Panicum	subalbidum	0	100	0	0	0	0	0	0	0	0	0
Pennisetum	glaucocladum	0	84	16	0	0	0	0	0	0	0	0
Pennisetum	natalense	0	80	0	20	0	0	0	0	0	0	0
Pennisetum	sphacelatum	41	59	0	0	0	0	0	0	0	0	0
Pennisetum	thunbergii	0	8	92	0	0	0	0	0	0	0	0
Pennisetum	unisetum	36	64	0	0	0	0	0	0	0	0	0
Pentameris	dregeana	0	0	0	0	0	0	0	0	51	40	9
Pentameris	macrocalycina	0	0	0	0	0	0	0	0	56	44	0
Pentameris	obtusifolia	0	0	0	0	0	0	0	0	37	0	63
Pentameris	thuarii	0	0	0	0	0	0	0	0	48	52	0
Pentaschistis	acinosa	0	0	86	0	0	0	0	0	0	0	14
Pentaschistis	airoides subs airoides	0	100	0	0	0	0	0	0	0	0	0
Pentaschistis	ampla	0	100	0	0	0	0	0	0	0	0	0
Pentaschistis	aristidoides	0	0	0	0	0	0	0	0	3	0	97
Pentaschistis	aristifolia	0	89	11	0	0	0	0	0	0	0	0
Pentaschistis	aspera	0	0	100	0	0	0	0	0	0	0	0
Pentaschistis	aurea	0	75	25	0	0	0	0	0	0	0	0
Pentaschistis	barbata	0	73	19	0	0	0	0	0	8	0	0
Pentaschistis	basutorium	0	0	0	0	0	0	0	0	21	0	79

Genus	Species	Bilobate Var1	Bilobate Var 2	Bilobate Var 3	Polylobate	Cross	Saddle Var 1	Saddle Var 2	Trapezoid	Rondel	Oblong	Reniform
Pentaschistis	capensis	0	0	0	0	0	0	0	1	0	0	0
Pentaschistis	capillaris	0	1	0	1	0	0	0	0	0	0	0
Pentaschistis	chippendallieae	0	1	1	0	0	0	0	0	0	0	1
Pentaschistis	colorata	0	1	1	0	0	0	0	0	0	0	1
Pentaschistis	curvifolia	0	0	0	0	0	0	0	1	0	0	1
Pentaschistis	densifolia	0	1	0	1	0	0	0	0	0	0	0
Pentaschistis	elegans	0	0	0	0	0	0	0	1	1	0	1
Pentaschistis	galpinii	0	1	1	0	0	0	0	0	0	0	0
Pentaschistis	glandulosa	0	1	1	0	0	0	0	1	0	0	0
Pentaschistis	natalensis	0	1	1	0	0	0	0	0	0	0	0
Pentaschistis	oreodoxa	0	1	1	0	0	0	0	0	0	0	0
Pentaschistis	lima	0	1	1	0	0	0	0	0	0	0	0
Pentaschistis	longipes	0	1	0	1	0	0	0	0	0	0	0
Pentaschistis	malouinensis	0	1	1	0	0	0	0	0	0	0	0
Pentaschistis	microphylla	0	1	1	0	0	0	0	1	0	0	0
Pentaschistis	pallescens	0	1	0	0	0	0	0	0	0	0	0
Pentaschistis	patula	0	1	0	0	0	0	0	0	0	0	0
Pentaschistis	pseudopallescens	0	1	0	1	0	0	0	0	0	0	0
Pentaschistis	rigidissima	0	0	0	0	0	0	0	1	0	0	1
Pentaschistis	rupestris	1	1	0	1	0	0	0	0	0	0	0
Pentaschistis	setifolia	0	1	1	0	0	0	0	0	0	0	0
Pentaschistis	tomentella	1	0	0	0	0	0	0	0	0	0	0
Pentaschistis	tortuosa	0	1	0	0	0	0	0	0	0	0	0
Pentaschistis	triseta	0	1	0	1	0	0	0	0	0	0	0
Pentaschistis	velutina	0	0	0	0	0	0	0	1	0	0	1
Perotis	patens	1	0	0	0	0	0	0	0	0	0	0
Phacelaris	franksae	0	0	0	0	0	0	0	1	0	0	1
Poa	bulbosa	0	0	0	0	0	0	0	0	0	1	0
Poa	binata	0	0	0	0	0	0	0	0	0	1	0
Pogonarthria	squarosa	0	0	0	0	0	1	0	0	0	0	0
Prosphytochloa	prehensilis	0	1	1	0	0	0	0	0	0	0	0
Pseudopentameris	macrantha	0	1	1	0	0	0	0	0	1	1	0
Puccinella	angusta	0	0	0	0	0	0	0	1	1	0	0
Puccinella	acroxantha	0	0	0	0	0	0	0	1	1	0	0
Rendlia	altera	0	0	0	0	0	1	0	0	0	0	0

Genus	Species	Bilobate Var. 1	Bilobate Var. 2	Bilobate Var. 3	Polylobate	Cross	Saddle Var. 1	Saddle Var. 2	Trapezoid	Rondel	Oblong	Reniform
Pentaschistis	capensis	0	0	0	0	0	0	0	100	0	0	0
Pentaschistis	capillaris	0	47	0	50	0	0	0	3	0	0	0
Pentaschistis	chippendallieae	0	77	11	0	0	0	0	0	0	0	12
Pentaschistis	colorata	0	69	15	0	0	0	0	0	0	0	16
Pentaschistis	curvifolia	0	0	0	0	0	0	0	78	0	0	22
Pentaschistis	densifolia	0	81	0	19	0	0	0	0	0	0	0
Pentaschistis	elegans	0	0	0	0	0	0	0	58	19	0	23
Pentaschistis	galpinii	0	88	12	0	0	0	0	0	0	0	0
Pentaschistis	glandulosa	0	89	5	0	0	0	0	6	0	0	0
Pentaschistis	natalensis	0	97	3	0	0	0	0	0	0	0	0
Pentaschistis	oreodoxa	0	83	17	0	0	0	0	0	0	0	0
Pentaschistis	lima	0	99	1	0	0	0	0	0	0	0	0
Pentaschistis	longipes	0	41	0	59	0	0	0	0	0	0	0
Pentaschistis	malouinensis	0	95	5	0	0	0	0	0	0	0	0
Pentaschistis	microphylla	0	27	19	0	0	0	0	54	0	0	0
Pentaschistis	pallescens	0	100	0	0	0	0	0	0	0	0	0
Pentaschistis	patula	0	100	0	0	0	0	0	0	0	0	0
Pentaschistis	pseudopallescens	0	94	0	6	0	0	0	0	0	0	0
Pentaschistis	rigidissima	0	0	0	0	0	0	0	89	0	0	11
Pentaschistis	rupestris	66	29	0	5	0	0	0	0	0	0	0
Pentaschistis	setifolia	0	85	15	0	0	0	0	0	0	0	0
Pentaschistis	tomentella	100	0	0	0	0	0	0	0	0	0	0
Pentaschistis	tortuosa	0	100	0	0	0	0	0	0	0	0	0
Pentaschistis	triseta	0	71	0	29	0	0	0	0	0	0	0
Pentaschistis	velutina	0	0	0	0	0	0	0	43	0	0	57
Perotis	patens	100	0	0	0	0	0	0	0	0	0	0
Phacelaris	franksae	0	0	0	0	0	0	0	80	0	0	20
Poa	bulbosa	0	0	0	0	0	0	0	0	0	100	0
Poa	binata	0	0	0	0	0	0	0	0	0	100	0
Pogonarthria	squarosa	0	0	0	0	0	100	0	0	0	0	0
Prosphytochloa	prehensilis	0	21	79	0	0	0	0	0	0	0	0
Pseudopentameris	macrantha	0	43	5	0	0	0	0	0	13	39	0
Puccinella	angusta	0	0	0	0	0	0	0	12	88	0	0
Puccinella	acroxantha	0	0	0	0	0	0	0	6	94	0	0
Rendlia	altera	0	0	0	0	0	100	0	0	0	0	0

Genus	Species	Bilobate Var1	Bilobate Var 2	Bilobate Var 3	Polylobate	Cross	Saddle Var 1	Saddle Var 2	Trapezoid	Rondel	Oblong	Reniform	Bilobate Var. 1	Bilobate Var. 2	Bilobate Var. 3	Polylobate	Cross	Saddle Var. 1	Saddle Var. 2	Trapezoid	Rondel	Oblong	Reniform
Rhytachne	latifolia	0	1	0	0	1	0	0	0	0	0	0	0	85	0	0	15	0	0	0	0	0	0
Rottboellia	cochinchinensis	0	1	0	0	0	0	0	0	0	0	0	0	100	0	0	0	0	0	0	0	0	0
Sacciolepis	curvata	0	1	0	1	0	0	0	0	0	0	0	0	66	0	34	0	0	0	0	0	0	0
Sacciolepis	typhura	0	1	1	1	1	0	0	0	0	0	0	0	32	27	19	22	0	0	0	0	0	0
Schismus	inermus	0	0	0	0	0	0	0	1	1	1	0	0	0	0	0	0	0	0	56	31	13	0
Schizachyrium	sanguineum	0	1	0	0	0	0	0	0	0	0	0	0	100	0	0	0	0	0	0	0	0	0
Schmidtia	pappophoroides	1	0	0	0	0	0	0	0	0	0	0	100	0	0	0	0	0	0	0	0	0	0
Schoenefeldia	transiensis	0	0	0	0	0	1	0	0	0	0	0	0	0	0	0	0	100	0	0	0	0	0
Setaria	sphacelata	0	1	0	0	0	0	0	0	0	0	0	0	100	0	0	0	0	0	0	0	0	0
Setaria	appendiculata	0	1	0	0	0	0	0	0	0	0	0	0	100	0	0	0	0	0	0	0	0	0
Setaria	incrassata	0	1	0	0	1	0	0	0	0	0	0	0	83	0	0	17	0	0	0	0	0	0
Setaria	lindenbergiana	0	1	0	0	0	0	0	0	0	0	0	0	100	0	0	0	0	0	0	0	0	0
Setaria	ustilata	0	1	0	0	0	0	0	0	0	0	0	0	100	0	0	0	0	0	0	0	0	0
Sorghastrum	friesii	0	1	0	0	0	0	0	0	0	0	0	0	100	0	0	0	0	0	0	0	0	0
Sorghum	bicolor	0	1	0	1	0	0	0	0	0	0	0	0	97	0	3	0	0	0	0	0	0	0
Sorghum	versicolor	1	1	0	1	0	0	0	0	0	0	0	27	4	0	69	0	0	0	0	0	0	0
Sporobolus	ludwiggi	0	1	0	0	0	0	0	0	0	0	0	0	100	0	0	0	0	0	0	0	0	0
Sporobolus	panicoides	0	0	0	0	0	1	1	0	0	0	0	0	0	0	0	0	0	94	6	0	0	0
Sporobolus	pectinatus	0	0	0	0	0	1	1	0	0	0	0	0	0	0	0	0	0	66	34	0	0	0
Sporobolus	africanus	0	0	0	0	0	1	1	0	0	0	1	0	0	0	0	0	0	61	39	0	0	0
Sporobolus	fimbriatus	0	0	0	0	0	1	1	0	0	0	0	0	0	0	0	0	0	59	41	0	0	0
Sporobolus	pyrimidalis	0	0	0	0	0	1	1	0	0	0	0	0	0	0	0	0	0	77	23	0	0	0
Sporobolus	centrifugus	0	0	0	0	0	1	1	0	0	0	0	0	0	0	0	0	0	83	17	0	0	0
Stenotaphrum	secundatum	0	1	0	0	0	0	0	0	0	0	0	0	100	0	0	0	0	0	0	0	0	0
Stipa	dregeana	0	1	0	1	0	0	0	0	0	0	0	0	52	0	48	0	0	0	0	0	0	0
Stipagrostis	anomala	0	0	0	0	0	0	1	0	0	0	0	0	0	0	0	0	0	0	100	0	0	0
Stipagrostis	brevifolia	0	0	0	0	0	0	1	0	0	0	0	0	0	0	0	0	0	0	100	0	0	0
Stipagrostis	damarensis	0	0	0	0	0	0	1	0	0	0	0	0	0	0	0	0	0	0	100	0	0	0
Stipagrostis	dregeana	0	0	0	0	0	0	1	0	0	0	0	0	0	0	0	0	0	0	100	0	0	0
Stipagrostis	fastigiata	0	0	0	0	0	0	1	0	0	0	0	0	0	0	0	0	0	0	100	0	0	0
Stipagrostis	garubensis	0	1	0	0	0	0	1	0	0	0	0	0	0	0	0	0	0	0	100	0	0	0
Stipagrostis	geminifolia	0	0	0	0	0	0	1	1	0	0	1	0	0	0	0	0	0	0	63	11	0	24
Stipagrostis	hermanii	0	1	0	0	0	0	1	1	1	0	0	0	29	0	0	0	0	0	60	9	2	0
Stipagrostis	lanipes	0	0	0	0	0	0	1	1	0	0	1	0	0	0	0	0	0	0	76	5	0	19
Stipagrostis	lutescens	0	0	0	0	0	0	1	0	0	0	1	0	0	0	0	0	0	0	56	0	0	44

Genus	Species	Bilobate Var1	Bilobate Var 2	Bilobate Var 3	Polylobate	Cross	Saddle Var 1	Saddle Var 2	Trapezoid	Rondel	Oblong	Reniform	Bilobate Var. 1	Bilobate Var. 2	Bilobate Var. 3	Polylobate	Cross	Saddle Var. 1	Saddle Var. 2	Trapezoid	Rondel	Oblong	Reniform
Stipagrostis	lutescens marlothii	0	0	0	0	0	0	1	0	0	0	1	0	0	0	0	0	0	52	0	0	0	48
Stipagrostis	namaquensis	0	0	0	0	0	0	1	0	0	0	0	0	0	0	0	0	0	100	0	0	0	0
Stipagrostis	proxima	0	0	0	0	0	0	1	0	0	0	0	0	0	0	0	0	0	100	0	0	0	0
Stipagrostis	sabulicola	0	0	0	0	0	0	1	0	0	0	0	0	0	0	0	0	0	100	0	0	0	0
Stipagrostis	schaeferi	0	0	0	0	0	0	1	0	0	0	0	0	0	0	0	0	0	100	0	0	0	0
Stipagrostis	subacaulis	1	1	0	0	0	0	0	0	0	0	0	61	39	0	0	0	0	0	0	0	0	0
Stipagrostis	uniplumis var neesii	0	0	0	0	0	0	1	0	0	0	0	0	0	0	0	0	0	100	0	0	0	0
Stipagrostis	zeyheri var barbata	0	0	0	0	0	0	1	0	0	0	0	0	0	0	0	0	0	100	0	0	0	0
Stipagrostis	zeyheri subs zeyheri	0	0	0	0	0	0	1	0	0	0	0	0	0	0	0	0	0	100	0	0	0	0
Stipagrostis	zeyheri subs macropus	0	0	0	0	0	0	1	0	1	0	0	0	0	0	0	0	0	67	0	33	0	0
Stypeiochloa	gynoglossa	1	0	0	0	0	0	0	0	0	0	0	100	0	0	0	0	0	0	0	0	0	0
Targidia	aequiglumis	0	1	0	0	0	0	0	0	0	0	0	0	100	0	0	0	0	0	0	0	0	0
Themeda	triandra	0	1	0	0	1	0	0	0	0	0	0	0	77	0	0	23	0	0	0	0	0	0
Tragus	berteronianus	0	0	0	0	0	1	0	0	0	0	0	0	0	0	0	0	100	0	0	0	0	0
Tribolium	acutiflorum	0	1	1	1	0	0	0	0	0	0	0	0	71	22	7	0	0	0	0	0	0	0
Tribolium	uniolae	0	1	0	1	0	0	0	1	0	0	1	0	66	0	19	0	0	0	11	0	0	14
Tribolium	brachystachyum	0	1	0	1	0	0	0	0	0	0	0	0	81	0	19	0	0	0	0	0	0	0
Tribolium	alternans	0	1	1	0	0	0	0	0	0	0	0	0	93	7	0	0	0	0	0	0	0	0
Tribolium	utriculosum	0	0	0	1	0	0	0	0	0	1	0	0	0	0	67	0	0	0	0	0	33	0
Tribolium	hispidum	0	1	0	0	0	0	0	0	0	0	0	0	100	0	0	0	0	0	0	0	0	0
Tricholaena	monachne	0	1	0	1	0	0	0	0	0	0	0	0	86	0	14	0	0	0	0	0	0	0
Trichopterix	dregeana	1	0	0	0	0	0	0	0	0	0	0	100	0	0	0	0	0	0	0	0	0	0
Triraphus	purpurea	1	1	0	0	0	0	0	0	0	0	0	44	56	0	0	0	0	0	0	0	0	0
Triraphus	andropogonoides	0	1	0	0	1	0	0	0	0	0	0	0	75	0	0	25	0	0	0	0	0	0
Tristachya	biserata	0	1	0	0	1	0	0	0	0	0	0	0	76	0	0	24	0	0	0	0	0	0
Tristachya	leucothrix	1	0	0	0	0	0	0	0	0	0	0	100	0	0	0	0	0	0	0	0	0	0
Tristachya	rehmannii	1	0	0	0	0	0	0	0	0	0	0	100	0	0	0	0	0	0	0	0	0	0
Urochloa	mossambicensis	0	1	0	0	0	0	0	0	0	0	0	0	100	0	0	0	0	0	0	0	0	0
Urochloa	brachyura	0	1	0	1	0	0	0	0	0	0	0	0	97	0	3	0	0	0	0	0	0	0
Vetiveria	nigritana	0	0	1	0	0	0	0	1	0	0	0	0	0	66	0	0	0	0	34	0	0	0

Appendix 4: Spearman's rank-order correlation between association through rate of recurrence of morphotypes and relative abundance of morphotypes.

Appendix 4.

Spearman's rank-order correlation between association through rate of recurrence of morphotypes and relative abundance of morphotypes. Bivariate plots with 95% confidence limits show positive covariation between the two categories.

Variable	Spearman Rank Order Correlations MD pairwise deleted. Matrix of two lists (Frequency vs Relative Abundance) Marked correlations are significant at p <.05000										
	Bilobate Var1	Bilobate Var2	Bilobate Var3	Polylobate	Cross	Saddle Var1	Saddle Var2	Trapezoid	Rondel	Oblong	Reniform
Bilobate Var1	0.937810	0.678471	0.277911	0.515292	0.605797	0.078268	-0.594274	-0.552979	-0.645940	-0.207638	-0.613666
Bilobate Var2	0.804054	0.956722	0.491987	0.851279	0.826738	-0.296315	-0.694867	-0.114950	-0.317882	0.349765	-0.366141
Bilobate Var3	0.406702	0.574033	0.742621	0.324950	0.582474	0.162495	-0.237840	-0.114950	-0.271135	0.247168	-0.247145
Polylobate	0.693439	0.876712	0.379135	0.938083	0.706213	-0.416745	-0.673081	0.000000	-0.253011	0.570249	-0.350921
Cross	0.861528	0.829676	0.440344	0.563979	0.850332	-0.104236	-0.673840	-0.408651	-0.461351	-0.101712	-0.526546
Saddle Var1	-0.020391	-0.544009	-0.149312	-0.601411	-0.494320	0.945941	0.452617	-0.315890	-0.183521	-0.567043	0.172188
Saddle Var2	-0.617766	-0.711950	-0.238528	-0.662421	-0.709437	0.486217	0.963558	0.380972	0.500096	-0.244558	0.624020
Trapezoid	-0.485936	-0.022989	0.299786	0.004619	-0.175405	-0.207403	0.418880	0.983761	0.849208	0.682446	0.812935
Rondel	-0.570856	-0.087358	0.084315	-0.036952	-0.274959	-0.236343	0.428293	0.937358	0.967153	0.480065	0.803697
Oblong	-0.160289	0.415010	0.396676	0.562136	0.283667	-0.520971	-0.152745	0.616513	0.373210	0.988070	0.203774
Reniform	-0.523570	-0.223235	0.264559	-0.274606	-0.375790	0.215067	0.690204	0.873621	0.850802	0.345102	0.915353

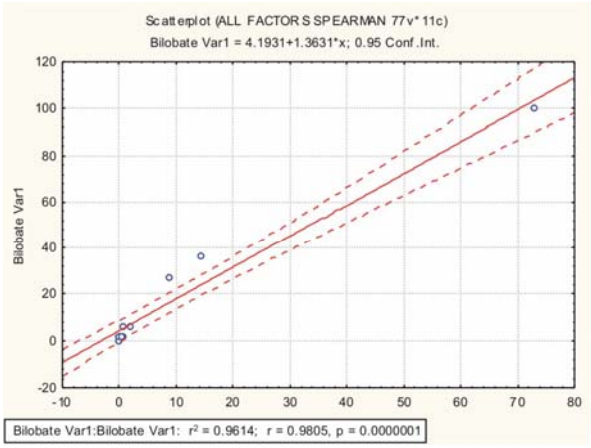
Scatterplot (ALL FACTORS SPEARMAN 77v*11c)
Bilobate Var1 = 4.1931+1.3631*x; 0.95 Conf.Int.
Bilobate Var1
Bilobate Var1:Bilobate Var1: r² = 0.9614; r = 0.9805, p = 0.0000001

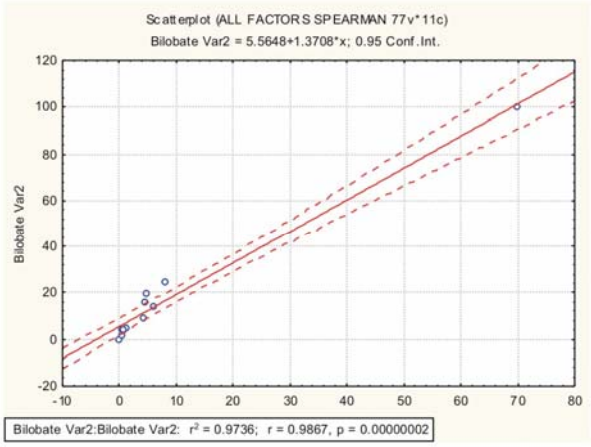
Scatterplot (ALL FACTORS SPEARMAN 77v*11c)
Bilobate Var2 = 5.5648+1.3708*x; 0.95 Conf.Int.
Bilobate Var2
Bilobate Var2:Bilobate Var2: r² = 0.9736; r = 0.9867, p = 0.00000002

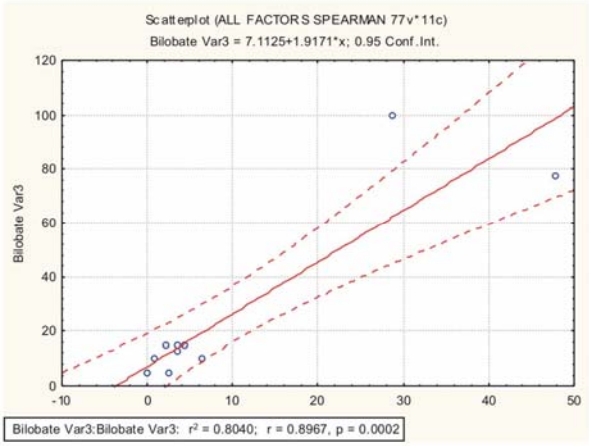
Scatterplot (ALL FACTORS SPEARMAN 77v*11c)
Bilobate Var3 = 7.1125+1.9171*x; 0.95 Conf.Int.
Bilobate Var3
Bilobate Var3:Bilobate Var3: r² = 0.8040; r = 0.8967, p = 0.0002

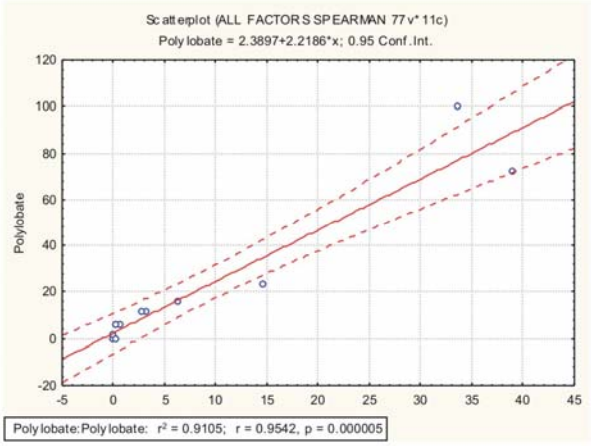
Scatterplot (ALL FACTORS SPEARMAN 77v*11c)
Polylobate = 2.3897+2.2186*x; 0.95 Conf.Int.
Polylobate
Polylobate:Polylobate: r² = 0.9105; r = 0.9542, p = 0.000005

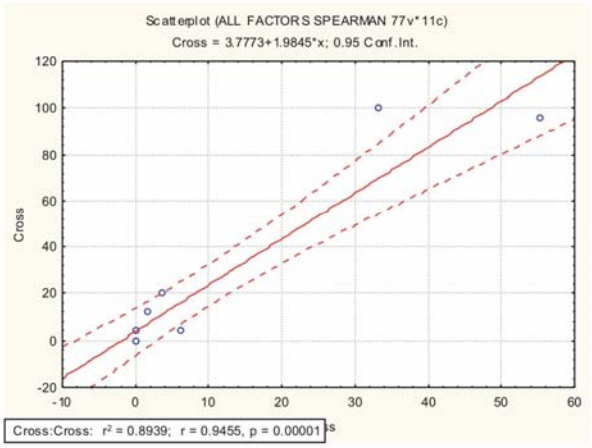
Scatterplot (ALL FACTORS SPEARMAN 77v*11c)
Cross = 3.7773+1.9845*x; 0.95 Conf.Int.
Cross
Cross:Cross: r² = 0.8939; r = 0.9455, p = 0.00001

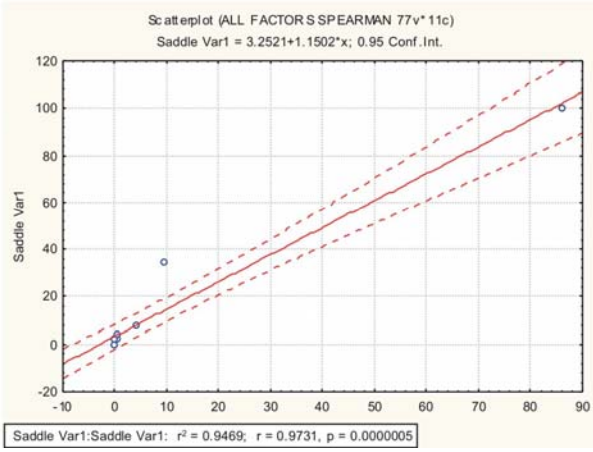
Scatterplot (ALL FACTORS SPEARMAN 77v*11c)
Saddle Var1 = 3.2521+1.1502*x; 0.95 Conf.Int.
Saddle Var1
Saddle Var1:Saddle Var1: r² = 0.9469; r = 0.9731, p = 0.0000005

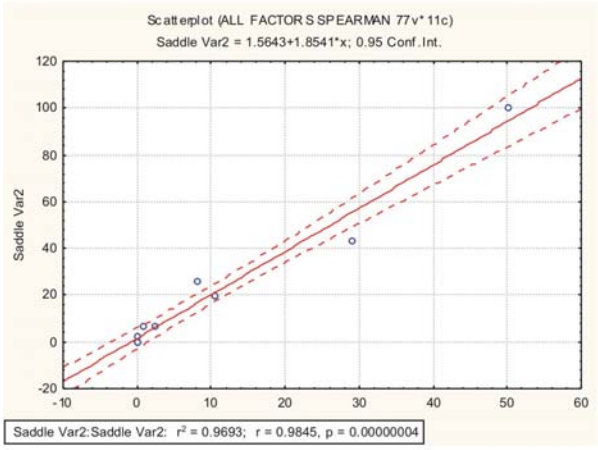
Scatterplot (ALL FACTORS SPEARMAN 77v*11c)
Saddle Var2 = 1.5643+1.8541*x; 0.95 Conf.Int.
Saddle Var2
Saddle Var2:Saddle Var2: r² = 0.9693; r = 0.9845, p = 0.00000004

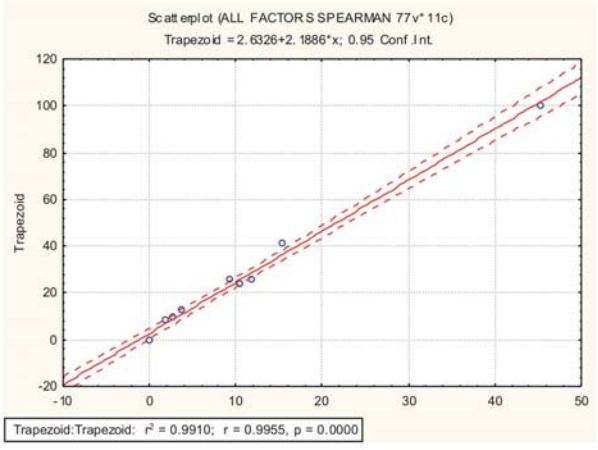
Scatterplot (ALL FACTORS SPEARMAN 77v*11c)
Trapezoid = 2.6326+2.1886*x; 0.95 Conf.Int.
Trapezoid
Trapezoid:Trapezoid: r² = 0.9910; r = 0.9955, p = 0.0000

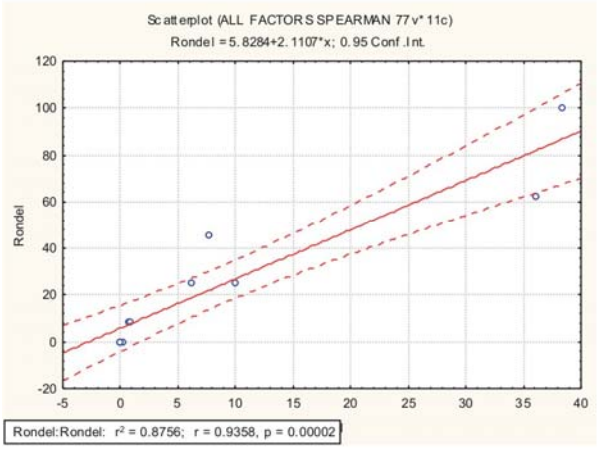
Scatterplot (ALL FACTORS SPEARMAN 77v*11c)
Rondel = 5.8284+2.1107*x; 0.95 Conf.Int.
Rondel
Rondel:Rondel: r² = 0.8756; r = 0.9358, p = 0.00002

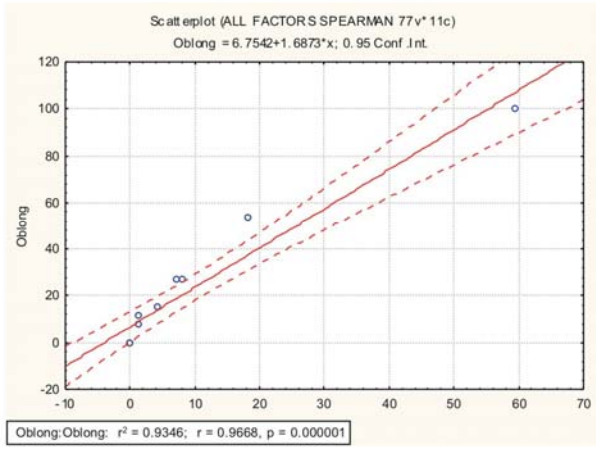
Scatterplot (ALL FACTORS SPEARMAN 77v*11c)
Oblong = 6.7542+1.6873*x; 0.95 Conf.Int.
Oblong
Oblong:Oblong: r² = 0.9346; r = 0.9668, p = 0.000001

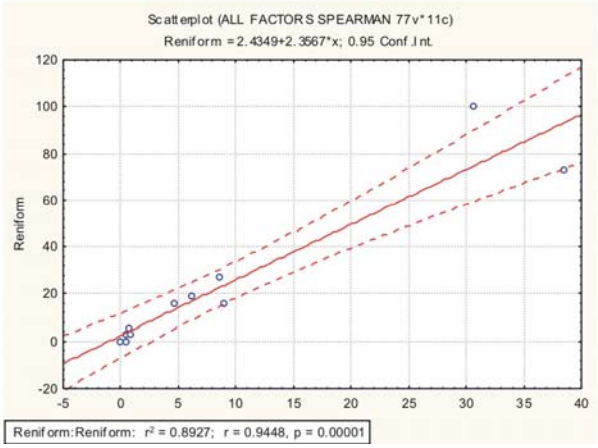
Scatterplot (ALL FACTORS SPEARMAN 77v*11c)
Reniform = 2.4349+2.3567*x; 0.95 Conf.Int.
Reniform
Reniform:Reniform: r² = 0.8927; r = 0.9448, p = 0.00001

Appendix 5: Basic statistics of the number of GSSC-morphotypes counted for each GSSC-morphotype subcategory.

Appendix 5

Basic statistics of the number of GSSC-phytoliths counted for each morphotype category.

Variable	BILOBATE VAR. 1					
	Valid N	Mean	Confidence -95.000%	Confidence +95.000%	Variance	Standard Error
Bilobate Var 1	52	73.01923	64.24020	81.79826	994.3722	4.372933
Bilobate Var 2	52	14.48077	7.62656	21.33498	606.1369	3.414159
Bilobate Var 3	52	0.76923	-0.37880	1.91726	17.0045	0.571848
Polylobate	52	8.86538	3.29898	14.43179	399.7658	2.772689
Cross	52	1.98077	-0.41698	4.37852	74.1761	1.194346
Saddle Var 1	52	0.65385	-0.65880	1.96650	22.2308	0.653846
Saddle Var 2	52	0.00000			0.0000	0.000000
Trapezoid	52	0.00000			0.0000	0.000000
Rondel	52	0.00000			0.0000	0.000000
Oblong	52	0.00000			0.0000	0.000000
Reniform	52	0.42308	-0.42629	1.27244	9.3077	0.423077

Variable	BILOBATE VAR. 2					
	Valid N	Mean	Confidence -95.000%	Confidence +95.000%	Variance	Standard Error
Bilobate Var 1	139	6.05036	3.01226	9.08846	328.1496	1.536486
Bilobate Var 2	139	69.94964	64.98669	74.91259	875.6859	2.509960
Bilobate Var 3	139	4.52518	2.40066	6.64970	160.4686	1.074453
Polylobate	139	8.02878	4.98293	11.07462	329.8253	1.540404
Cross	139	4.38849	2.40928	6.36770	139.2683	1.000965
Saddle Var 1	139	0.00000			0.0000	0.000000
Saddle Var 2	139	0.52518	-0.34683	1.39719	27.0338	0.441008
Trapezoid	139	4.25899	1.80147	6.71651	214.7150	1.242865
Rondel	139	0.41007	-0.03311	0.85325	6.9828	0.224134
Oblong	139	1.20144	-0.12793	2.53081	62.8287	0.672313
Reniform	139	0.76259	0.13228	1.39289	14.1244	0.318770

Variable	BILOBATE VAR. 3					
	Valid N	Mean	Confidence -95.000%	Confidence +95.000%	Variance	Standard Error
Bilobate Var 1	40	2.60000	-1.86087	7.06087	194.554	2.205413
Bilobate Var 2	40	46.02500	34.22290	57.82710	1361.820	5.834852
Bilobate Var 3	40	29.45000	21.03137	37.86863	692.921	4.162092
Polylobate	40	3.80000	0.25700	7.34300	122.728	1.751629
Cross	40	3.77500	0.09526	7.45474	132.384	1.819230
Saddle Var 1	40	6.75000	0.46923	13.03077	385.679	3.105155
Saddle Var 2	40	0.00000			0.000	0.000000
Trapezoid	40	4.32500	0.52679	8.12321	141.046	1.877801
Rondel	40	0.05000	-0.05113	0.15113	0.100	0.050000
Oblong	40	0.87500	-0.31326	2.06326	13.804	0.587462
Reniform	40	2.27500	0.45575	4.09425	32.358	0.899421

Variable	POLYLOBATE					
	Valid N	Mean	Confidence -95.000%	Confidence +95.000%	Variance	Standard Error
Bilobate Var 1	51	14.52941	6.50239	22.55643	814.534	3.996406
Bilobate Var 2	51	38.90196	29.33711	48.46681	1156.530	4.762044
Bilobate Var 3	51	3.19608	0.20841	6.18375	112.841	1.487469
Polylobate	51	33.56863	25.76955	41.36770	768.930	3.882919
Cross	51	0.68627	-0.31127	1.68382	12.580	0.496648
Saddle Var 1	51	0.00000			0.000	0.000000
Saddle Var 2	51	0.00000			0.000	0.000000
Trapezoid	51	2.74510	0.08529	5.40491	89.434	1.324237
Rondel	51	0.17647	-0.17798	0.53092	1.588	0.176471
Oblong	51	6.31373	0.92024	11.70721	367.740	2.685252
Reniform	51	0.27451	-0.27686	0.82588	3.843	0.274510

Variable	CROSS					
	Valid N	Mean	Confidence -95.000%	Confidence +95.000%	Variance	Standard Error
Bilobate Var 1	25	6.00000	-0.99598	12.99598	287.2500	3.389690
Bilobate Var 2	25	54.20000	42.94907	65.45093	742.9167	5.451300
Bilobate Var 3	25	3.48000	0.18181	6.77819	63.8433	1.598040
Polylobate	25	1.80000	-0.45460	4.05460	29.8333	1.092398
Cross	25	34.52000	25.97194	43.06806	428.8433	4.141707
Saddle Var 1	25	0.00000			0.0000	0.000000
Saddle Var 2	25	0.00000			0.0000	0.000000
Trapezoid	25	0.00000			0.0000	0.000000
Rondel	25	0.00000			0.0000	0.000000
Oblong	25	0.00000			0.0000	0.000000
Reniform	25	0.00000			0.0000	0.000000

Variable	SADDLE VAR. 1					
	Valid N	Mean	Confidence -95.000%	Confidence +95.000%	Variance	Standard Error
Bilobate Var 1	49	0.34694	-0.35063	1.04451	5.8980	0.346939
Bilobate Var 2	49	0.00000			0.0000	0.000000
Bilobate Var 3	49	4.06122	-0.00358	8.12603	200.2670	2.021653
Polylobate	49	0.00000			0.0000	0.000000
Cross	49	0.00000			0.0000	0.000000
Saddle Var 1	49	85.75510	79.80857	91.70164	428.6054	2.957541
Saddle Var 2	49	9.55102	4.79102	14.31102	274.6276	2.367413
Trapezoid	49	0.00000			0.0000	0.000000
Rondel	49	0.00000			0.0000	0.000000
Oblong	49	0.00000			0.0000	0.000000
Reniform	49	0.44898	-0.45375	1.35171	9.8776	0.448980

Variable	SADDLE VAR. 2					
	Valid N	Mean	Confidence -95.000%	Confidence +95.000%	Variance	Standard Error
Bilobate Var 1	46	0.00000			0.000	0.000000
Bilobate Var 2	46	0.80435	-0.50532	2.11401	19.450	0.650247
Bilobate Var 3	46	0.00000			0.000	0.000000
Polylobate	46	0.00000			0.000	0.000000
Cross	46	0.00000			0.000	0.000000
Saddle Var 1	46	28.06522	16.91172	39.21871	1410.640	5.537697
Saddle Var 2	46	50.10870	38.85309	61.36430	1436.588	5.588396
Trapezoid	46	10.58696	3.66614	17.50777	543.137	3.436178
Rondel	46	2.34783	0.06877	4.62688	58.899	1.131549
Oblong	46	0.00000			0.000	0.000000
Reniform	46	8.13043	3.06226	13.19861	291.271	2.516344

Variable	TRAPEZOID					
	Valid N	Mean	Confidence -95.000%	Confidence +95.000%	Variance	Standard Error
Bilobate Var 1	70	0.00000			0.0000	0.000000
Bilobate Var 2	70	10.45714	5.41148	15.50281	447.7880	2.529223
Bilobate Var 3	70	2.61429	0.26914	4.95943	96.7331	1.175543
Polylobate	70	1.87143	0.13250	3.61035	53.1861	0.871666
Cross	70	0.00000			0.0000	0.000000
Saddle Var 1	70	0.00000			0.0000	0.000000
Saddle Var 2	70	3.62857	0.36877	6.88837	186.9035	1.634029
Trapezoid	70	46.54286	39.29126	53.79446	924.9184	3.634986
Rondel	70	9.34286	4.20332	14.48240	464.6054	2.576280
Oblong	70	10.41429	4.38016	16.44841	640.4201	3.024708
Reniform	70	15.20000	9.60560	20.79440	550.4812	2.804285

Variable	RONDEL					
	Valid N	Mean	Confidence -95.000%	Confidence +95.000%	Variance	Standard Error
Bilobate Var 1	24	0.00000			0.000	0.000000
Bilobate Var 2	24	9.50000	2.14286	16.85714	303.565	3.556480
Bilobate Var 3	24	0.62500	-0.66791	1.91791	9.375	0.625000
Polylobate	24	0.29167	-0.13021	0.71355	0.998	0.203939
Cross	24	0.00000			0.000	0.000000
Saddle Var 1	24	0.00000			0.000	0.000000
Saddle Var 2	24	7.29167	-0.57519	15.15852	347.085	3.802878
Trapezoid	24	34.50000	23.41016	45.58984	689.739	5.360889
Rondel	24	40.00000	25.80215	54.19785	1130.522	6.863314
Oblong	24	0.79167	-0.42186	2.00519	8.259	0.586624
Reniform	24	7.33333	2.90344	11.76323	110.058	2.141436

Variable	OBLONG					
	Valid N	Mean	Confidence -95.000%	Confidence +95.000%	Variance	Standard Error
Bilobate Var 1	26	0.00000			0.000	0.000000
Bilobate Var 2	26	8.15385	0.99229	15.31540	314.375	3.477263
Bilobate Var 3	26	4.11538	-1.13024	9.36101	168.666	2.546990
Polylobate	26	7.23077	0.87585	13.58569	247.545	3.085603
Cross	26	0.00000			0.000	0.000000
Saddle Var 1	26	0.00000			0.000	0.000000
Saddle Var 2	26	0.00000			0.000	0.000000
Trapezoid	26	18.19231	8.23613	28.14849	607.602	4.834179
Rondel	26	1.26923	-1.18515	3.72361	36.925	1.191712
Oblong	26	59.42308	45.34285	73.50330	1215.214	6.836592
Reniform	26	1.19231	-0.35744	2.74205	14.722	0.752471

Variable	RENIFORM					
	Valid N	Mean	Confidence -95.000%	Confidence +95.000%	Variance	Standard Error
Bilobate Var 1	37	0.45946	-0.47237	1.39129	7.8108	0.459459
Bilobate Var 2	37	8.16216	1.42862	14.89571	407.8619	3.320135
Bilobate Var 3	37	5.13514	-0.14142	10.41169	250.4535	2.601733
Polylobate	37	0.08108	-0.08336	0.24552	0.2432	0.081081
Cross	37	0.02703	-0.02779	0.08184	0.0270	0.027027
Saddle Var 1	37	0.91892	-0.94474	2.78257	31.2432	0.918919
Saddle Var 2	37	9.43243	2.17917	16.68570	473.2523	3.576395
Trapezoid	37	38.40541	28.01928	48.79153	970.3589	5.121124
Rondel	37	6.89189	0.97184	12.81195	315.2658	2.919023
Oblong	37	0.81081	-0.22832	1.84994	9.7132	0.512366
Reniform	37	29.29730	21.67806	36.91654	522.2147	3.756849

Appendix 6: GSSC-phytolith abundance as a proportion of all morphotypes per category.

Appendix 6

GSSC-phytolith abundance as a proportion of all morphotypes per category.

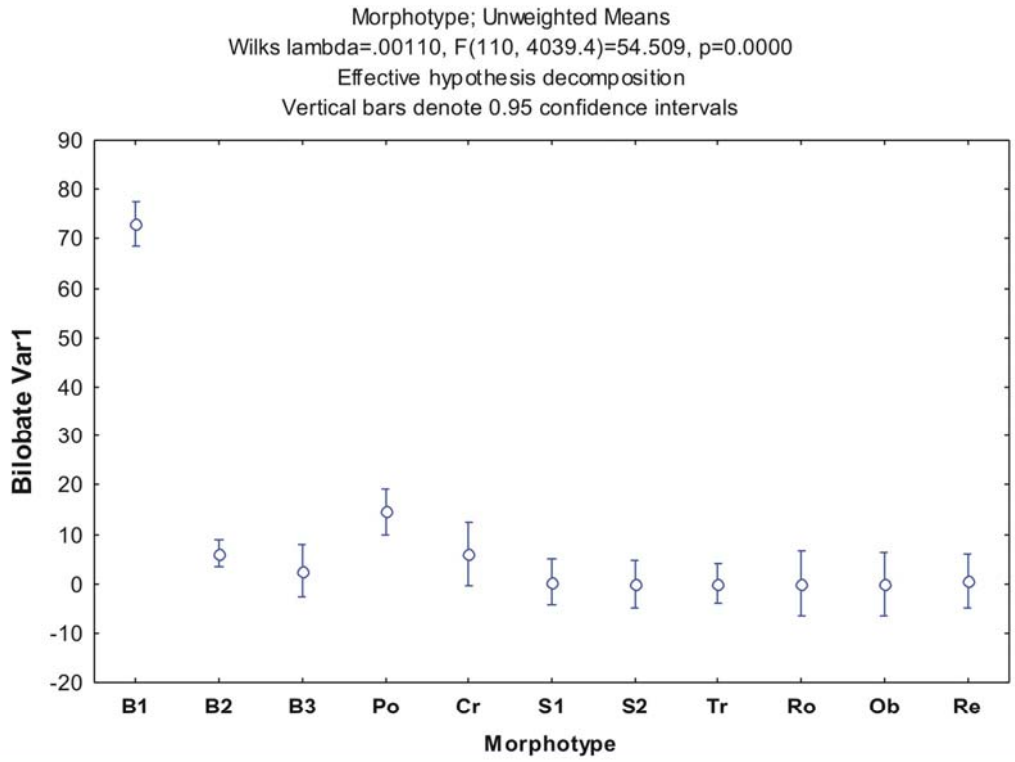

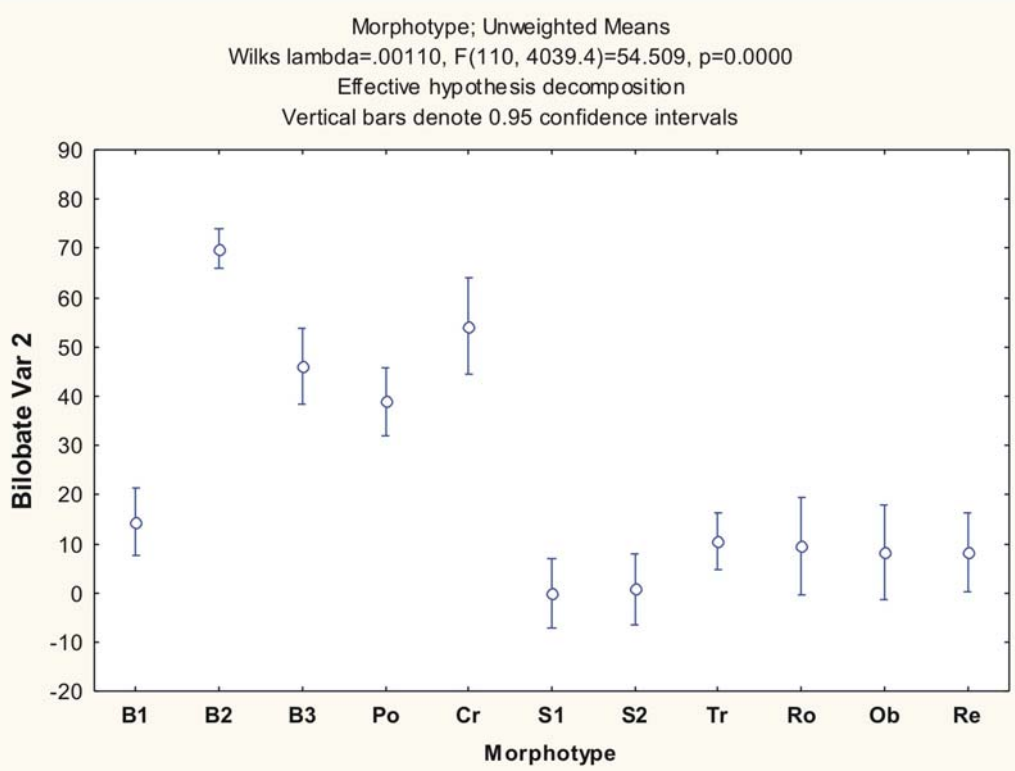

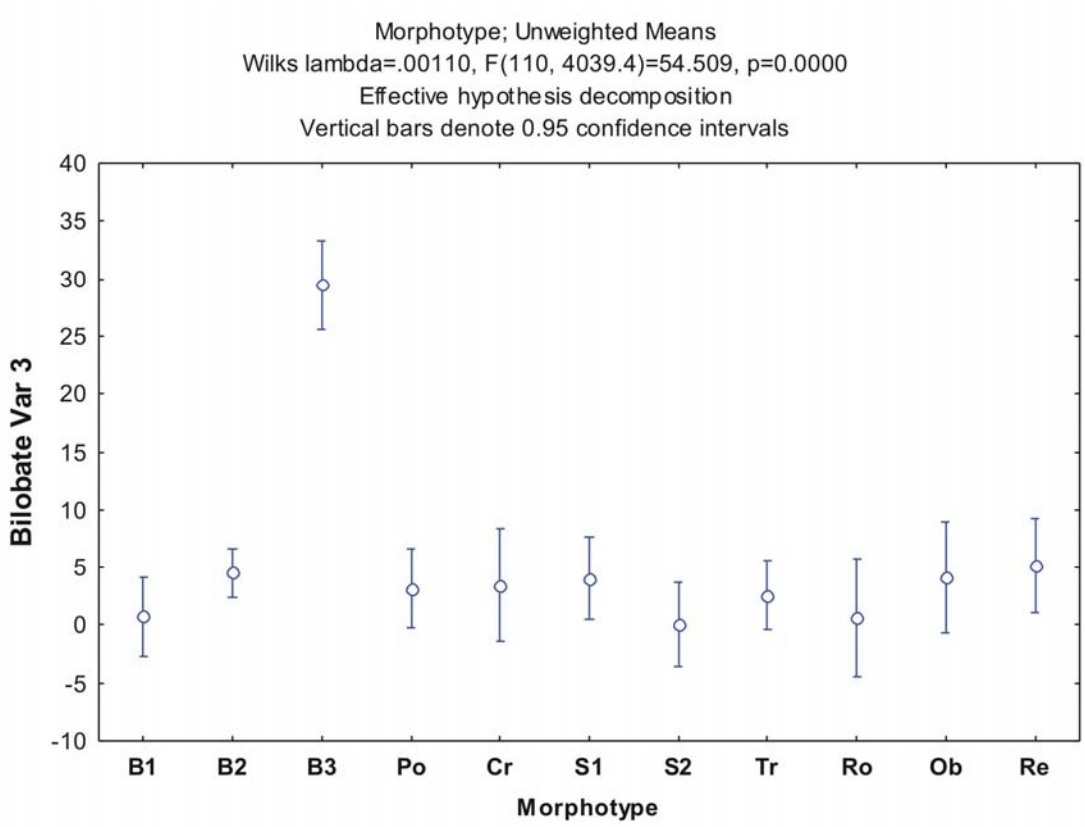
Morphotype; Unweighted Means
Wilks lambda=.00110, F(110, 4039.4)=54.509, p=0.0000
Effective hypothesis decomposition
Vertical bars denote 0.95 confidence intervals
Bilobate Var 3
40
35
30
25
20
15
10
5
0
-5
-10
B1
B2
B3
Po
Cr
S1
S2
Tr
Ro
Ob
Re
Morphotype

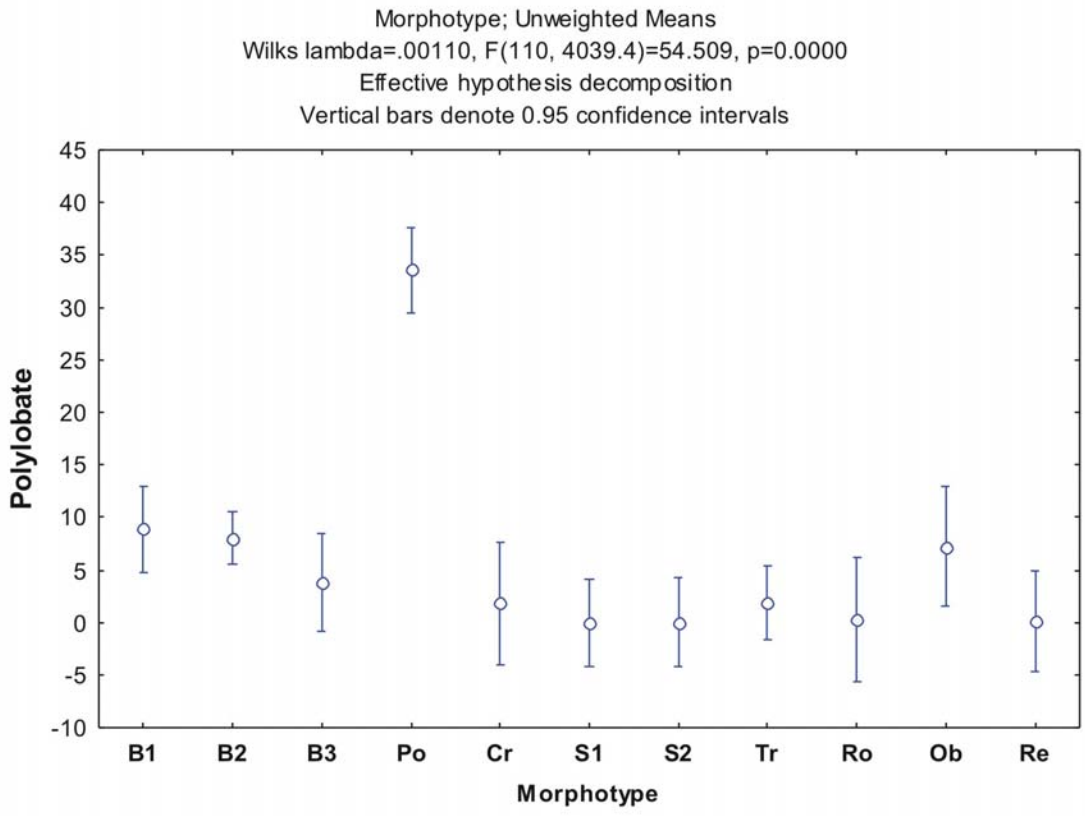
Morphotype; Unweighted Means
Wilks lambda=.00110, F(110, 4039.4)=54.509, p=0.0000
Effective hypothesis decomposition
Vertical bars denote 0.95 confidence intervals
Polylobate
45
40
35
30
25
20
15
10
5
0
-5
-10
B1
B2
B3
Po
Cr
S1
S2
Tr
Ro
Ob
Re
Morphotype

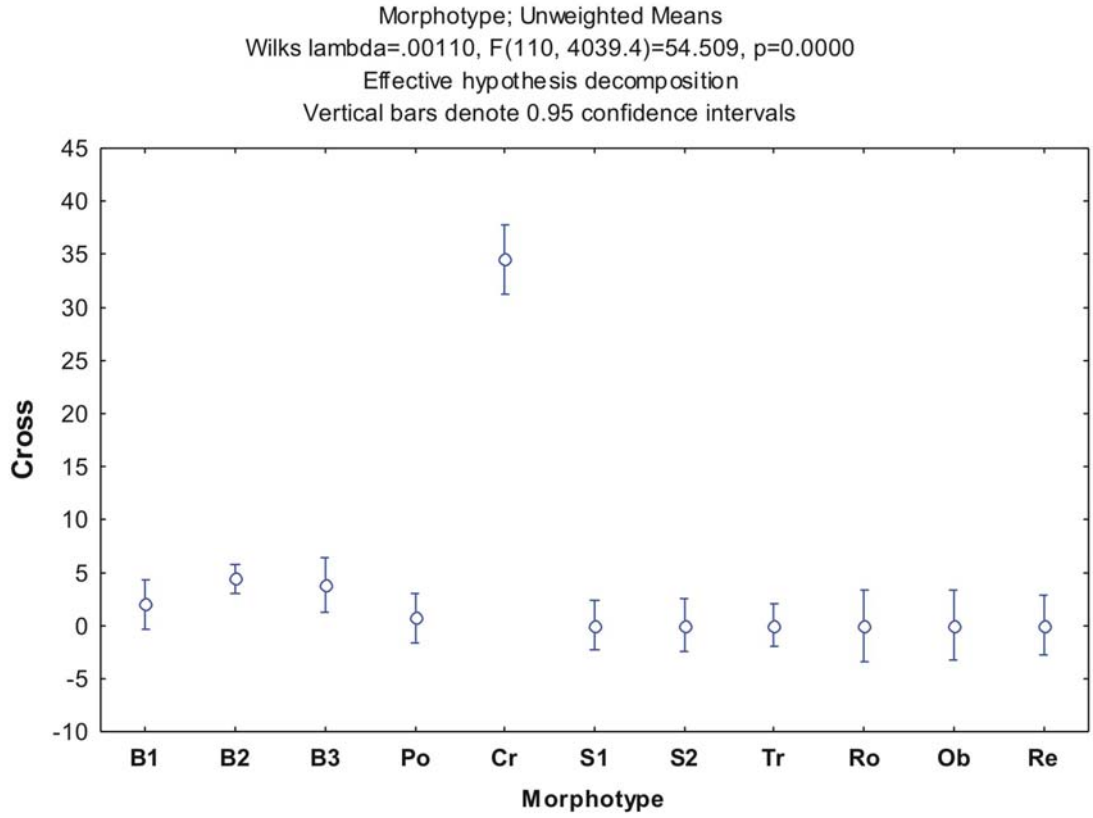
Morphotype; Unweighted Means
Wilks lambda=.00110, F(110, 4039.4)=54.509, p=0.0000
Effective hypothesis decomposition
Vertical bars denote 0.95 confidence intervals
Cross
45
40
35
30
25
20
15
10
5
0
-5
-10
B1
B2
B3
Po
Cr
S1
S2
Tr
Ro
Ob
Re
Morphotype

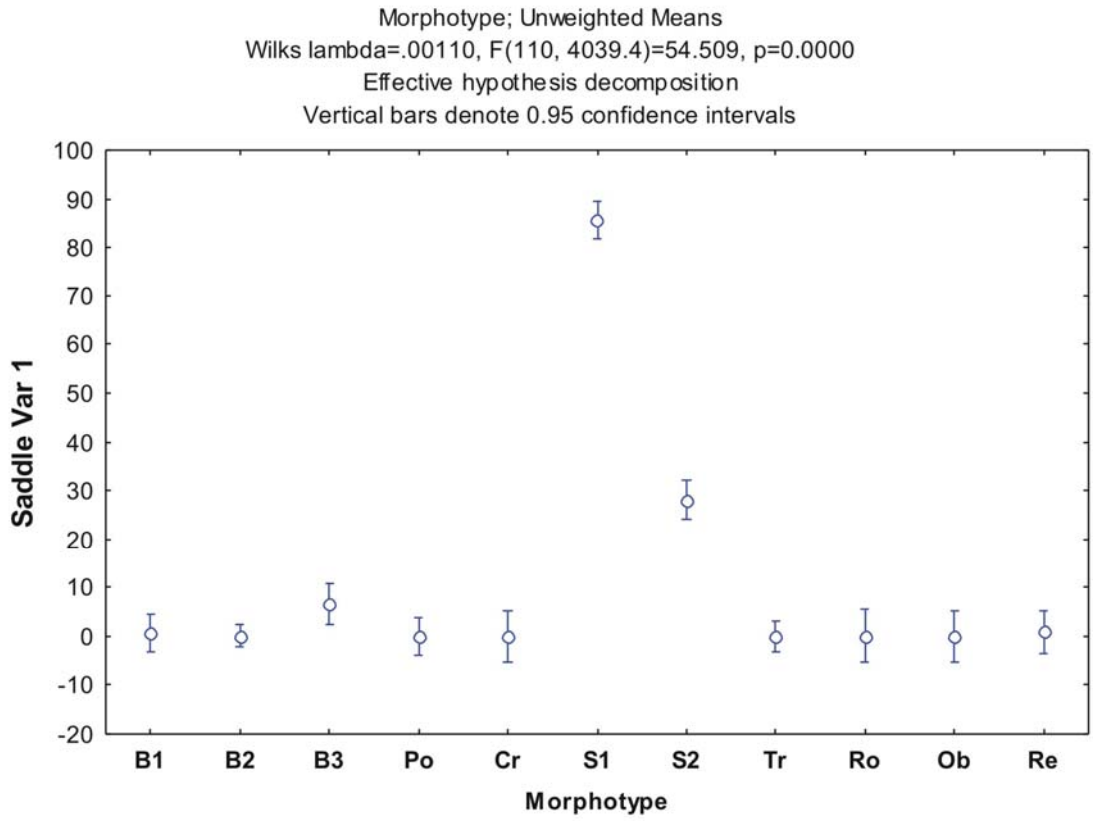
Morphotype; Unweighted Means
Wilks lambda=.00110, F(110, 4039.4)=54.509, p=0.0000
Effective hypothesis decomposition
Vertical bars denote 0.95 confidence intervals
Saddle Var 1
100
90
80
70
60
50
40
30
20
10
0
-10
-20
B1
B2
B3
Po
Cr
S1
S2
Tr
Ro
Ob
Re
Morphotype

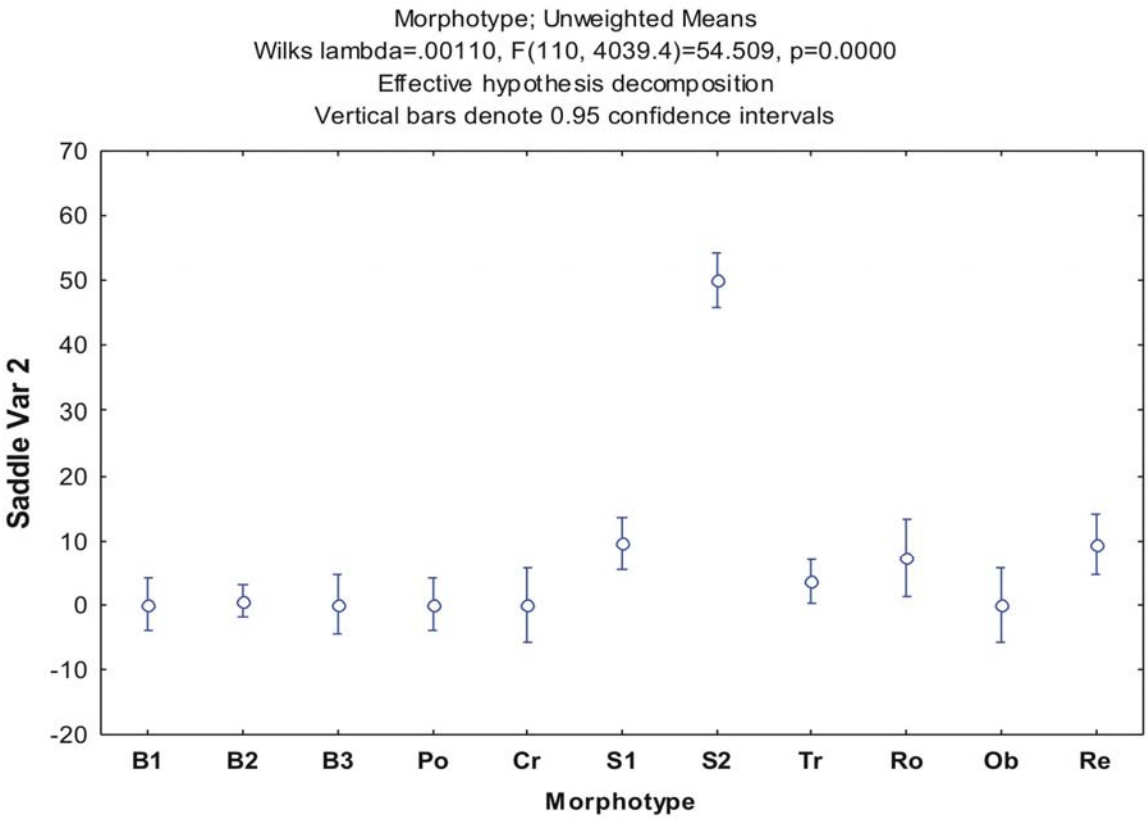
Morphotype; Unweighted Means
Wilks lambda=.00110, F(110, 4039.4)=54.509, p=0.0000
Effective hypothesis decomposition
Vertical bars denote 0.95 confidence intervals
Saddle Var 2
70
60
50
40
30
20
10
0
-10
-20
B1
B2
B3
Po
Cr
S1
S2
Tr
Ro
Ob
Re
Morphotype

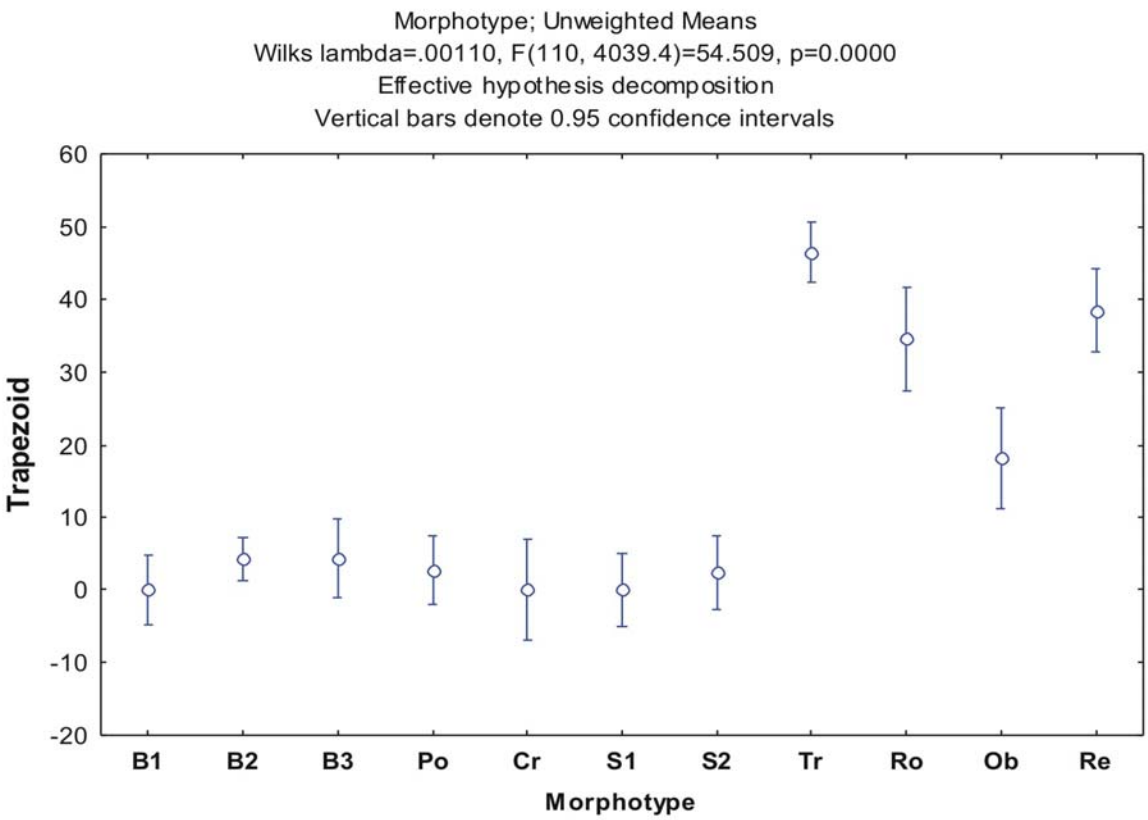
Morphotype; Unweighted Means
Wilks lambda=.00110, F(110, 4039.4)=54.509, p=0.0000
Effective hypothesis decomposition
Vertical bars denote 0.95 confidence intervals
Trapezoid
60
50
40
30
20
10
0
-10
-20
B1
B2
B3
Po
Cr
S1
S2
Tr
Ro
Ob
Re
Morphotype

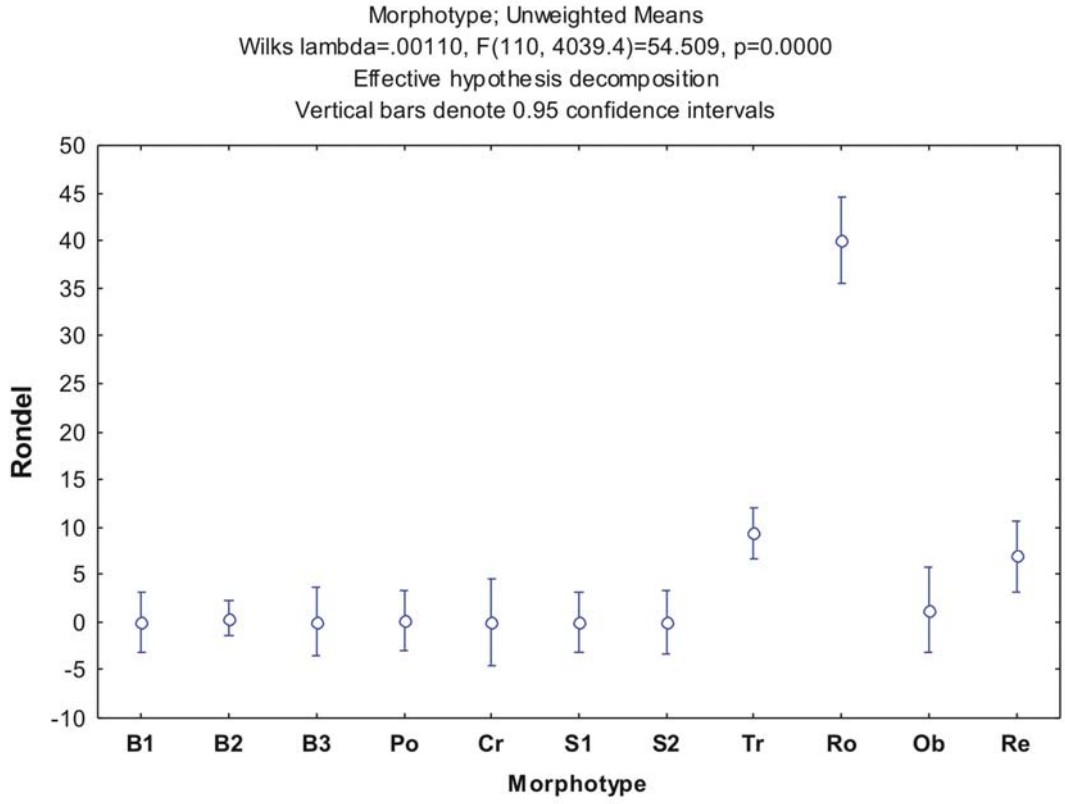
Morphotype; Unweighted Means
Wilks lambda=.00110, F(110, 4039.4)=54.509, p=0.0000
Effective hypothesis decomposition
Vertical bars denote 0.95 confidence intervals
Rondel
50
45
40
35
30
25
20
15
10
5
0
-5
-10
B1
B2
B3
Po
Cr
S1
S2
Tr
Ro
Ob
Re
Morphotype

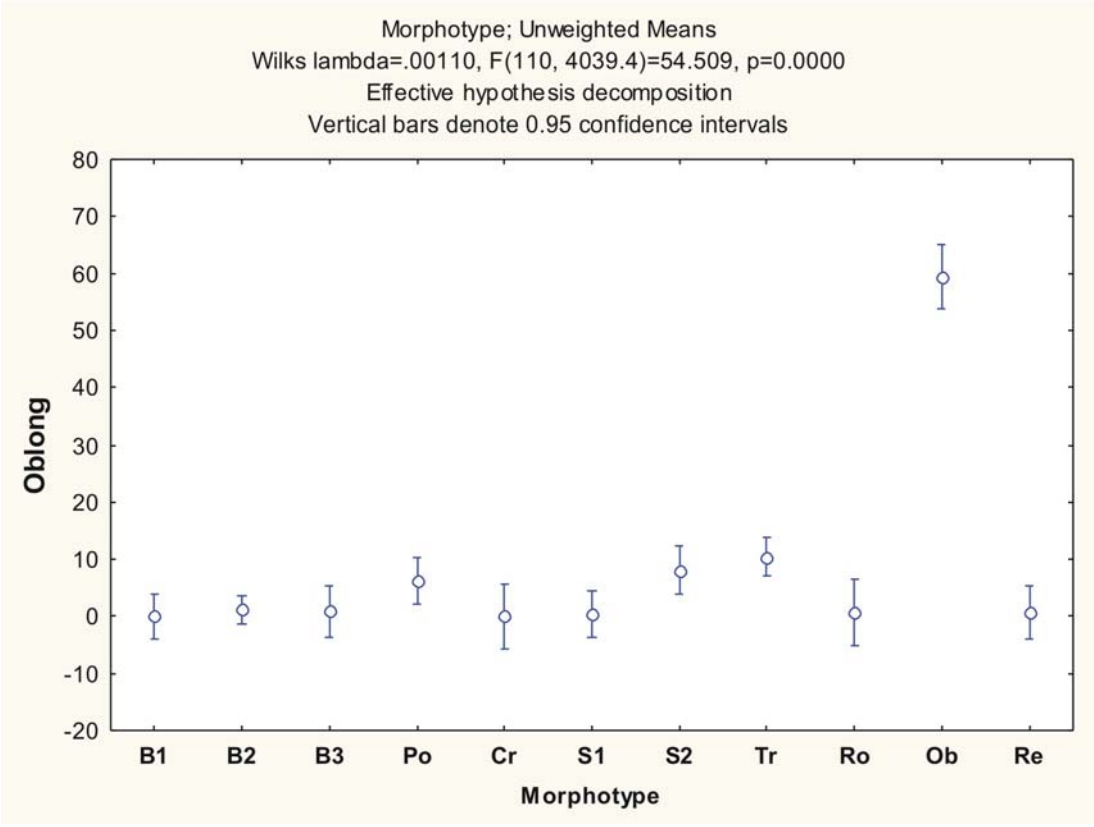
Morphotype; Unweighted Means
Wilks lambda=.00110, F(110, 4039.4)=54.509, p=0.0000
Effective hypothesis decomposition
Vertical bars denote 0.95 confidence intervals
Oblong
80
70
60
50
40
30
20
10
0
-10
-20
B1
B2
B3
Po
Cr
S1
S2
Tr
Ro
Ob
Re
Morphotype

Appendix 7: Basic statistics of the number of GSSC-morphotypes counted for each subfamily subcategory.

Appendix 7

Basic statistics of GSSC-morphotypes counted for each subfamily subcategory.

Variable	Aristidoideae					
	Valid N	Mean	Confidence -95.000%	Confidence +95.000%	Variance	Standard Error
Bilobate Var 1	29	26.82759	10.25686	43.39831	1897.791	8.089565
Bilobate Var 2	29	2.34483	-1.02883	5.71849	78.663	1.646968
Bilobate Var 3	29	0.93103	-0.97610	2.83817	25.138	0.931034
Polylobate	29	0.00000			0.000	0.000000
Cross	29	0.00000			0.000	0.000000
Saddle Var 1	29	2.37931	-1.00527	5.76389	79.172	1.652296
Saddle Var 2	29	59.96552	43.31999	76.61104	1914.963	8.126082
Trapezoid	29	0.86207	-0.16829	1.89243	7.337	0.503006
Rondel	29	1.20690	-1.12328	3.53708	37.527	1.137558
Oblong	29	0.00000			0.000	0.000000
Reniform	29	5.41379	0.42773	10.39985	171.823	2.434116

Variable	Chloridoideae					
	Valid N	Mean	Confidence -95.000%	Confidence +95.000%	Variance	Standard Error
Bilobate Var 1	62	8.51613	1.65475	15.37751	729.992	3.431335
Bilobate Var 2	62	12.85484	4.88974	20.81993	983.733	3.983297
Bilobate Var 3	62	5.03226	0.50948	9.55503	317.179	2.261812
Polylobate	62	1.62903	-1.62842	4.88648	164.532	1.629032
Cross	62	2.24194	-1.11886	5.60273	175.137	1.680712
Saddle Var 1	62	69.93548	59.86731	80.00366	1571.799	5.035037
Saddle Var 2	62	8.12903	3.58492	12.67315	320.180	2.272485
Trapezoid	62	1.62903	-1.62842	4.88648	164.532	1.629032
Rondel	62	1.62903	-1.62842	4.88648	164.532	1.629032
Oblong	62	1.62903	-1.62842	4.88648	164.532	1.629032
Reniform	62	1.62903	-1.62842	4.88648	164.532	1.629032

Variable	Danthonioideae					
	Valid N	Mean	Confidence -95.000%	Confidence +95.000%	Variance	Standard Error
Bilobate Var 1	65	2.55385	-1.10208	6.20978	217.688	1.830042
Bilobate Var 2	65	40.60000	30.16384	51.03616	1773.869	5.224011
Bilobate Var 3	65	5.73846	1.54609	9.93083	286.259	2.098566
Polylobate	65	4.63077	1.30186	7.95968	180.487	1.666348
Cross	65	0.00000			0.000	0.000000
Saddle Var 1	65	0.00000			0.000	0.000000
Saddle Var 2	65	0.84615	0.20652	1.48579	6.663	0.320179
Trapezoid	65	23.90769	15.96848	31.84691	1026.585	3.974118
Rondel	65	7.41538	2.44573	12.38504	402.247	2.487651
Oblong	65	1.83077	-0.64113	4.30267	99.518	1.237353
Reniform	65	11.15385	5.80372	16.50397	466.195	2.678101

Variable	Ehrhartoideae					
	Valid N	Mean	Confidence -95.000%	Confidence +95.000%	Variance	Standard Error
Bilobate Var 1	18	5.55556	-6.16564	17.27675	555.556	5.555556
Bilobate Var 2	18	37.55556	21.36482	53.74629	1060.026	7.674004
Bilobate Var 3	18	10.66667	0.03928	21.29405	456.706	5.037117
Polylobate	18	1.50000	-1.20903	4.20903	29.676	1.284014
Cross	18	1.33333	-1.47975	4.14642	32.000	1.333333
Saddle Var 1	18	0.00000			0.000	0.000000
Saddle Var 2	18	0.00000			0.000	0.000000
Trapezoid	18	26.50000	12.72587	40.27413	767.206	6.528595
Rondel	18	2.11111	0.27491	3.94731	13.634	0.870312
Oblong	18	3.66667	-2.54446	9.87780	156.000	2.943920
Reniform	18	10.16667	-0.07632	20.40966	424.265	4.854921

Variable	Panicoideae					
	Valid N	Mean	Confidence -95.000%	Confidence +95.000%	Variance	Standard Error
Bilobate Var 1	104	21.40385	14.41211	28.39558	1292.534	3.525367
Bilobate Var 2	104	54.43269	46.40445	62.46093	1704.170	4.047994
Bilobate Var 3	104	2.82692	0.49772	5.15613	143.445	1.174429
Polylobate	104	11.43269	6.66806	16.19732	600.248	2.402418
Cross	104	6.86538	3.60657	10.12420	280.797	1.643160
Saddle Var 1	104	0.00000			0.000	0.000000
Saddle Var 2	104	0.64423	-0.63345	1.92191	43.163	0.644231
Trapezoid	104	2.07692	-0.33458	4.48842	153.761	1.215924
Rondel	104	0.00000			0.000	0.000000
Oblong	104	0.00000			0.000	0.000000
Reniform	104	0.50962	-0.22307	1.24230	14.194	0.369434

Variable	Pooideae					
	Valid N	Mean	Confidence -95.000%	Confidence +95.000%	Variance	Standard Error
Bilobate Var 1	31	0.00000			0.000	0.000000
Bilobate Var 2	31	7.70968	0.65714	14.76222	369.680	3.453281
Bilobate Var 3	31	3.45161	-1.00655	7.90978	147.723	2.182944
Polylobate	31	6.83871	1.75517	11.92225	192.073	2.489158
Cross	31	0.64516	-0.67243	1.96276	12.903	0.645161
Saddle Var 1	31	0.00000			0.000	0.000000
Saddle Var 2	31	0.00000			0.000	0.000000
Trapezoid	31	22.41935	11.85069	32.98802	830.185	5.174955
Rondel	31	10.58065	0.14564	21.01565	809.318	5.109505
Oblong	31	43.87097	28.44728	59.29466	1768.116	7.552218
Reniform	31	4.48387	-0.62148	9.58922	193.725	2.499837

Appendix 8: Subfamily: Tukey's HSD test for unequal sample sizes.

Appendix 8

Subfamily: Tukey's HSD for unequal sample sizes. Marked values are significant at p < .05000.

Cell No.	SUBFAM	{1} 7.0000	{2} 26.828	{3} 0.0000	{4} 2.5538	{5} 5.5556	{6} 21.404	{7} 0.0000
	Tukey HSD test; variable **Bilobate Var1**							
	Approximate Probabilities for Post Hoc Tests							
	Error: Between MS = 807.51, df = 304.00							
1	Chlo		0.032488	0.999601	0.975921	0.999996	0.027868	0.923218
2	Arist	0.032488		0.710102	0.002508	0.161036	0.971297	0.004817
4	Dan	0.975921	0.002508	0.999999		0.999700	0.000556	0.999627
5	Ehrh	0.999996	0.161036	0.999924	0.999700		0.303763	0.994660
6	Pa	0.027868	0.971297	0.858560	0.000556	0.303763		0.004362
7	Po	0.923218	0.004817	1.000000	0.999627	0.994660	0.004362	

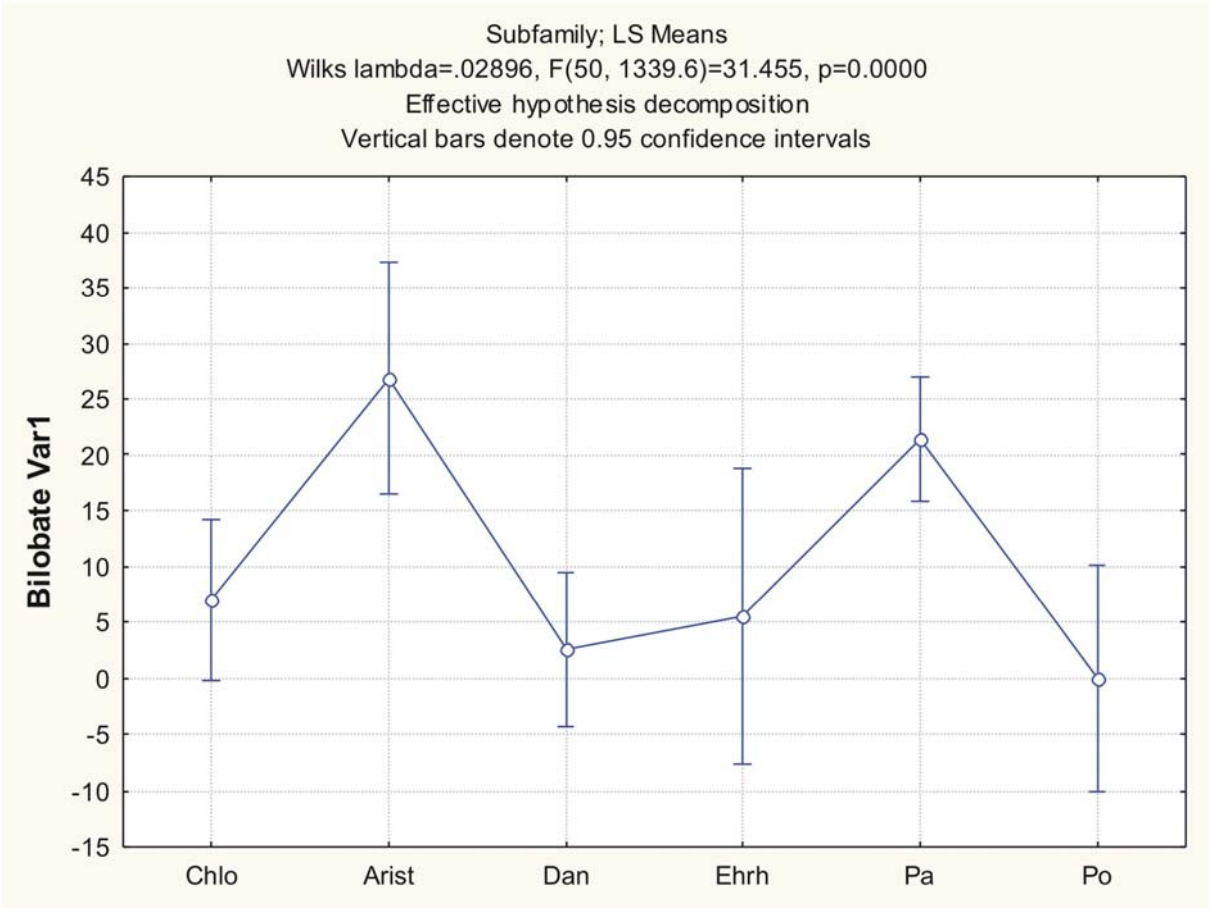

Cell No.	SUBFAM	{1} 11.410	{2} 2.3448	{3} 12.333	{4} 40.600	{5} 37.556	{6} 54.433	{7} 7.7097
	Tukey HSD test; variable **Bilobate Var 2** Approximate Probabilities for Post Hoc Tests Error: Between MS = 1228.3, df = 304.00							
1	Chlo		0.913526	1.000000	0.000083	0.079435	0.000026	0.999114
2	Arist	0.913526		0.999202	0.000045	0.014305	0.000026	0.997046
4	Dan	0.000083	0.000045	0.820100		0.999904	0.160476	0.000359
5	Ehrh	0.079435	0.014305	0.911047	0.999904		0.489385	0.061751
6	Pa	0.000026	0.000026	0.382227	0.160476	0.489385		0.000026
7	Po	0.999114	0.997046	0.999991	0.000359	0.061751	0.000026	

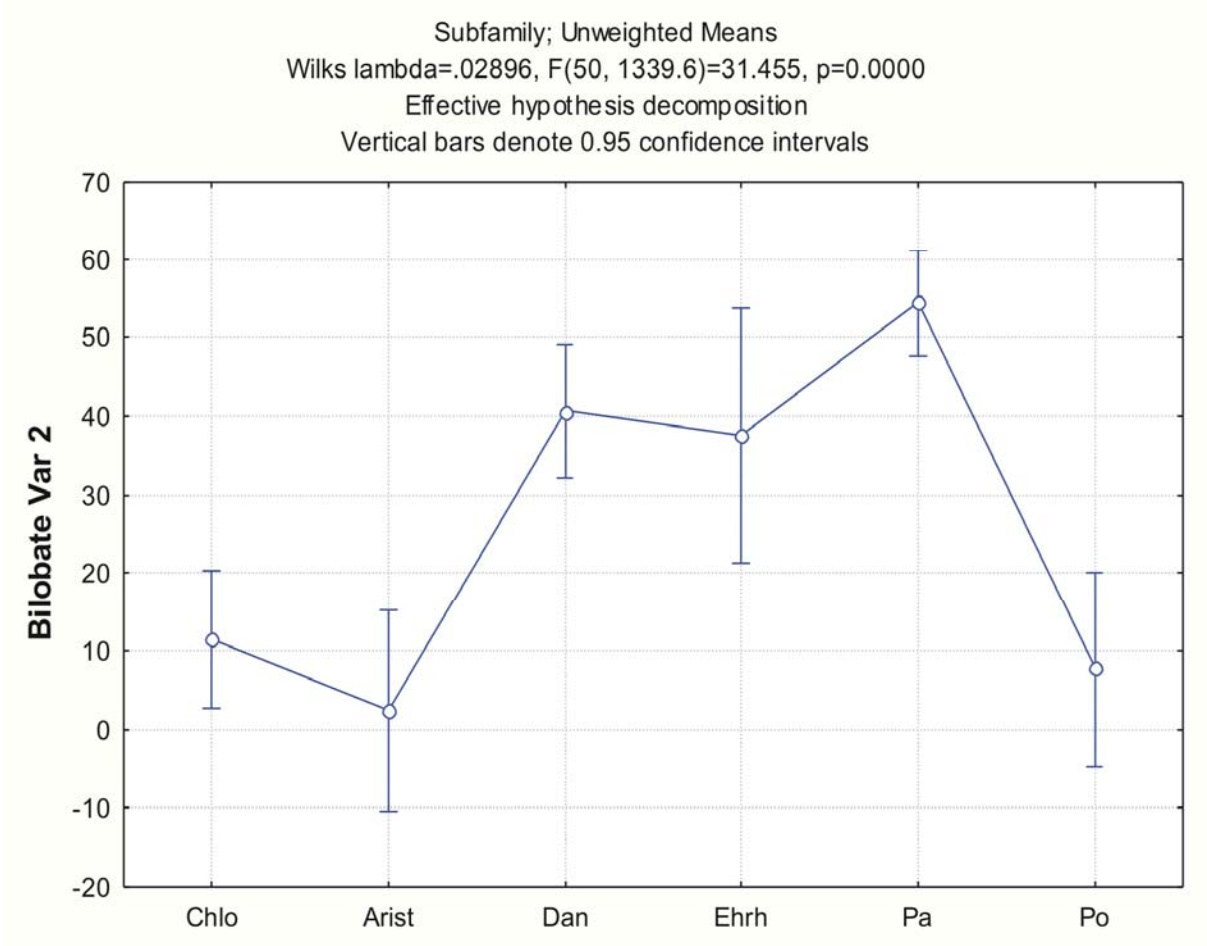

Cell No.	SUBFAM	{1} 0.0000	{2} 0.0000	{3} 0.0000	{4} 4.6308	{5} 1.5000	{6} 11.433	{7} 6.8387
	Tukey HSD test; variable **Polylobate**							
	Approximate Probabilities for Post Hoc Tests							
	Error: Between MS = 261.98, df = 304.00							
1	Chlo		1.000000	1.000000	0.679206	0.999866	0.000257	0.469847
2	Arist	1.000000		1.000000	0.860816	0.999930	0.013582	0.659195
4	Dan	0.679206	0.860816	0.999050		0.991029	0.109195	0.996032
5	Ehrh	0.999866	0.999930	0.999999	0.991029		0.196761	0.924379
6	Pa	0.000257	0.013582	0.892091	0.109195	0.196761		0.809045
7	Po	0.469847	0.659195	0.992705	0.996032	0.924379	0.809045	

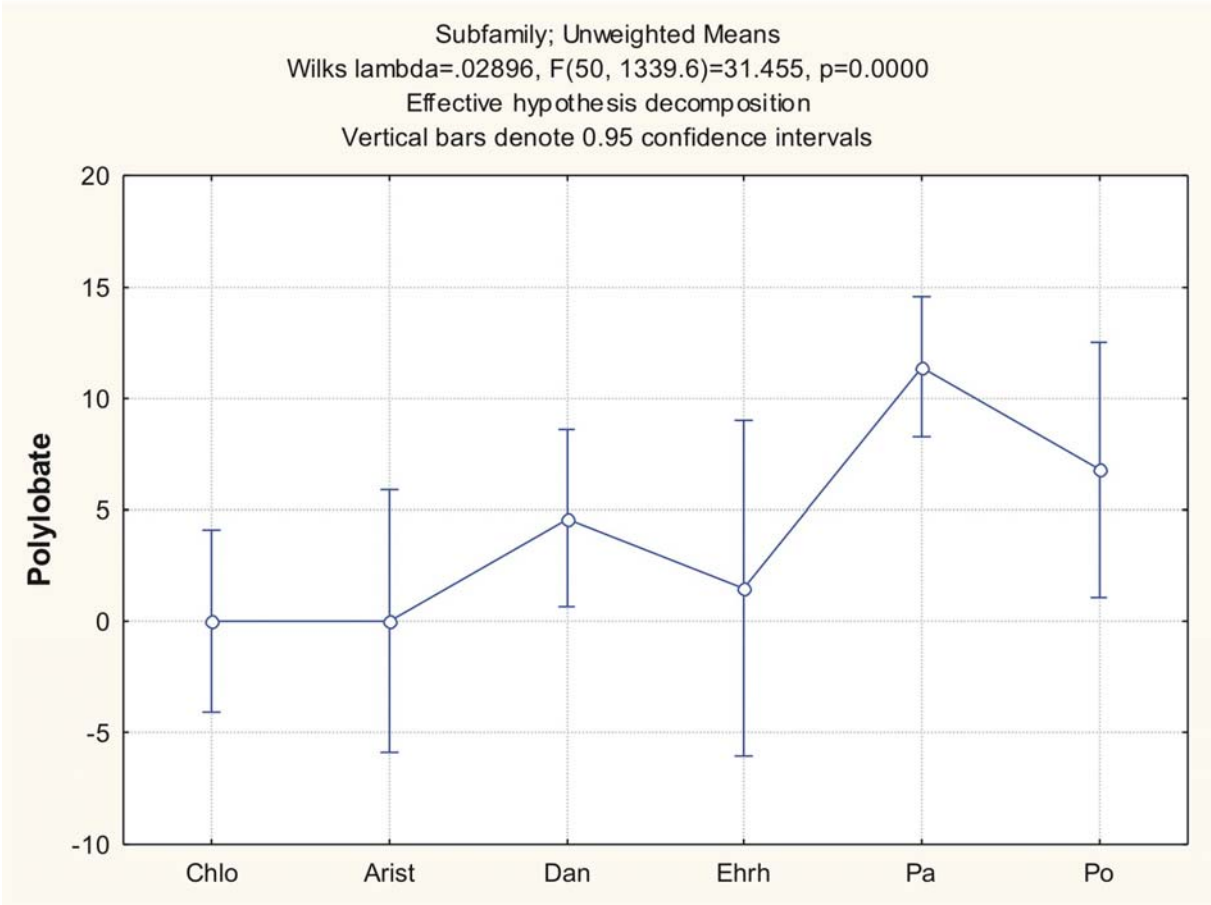

Cell No.	Tukey HSD test; variable **Cross** Approximate Probabilities for Post Hoc Tests Error: Between MS = 107.13, df = 304.00 SUBFAM	{1} .62295	{2} 0.0000	{3} 18.000	{4} 0.0000	{5} 1.3333	{6} 6.8654	{7} .64516
1	Chlo		0.999971	0.067986	0.999883	0.999977	0.003490	1.000000
2	Arist	0.999971		0.062843	1.000000	0.999525	0.026536	0.999984
4	Dan	0.999883	1.000000	0.050495		0.999059	0.000557	0.999956
5	Ehrh	0.999977	0.999525	0.131360	0.999059		0.356323	0.999989
6	Pa	0.003490	0.026536	0.522813	0.000557	0.356323		0.051685
7	Po	1.000000	0.999984	0.081172	0.999956	0.999989	0.051685	

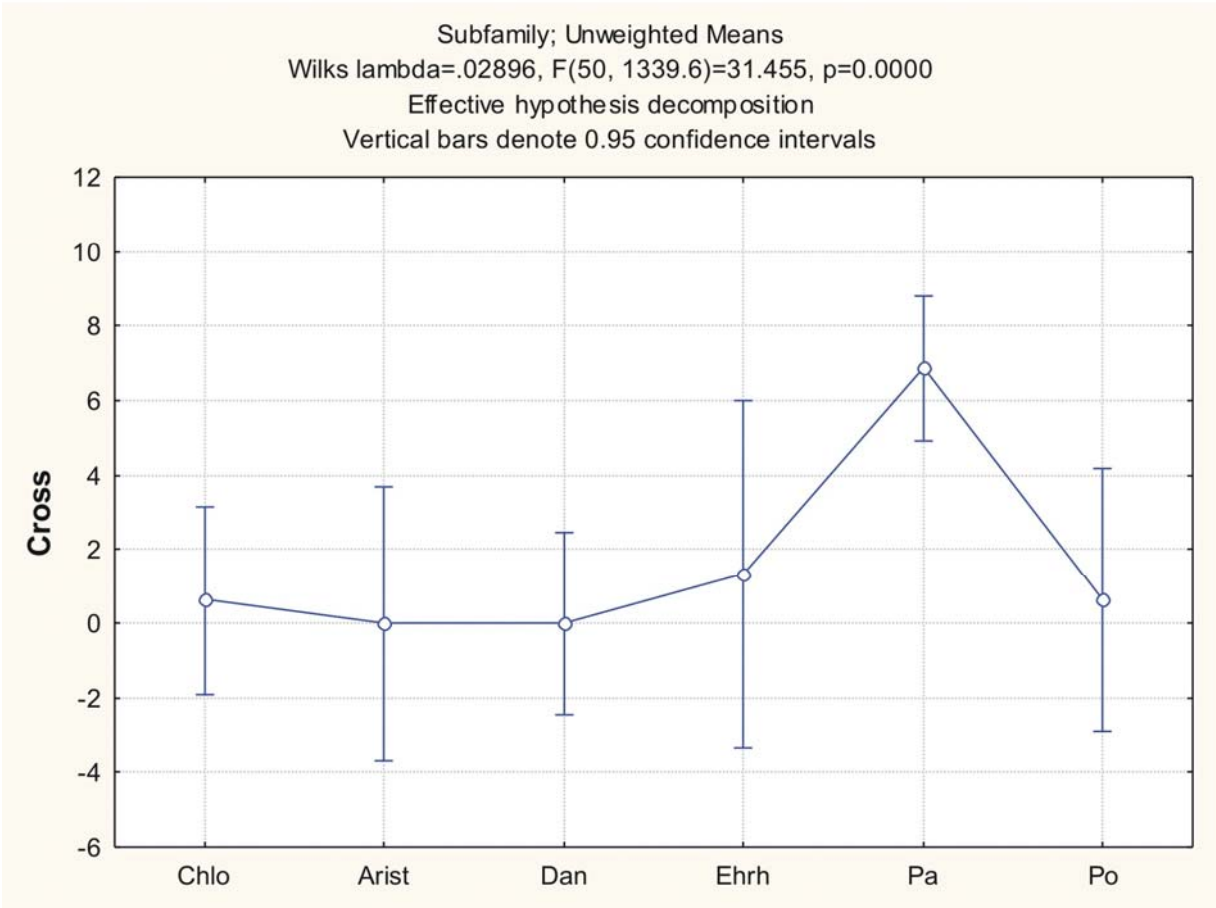

Cell No.	SUBFAM	{1} 69.426	{2} 2.3793	{3} 0.0000	{4} 0.0000	{5} 0.0000	{6} 0.0000	{7} 0.0000
	Tukey HSD test; variable **Saddle Var 1**							
	Approximate Probabilities for Post Hoc Tests							
	Error: Between MS = 319.46, df = 304.00							
1	Chlo		0.000026	0.000026	0.000026	0.000026	0.000026	0.000026
2	Arist	0.000026		0.999991	0.996945	0.999426	0.995709	0.998652
4	Dan	0.000026	0.996945	1.000000		1.000000	1.000000	1.000000
5	Ehrh	0.000026	0.999426	1.000000	1.000000		1.000000	1.000000
6	Pa	0.000026	0.995709	1.000000	1.000000	1.000000		1.000000
7	Po	0.000026	0.998652	1.000000	1.000000	1.000000	1.000000	

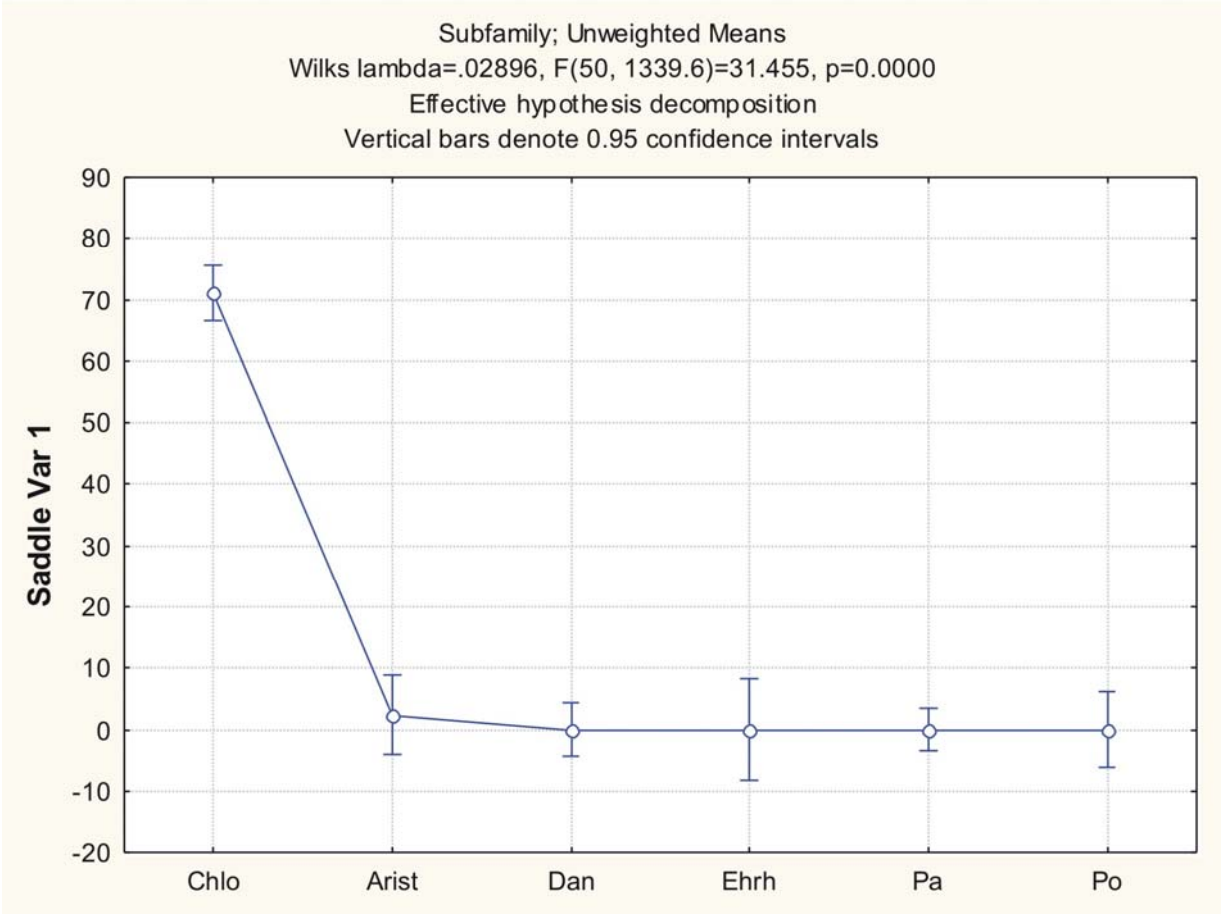

Cell No.	Tukey HSD test; variable **Saddle Var 2** Approximate Probabilities for Post Hoc Tests Error: Between MS = 227.82, df = 304.00 SUBFAM	{1} 6.6066	{2} 59.966	{3} 0.0000	{4} .84615	{5} 0.0000	{6} .64423	{7} 0.0000
1	Chlo		0.000026	0.990072	0.328486	0.661598	0.178205	0.424566
2	Arist	0.000026		0.000026	0.000026	0.000026	0.000026	0.000026
4	Dan	0.328486	0.000026	1.000000		0.999993	1.000000	0.999977
5	Ehrh	0.661598	0.000026	1.000000	0.999993		0.999998	1.000000
6	Pa	0.178205	0.000026	1.000000	1.000000	0.999998		0.999993
7	Po	0.424566	0.000026	1.000000	0.999977	1.000000	0.999993	

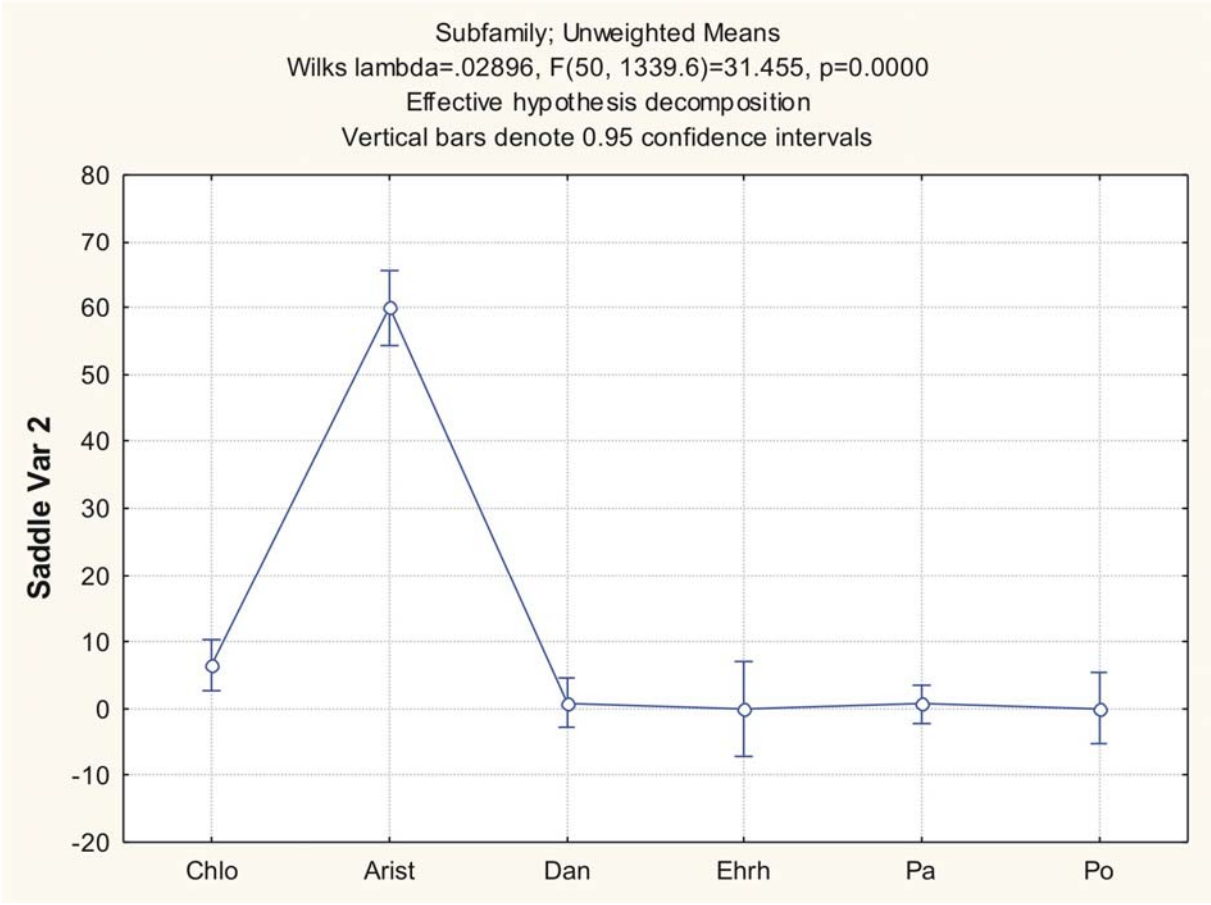

Cell No.	SUBFAM	{1} 0.0000	{2} .86207	{3} 66.667	{4} 23.908	{5} 26.500	{6} 2.0769	{7} 22.419
	Tukey HSD test; variable **Trapezoid**							
	Approximate Probabilities for Post Hoc Tests							
	Error: Between MS = 415.65, df = 304.00							
1	Chlo		0.999996	0.000026	0.000026	0.000049	0.995792	0.000037
2	Arist	0.999996		0.000027	0.000033	0.000566	0.999958	0.000852
4	Dan	0.000026	0.000033	0.007039		0.999127	0.000026	0.999889
5	Ehrh	0.000049	0.000566	0.026482	0.999127		0.000077	0.993931
6	Pa	0.995792	0.999958	0.000027	0.000026	0.000077		0.000046
7	Po	0.000037	0.000852	0.006123	0.999889	0.993931	0.000046	

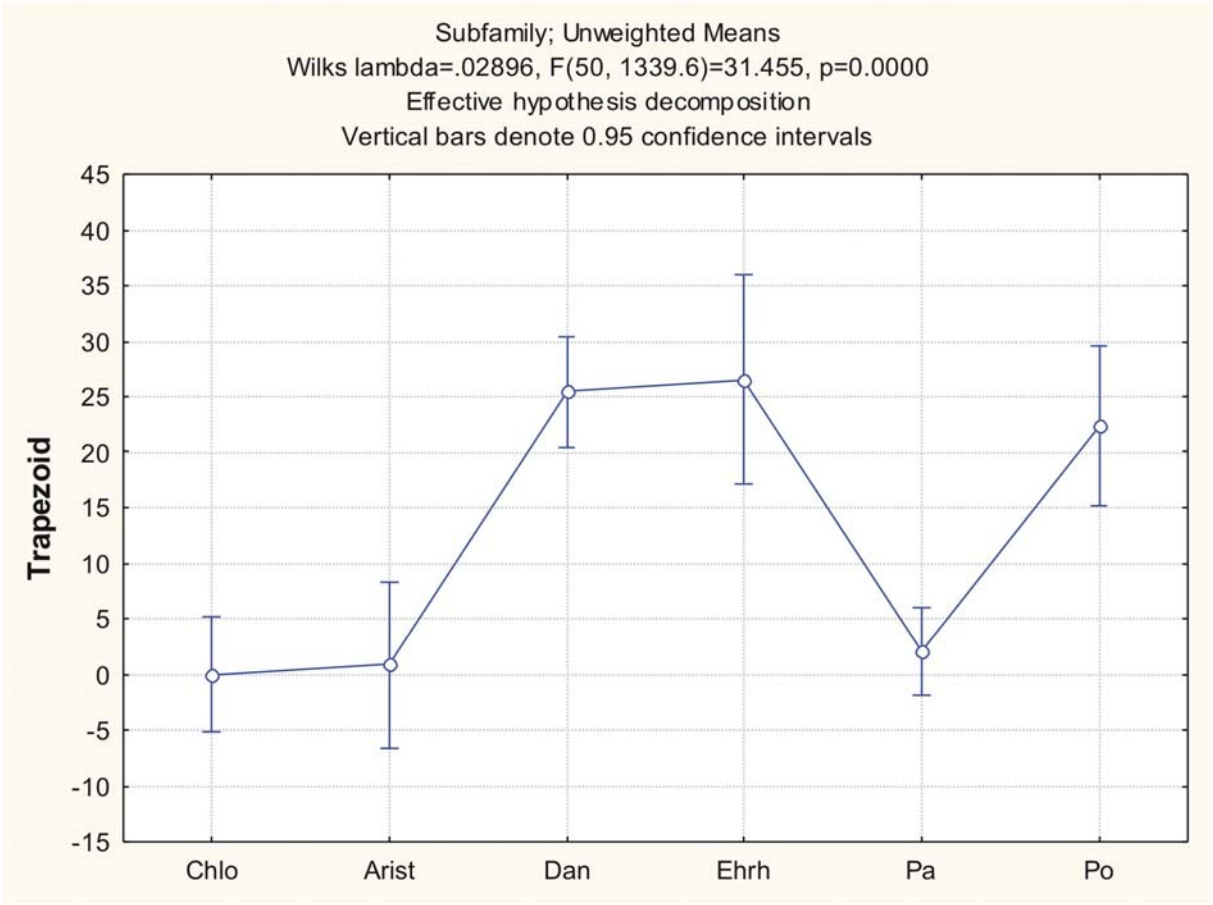

Cell No.	Tukey HSD test; variable **Rondel** Approximate Probabilities for Post Hoc Tests Error: Between MS = 168.77, df = 304.00 SUBFAM	{1} 0.0000	{2} 1.2069	{3} 0.0000	{4} 7.4154	{5} 2.1111	{6} 0.0000	{7} 10.581
1	Chlo		0.999626	1.000000	0.023126	0.996659	1.000000	0.004176
2	Arist	0.999626		0.999999	0.328961	0.999987	0.999436	0.076985
4	Dan	0.023126	0.328961	0.961105		0.724897	0.005676	0.923388
5	Ehrh	0.996659	0.999987	0.999974	0.724897		0.995610	0.295308
6	Pa	1.000000	0.999436	1.000000	0.005676	0.995610		0.001353
7	Po	0.004176	0.076985	0.829628	0.923388	0.295308	0.001353	

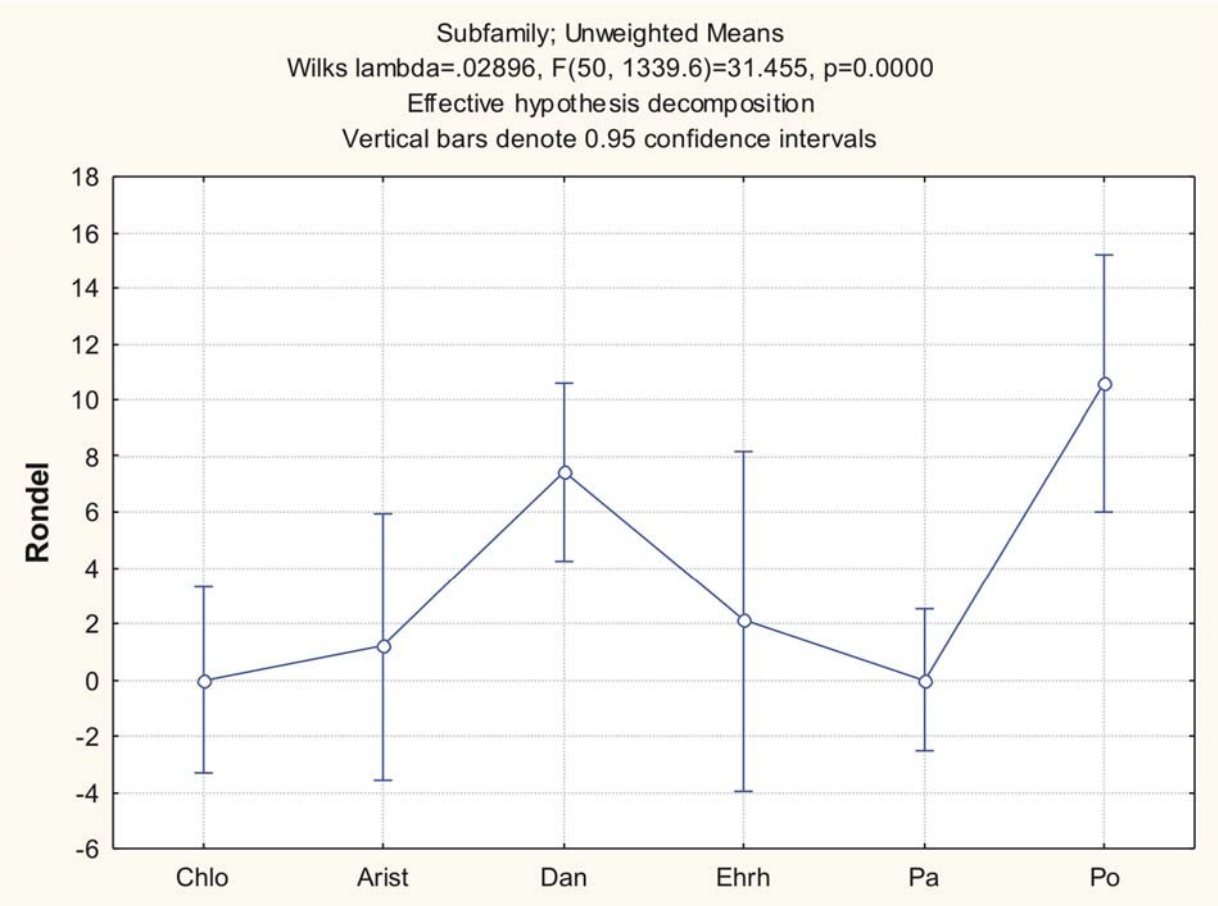

Cell No.	Tukey HSD test; variable **Oblong** Approximate Probabilities for Post Hoc Tests Error: Between MS = 204.34, df = 304.00 SUBFAM	{1} 0.0000	{2} 0.0000	{3} 3.0000	{4} 1.8308	{5} 3.6667	{6} 0.0000	{7} 43.871
1	Chlo		1.000000	0.999843	0.991531	0.963093	1.000000	0.000026
2	Arist	1.000000		0.999864	0.997537	0.978945	1.000000	0.000026
4	Dan	0.991531	0.997537	0.999999		0.999075	0.984046	0.000026
5	Ehrh	0.963093	0.978945	1.000000	0.999075		0.953100	0.000026
6	Pa	1.000000	1.000000	0.999834	0.984046	0.953100		0.000026
7	Po	0.000026	0.000026	0.000069	0.000026	0.000026	0.000026	

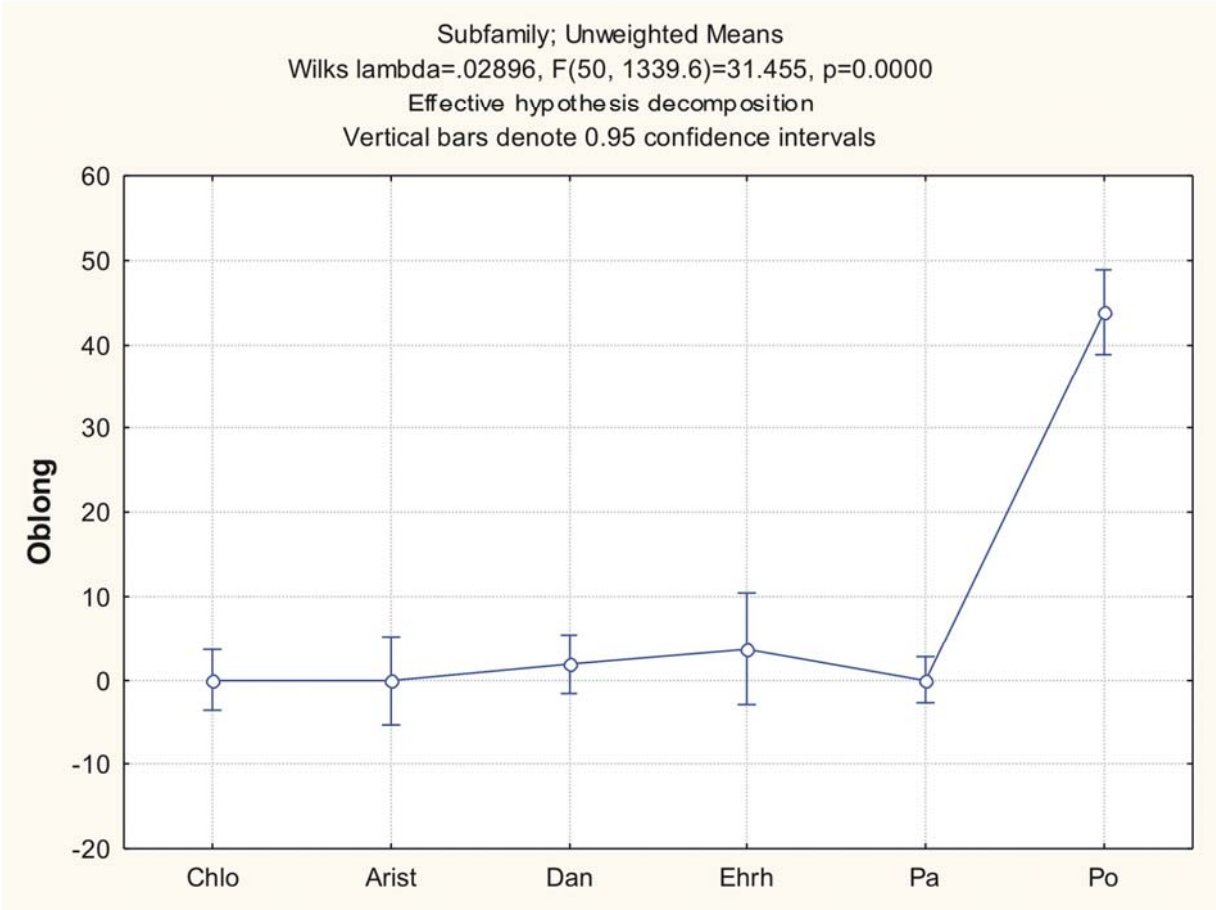

Cell No.	Tukey HSD test; variable **Reniform** Approximate Probabilities for Post Hoc Tests Error: Between MS = 161.62, df = 304.00 SUBFAM	{1} 0.0000	{2} 5.4138	{3} 0.0000	{4} 11.154	{5} 10.167	{6} .50962	{7} 4.4839
1	Chlo		0.488314	1.000000	0.000041	0.045444	0.999981	0.683033
2	Arist	0.488314		0.992513	0.400615	0.876088	0.522818	0.999958
4	Dan	0.000041	0.400615	0.753551		0.999950	0.000028	0.196829
5	Ehrh	0.045444	0.876088	0.860279	0.999950		0.046222	0.739920
6	Pa	0.999981	0.522818	1.000000	0.000028	0.046222		0.728160
7	Po	0.683033	0.999958	0.997293	0.196829	0.739920	0.728160	

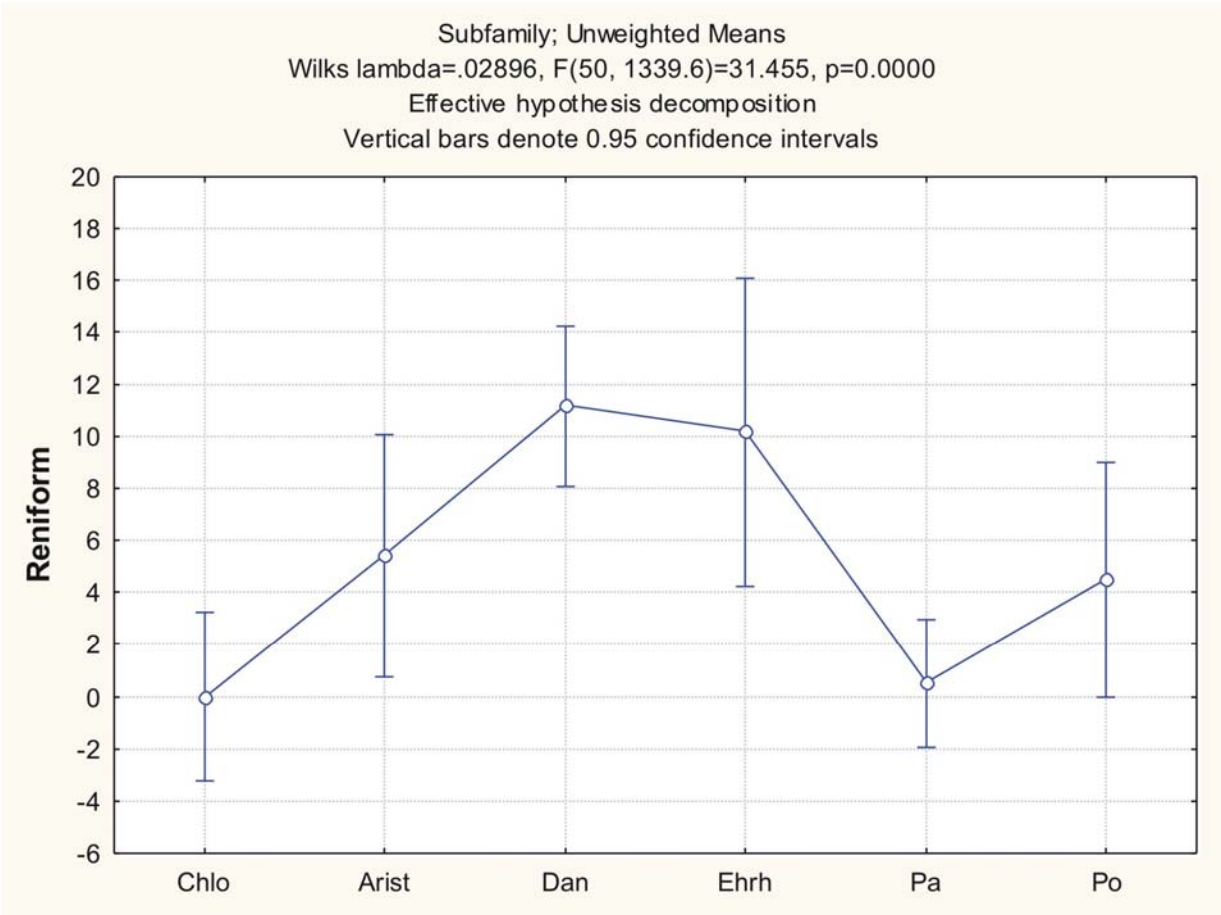

Appendix 9: Basic statistics of the number of GSSC-morphotypes counted for each photosynthetic pathway subcategory, including C_4 subtypes.

Appendix 9

Basic statistics of GSSC-morphotypes counted for each photosynthetic subcategory.

Variable	C3					
	Valid N	Mean	Confidence -95.000%	Confidence +95.000%	Variance	Standard Error
Bilobate Var 1	127	3.84252	0.65591	7.02913	329.292	1.610234
Bilobate Var 2	127	30.79528	24.10157	37.48898	1452.974	3.382416
Bilobate Var 3	127	5.91339	3.08166	8.74511	260.032	1.430908
Polylobate	127	5.98425	3.26550	8.70301	239.698	1.373822
Cross	127	1.30709	-0.35171	2.96589	89.230	0.838213
Saddle Var 1	127	0.00000			0.000	0.000000
Saddle Var 2	127	0.43307	0.10151	0.76463	3.565	0.167542
Trapezoid	127	23.66929	18.15433	29.18425	986.302	2.786783
Rondel	127	6.67717	3.11944	10.23489	410.458	1.797764
Oblong	127	12.16535	7.13500	17.19571	820.584	2.541906
Reniform	127	8.40157	5.08787	11.71528	356.083	1.674457

Variable	C4					
	Valid N	Mean	Confidence -95.000%	Confidence +95.000%	Variance	Standard Error
Bilobate Var 1	175	17.93143	12.66813	23.19473	1244.501	2.666727
Bilobate Var 2	175	31.83429	25.59663	38.07194	1747.921	3.160398
Bilobate Var 3	175	2.58857	0.84555	4.33159	136.485	0.883127
Polylobate	175	4.41143	2.02721	6.79564	255.370	1.207997
Cross	175	2.82857	1.41466	4.24248	89.810	0.716378
Saddle Var 1	175	24.59429	18.55135	30.63722	1640.495	3.061741
Saddle Var 2	175	12.64571	8.28930	17.00213	852.586	2.207243
Trapezoid	175	1.37714	-0.06162	2.81591	92.995	0.728971
Rondel	175	0.20000	-0.17274	0.57274	6.241	0.188852
Oblong	175	0.00000			0.000	0.000000
Reniform	175	1.17714	0.24916	2.10513	38.687	0.470178

Variable	NAD					
	Valid N	Mean	Confidence -95.000%	Confidence +95.000%	Variance	Standard Error
Bilobate Var 1	42	4.88095	-1.01087	10.77278	357.473	2.917408
Bilobate Var 2	42	7.21429	0.40904	14.01953	476.904	3.369698
Bilobate Var 3	42	2.92857	-0.88700	6.74415	149.922	1.889328
Polylobate	42	0.00000			0.000	0.000000
Cross	42	0.30952	-0.31557	0.93462	4.024	0.309524
Saddle Var 1	42	43.00000	28.73911	57.26089	2094.293	7.061453
Saddle Var 2	42	35.97619	22.76496	49.18742	1797.341	6.541699
Trapezoid	42	0.59524	-0.11357	1.30404	5.174	0.350973
Rondel	42	0.04762	-0.04855	0.14379	0.095	0.047619
Oblong	42	0.00000			0.000	0.000000
Reniform	42	2.85714	-0.07064	5.78493	88.272	1.449727

Variable	NADP					
	Valid N	Mean	Confidence -95.000%	Confidence +95.000%	Variance	Standard Error
Bilobate Var 1	28	25.50000	10.50013	40.49987	1496.407	7.310480
Bilobate Var 2	28	55.32143	38.87118	71.77167	1799.782	8.017351
Bilobate Var 3	28	1.42857	-0.73535	3.59249	31.143	1.054630
Polylobate	28	11.67857	0.55576	22.80138	822.819	5.420921
Cross	28	6.42857	1.23327	11.62387	179.513	2.532032
Saddle Var 1	28	0.00000			0.000	0.000000
Saddle Var 2	28	0.00000			0.000	0.000000
Trapezoid	28	0.00000			0.000	0.000000
Rondel	28	0.00000			0.000	0.000000
Oblong	28	0.00000			0.000	0.000000
Reniform	28	0.00000			0.000	0.000000

Variable	PCK					
	Valid N	Mean	Confidence -95.000%	Confidence +95.000%	Variance	Standard Error
Bilobate Var 1	16	16.06250	-2.96247	35.08747	1274.729	8.92584
Bilobate Var 2	16	20.81250	1.48375	40.14125	1315.762	9.06836
Bilobate Var 3	16	1.87500	-0.88270	4.63270	26.783	1.29382
Polylobate	16	4.37500	-2.63202	11.38202	172.917	3.28744
Cross	16	6.87500	-2.01784	15.76784	278.517	4.17220
Saddle Var 1	16	43.00000	18.46826	67.53174	2119.467	11.50942
Saddle Var 2	16	7.00000	-0.52576	14.52576	199.467	3.53082
Trapezoid	16	0.00000			0.000	0.00000
Rondel	16	0.00000			0.000	0.00000
Oblong	16	0.00000			0.000	0.00000
Reniform	16	0.00000			0.000	0.00000

Appendix 10: Tukey's HSD test for unequal sample sizes in the Photosynthetic pathway -category (including C_3 and C_4).

Appendix 10

Photosynthetic pathway (C3 and C4 subcategories): Tukey's HSD for unequal sample sizes. Marked values are significant at p < .05000.

Cell No.	Tukey HSD test; variable Bilobate Var1 Approximate Probabilities for Post Hoc Tests Error: Between MS = 553.45, df = 209.00 Photosynthetic pathway	{1} 3.8425	{2} 4.8810	{3} 25.500	{4} 16.062
1	C3		0.994649	0.000067	0.204081
2	NAD	0.994649		0.001874	0.368464
3	NADP	0.000067	0.001874		0.575672
4	PCK	0.204081	0.368464	0.575672	

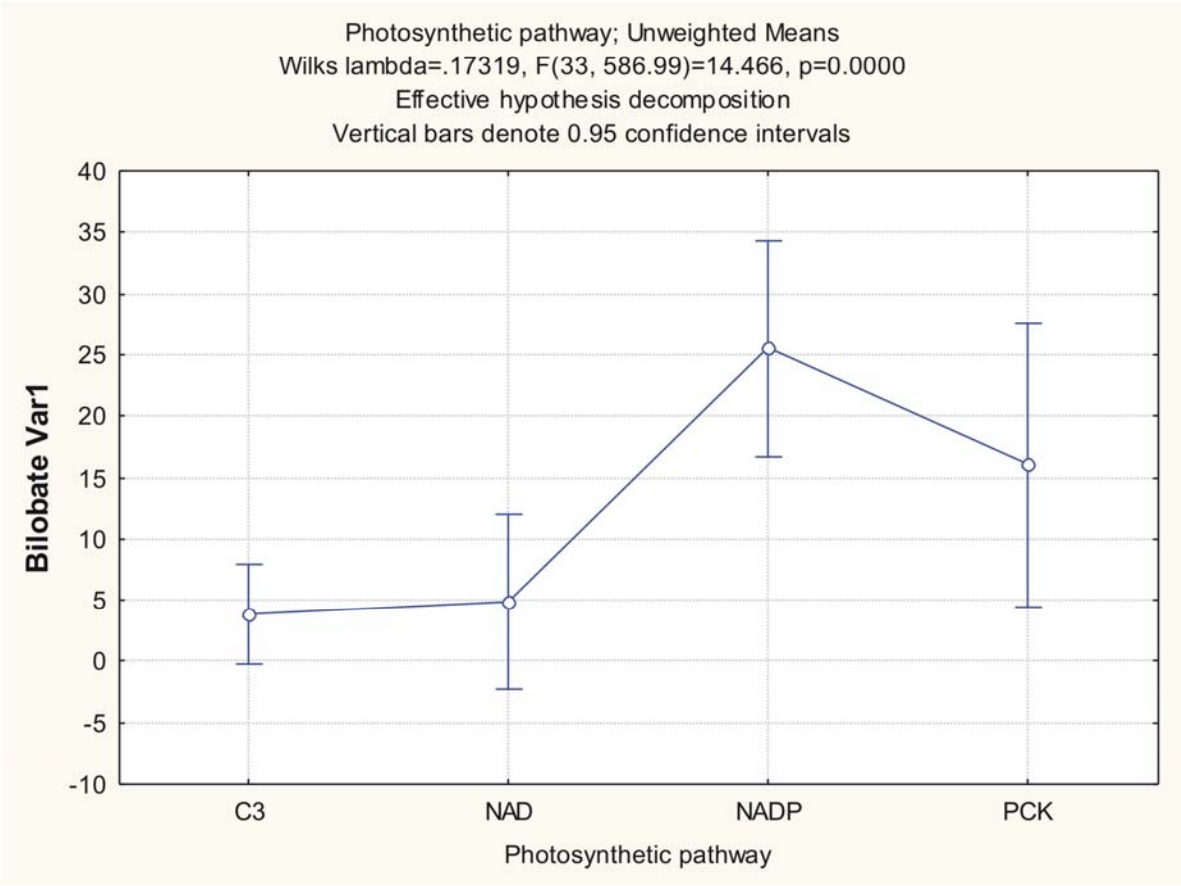

Cell No.	Photosynthetic pathway	{1} 30.795	{2} 7.2143	{3} 55.321	{4} 20.813
	Tukey HSD test; variable Bilobate Var 2 Approximate Probabilities for Post Hoc Tests Error: Between MS = 1296.5, df = 209.00				
1	C3		0.001352	0.006083	0.722837
2	NAD	0.001352		0.000008	0.572183
3	NADP	0.006083	0.000008		0.011946
4	PCK	0.722837	0.572183	0.011946	

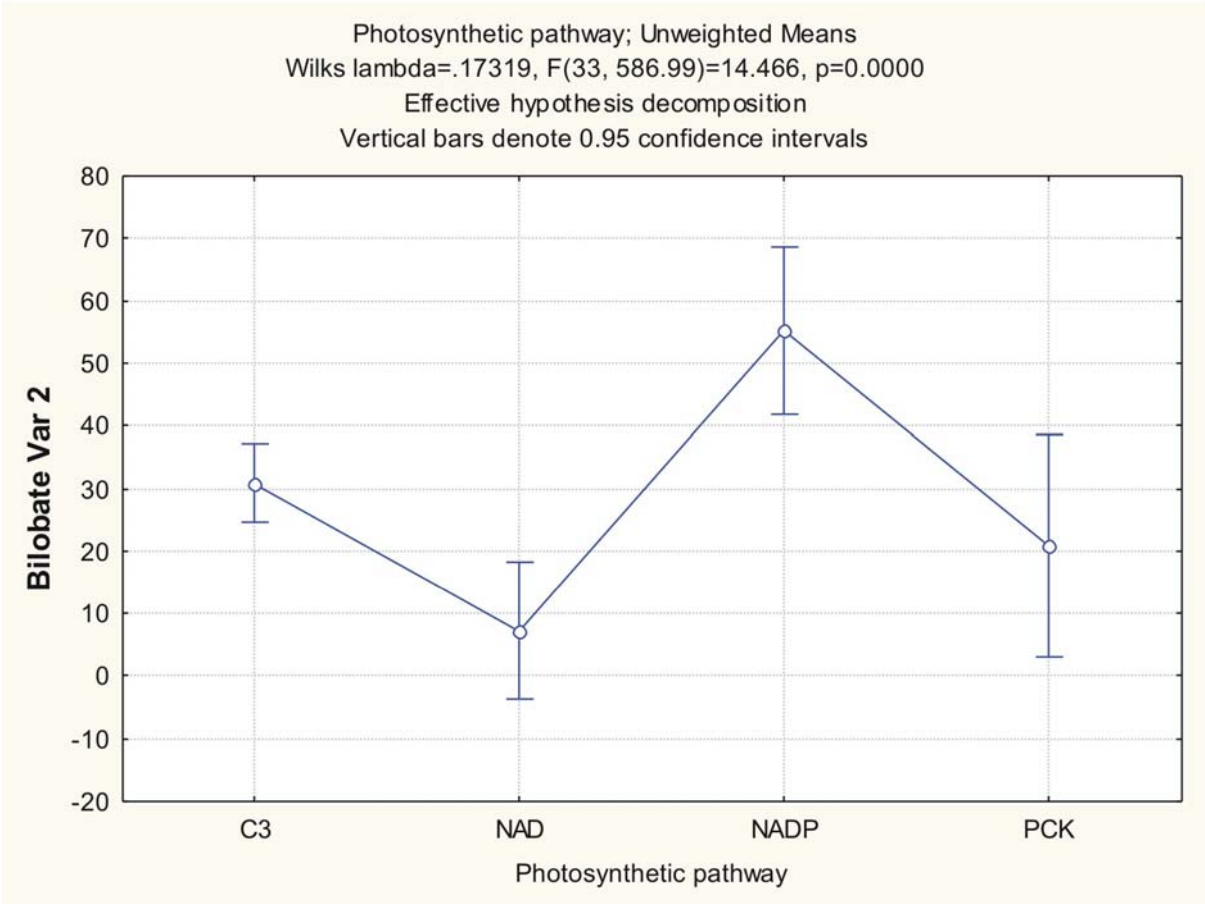

Cell No.	Photosynthetic pathway	{1} 5.9843	{2} 0.0000	{3} 11.679	{4} 4.3750
	Tukey HSD test; variable Polylobate Approximate Probabilities for Post Hoc Tests Error: Between MS = 263.21, df = 209.00				
1	C3		0.162221	0.333652	0.982183
2	NAD	0.162221		0.016748	0.795297
3	NADP	0.333652	0.016748		0.476479
4	PCK	0.982183	0.795297	0.476479	

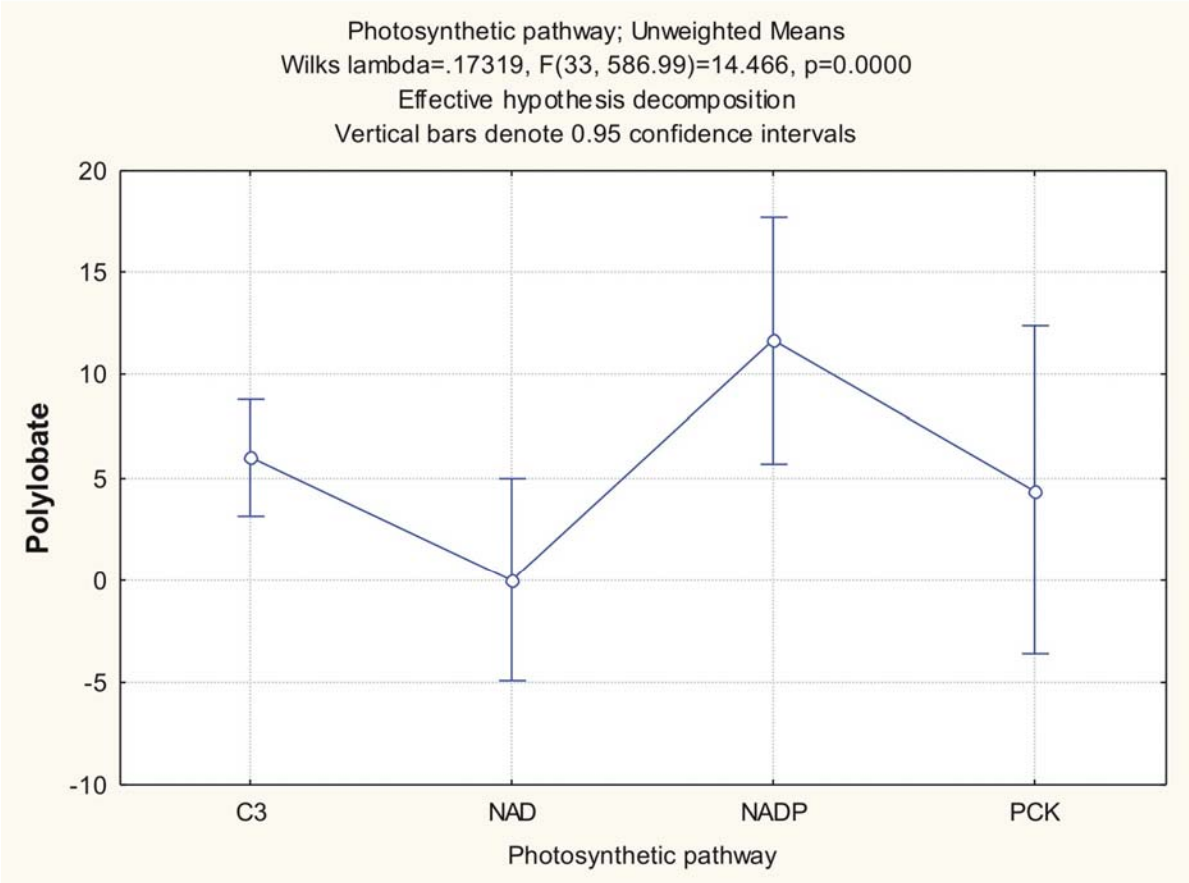

Cell No.	Tukey HSD test; variable Cross Approximate Probabilities for Post Hoc Tests Error: Between MS = 97.764, df = 209.00 Photosynthetic pathway	{1} 1.3071	{2} .30952	{3} 6.4286	{4} 6.8750
1	C3		0.941936	0.062893	0.145833
2	NAD	0.941936		0.054469	0.107485
3	NADP	0.062893	0.054469		0.998935
4	PCK	0.145833	0.107485	0.998935	

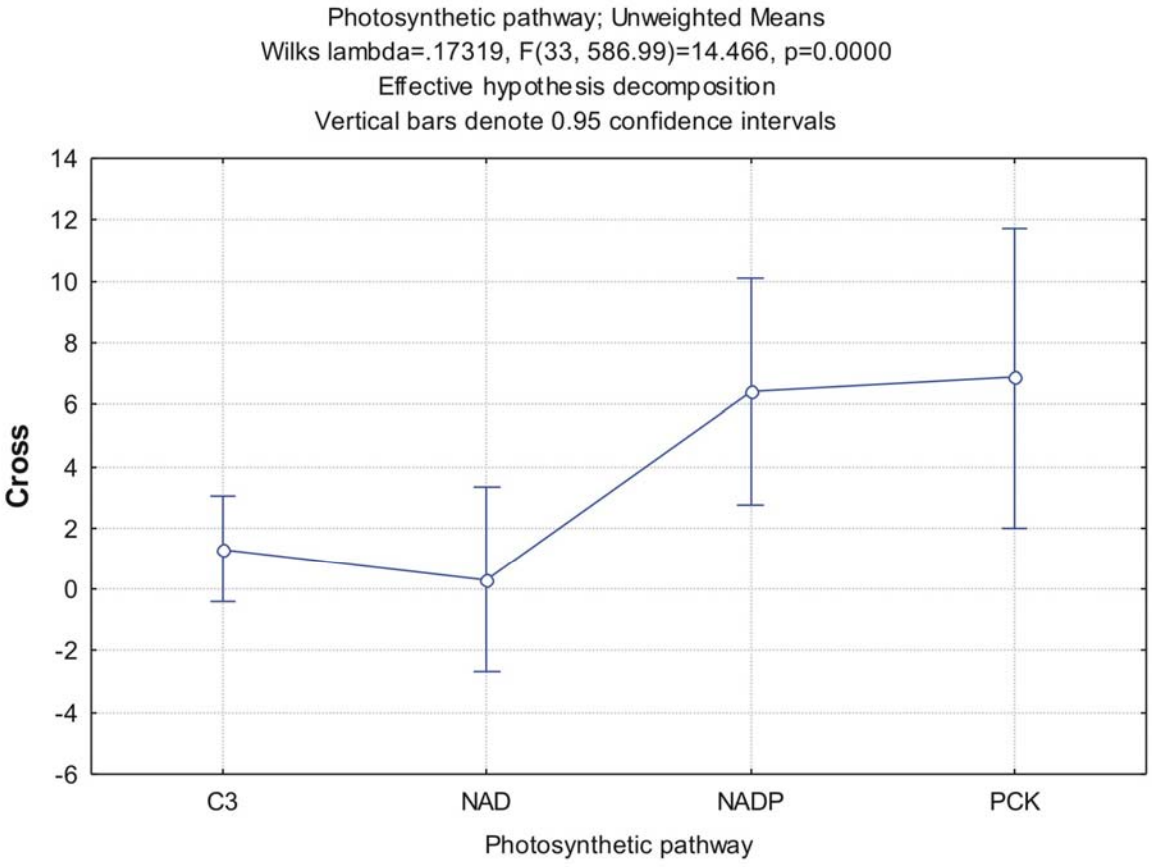

Cell No.	Photosynthetic pathway	{1} 0.0000	{2} 43.000	{3} 0.0000	{4} 43.000
	Tukey HSD test; variable Saddle Var 1 Approximate Probabilities for Post Hoc Tests Error: Between MS = 562.96, df = 209.00				
1	C3		0.000008	1.000000	0.000008
2	NAD	0.000008		0.000008	1.000000
3	NADP	1.000000	0.000008		0.000008
4	PCK	0.000008	1.000000	0.000008	

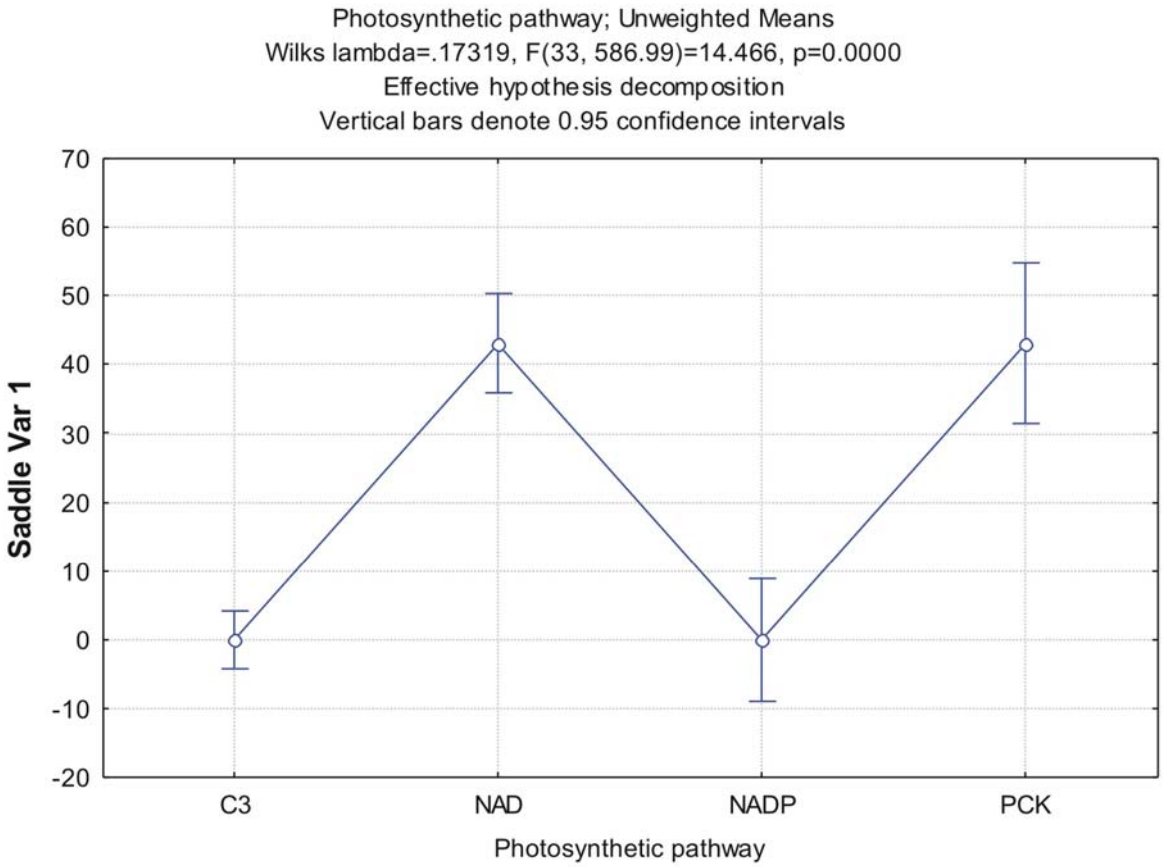

Cell No.	Photosynthetic pathway	{1} .43307	{2} 35.976	{3} 0.0000	{4} 7.0000
	Tukey HSD test; variable Saddle Var 2 Approximate Probabilities for Post Hoc Tests Error: Between MS = 369.05, df = 209.00				
1	C3		0.000008	0.999550	0.570214
2	NAD	0.000008		0.000008	0.000009
3	NADP	0.999550	0.000008		0.650453
4	PCK	0.570214	0.000009	0.650453	

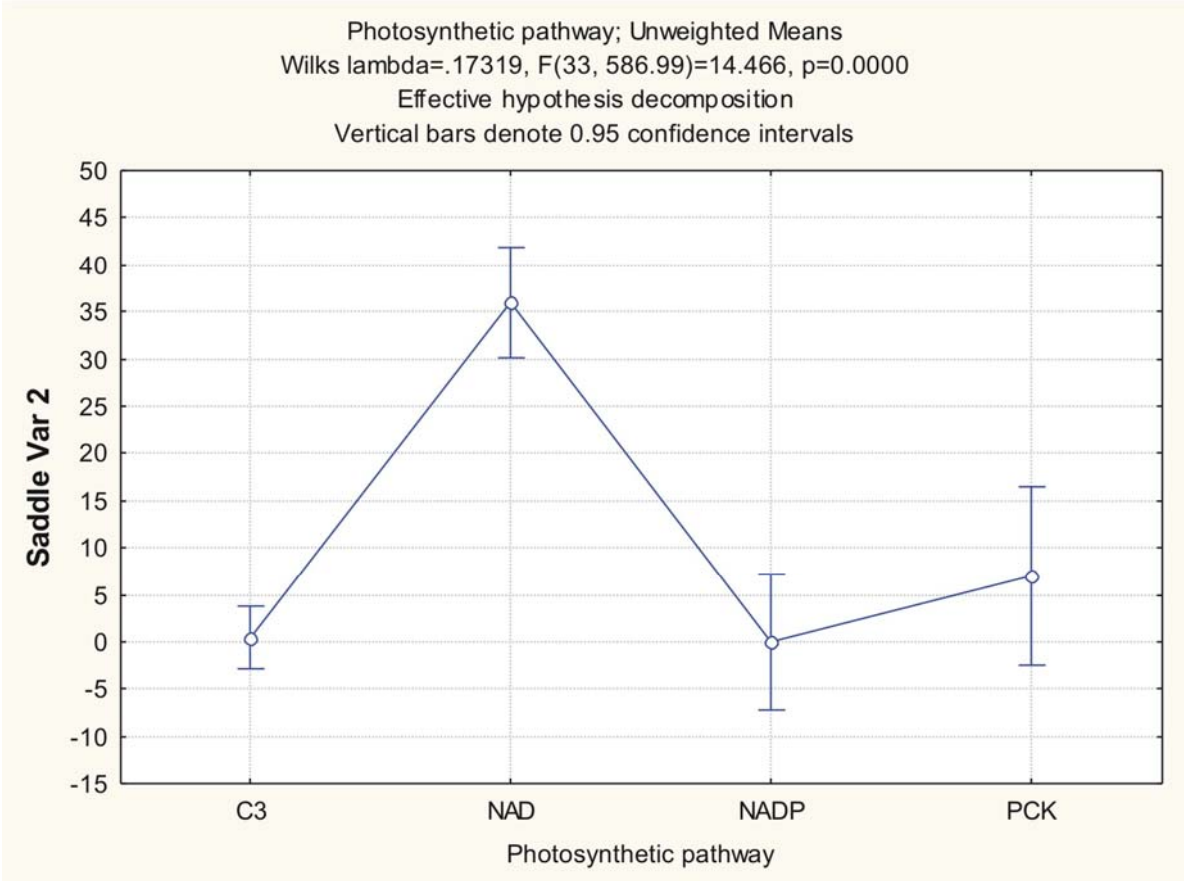

Cell No.	Tukey HSD test; variable Trapezoid Approximate Probabilities for Post Hoc Tests Error: Between MS = 595.63, df = 209.00 Photosynthetic pathway	{1} 23.669	{2} .59524	{3} 0.0000	{4} 0.0000
1	C3		0.000008	0.000027	0.001477
2	NAD	0.000008		0.999643	0.999795
3	NADP	0.000027	0.999643		1.000000
4	PCK	0.001477	0.999795	1.000000	

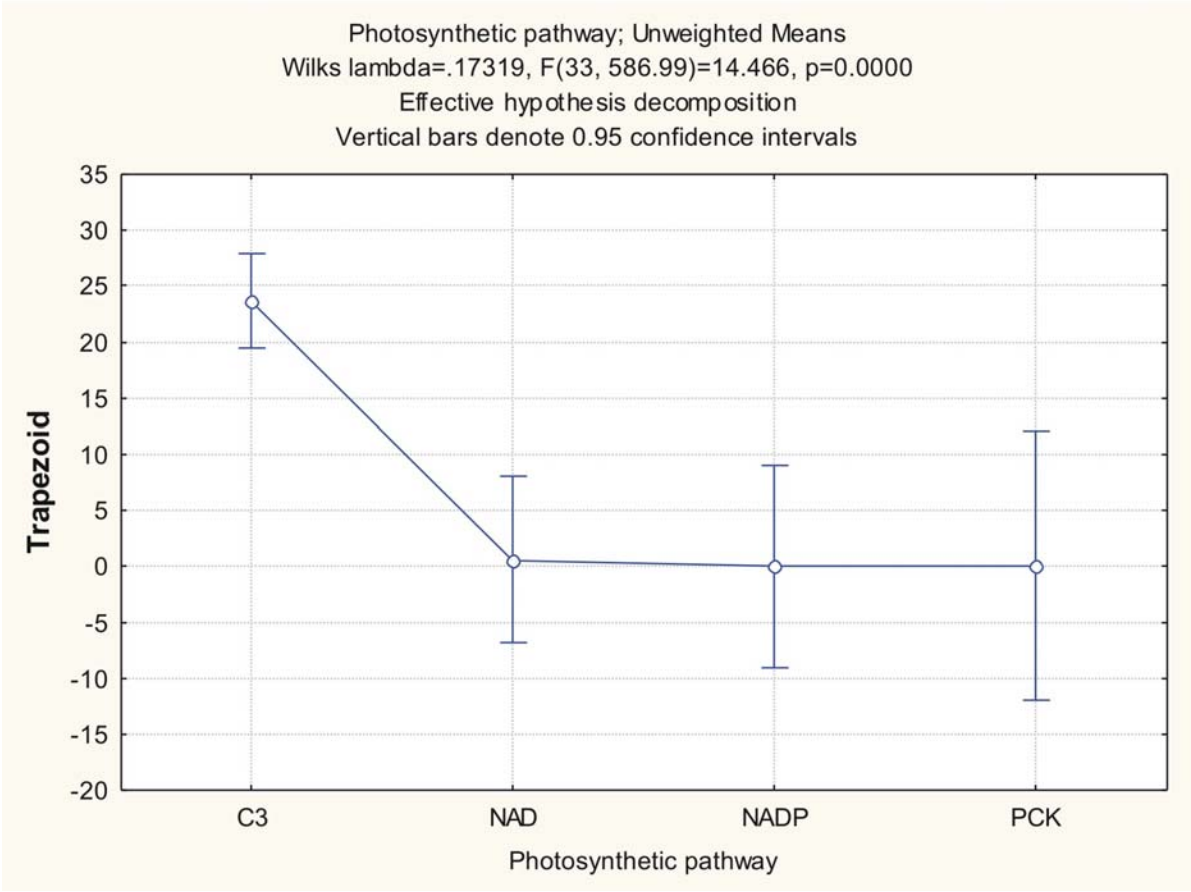

Cell No.	Photosynthetic pathway	{1} 6.6772	{2} .04762	{3} 0.0000	{4} 0.0000
	Tukey HSD test; variable Rondel Approximate Probabilities for Post Hoc Tests Error: Between MS = 247.47, df = 209.00				
1	C3		0.083407	0.175831	0.378568
2	NAD	0.083407		0.999999	1.000000
3	NADP	0.175831	0.999999		1.000000
4	PCK	0.378568	1.000000	1.000000	

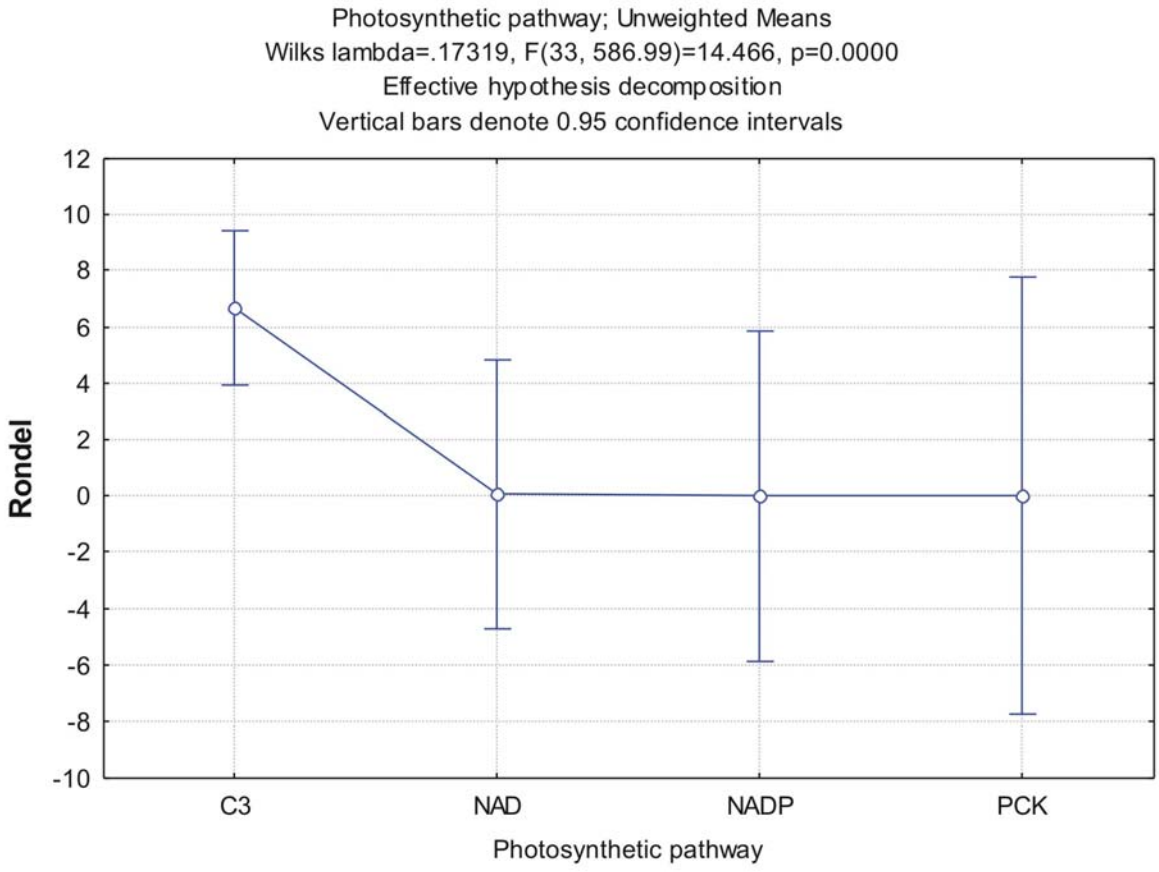

Cell No.	Photosynthetic pathway	{1} 6.6772	{2} .04762	{3} 0.0000	{4} 0.0000
	Tukey HSD test; variable Rondel Approximate Probabilities for Post Hoc Tests Error: Between MS = 247.47, df = 209.00				
1	C3		0.083407	0.175831	0.378568
2	NAD	0.083407		0.999999	1.000000
3	NADP	0.175831	0.999999		1.000000
4	PCK	0.378568	1.000000	1.000000	

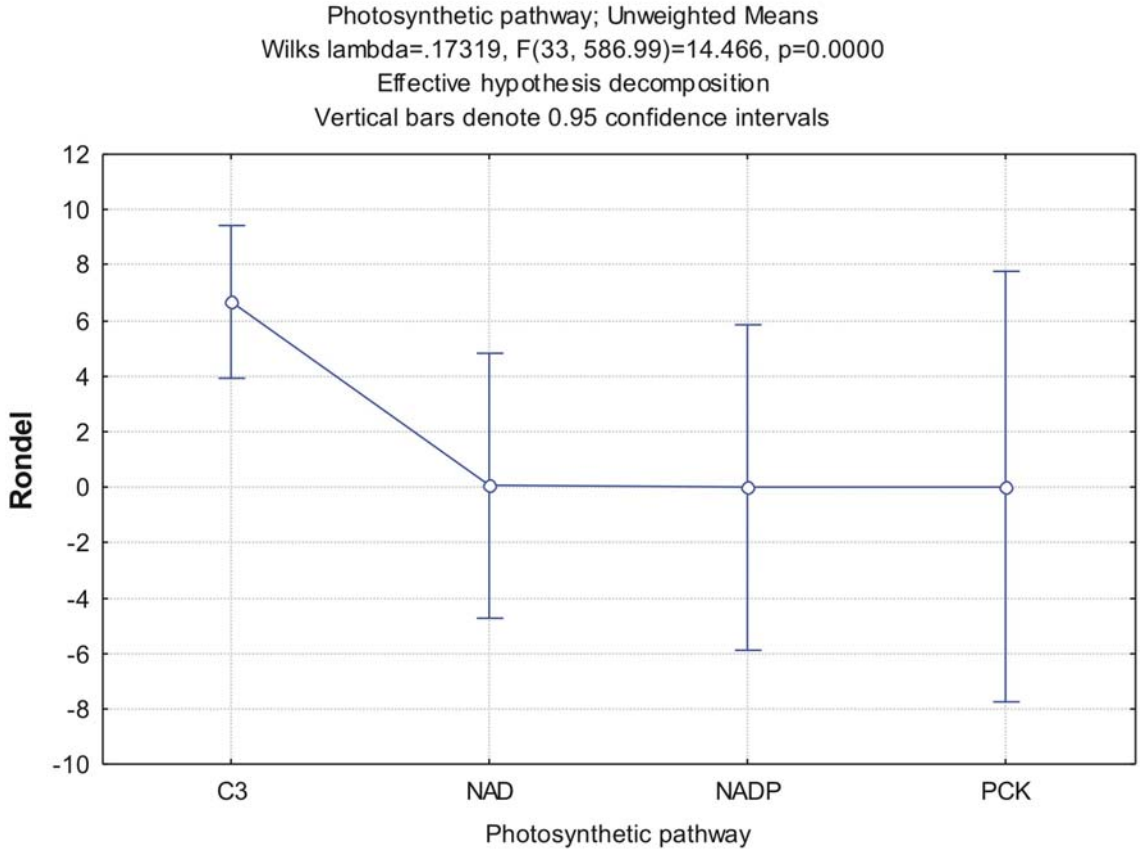

Cell No.	Tukey HSD test; variable Oblong Approximate Probabilities for Post Hoc Tests Error: Between MS = 494.71, df = 209.00 Photosynthetic pathway	{1} 12.165	{2} 0.0000	{3} 0.0000	{4} 0.0000
1	C3		0.011401	0.043639	0.165769
2	NAD	0.011401		1.000000	1.000000
3	NADP	0.043639	1.000000		1.000000
4	PCK	0.165769	1.000000	1.000000	

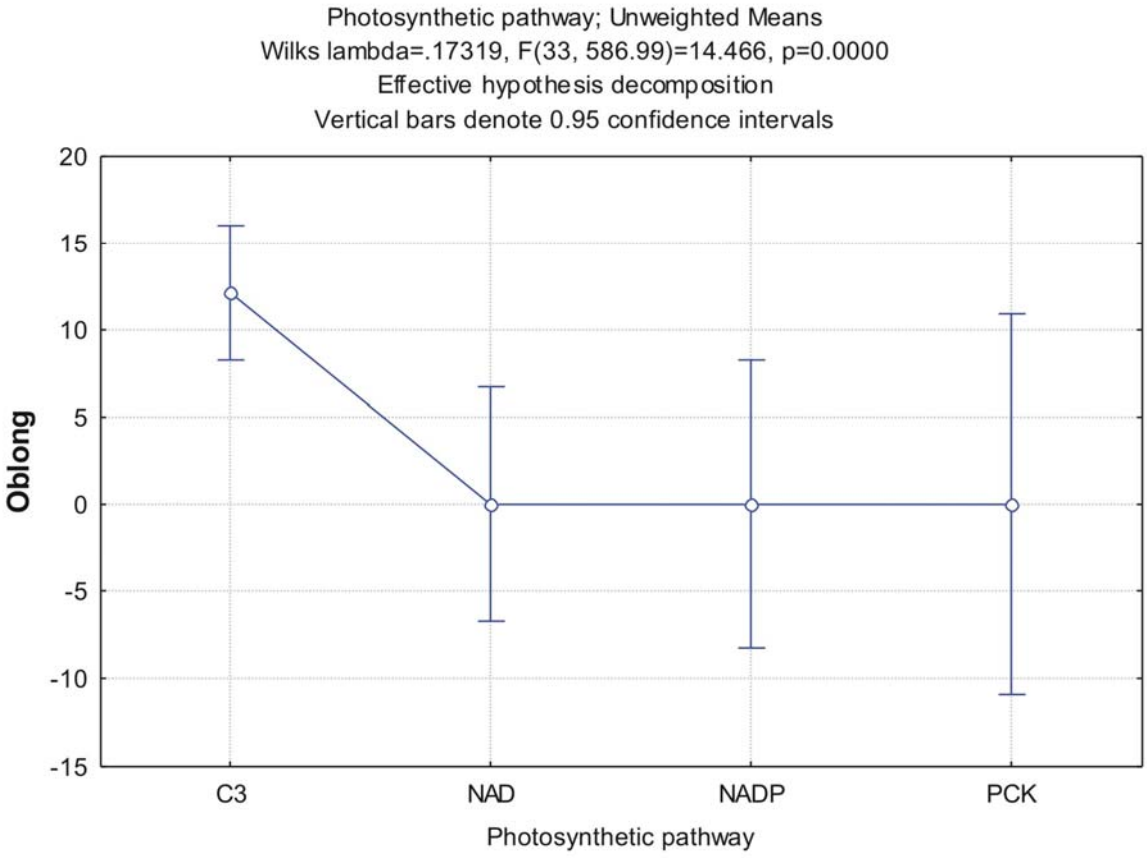

Cell No.	Photosynthetic pathway	{1} 8.4016	{2} 2.8571	{3} 0.0000	{4} 0.0000
	Tukey HSD test; variable Reniform Approximate Probabilities for Post Hoc Tests Error: Between MS = 231.99, df = 209.00				
1	C3		0.171570	0.041071	0.159844
2	NAD	0.171570		0.868514	0.919563
3	NADP	0.041071	0.868514		1.000000
4	PCK	0.159844	0.919563	1.000000	

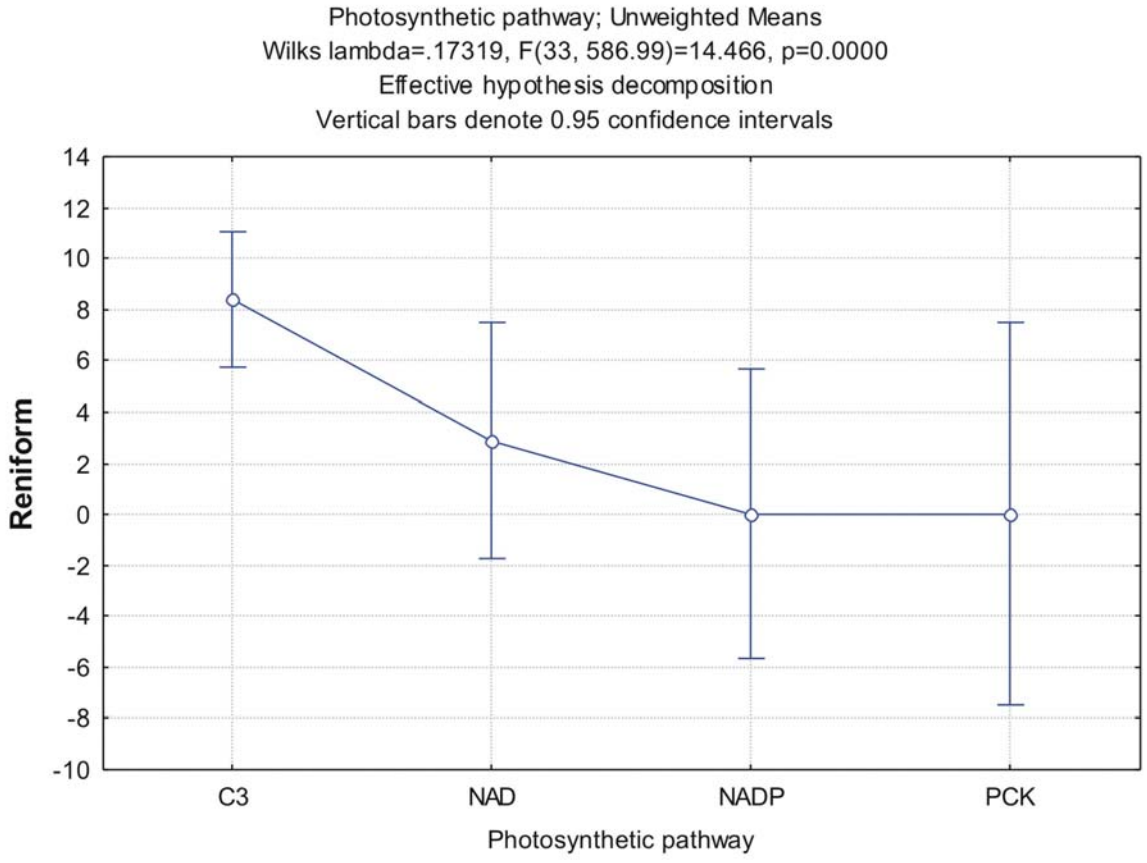

Appendix 11: Tukey's HSD test for unequal sample sizes in the photosynthetic pathway - category (C_4 only).

Appendix 11

Photosynthetic pathway (C4 subtypes): Tukey's HSD for unequal sample sizes. Marked values are significant at p < .05000.

Cell No.	Photosynthetic pathway	{1} 4.8810	{2} 25.500	{3} 16.062
	Tukey HSD test; variable Bilobate Var1 Approximate Probabilities for Post Hoc Tests Error: Between MS = 893.74, df = 83.000			
1	NAD		0.016175	0.414377
2	NADP	0.016175		0.574444
3	PCK	0.414377	0.574444	

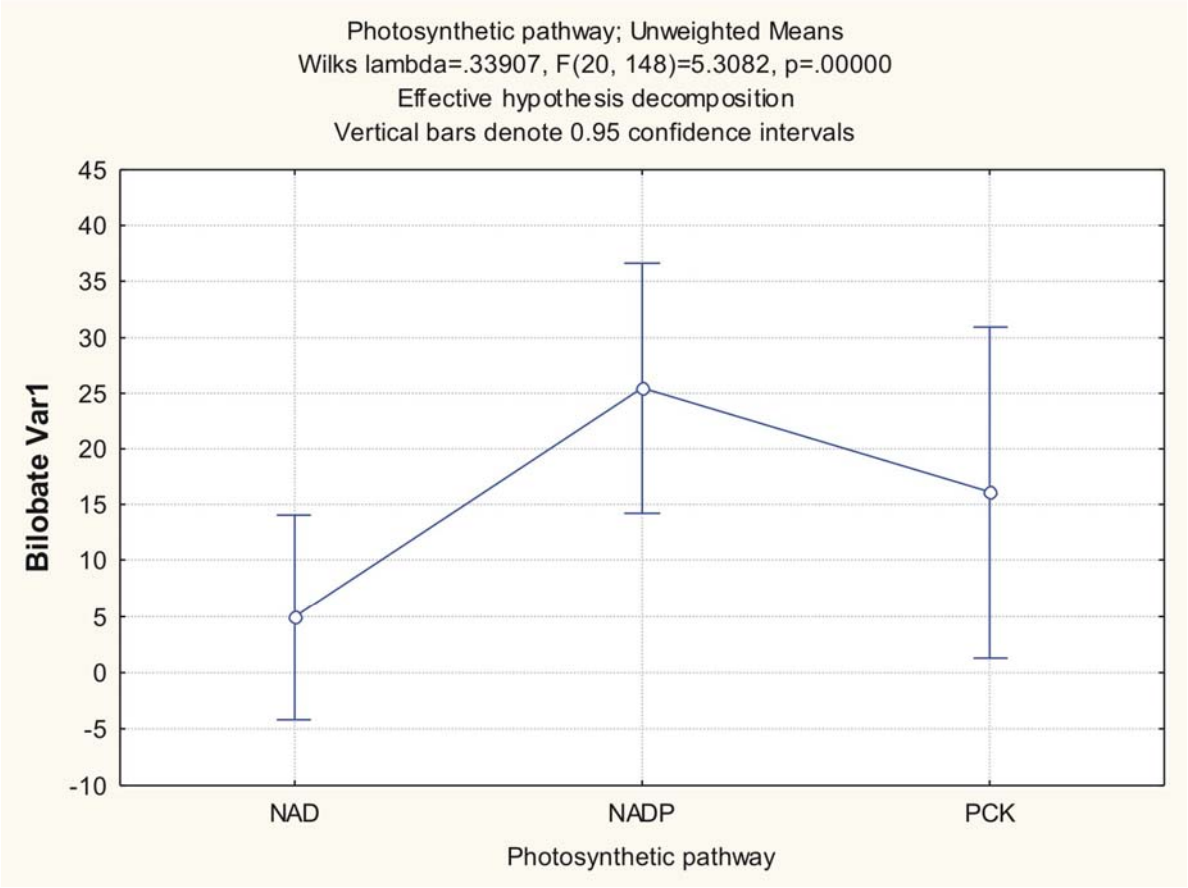

Cell No.	Photosynthetic pathway	{1} 7.2143	{2} 55.321	{3} 20.813
	Tukey HSD test; variable Bilobate Var 2 Approximate Probabilities for Post Hoc Tests Error: Between MS = 1058.8, df = 83.000			
1	NAD		0.000108	0.334196
2	NADP	0.000108		0.003198
3	PCK	0.334196	0.003198	

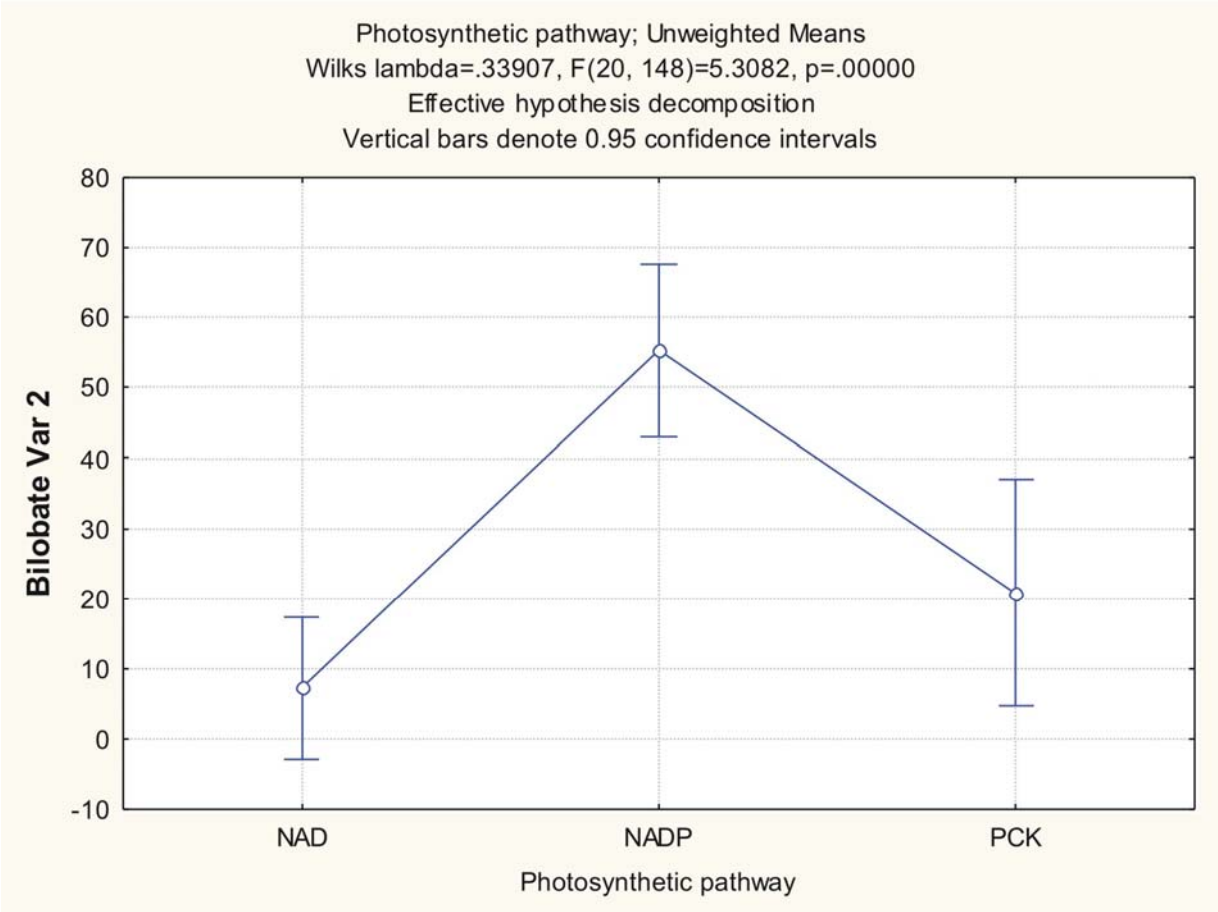

Cell No.	Tukey HSD test; variable Polylobate Approximate Probabilities for Post Hoc Tests Error: Between MS = 298.91, df = 83.000 Photosynthetic pathway	{1} 0.0000	{2} 11.679	{3} 4.3750
1	NAD		0.018942	0.666129
2	NADP	0.018942		0.373079
3	PCK	0.666129	0.373079	

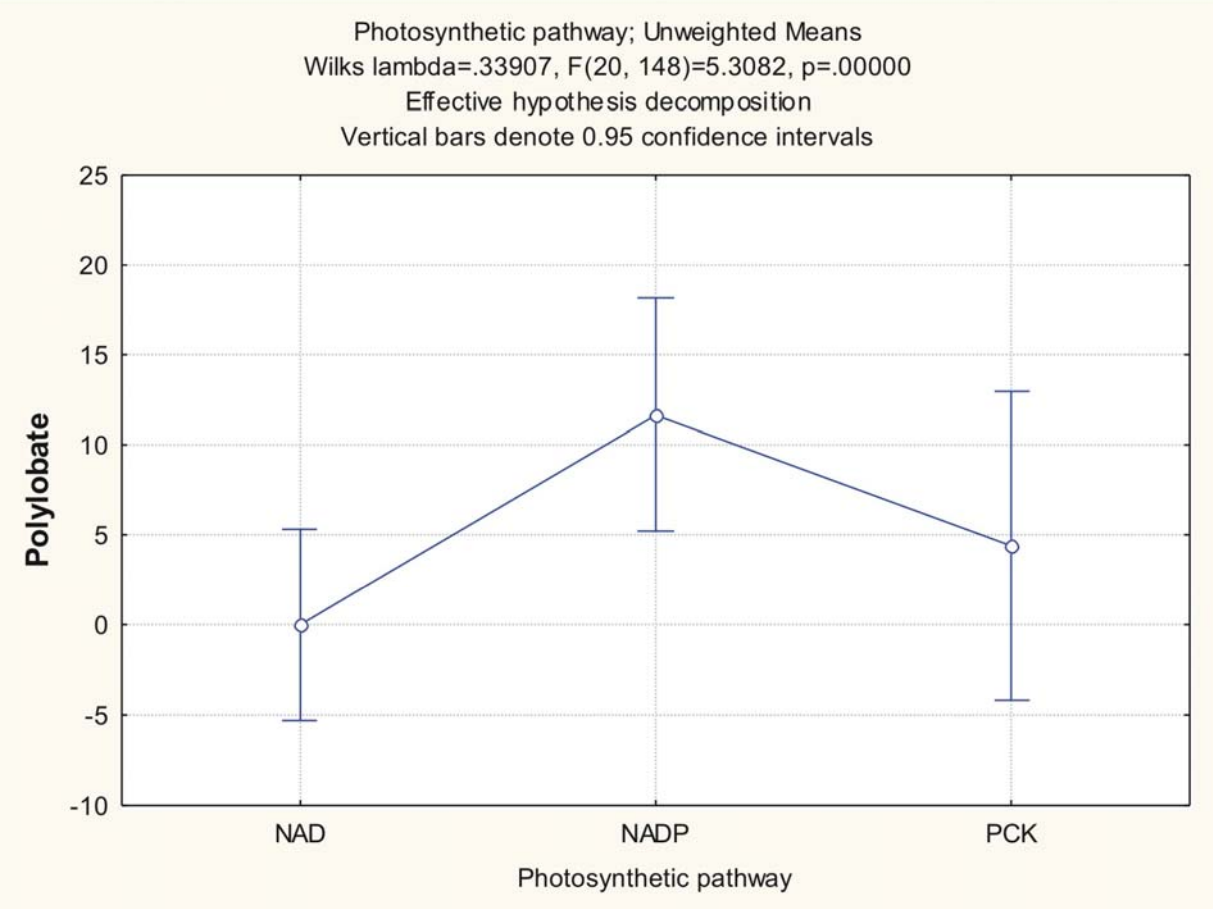

Cell No.	Tukey HSD test; variable Cross Approximate Probabilities for Post Hoc Tests Error: Between MS = 110.72, df = 83.000 Photosynthetic pathway	{1} .30952	{2} 6.4286	{3} 6.8750
1	NAD		0.050424	0.091269
2	NADP	0.050424		0.990032
3	PCK	0.091269	0.990032	

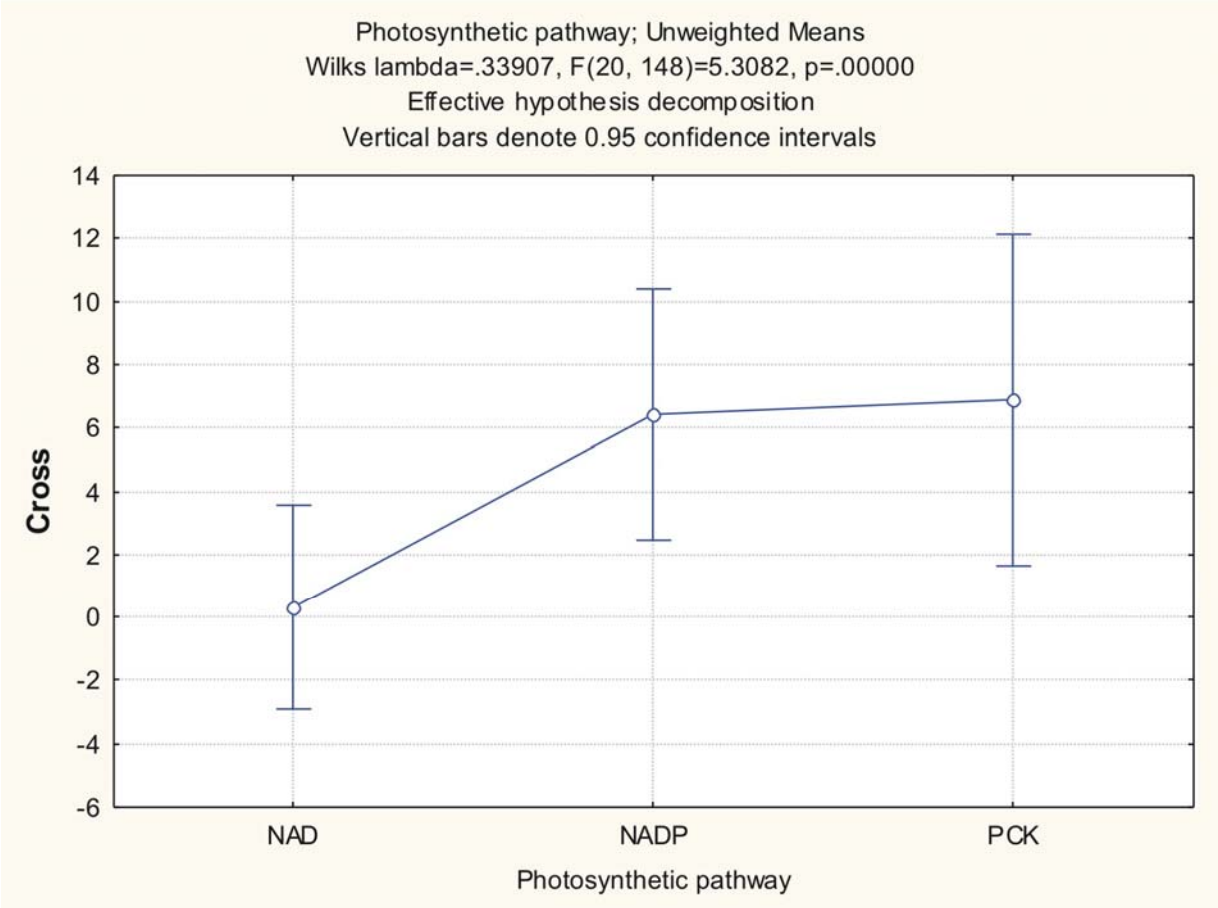

Cell No.	Tukey HSD test; variable Saddle Var 1 Approximate Probabilities for Post Hoc Tests Error: Between MS = 1417.6, df = 83.000 Photosynthetic pathway	{1} 43.000	{2} 0.0000	{3} 43.000
1	NAD		0.000136	1.000000
2	NADP	0.000136		0.001436
3	PCK	1.000000	0.001436	

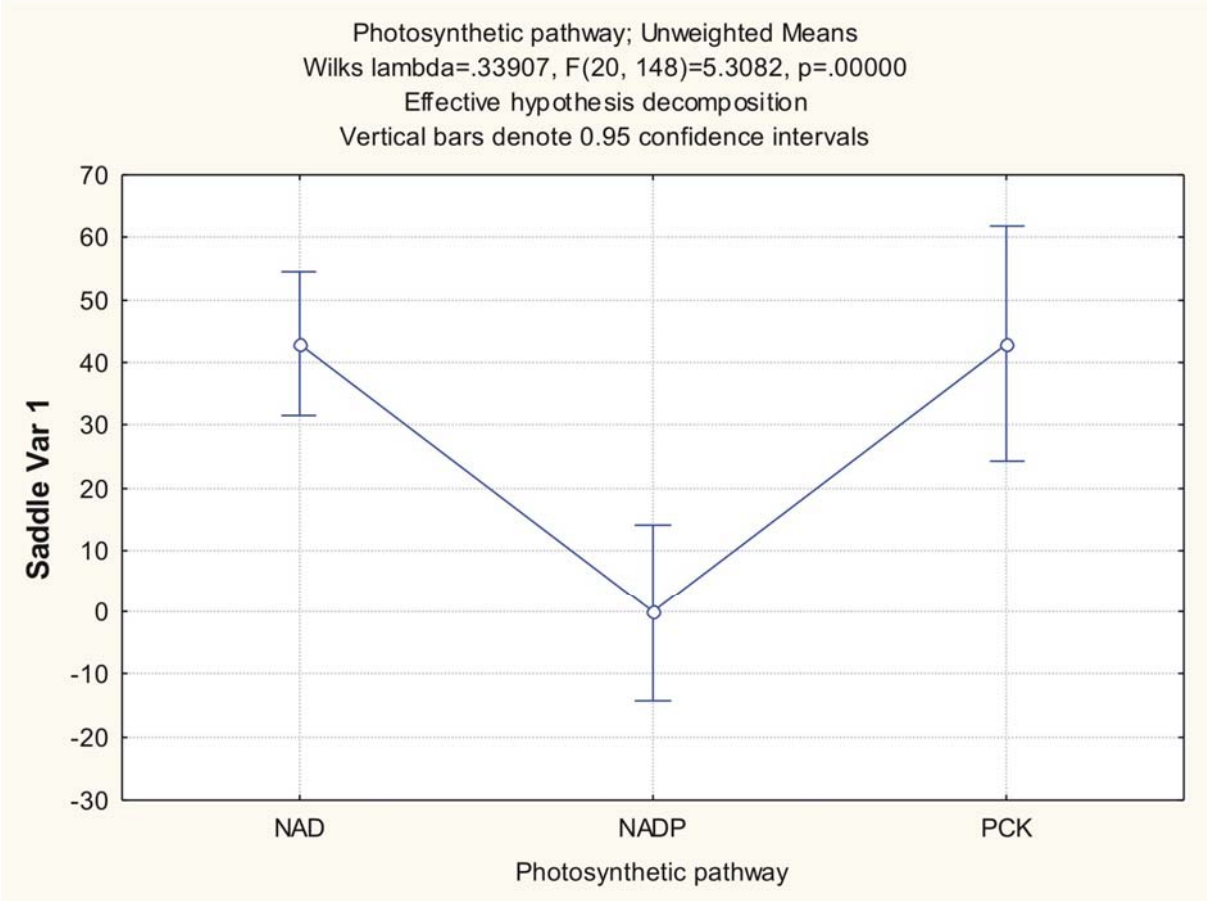

Cell No.	Tukey HSD test; variable Saddle Var 2 Approximate Probabilities for Post Hoc Tests Error: Between MS = 923.89, df = 83.000 Photosynthetic pathway	{1} 35.976	{2} 0.0000	{3} 7.0000
1	NAD		0.000122	0.004873
2	NADP	0.000122		0.743611
3	PCK	0.004873	0.743611	

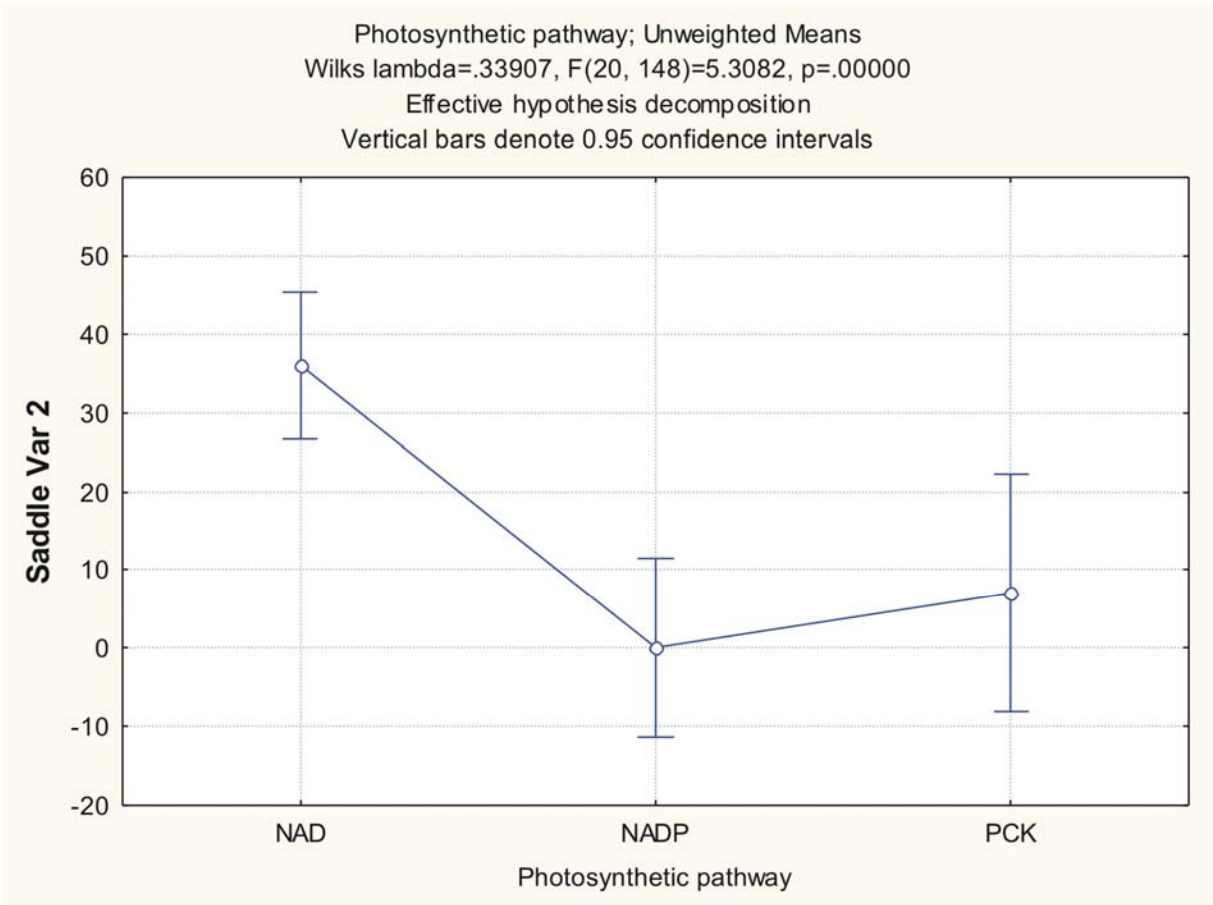

Appendix 12: Basic statistics of the number of GSSC-morphotypes counted for each Rainfall subcategory.

Appendix 12

Basic statistics of GSSC-morphotypes counted for each rainfall subcategory.

Variable	>500mm S					
	Valid N	Mean	Confidence -95.000%	Confidence +95.000%	Variance	Standard Error
Bilobate Var 1	176	16.66477	11.57889	21.75066	1168.750	2.576941
Bilobate Var 2	176	35.69318	29.47609	41.91027	1746.477	3.150105
Bilobate Var 3	176	3.10227	1.28540	4.91915	149.155	0.920583
Polylobate	176	6.80114	4.02711	9.57516	347.703	1.405555
Cross	176	3.84659	1.91106	5.78212	169.273	0.980704
Saddle Var 1	176	15.96023	10.70890	21.21156	1246.027	2.660770
Saddle Var 2	176	1.34091	0.43568	2.24614	37.026	0.458666
Trapezoid	176	6.32386	3.57130	9.07643	342.346	1.394685
Rondel	176	2.31818	0.34367	4.29270	176.161	1.000457
Oblong	176	5.25568	2.30739	8.20398	392.763	1.493856
Reniform	176	2.23864	0.81243	3.66485	91.908	0.722639

Variable	<500mm S					
	Valid N	Mean	Confidence -95.000%	Confidence +95.000%	Variance	Standard Error
Bilobate Var 1	97	6.85567	2.38718	11.32416	491.562	2.251145
Bilobate Var 2	97	29.30928	21.34240	37.27615	1562.549	4.013571
Bilobate Var 3	97	2.85567	0.79682	4.91452	104.354	1.037215
Polylobate	97	6.84536	2.63826	11.05246	435.736	2.119464
Cross	97	4.43299	1.40424	7.46174	225.831	1.525831
Saddle Var 1	97	27.78351	19.26997	36.29704	1784.338	4.288967
Saddle Var 2	97	15.74227	9.04576	22.43878	1103.964	3.373585
Trapezoid	97	2.31959	-0.25349	4.89266	162.991	1.296270
Rondel	97	2.34021	-0.51524	5.19565	200.727	1.438523
Oblong	97	0.24742	-0.09927	0.59411	2.959	0.174657
Reniform	97	0.34021	-0.33510	1.01551	11.227	0.340206

Variable	>40% W					
	Valid N	Mean	Confidence -95.000%	Confidence +95.000%	Variance	Standard Error
Bilobate Var 1	125	3.88800	0.85701	6.91899	293.133	1.531359
Bilobate Var 2	125	33.49600	26.55845	40.43355	1535.704	3.505086
Bilobate Var 3	125	5.42400	2.41225	8.43575	289.424	1.521640
Polylobate	125	4.49600	2.26965	6.72235	158.155	1.124830
Cross	125	2.88000	0.70592	5.05408	150.816	1.098421
Saddle Var 1	125	3.12800	0.47595	5.78005	224.419	1.339907
Saddle Var 2	125	10.16000	5.42303	14.89697	715.974	2.393281
Trapezoid	125	17.42400	12.23774	22.61026	858.230	2.620275
Rondel	125	3.92000	1.35539	6.48461	209.865	1.295730
Oblong	125	7.67200	3.58676	11.75724	532.513	2.064001
Reniform	125	6.67200	3.61489	9.72911	298.206	1.544554

Appendix 13: Tukey's HSD test for unequal sample sizes in the Rainfall-category

Appendix 13

Rainfall: Tukey's HSD for unequal sample sizes. Marked values are significant at p < .05000.

Cell No.	Rainfall	{1} 3.8880	{2} 6.8557	{3} 16.665
		Tukey HSD test; variable Bilobate Var1 Approximate Probabilities for Post Hoc Tests Error: Between MS = 729.29, df = 395.00		
1	>40%W		0.695497	0.000172
2	<500S	0.695497		0.011362
3	>500 S	0.000172	0.011362	

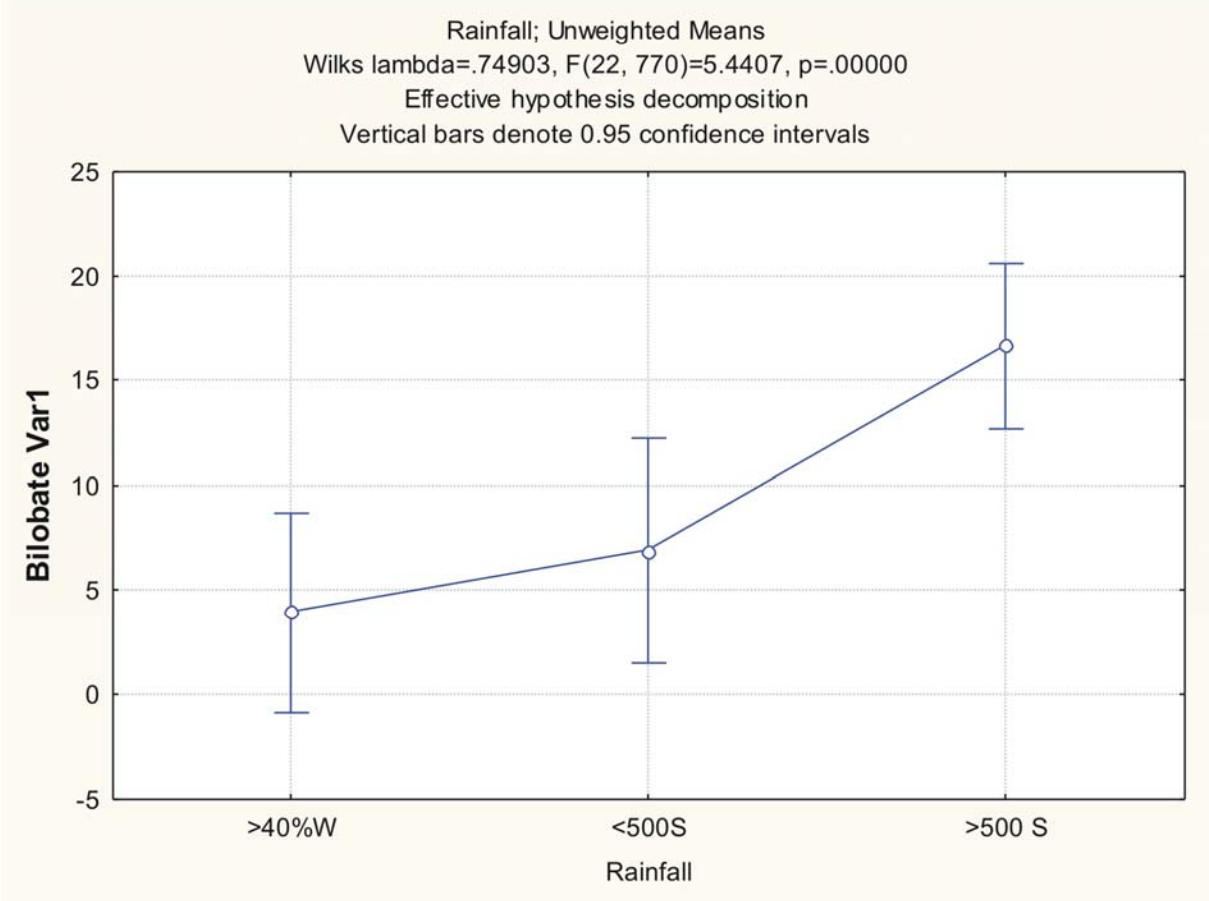

Cell No.	Rainfall	{1} 3.1280	{2} 27.784	{3} 15.960
	Tukey HSD test; variable Saddle Var 1 Approximate Probabilities for Post Hoc Tests Error: Between MS = 1056.1, df = 395.00			
1	>40%W		0.000022	0.002135
2	<500S	0.000022		0.011202
3	>500 S	0.002135	0.011202	

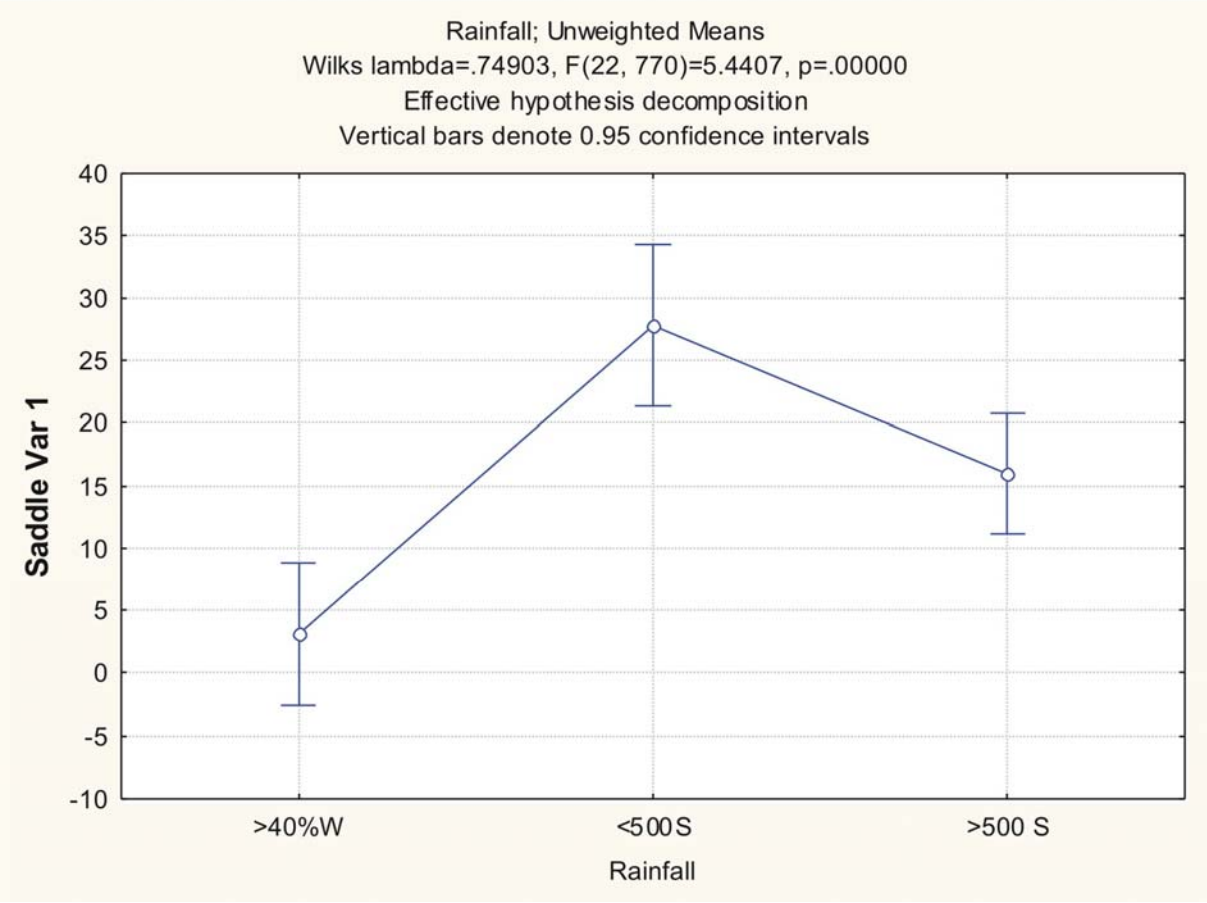

Cell No.	Rainfall	{1} 10.160	{2} 15.742	{3} 1.3409
1	>40%W		0.160526	0.002420
2	<500S	0.160526		0.000023
3	>500 S	0.002420	0.000023	

Tukey HSD test; variable Saddle Var 2
Approximate Probabilities for Post Hoc Tests
Error: Between MS = 509.47, df = 395.00

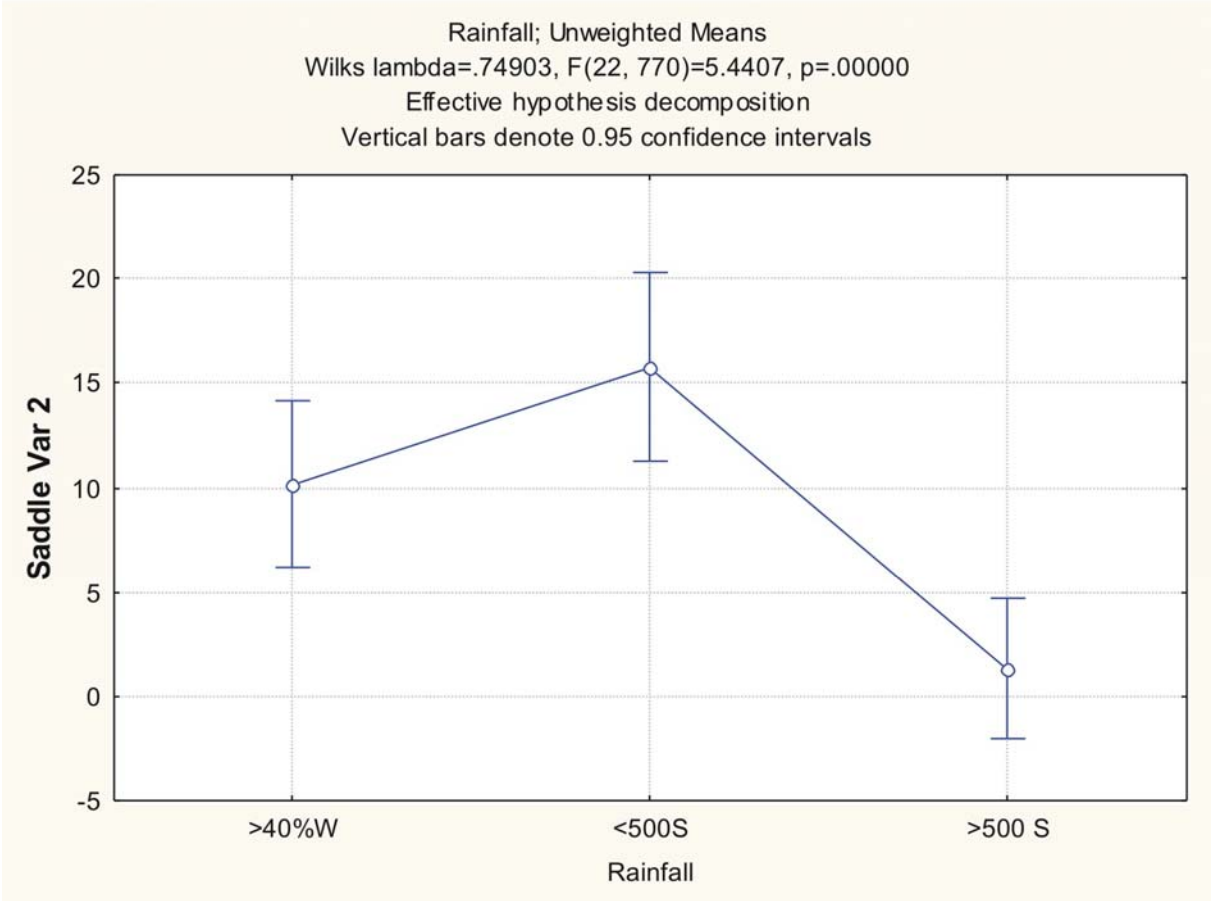

Cell No.	Rainfall	{1} 17.424	{2} 2.3196	{3} 6.3239
1	>40%W		0.000022	0.000049
2	<500S	0.000022		0.302847
3	>500 S	0.000049	0.302847	

Tukey HSD test; variable Trapezoid
Approximate Probabilities for Post Hoc Tests
Error: Between MS = 460.70, df = 395.00

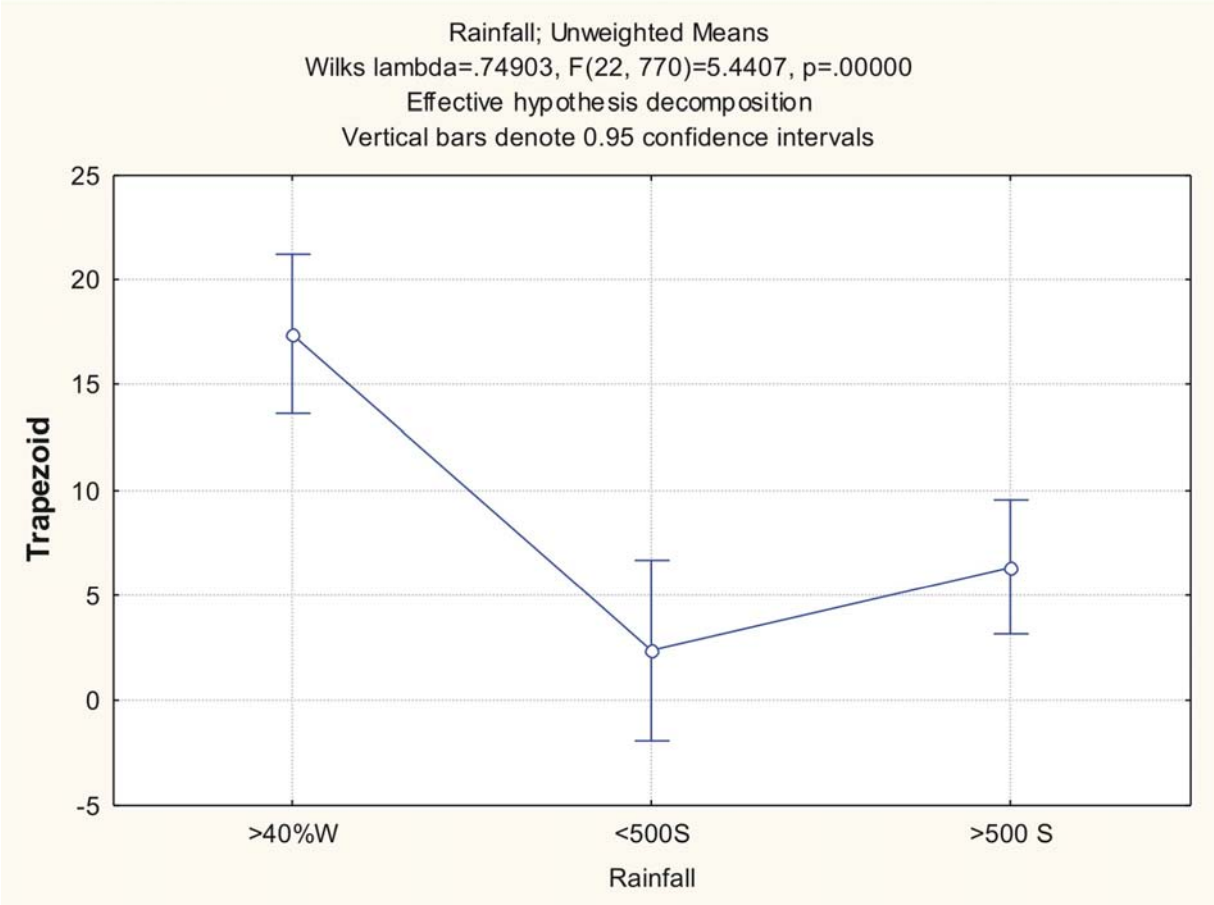

Cell No.	Rainfall	{1} 7.6720	{2} .24742	{3} 5.2557
1	>40%W		0.008444	0.503409
2	<500S	0.008444		0.081575
3	>500 S	0.503409	0.081575	

Tukey HSD test; variable Oblong
Approximate Probabilities for Post Hoc Tests
Error: Between MS = 341.90, df = 395.00

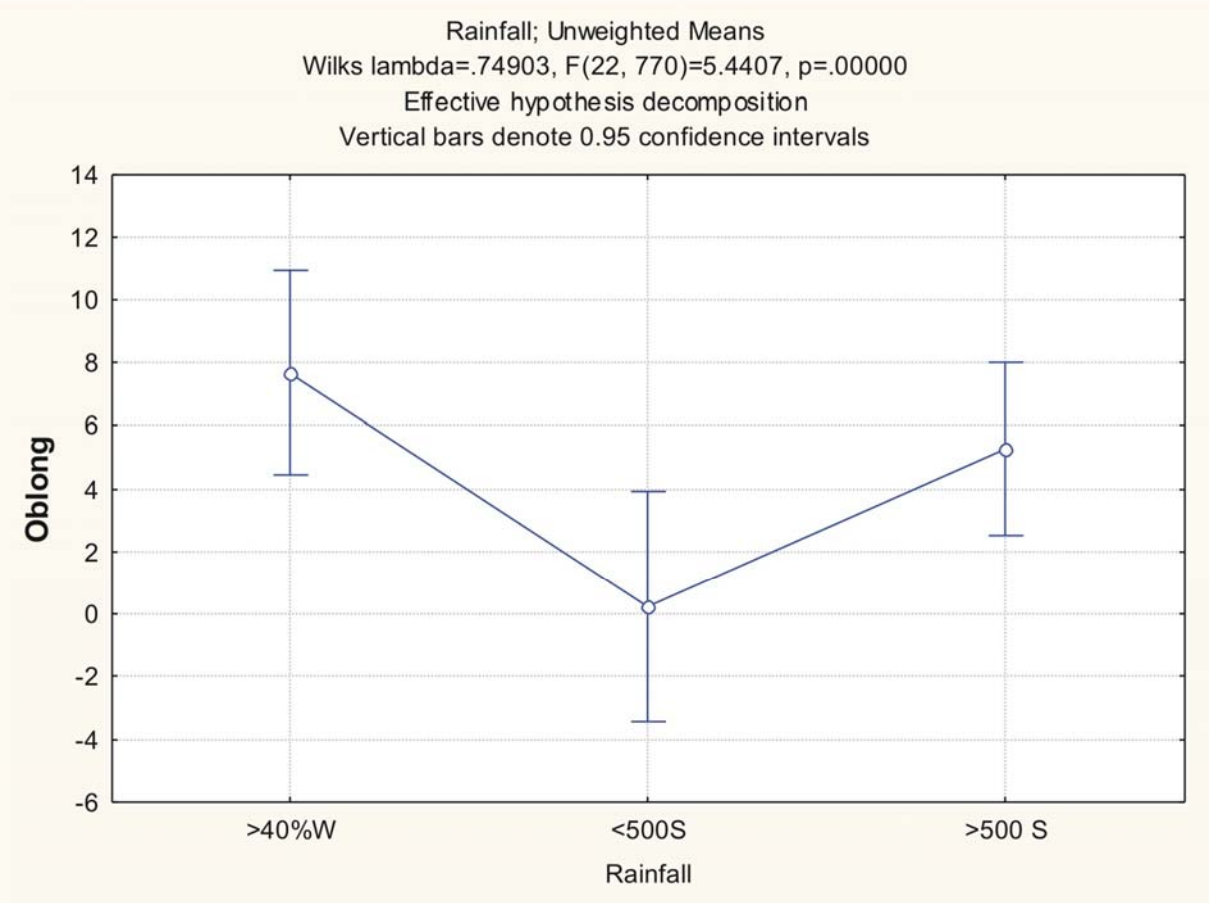

Cell No.	Rainfall	{1} 6.6720	{2} .34021	{3} 2.2386
	Tukey HSD test; variable Reniform Approximate Probabilities for Post Hoc Tests Error: Between MS = 137.06, df = 395.00			
1	>40%W		0.000206	0.003463
2	<500S	0.000206		0.405157
3	>500 S	0.003463	0.405157	

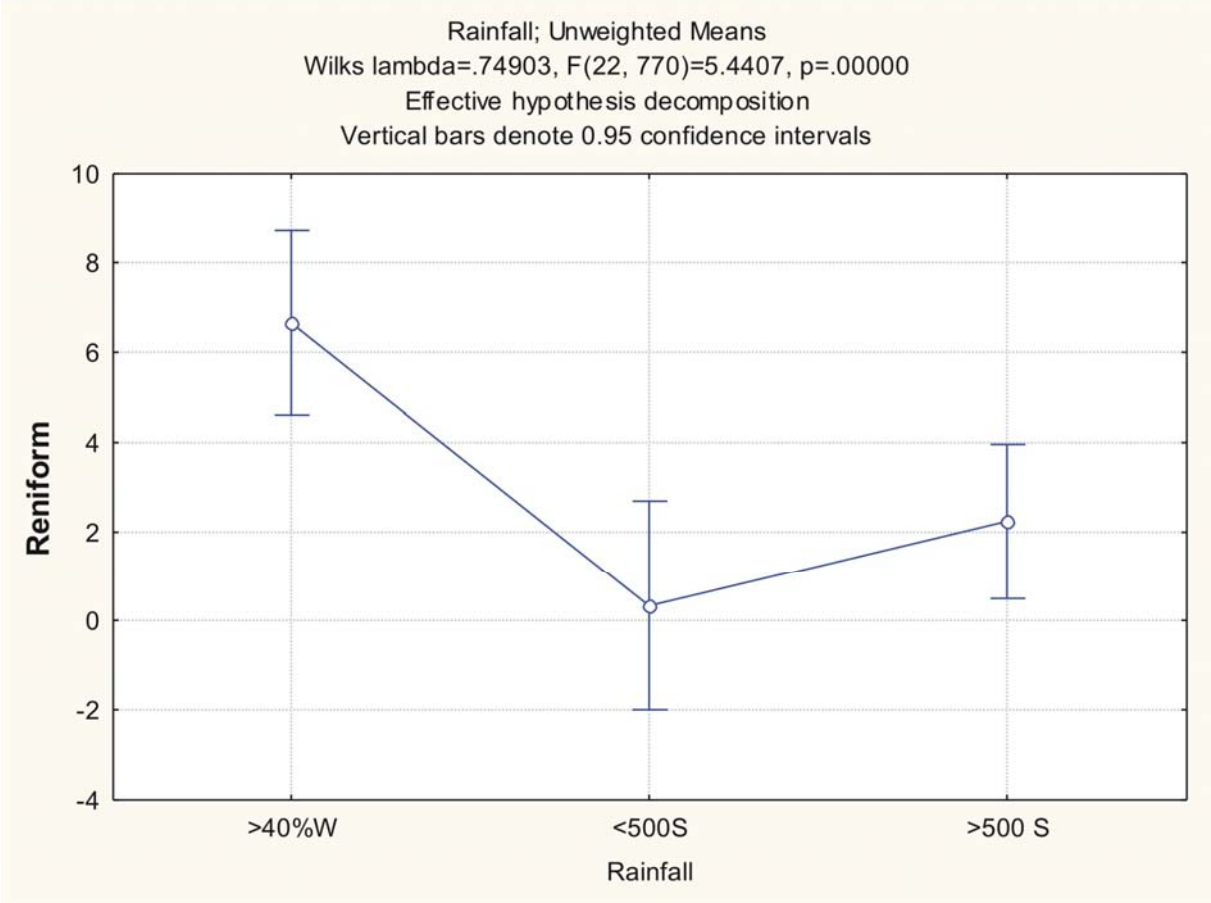

Appendix 14: Basic statistics of the number of GSSC-morphotypes counted for each habitat subcategory.

Appendix 14

Basic statistics of GSSC-morphotypes counted for each habitat subcategory.

Variable	Desert grasses					
	Valid N	Mean	Confidence -95.000%	Confidence +95.000%	Variance	Standard Error
Bilobate Var 1	26	15.57692	1.73791	29.41593	1173.934	6.719472
Bilobate Var 2	26	16.50000	3.97792	29.02208	961.140	6.080043
Bilobate Var 3	26	1.19231	-1.26330	3.64791	36.962	1.192308
Polylobate	26	0.88462	-0.93728	2.70651	20.346	0.884615
Cross	26	0.00000			0.000	0.000000
Saddle Var 1	26	18.92308	4.15706	33.68910	1336.474	7.169577
Saddle Var 2	26	24.34615	9.15062	39.54169	1415.355	7.378126
Trapezoid	26	16.84615	2.99276	30.69955	1176.375	6.726456
Rondel	26	3.46154	-3.50467	10.42775	297.458	3.382412
Oblong	26	0.00000			0.000	0.000000
Reniform	26	2.26923	-1.59744	6.13590	91.645	1.877443

Variable	Succulent Karroo grasses					
	Valid N	Mean	Confidence -95.000%	Confidence +95.000%	Variance	Standard Error
Bilobate Var1	46	3.50000	-1.57789	8.57789	292.389	2.521166
Bilobate Var 2	46	23.41304	13.08988	33.73621	1208.426	5.125439
Bilobate Var 3	46	3.52174	0.64820	6.39528	93.633	1.426708
Polylobate	46	3.47826	-0.27270	7.22923	159.544	1.862350
Cross	46	3.80435	-1.08273	8.69143	270.828	2.426428
Saddle Var 1	46	7.82609	0.60057	15.05160	592.014	3.587459
Saddle Var 2	46	24.32609	12.79989	35.85229	1506.491	5.722745
Trapezoid	46	15.08696	6.47085	23.70306	841.814	4.277887
Rondel	46	1.95652	-0.17937	4.09242	51.731	1.060470
Oblong	46	9.95652	2.25709	17.65595	672.220	3.822759
Reniform	46	2.93478	0.47367	5.39590	68.685	1.221942

Variable	Nama-Karroo grasses					
	Valid N	Mean	Confidence -95.000%	Confidence +95.000%	Variance	Standard Error
Bilobate Var1	85	8.11765	2.72708	13.50822	624.581	2.710722
Bilobate Var 2	85	30.31765	21.83687	38.79842	1545.934	4.264675
Bilobate Var 3	85	2.62353	0.49346	4.75360	97.523	1.071136
Polylobate	85	4.70588	1.28105	8.13071	252.115	1.722224
Cross	85	5.24706	1.90140	8.59272	240.593	1.682411
Saddle Var 1	85	22.60000	14.01614	31.18386	1583.743	4.316511
Saddle Var 2	85	9.38824	3.63565	15.14082	711.288	2.892766
Trapezoid	85	7.07059	2.51906	11.62211	445.281	2.288798
Rondel	85	2.80000	-0.06554	5.66554	176.495	1.440977
Oblong	85	5.97647	1.34770	10.60524	460.523	2.327643
Reniform	85	0.14118	-0.13957	0.42192	1.694	0.141176

Variable	Savanna grassland					
	Valid N	Mean	Confidence -95.000%	Confidence +95.000%	Variance	Standard Error
Bilobate Var1	157	16.96178	11.55610	22.36747	1175.819	2.736657
Bilobate Var 2	157	36.58599	29.84271	43.32927	1829.706	3.413821
Bilobate Var 3	157	2.67516	1.02647	4.32385	109.375	0.834658
Polylobate	157	6.08917	3.28480	8.89354	316.454	1.419728
Cross	157	4.12739	2.09669	6.15809	165.932	1.028054
Saddle Var 1	157	23.90446	17.42467	30.38425	1689.510	3.280428
Saddle Var 2	157	4.51592	1.72995	7.30190	312.315	1.410415
Trapezoid	157	2.23567	0.41000	4.06134	134.117	0.924256
Rondel	157	0.05732	-0.05591	0.17056	0.516	0.057325
Oblong	157	2.19108	0.21498	4.16719	157.130	1.000414
Reniform	157	0.21019	-0.20500	0.62538	6.936	0.210191

Variable	Grassland Biome grassland					
	Valid N	Mean	Confidence -95.000%	Confidence +95.000%	Variance	Standard Error
Bilobate Var1	134	15.19403	9.76983	20.61823	1007.721	2.742318
Bilobate Var 2	134	35.39552	28.27494	42.51610	1736.602	3.599960
Bilobate Var 3	134	2.29851	0.47869	4.11832	113.429	0.920046
Polylobate	134	7.27612	4.03001	10.52223	360.908	1.641141
Cross	134	4.85821	2.47208	7.24434	195.010	1.206357
Saddle Var 1	134	18.02239	11.72717	24.31760	1357.345	3.182679
Saddle Var 2	134	1.63433	0.45487	2.81379	47.647	0.596302
Trapezoid	134	3.52239	1.30967	5.73510	167.695	1.118685
Rondel	134	3.19403	0.36792	6.02014	273.556	1.428798
Oblong	134	6.90299	3.06188	10.74409	505.336	1.941949
Reniform	134	0.95522	-0.16414	2.07459	42.915	0.565918

Variable	Fynbos grasses					
	Valid N	Mean	Confidence -95.000%	Confidence +95.000%	Variance	Standard Error
Bilobate Var1	104	4.08654	0.61716	7.55591	318.255	1.749326
Bilobate Var 2	104	35.99038	28.20042	43.78035	1604.514	3.927852
Bilobate Var 3	104	5.49038	2.08124	8.89953	307.301	1.718958
Polylobate	104	3.82692	1.73896	5.91489	115.271	1.052793
Cross	104	3.25962	0.90259	5.61664	146.893	1.188459
Saddle Var 1	104	8.64423	3.52653	13.76193	692.503	2.580443
Saddle Var 2	104	4.26923	1.00679	7.53167	281.422	1.644986
Trapezoid	104	16.80769	11.32931	22.28608	793.555	2.762306
Rondel	104	4.21154	1.19306	7.23002	240.906	1.521975
Oblong	104	5.77885	2.01534	9.54235	374.504	1.897630
Reniform	104	6.60577	3.14155	10.06999	317.309	1.746725

Variable	Forest grasses					
	Valid N	Mean	Confidence -95.000%	Confidence +95.000%	Variance	Standard Error
Bilobate Var 1	15	6.20000	-7.09768	19.49768	576.600	6.20000
Bilobate Var 2	15	36.73333	13.62145	59.84521	1741.781	10.77584
Bilobate Var 3	15	9.20000	-4.13387	22.53387	579.743	6.21687
Polylobate	15	13.46667	-1.48817	28.42150	729.267	6.97264
Cross	15	1.13333	-1.29742	3.56409	19.267	1.13333
Saddle Var 1	15	13.33333	-6.15234	32.81901	1238.095	9.08514
Saddle Var 2	15	0.00000			0.000	0.00000
Trapezoid	15	6.40000	-1.87184	14.67184	223.114	3.85672
Rondel	15	6.53333	-6.16552	19.23219	525.838	5.92080
Oblong	15	7.00000	-2.13080	16.13080	271.857	4.25721
Reniform	15	0.00000			0.000	0.00000

Variable	Montane grassland					
	Valid N	Mean	Confidence -95.000%	Confidence +95.000%	Variance	Standard Error
Bilobate Var 1	70	11.48571	4.17616	18.79526	939.761	3.664035
Bilobate Var 2	70	24.30000	15.60202	32.99798	1330.677	4.360008
Bilobate Var 3	70	2.21429	0.59054	3.83803	46.374	0.813930
Polylobate	70	3.61429	1.43297	5.79560	83.690	1.093420
Cross	70	0.88571	-0.17096	1.94239	19.639	0.529675
Saddle Var 1	70	1.67143	-0.87175	4.21461	113.760	1.274811
Saddle Var 2	70	0.68571	0.04701	1.32442	7.175	0.320160
Trapezoid	70	24.62857	16.79635	32.46079	1078.961	3.926033
Rondel	70	6.31429	1.30026	11.32831	442.190	2.513363
Oblong	70	13.24286	5.92118	20.56454	942.882	3.670115
Reniform	70	10.95714	5.99185	15.92243	433.636	2.488935

Variable	High alt. grassland					
	Valid N	Mean	Confidence -95.000%	Confidence +95.000%	Variance	Standard Error
Bilo thin Var1	18	21.83333	0.91921	42.74746	1768.735	9.912773
Bilo thick Var 2	18	7.55556	-3.89951	19.01063	530.614	5.429418
Bilo Var 3	18	0.66667	-0.73988	2.07321	8.000	0.666667
Polylobate	18	0.38889	-0.43159	1.20937	2.722	0.388889
Cross	18	0.00000			0.000	0.000000
Saddle Var 1	18	0.00000			0.000	0.000000
Saddle Var 2	18	0.22222	-0.24663	0.69107	0.889	0.222222
Trapezoid	18	25.55556	10.68552	40.42559	894.144	7.048025
Rondel	18	14.05556	-1.65479	29.76590	998.056	7.446310
Oblong	18	15.00000	-2.25695	32.25695	1204.235	8.179362
Reniform	18	14.72222	5.35212	24.09233	355.036	4.441196

Variable	Damp Soils					
	Valid N	Mean	Confidence -95.000%	Confidence +95.000%	Variance	Standard Error
Bilobate Var 1	82	11.73171	5.47729	17.98612	810.248	3.143418
Bilobate Var 2	82	36.43902	27.36930	45.50875	1703.854	4.558367
Bilobate Var 3	82	3.92683	0.84512	7.00854	196.711	1.548842
Polylobate	82	5.08537	1.63374	8.53700	246.770	1.734761
Cross	82	5.48780	1.76805	9.20756	286.599	1.869520
Saddle Var 1	82	6.52439	1.48660	11.56218	525.685	2.531953
Saddle Var 2	82	0.58537	-0.41468	1.58541	20.715	0.502613
Trapezoid	82	10.89024	5.96023	15.82026	503.432	2.477785
Rondel	82	3.14634	0.23421	6.05847	175.657	1.463613
Oblong	82	12.92683	6.16463	19.68903	947.155	3.398628
Reniform	82	3.37805	0.70173	6.05437	148.361	1.345097

Variable	Swamps / Vleis					
	Valid N	Mean	Confidence -95.000%	Confidence +95.000%	Variance	Standard Error
Bilobate Var 1	21	13.95238	-1.99923	29.90400	1228.048	7.647121
Bilobate Var 2	21	40.28571	20.84824	59.72318	1823.414	9.318221
Bilobate Var 3	21	5.04762	0.13979	9.95544	116.248	2.352786
Polylobate	21	11.38095	-1.78785	24.54975	836.948	6.313054
Cross	21	5.52381	-0.16270	11.21032	156.062	2.726081
Saddle Var 1	21	4.76190	-5.17125	14.69506	476.190	4.761905
Saddle Var 2	21	0.19048	-0.20685	0.58780	0.762	0.190476
Trapezoid	21	7.76190	-2.88411	18.40792	546.990	5.103642
Rondel	21	5.85714	-4.22342	15.93771	490.429	4.832571
Oblong	21	3.76190	-4.08529	11.60910	297.190	3.761905
Reniform	21	1.47619	-1.60309	4.55547	45.762	1.476190

Variable	Shady grasses					
	Valid N	Mean	Confidence -95.000%	Confidence +95.000%	Variance	Standard Error
Bilobate Var 1	43	16.74419	6.48597	27.00240	1111.052	5.083151
Bilobate Var 2	43	31.13953	19.32618	42.95289	1473.456	5.853753
Bilobate Var 3	43	3.48837	-1.03636	8.01310	216.161	2.242095
Polylobate	43	12.93023	5.25650	20.60396	621.733	3.802487
Cross	43	0.74419	-0.30720	1.79557	11.671	0.520981
Saddle Var 1	43	6.02326	-1.00763	13.05414	521.928	3.483943
Saddle Var 2	43	1.11628	-0.82806	3.06061	39.915	0.963457
Trapezoid	43	11.74419	4.21262	19.27575	598.909	3.732040
Rondel	43	4.27907	-0.64561	9.20375	256.063	2.440278
Oblong	43	10.09302	1.92604	18.26000	704.229	4.046903
Reniform	43	1.69767	-0.89163	4.28697	70.787	1.283050

Appendix 15: Tukey's HSD test for unequal sample sizes in the Habitat-category.

Appendix 15

Habitat: Tukey's HSD for unequal sample sizes. Marked values are significant at p < .05000.

Tukey HSD test; variable **Bilobate Var 1**
Approximate Probabilities for Post Hoc Tests
Error: Between MS = 868.24, df = 789.00

Ce	Habitat	{1} 6.2000	{2} 16.744	{3} 13.952	{4} 4.0865	{5} 15.194	{6} 8.1176	{7} 16.962	{8} 3.5000	{9} 15.577	{10} 21.833	{11} 11.732	{12} 11.486
1	Forest		0.989580	0.999785	1.000000	0.993824	1.000000	0.972183	1.000000	0.998085	0.936152	0.999953	0.999974
2	Shade	0.989580		1.000000	0.427125	1.000000	0.921819	1.000000	0.609042	1.000000	0.999980	0.999107	0.998931
3	Swamps	0.999785	1.000000		0.963929	1.000000	0.999674	0.999999	0.972874	1.000000	0.999587	1.000000	1.000000
4	Fynbos	1.000000	0.427125	0.963929		0.146265	0.998764	0.027329	1.000000	0.830057	0.434200	0.841279	0.900549
5	Grassland	0.993824	1.000000	1.000000	0.146265		0.853682	0.999997	0.460354	1.000000	0.999160	0.999561	0.999478
6	Nama-Karoo	1.000000	0.921819	0.999674	0.998764	0.853682		0.528347	0.999462	0.993416	0.821732	0.999744	0.999915
7	Savanna	0.972183	1.000000	0.999999	0.027329	0.999997	0.528347		0.213757	1.000000	0.999955	0.978993	0.980167
8	Succulent Karoo	1.000000	0.609042	0.972874	1.000000	0.460354	0.999462	0.213757		0.881793	0.521706	0.936456	0.958282
9	Desert	0.998085	1.000000	1.000000	0.830057	1.000000	0.993416	1.000000	0.881793		0.999932	0.999989	0.999983
10	High alt.	0.936152	0.999980	0.999587	0.434200	0.999160	0.821732	0.999955	0.521706	0.999932		0.977134	0.975527
11	Damp soils	0.999953	0.999107	1.000000	0.841279	0.999561	0.999744	0.978993	0.936456	0.999989	0.977134		1.000000
12	Montane	0.999974	0.998931	1.000000	0.900549	0.999478	0.999915	0.980167	0.958282	0.999983	0.975527	1.000000	

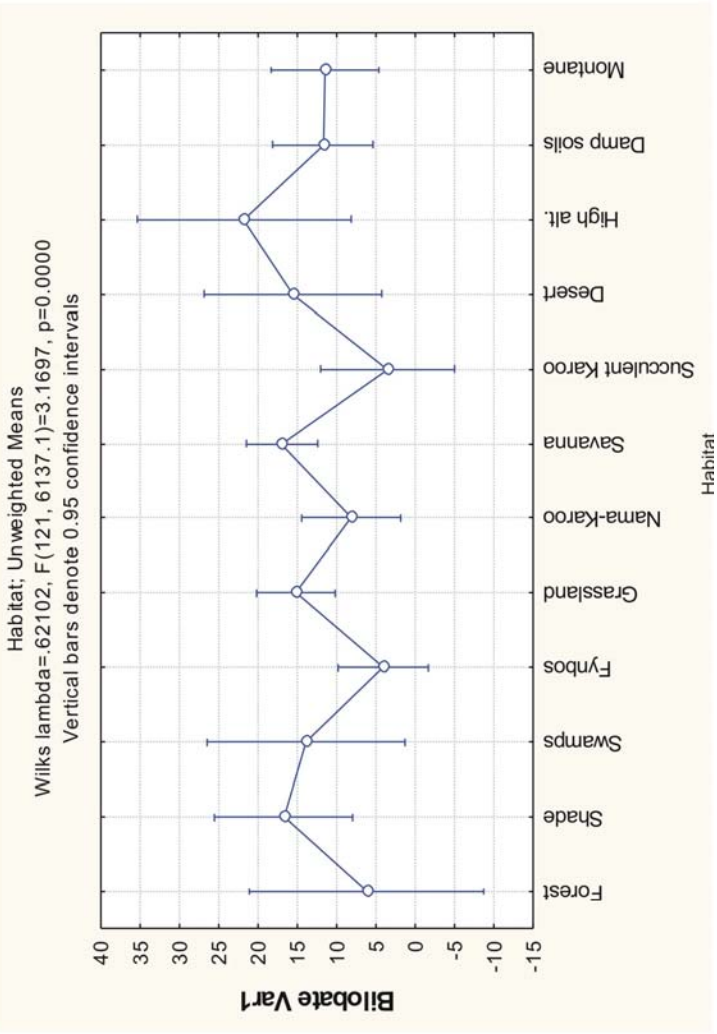

Tukey HSD test; variable **Bilobate Var 2**
Approximate Probabilities for Post Hoc Tests
Error: Between MS = 1586.2, df = 789.00

Ce	Habitat	{1} 36.733	{2} 31.140	{3} 40.286	{4} 35.990	{5} 35.396	{6} 30.318	{7} 36.586	{8} 23.413	{9} 16.500	{10} 7.5556	{11} 36.439	{12} 24.300
1	Forest		0.999999	1.000000	1.000000	1.000000	0.999990	1.000000	0.993646	0.921022	0.626048	1.000000	0.994865
2	Shade	0.999999		0.999422	0.999950	0.999981	1.000000	0.999738	0.998999	0.946349	0.616058	0.999917	0.999254
3	Swamps	1.000000	0.999422		0.999999	0.999996	0.997121	1.000000	0.906432	0.668904	0.303659	1.000000	0.904731
4	Fynbos	1.000000	0.999950	0.999999		1.000000	0.998212	1.000000	0.827415	0.526139	0.181171	1.000000	0.760445
5	Grassland	1.000000	0.999981	0.999996	1.000000		0.998948	1.000000	0.839358	0.539356	0.186422	1.000000	0.766381
6	Nama-Karoo	0.999990	1.000000	0.997121	0.998212	0.998948		0.991228	0.998617	0.927054	0.547580	0.997873	0.998758
7	Savanna	1.000000	0.999738	1.000000	1.000000	1.000000	0.991228		0.712169	0.418355	0.130591	1.000000	0.588963
8	Succulent Karoo	0.993646	0.998999	0.906432	0.827415	0.839358	0.998617	0.712169		0.999916	0.957384	0.831641	1.000000
9	Desert	0.921022	0.946349	0.668904	0.526139	0.539356	0.927054	0.418355	0.999916		0.999882	0.531665	0.999482
10	High alt.	0.626048	0.616058	0.303659	0.181171	0.186422	0.547580	0.130591	0.957384	0.999882		0.185703	0.912834
11	Damp soils	1.000000	0.999917	1.000000	1.000000	1.000000	0.997873	1.000000	0.831641	0.531665	0.185703		0.776255
12	Montane	0.994865	0.999254	0.904731	0.760445	0.766381	0.998758	0.588963	1.000000	0.999482	0.912834	0.776255	

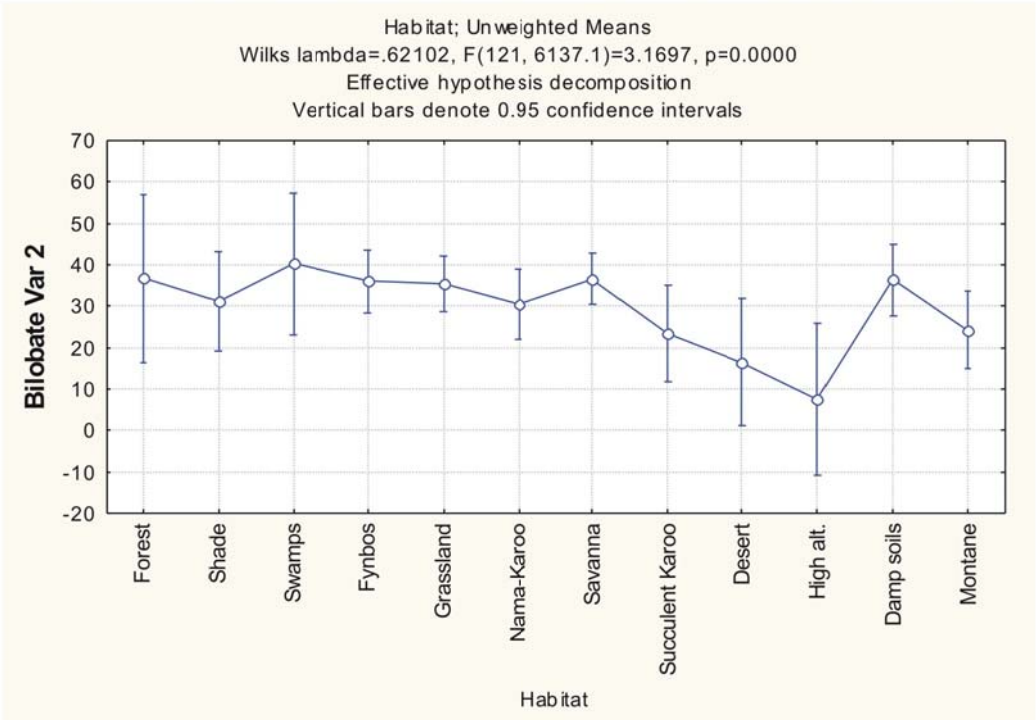

Tukey HSD test; variable **Polylobate**
Approximate Probabilities for Post Hoc Tests
Error: Between MS = 275.00, df = 789.00

Cel	Habitat	{1} 13.467	{2} 12.930	{3} 11.381	{4} 3.8269	{5} 7.2761	{6} 4.7059	{7} 6.0892	{8} 3.4783	{9} .88462	{10} .38889	{11} 5.0854	{12} 3.6143
1	Forest		1.000000	1.000000	0.619427	0.969004	0.768058	0.891910	0.675779	0.447775	0.508647	0.818606	0.631403
2	Shade	1.000000		1.000000	0.100529	0.730443	0.251730	0.408081	0.232511	0.132375	0.229038	0.331819	0.140904
3	Swamps	1.000000	1.000000		0.757028	0.996360	0.889618	0.968621	0.813223	0.580960	0.649021	0.925732	0.770531
4	Fynbos	0.619427	0.100529	0.757028		0.912580	1.000000	0.995558	1.000000	0.999687	0.999676	0.999997	1.000000
5	Grassland	0.969004	0.730443	0.996360	0.912580		0.993979	0.999982	0.973886	0.819277	0.888538	0.998681	0.941746
6	Nama-Karoo	0.768058	0.251730	0.889618	1.000000	0.993979		0.999978	1.000000	0.997093	0.997664	1.000000	1.000000
7	Savanna	0.891910	0.408081	0.968621	0.995558	0.999982	0.999978		0.998721	0.945672	0.967245	0.999999	0.996826
8	Succulent Karoo	0.675779	0.232511	0.813223	1.000000	0.973886	1.000000	0.998721		0.999971	0.999951	0.999996	1.000000
9	Desert	0.447775	0.132375	0.580960	0.999687	0.819277	0.997093	0.945672	0.999971		1.000000	0.993615	0.999905
10	High alt.	0.508647	0.229038	0.649021	0.999676	0.888538	0.997664	0.967245	0.999951	1.000000		0.995224	0.999876
11	Damp soils	0.818606	0.331819	0.925732	0.999997	0.998681	1.000000	0.999999	0.999996	0.993615	0.995224		0.999994
12	Montane	0.631403	0.140904	0.770531	1.000000	0.941746	1.000000	0.996826	1.000000	0.999905	0.999876	0.999994	

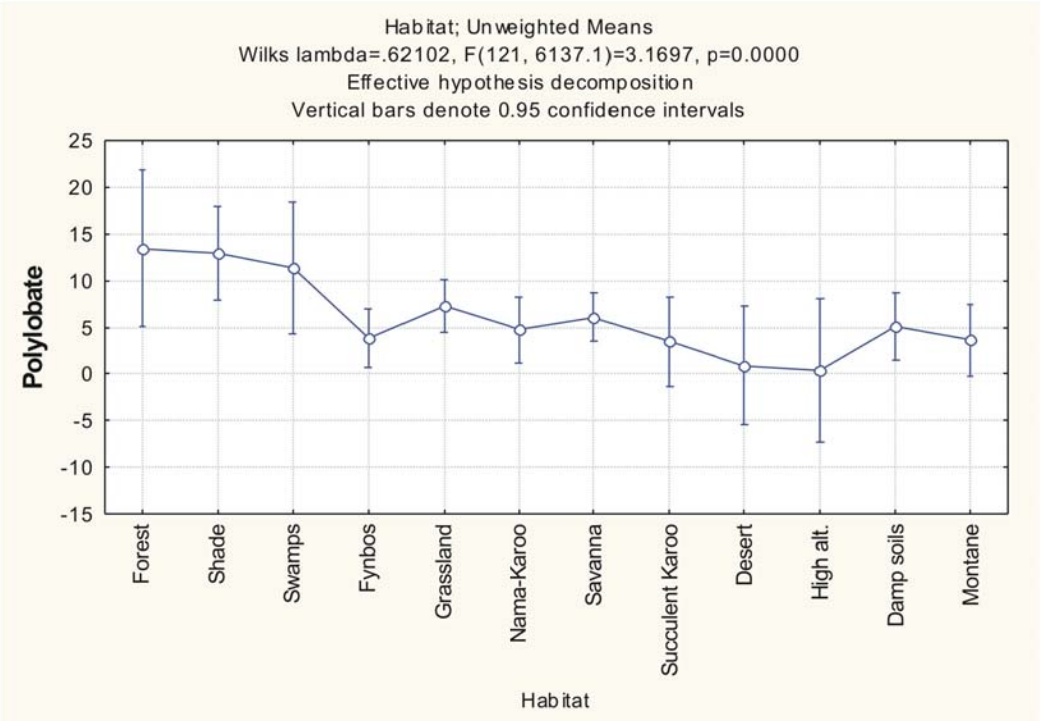

Tukey HSD test; variable **Saddle Var 1**
Approximate Probabilities for Post Hoc Tests
Error: Between MS = 1023.7, df = 789.00

Cel	Habitat	{1} 13.333	{2} 6.0233	{3} 4.7619	{4} 8.6442	{5} 18.022	{6} 22.600	{7} 23.904	{8} 7.8261	{9} 18.923	{10} 0.0000	{11} 6.5244	{12} 1.6714
1	Forest		0.999826	0.999744	0.999996	0.999995	0.996940	0.987305	0.999989	0.999995	0.989675	0.999835	0.981568
2	Shade	0.999826		1.000000	0.999999	0.593864	0.193523	0.053336	1.000000	0.901070	0.999951	1.000000	0.999922
3	Swamps	0.999744	1.000000		0.999997	0.836631	0.485275	0.293939	1.000000	0.938696	0.999999	1.000000	1.000000
4	Fynbos	0.999996	0.999999	0.999997		0.518065	0.113404	0.008889	1.000000	0.949899	0.996249	0.999999	0.961985
5	Grassland	0.999995	0.593864	0.836631	0.518065		0.997001	0.922241	0.781169	1.000000	0.517380	0.300906	0.026497
6	Nama-Karoo	0.996940	0.193523	0.485275	0.113404	0.997001		1.000000	0.325477	0.999997	0.215015	0.053507	0.002970
7	Savanna	0.987305	0.053336	0.293939	0.008889	0.922241	1.000000		0.109161	0.999877	0.107706	0.003873	0.000098
8	Succulent Karoo	0.999989	1.000000	1.000000	1.000000	0.781169	0.325477	0.109161		0.961211	0.999304	1.000000	0.997444
9	Desert	0.999995	0.901070	0.938696	0.949899	1.000000	0.999997	0.999877	0.961211		0.741201	0.858588	0.442351
10	High alt.	0.989675	0.999951	0.999999	0.996249	0.517380	0.215015	0.107706	0.999304	0.741201		0.999771	1.000000
11	Damp soils	0.999835	1.000000	1.000000	0.999999	0.300906	0.053507	0.003873	1.000000	0.858588	0.999771		0.998807
12	Montane	0.981568	0.999922	1.000000	0.961985	0.026497	0.002970	0.000098	0.997444	0.442351	1.000000	0.998807	

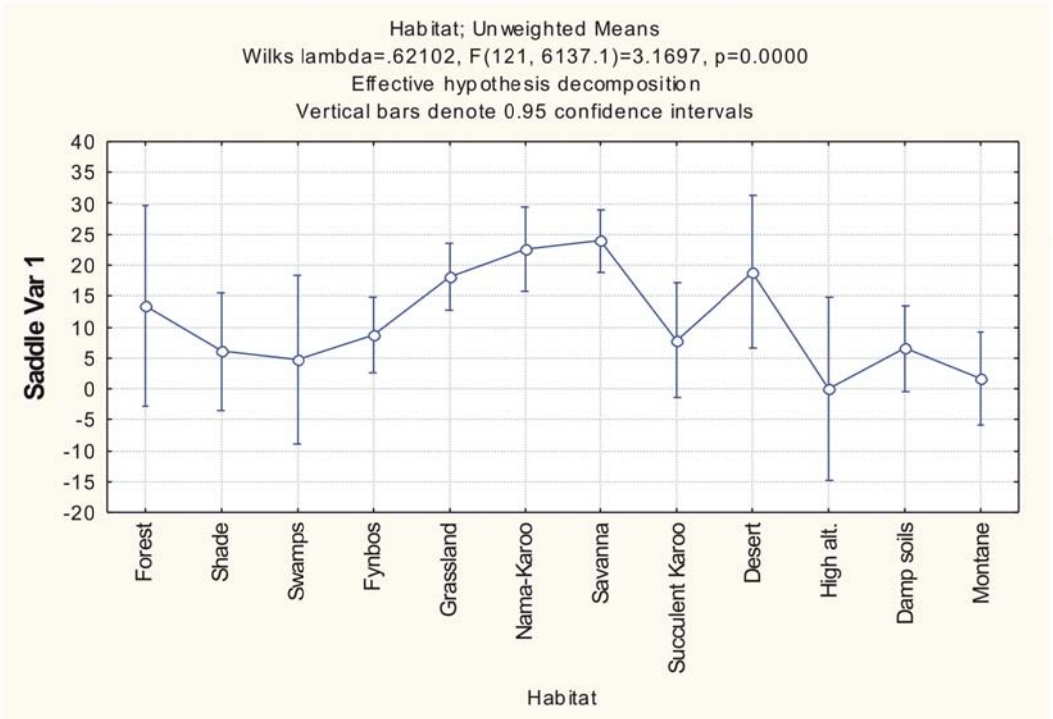

Ce	Tukey HSD test; variable **Saddle Var 2** Approximate Probabilities for Post Hoc Tests Error: Between MS = 317.93, df = 789.00 Habitat	{1} 0.0000	{2} 1.1163	{3} .19048	{4} 4.2692	{5} 1.6343	{6} 9.3882	{7} 4.5159	{8} 24.326	{9} 24.346	{10} .22222	{11} .58537	{12} .68571
1	Forest		1.000000	1.000000	0.999394	1.000000	0.771947	0.998745	0.000289	0.001545	1.000000	1.000000	1.000000
2	Shade	1.000000		1.000000	0.998192	1.000000	0.353122	0.994426	0.000018	0.000027	1.000000	1.000000	1.000000
3	Swamps	1.000000	1.000000		0.998491	1.000000	0.610611	0.996671	0.000034	0.000254	1.000000	1.000000	1.000000
4	Fynbos	0.999394	0.998192	0.998491		0.993355	0.718461	1.000000	0.000018	0.000034	0.999232	0.964039	0.979333
5	Grassland	1.000000	1.000000	1.000000	0.993355		0.074146	0.968492	0.000018	0.000018	1.000000	1.000000	1.000000
6	Nama-Karoo	0.771947	0.353122	0.610611	0.718461	0.074146		0.673387	0.000304	0.009914	0.706455	0.063417	0.101590
7	Savanna	0.998745	0.994426	0.996671	1.000000	0.968492	0.673387		0.000018	0.000026	0.998316	0.902978	0.942457
8	Succulent Karoo	0.000289	0.000018	0.000034	0.000018	0.000018	0.000304	0.000018		1.000000	0.000087	0.000018	0.000018
9	Desert	0.001545	0.000027	0.000254	0.000034	0.000018	0.009914	0.000026	1.000000		0.000635	0.000018	0.000018
10	High alt.	1.000000	1.000000	1.000000	0.999232	1.000000	0.706455	0.998316	0.000087	0.000635		1.000000	1.000000
11	Damp soils	1.000000	1.000000	1.000000	0.964039	1.000000	0.063417	0.902978	0.000018	0.000018	1.000000		1.000000
12	Montane	1.000000	1.000000	1.000000	0.979333	1.000000	0.101590	0.942457	0.000018	0.000018	1.000000	1.000000	

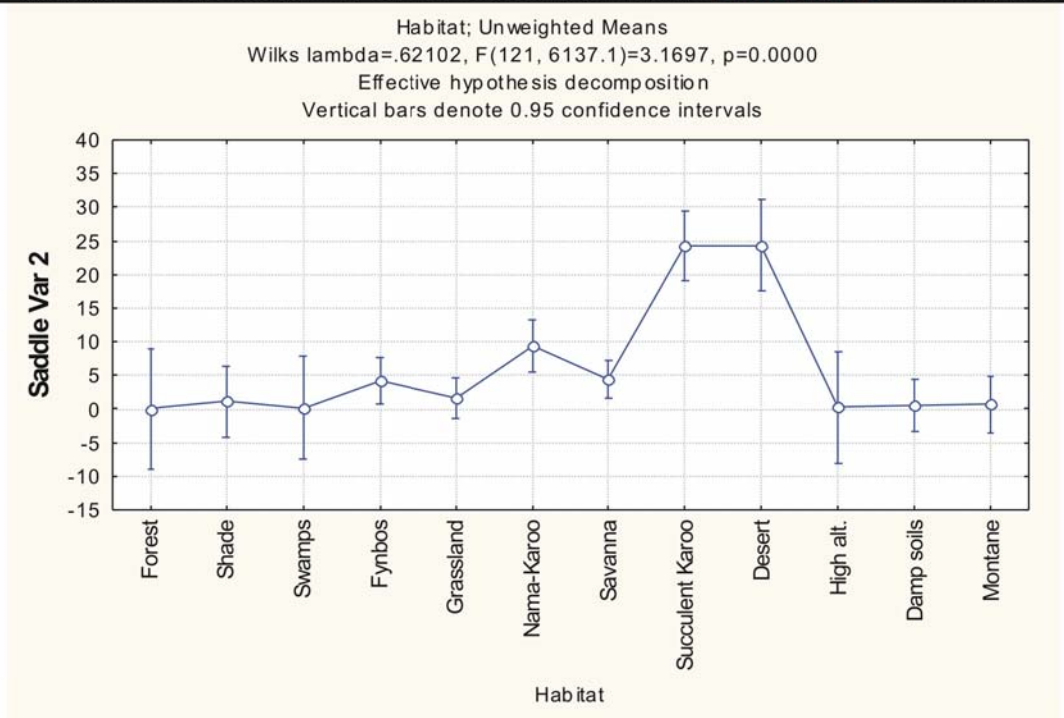

Tukey HSD test; variable **Trapezoid**
Approximate Probabilities for Post Hoc Tests
Error: Between MS = 506.08, df = 789.00

Cel	Habitat	{1} 6.4000	{2} 11.744	{3} 7.7619	{4} 16.808	{5} 3.5224	{6} 7.0706	{7} 2.2357	{8} 15.087	{9} 16.846	{10} 25.556	{11} 10.890	{12} 24.629
1	Forest		0.999745	1.000000	0.879809	0.999999	1.000000	0.999939	0.979486	0.957380	0.381693	0.999912	0.160154
2	Shade	0.999745		0.999955	0.985632	0.633492	0.994321	0.368362	0.999924	0.999016	0.559214	1.000000	0.121809
3	Swamps	1.000000	0.999955		0.877330	0.999709	1.000000	0.996282	0.986098	0.968111	0.363908	0.999991	0.104535
4	Fynbos	0.879809	0.985632	0.877330		0.000395	0.120474	0.000035	0.999999	1.000000	0.934534	0.828656	0.513796
5	Grassland	0.999999	0.633492	0.999709	0.000395		0.993015	0.999998	0.105999	0.195685	0.005423	0.450690	0.000018
6	Nama-Karoo	1.000000	0.994321	1.000000	0.120474	0.993015		0.911019	0.729493	0.734638	0.067790	0.994877	0.000098
7	Savanna	0.999939	0.368362	0.996282	0.000035	0.999998	0.911019		0.032107	0.090132	0.001867	0.169928	0.000018
8	Succulent Karoo	0.979486	0.999924	0.986098	0.999999	0.105999	0.729493	0.032107		1.000000	0.880358	0.997461	0.524110
9	Desert	0.957380	0.999016	0.968111	1.000000	0.195685	0.734638	0.090132	1.000000		0.983559	0.990746	0.939322
10	High alt.	0.381693	0.559214	0.363908	0.934534	0.005423	0.067790	0.001867	0.880358	0.983559		0.336834	1.000000
11	Damp soils	0.999912	1.000000	0.999991	0.828656	0.450690	0.994877	0.169928	0.997461	0.990746	0.336834		0.009564
12	Montane	0.160154	0.121809	0.104535	0.513796	0.000018	0.000098	0.000018	0.524110	0.939322	1.000000	0.009564	

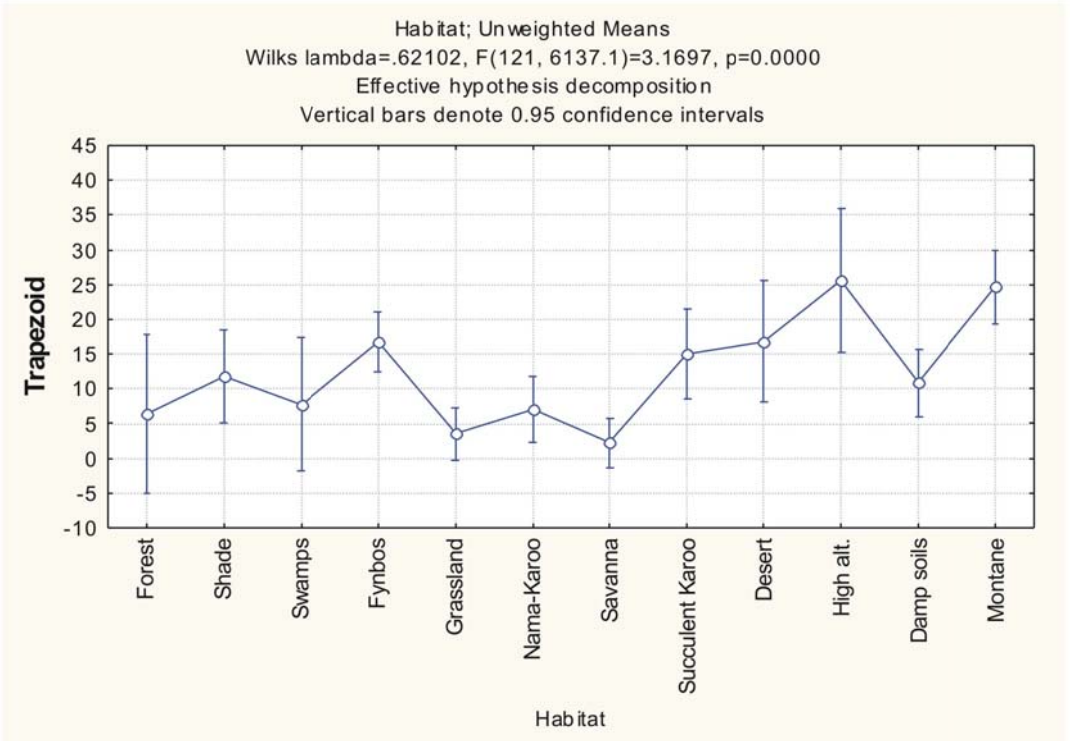

Tukey HSD test; variable **Rondel**
Approximate Probabilities for Post Hoc Tests
Error: Between MS = 222.43, df = 789.00

Ce	Habitat	{1} 6.5333	{2} 4.2791	{3} 5.8571	{4} 4.2115	{5} 3.1940	{6} 2.8000	{7} .05732	{8} 1.9565	{9} 3.4615	{10} 14.056	{11} 3.1463	{12} 6.3143
1	Forest		0.999997	1.000000	0.999992	0.999634	0.999192	0.907131	0.996993	0.999972	0.955085	0.999689	1.000000
2	Shade	0.999997		1.000000	1.000000	1.000000	0.999996	0.892536	0.999879	1.000000	0.451346	1.000000	0.999920
3	Swamps	1.000000	1.000000		0.999999	0.999828	0.999545	0.880418	0.997870	0.999994	0.863477	0.999863	1.000000
4	Fynbos	0.999992	1.000000	0.999999		0.999996	0.999966	0.547286	0.999475	1.000000	0.287743	0.999998	0.999025
5	Grassland	0.999634	1.000000	0.999828	0.999996		1.000000	0.824831	0.999998	1.000000	0.140293	1.000000	0.960185
6	Nama-Karoo	0.999192	0.999996	0.999545	0.999966	1.000000		0.969916	1.000000	1.000000	0.137612	1.000000	0.951143
7	Savanna	0.907131	0.892536	0.880418	0.547286	0.824831	0.969916		0.999831	0.995592	0.008910	0.935426	0.133995
8	Succulent Karoo	0.996993	0.999879	0.997870	0.999475	0.999998	1.000000	0.999831		1.000000	0.134396	0.999999	0.929711
9	Desert	0.999972	1.000000	0.999994	1.000000	1.000000	1.000000	0.995592	1.000000		0.464484	1.000000	0.999587
10	High alt.	0.955085	0.451346	0.863477	0.287743	0.140293	0.137612	0.008910	0.134396	0.464484		0.175440	0.718022
11	Damp soils	0.999689	1.000000	0.999863	0.999998	1.000000	1.000000	0.935426	0.999999	1.000000	0.175440		0.978665
12	Montane	1.000000	0.999920	1.000000	0.999025	0.960185	0.951143	0.133995	0.929711	0.999587	0.718022	0.978665	

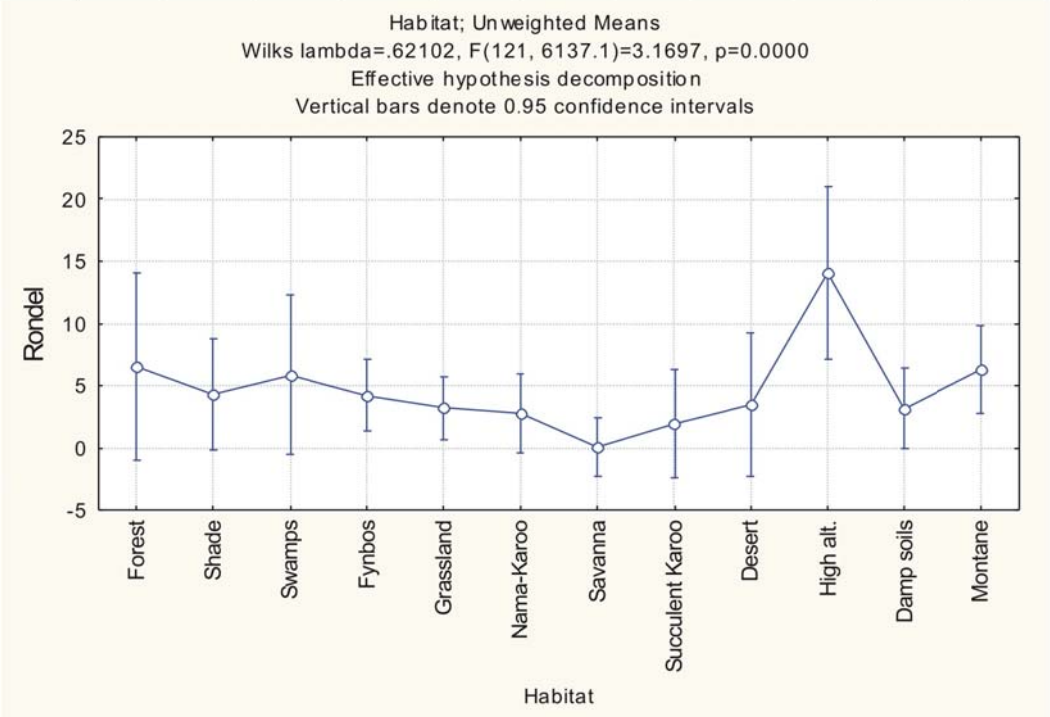

Tukey HSD test; variable **Oblong**
Approximate Probabilities for Post Hoc Tests
Error: Between MS = 507.99, df = 789.00

Ce	Habitat	{1} 7.0000	{2} 10.093	{3} 3.7619	{4} 5.7788	{5} 6.9030	{6} 5.9765	{7} 2.1911	{8} 9.9565	{9} 0.0000	{10} 15.000	{11} 12.927	{12} 13.243
1	Forest		0.999999	1.000000	1.000000	1.000000	1.000000	0.999753	0.999999	0.998466	0.997403	0.998754	0.998222
2	Shade	0.999999		0.996346	0.996327	0.999693	0.998180	0.667946	1.000000	0.817062	0.999793	0.999953	0.999898
3	Swamps	1.000000	0.996346		1.000000	0.999986	1.000000	1.000000	0.996683	0.999991	0.925720	0.885110	0.872942
4	Fynbos	1.000000	0.996327	1.000000		1.000000	1.000000	0.983925	0.996593	0.991191	0.908632	0.588217	0.592152
5	Grassland	1.000000	0.999693	0.999986	1.000000		1.000000	0.830538	0.999743	0.958008	0.957607	0.755658	0.754935
6	Nama-Karoo	1.000000	0.998180	1.000000	1.000000	1.000000		0.985092	0.998362	0.990289	0.928614	0.698992	0.695386
7	Savanna	0.999753	0.667946	1.000000	0.983925	0.830538	0.985092		0.655128	0.999999	0.488233	0.023897	0.031638
8	Succulent Karoo	0.999999	1.000000	0.996683	0.996593	0.999743	0.998362	0.655128		0.818225	0.999703	0.999906	0.999811
9	Desert	0.998466	0.817062	0.999991	0.991191	0.958008	0.990289	0.999999	0.818225		0.571289	0.309794	0.303761
10	High alt.	0.997403	0.999793	0.925720	0.908632	0.957607	0.928614	0.488233	0.999703	0.571289		1.000000	1.000000
11	Damp soils	0.998754	0.999953	0.885110	0.588217	0.755658	0.698992	0.023897	0.999906	0.309794	1.000000		1.000000
12	Montane	0.998222	0.999898	0.872942	0.592152	0.754935	0.695386	0.031638	0.999811	0.303761	1.000000	1.000000	

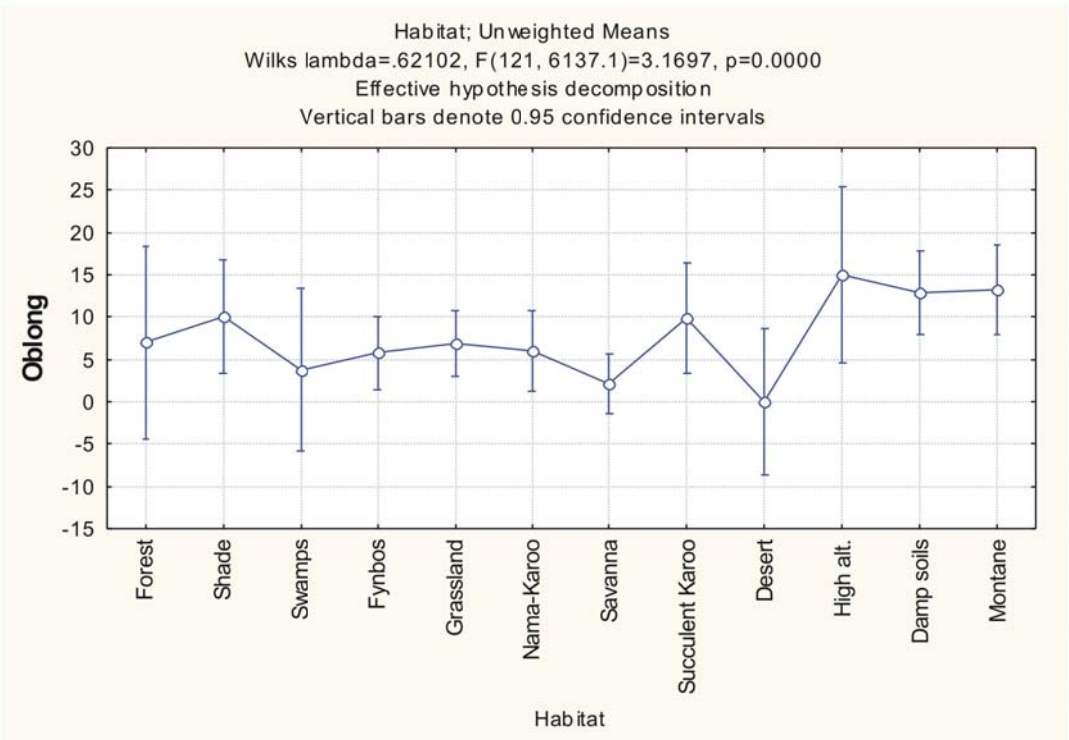

Tukey HSD test; variable **Reniform**
Approximate Probabilities for Post Hoc Tests
Error: Between MS = 122.76, df = 789.00

Ce	Habitat	{1} 0.0000	{2} 1.6977	{3} 1.4762	{4} 6.6058	{5} .95522	{6} .14118	{7} .21019	{8} 2.9348	{9} 2.2692	{10} 14.722	{11} 3.3780	{12} 10.957
1	Forest		0.999997	1.000000	0.579997	1.000000	1.000000	1.000000	0.999217	0.999973	0.007989	0.995313	0.025580
2	Shade	0.999997		1.000000	0.376570	1.000000	0.999849	0.999781	0.999996	1.000000	0.001706	0.999700	0.000983
3	Swamps	1.000000	1.000000		0.737091	1.000000	0.999998	0.999998	0.999998	1.000000	0.010724	0.999923	0.028906
4	Fynbos	0.579997	0.376570	0.737091		0.005403	0.003819	0.000320	0.777395	0.826570	0.151849	0.712326	0.314621
5	Grassland	1.000000	1.000000	1.000000	0.005403		0.999996	0.999990	0.996629	0.999993	0.000062	0.923376	0.000018
6	Nama-Karoo	1.000000	0.999849	0.999998	0.003819	0.999996		1.000000	0.967913	0.999457	0.000041	0.767460	0.000018
7	Savanna	1.000000	0.999781	0.999998	0.000320	0.999990	1.000000		0.949521	0.999319	0.000026	0.623966	0.000018
8	Succulent Karoo	0.999217	0.999996	0.999998	0.777395	0.996629	0.967913	0.949521		1.000000	0.007241	1.000000	0.007574
9	Desert	0.999973	1.000000	1.000000	0.826570	0.999993	0.999457	0.999319	1.000000		0.013177	0.999999	0.031397
10	High alt.	0.007989	0.001706	0.010724	0.151849	0.000062	0.000041	0.000026	0.007241	0.013177		0.004783	0.981021
11	Damp soils	0.995313	0.999700	0.999923	0.712326	0.923376	0.767460	0.623966	1.000000	0.999999	0.004783		0.001594
12	Montane	0.025580	0.000983	0.028906	0.314621	0.000018	0.000018	0.000018	0.007574	0.031397	0.981021	0.001594	

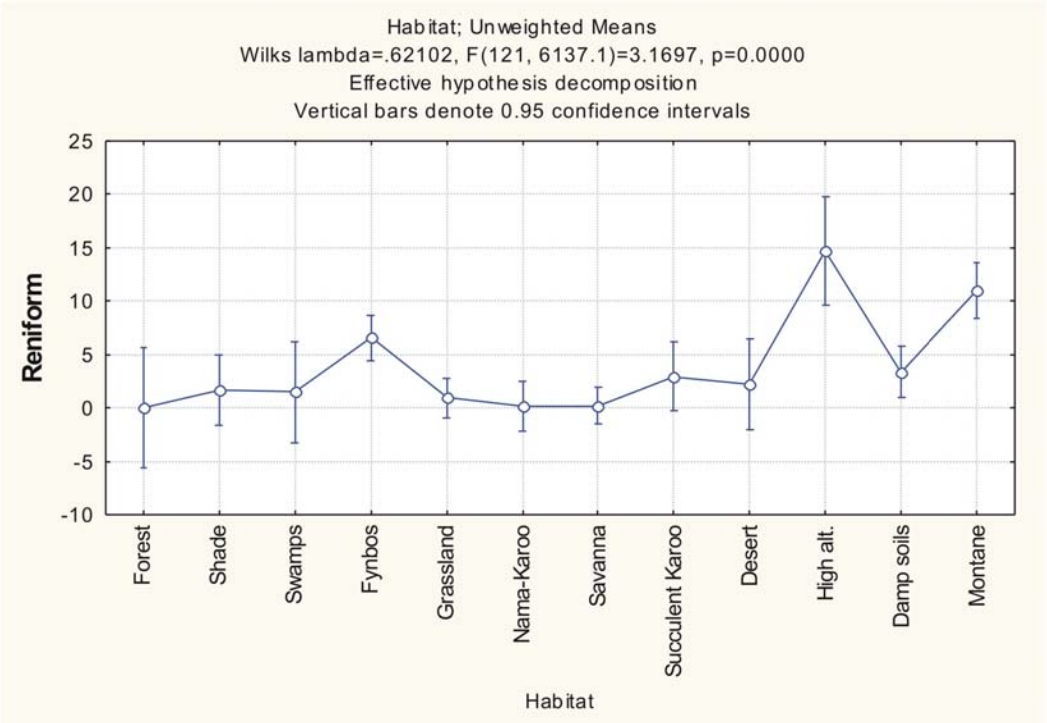

Appendix 16: Comparison of GSSC-phytoliths against three Palaeoenvironmental Scenarios.

Introduction

GSSC-phytolith morphotypes demonstrated their likely ability to predict a range of ecological and climatic conditions within the South African environment. The potential strength of the method was evaluated against several palaeoenvironmental interpretations provided by three fossil faunal assemblages located in the Grassland Biome (Figure 1). The faunal assemblages reflect palaeoenvironmental conditions at important stages of mammalian evolution in the central interior of southern Africa (Figure 2). The aim of this exercise was to compare these palaeoenvironmental interpretations with the results of analyses done on fossil phytolith samples, by using the Habitat- and Rainfall-categories as frameworks for interpretation.

Two assemblages are derived from Cornelia-Uitzoek and Florisbad, which are respectively the type localities of the Cornelian and Florisian Land Mammal Ages Age (*vide* Hendey 1974; Brink 1987, 1988; Brink and Rossouw 2000). A Land Mammal Age (LMA) is a period of geological time defined by its distinguishing faunal character (Hendey 1974).

The site of Cornelia-Uitzoek consists of fossil-bearing clays and fluvial gravels that are exposed along erosional gullies next to the Schoonspruit River on the Uitzoek farm near the town of Cornelia (Figure 3; Butzer 1974; Bender and Brink 1992) The vertebrate fauna from Cornelia-Uitzoek is an important representative sample of the southern African Middle Pleistocene (Cooke 1974; Bender and Brink 1992) and

considered to be coeval with the upper Beds of Olduvai, which suggests an age of between 800 000 and 1 million years ago for the site (Brink and Rossouw 2000). Latest excavations at the site suggest that carnivores may have been the primary collecting agent of the fossil accumulation (Brink and Rossouw 2000). The occurrence is rich in medium-sized ungulates with the extinct bovids, *Antidorcas bondi*, *Damaliscus niro* and *Connochaetes gnou laticornutus* representing the dominant taxonomic component (Brink and Rossouw 2000). These species, along with other extinct ungulates including the bovids, *Megalotragus eucornutus*, *Pelorovis antiquus*, and three equid species are regarded as indicator taxa for the incipient development of an open grassland ecosystem in the central interior of southern Africa (Brink and Rossouw 2000).

Florisbad, situated forty-five kilometers northwest of Bloemfontein, is the type locality of the Florisian Land Mammal Age (Hendey 1974) and consists of a fossil-bearing and archaeologically rich spring mound that has produced two distinct faunal assemblages, a Middle Stone Age land surface assemblage with evidence of human habitation and an older spring assemblage (Brink 1987, 1988). The Florisbad spring assemblage is between 100 000 and 400 000 years old and has produced hominid remains that yielded an ESR–date of 259 000 ± 35 000 yrs BP (Grün *et al*. 1996). Fossils from this occurrence are primarily derived from a carnivore- accumulated assemblage, excavated from intrusive spring vent structures that continually reworked and included fresh faunal material from around the spring and associated waterholes (Figure 4). Despite the temporal range of ESR age estimates, the spring assemblage is regarded as a homogeneous taphonomic entity (Brink 1988).

Classification of taxa according to habitat types, reflect a local spring environment indicated by the occurrence of hippopotamus and lechwe, as well as an open regional environment, indicated by a number of extinct grazers, including *Equus capensis, Pelorovis antiquus, Damaliscus niro, Megalotragus priscus* and *Antidorcas bondi,* The faunal composition reflect productive grassland conditions and a grazing system that is analogous to the grazing succession described for the modern sub-Saharan savannas in East Africa (Bell 1971; Brink 1987, 1988; Brink and Lee Thorp 1992). In addition, a study on the feeding niche of the extinct springbok *A. bondi* also established the existence of C_4 grasslands in the region (Brink & Lee Thorp 1992). The third faunal assemblage is derived from a recent discovery of fossiliferous fluvial sediments at Erfkroon, sixty kilometers southwest of Florisbad, which in part represent the terminal period of the Florisian LMA in the central interior of southern Africa (Figure 5). The site covers several hectares of river channel and overbank silts and clays flanking the modern Modder River (Churchill *et al.* 2000). New excavations are currently in progress and preliminary luminescence dating indicates that the overbank sediments span the last 160 000 years with several distinctive pedostratigraphic units dating to just before the start of the Last Glacial Maximum (Figure 3C; Churchill *et al.* 2000; J.S. Brink pers. com.). The site preserves vertebrate fossils that are typically Florisian in character, as well as birds, amphibians, small reptiles, fish and micromammals, which is also representative of a more complex riverine environment (Churchill *et al.* 2000; J.S. Brink pers. com.). Geologically, the exposed sediments reflect the evolution of the Modder River system during the Late Pleistocene, and it has been suggested that the extensive channel sedimentation and

overbank deposits developed under changing palaeoclimates that ranged from semiarid to arid (Churchill *et al.* 2000).

Materials and Methods

Materials

Four sediment samples, were collected from the temporally homogenous, fossil bearing yellow clay unit at the Cornelia-Uitzoek type site (Figure 3). Each sample was removed from the fossil-bearing unit in the form of consolidate blocks. Three hyaena coprolites were sampled from the Florisbad spring assemblage collection stored at the Florisbad Quaternary Research Station. Two of those (FLO1050 and FLO1051) were previously sampled for the extraction of pollen (Scott and Brink 1992) while the third had been analysed for phytoliths as part of a preliminary study (Scott and Rossouw 2005). The coprolites were analysed with consideration that the context of the spring assemblage was disturbed as a result of vertical displacement and post-depositional modification of bone by ancient intrusive spring vent structures (Figure 2B; Brink 1988). Although direct proof is difficult to establish at present, the possibility exist that the fossil coprolites may be temporally and taphonomically linked to the dated hominid remains due to their direct association with hyaena activity at the spring. Six sediment samples were collected from a pedostratigraphic sequence dated to between 25 600 ± 1200 years and 42 000 ± 2000 years BP by luminescence dating (Figure 5; J.S. Brink pers. com.). The samples were extracted with a small corer after initial cleaning of the section facies.

Phytolith extraction and assemblage analysis

The procedure for recovering phytoliths from coprolite and soil samples is based on published techniques (Piperno, 1988; Lentfer and Boyd, 1998, 1999; Albert and

Weiner, 2001; Horrocks, 2005). Only half of each fossil coprolite sample was used for the extraction of phytoliths. To avoid potential contamination, the outer layer of each sample was removed by submerging the coprolites in a solution of HCl (10%) for five minutes where after it was rinsed at treated the same as the sediment samples. The sediment samples were collected in consolidated blocks to minimize potential contamination. Ten different modern soil samples were collected in the vicinity of each fossil locality. Each set was then mixed up and analysed as one representative sample per site. Twenty grams of soil for each sample was used for each phytolith extraction. Essential steps included deflocculation, removal of clays by means of sedimentation and the elimination of carbonates using HCl in low concentration (10%). Phytolith extraction involved mineral separation with a heavy liquid solution of sodium polytungstate (specific gravity = 2.3). Fractions were mounted on microscope slides in glycerin jelly or DPX mountant. The phytolith counts are based on systematic scanning following standardized transects for each slide and identification at X400 magnification (Table 1).

Phytolith counts were normalized as percentages of the short-cell sum for each sample (Figure 6), based on the total count of the eleven GSSC-morphotypes (acknowledged in Chapter 2, Table 2), and incorporated into the modern dataset of GSSC-profiles that were created for the Habitat- and Rainfall-category in Chapter 2, Table 6 (Table 2). The combined dataset was analyzed using CA by applying the GSSC-morphotypes that were found to be significant for the Habitat- and Rainfall-categories (see Chapter 5, Table 22). The CA for the Rainfall-category was carried out in order to substantiate the trends observed in the CA conducted for the Habitat-

category.

Results

The first CA carried out for the Habitat-category resulted in two dimensions explaining a cumulative 90.2% of inertia, with a total of three dimensions extracted (Table3, Figure 7). While there is some overlap amongst habitat-subcategories, the CA did show that the inertia created by the matrix apparently distributed the fossil samples across the plot according to a climatic gradient. The first dimension accounted for 65.7% of the inertia and was clearly driven by growing temperature, with predominantly C_4, warm growing-temperature environments represented by the Savanna grassland-subcategory (highest contribution to total relative inertia = 0.051476), and predominantly C_3, cool growing-temperature environments marked by the High altitude grassland- category on the other end of the graph (highest contribution to total relative inertia = 0.214589). Dimension 2, accounting for 26% of the inertia, indicated a moisture gradient, with wetter habitats marked by the High altitude grassland- category and drier habitats marked by the Succulent Karoo-subcategory at the bottom of the graph (Figure 7).

The second CA conducted for the Rainfall-category confirmed the trends observed in the first CA. It resulted in two dimensions explaining a cumulative 77.8% with a total of five dimensions extracted. Dimension 1 accounted for 53.4% of the inertia and clearly showed a seasonal grade marked by the >500mm Summer Rainfall- and >40% Winter Rainfall-subcategory, while the second dimension accounted for 24.4% of the inertia and reflected a wetness gradient (Table 4, Figure 8).

The Cornelia specimens indicated their affiliation with the Savanna grassland- and Nama-Karoo grasses – subcategories in the first CA and the <500mm Summer Rainfall-subcategory in the second CA. The Florisbad spring assemblage material demonstrated more diverse trends. COR59 did not plot closely to any subcategory, but was more inclined towards the Fynbos grasses-, and Swamps/Vleis-subcategories in the first CA and the >40% Winter Rainfall subcategory in the second CA. FLO1050 and FLO1051 fell closer to the Nama-Karoo grasses and >500mm Summer Rainfall subcategories. Alliances amongst the Erfkroon samples were mainly with the Desert grasses-subcategory in the first CA, except for ERF5 and ERF7a, which respectively associated closer to the Fynbos grasses- and Nama-Karoo grasses-subcategories. The second CA indicated that the Erfkroon samples associated closely with the >40 Winter Rainfall-subcategory.

Discussion and Conclusion

The fossil phytolith data from Cornelia-Uitzoek suggests that relatively warm and dry C_4 grassland conditions, analogous to Savanna grassland or Nama-Karoo environments, prevailed during the time of bone accumulation at the site. The plots indicated a wooded grassland component, represented by the Savanna grassland-subcategory, but also warmer and drier than present summer rainfall environments, as represented by the Nama-Karoo grasses subcategory. The Nama-Karoo Biome today is a complex of extensive plains dominated by low shrubs intermixed with grasses where small trees occur only along drainage lines or rocky outcrops (Mucina *et al*. 2006b) Nama-Karoo-type conditions could be indicative of incipient treeless grassland development. However, the data also implies that open grasslands were

probably not as established as previously inferred from the faunal record (Brink and Rossouw 2000).

Phytolith data from Florisbad samples, FLO1050 and FLO1051 affiliated closely with the Nama-Karoo grasses-subcategory in the first CA and more generally with the >500mm Summer Rainfall-subcategory in the second CA. The Nama-Karoo Biome forms a dry ecotone between the winter-rainfall Fynbos Biome in the south and the summer rainfall Savanna Biome in the north, with summer rainfall occurring mostly in late summer (Mucina *et al.* 2006c). This trend concurs partly with pollen results of FLO1050 and FLO1051 from the Scott and Brink (1992) study, which showed dry pan floor elements like Chenopodiaceae pollen, and relatively high proportions of Asteraceae pollen, which is a dominant plant family in the Nama-Karoo Biome. The Asteraceae pollen was associated with low rainfall, but with a seasonality-shift away from summer rains (Scott & Nyakale 2002; Scott & Lee-Thorp 2004; Scott and Rossouw 2005). However, the absence and comparatively low amount of *Stoebe*-type pollen in FLO1050 and FLO1051 respectively, is probably related to a mesic C_4, summer rainfall environment (Scott and Rossouw 2005), which is also indicated by the plots in the second CA. The position of FLO59 in the two-dimensional matrix of the first CA was more representative of swampy conditions at the local spring environment than of the wider regional grassland, while its position in the second CA also corresponded to a mesic C_4, summer rainfall environment. An indication of swampy conditions was pointed out by the comparatively high proportions of Trapeziform morphotypes in the sample (Figure 6), which appear to be generally good indicators of swampy conditions and permanently damp soils (Table 22).

The phytolith data from the spring assemblage coprolites demonstrated the presence of a C_4 grassland ecosystem with a local aquatic component at Florisbad, which is in accordance with the faunal evidence (Brink 1988; Brink and Lee Thorp 1992). However, there were no association between the phytolith data and the modern Grassland Biome-subcategory. Although the results are in line with the pollen data from FLO1050 and 1051, reconciling summer rainfall and Nama-Karoo-type conditions with a productive grassland ecosystem in the spring assemblage most likely suggest that a unique grassland ecosystem with no modern analogue existed at the time.

Phytolith data from Erfkroon indicated cool and dry Desert- to Fynbos-like conditions between 42 000 years and 26 000 years ago. The results are supported by pollen evidence from the Tswaing Crater sequence in the current Savanna Biome about five hundred kilometers north of Erfkroon, that indicate aridification of grasslands between 33 000 and 40 000 thousand years ago, and cool dry grassland with fynbos elements at around 33 000 years ago (Scott 1999), while grass phytoliths from the same sequence suggest that C_3 grasses increased in the region between 29 000 and 8000 years ago (McLean and Scott 1999). The evidence support the hypothesis that the fluvial overbank deposits at Erfkroon developed under conditions that ranged from semiarid to arid (Churchill *et al.* 2000).

References

Albert, R.M., Weiner, S., 2001. Study of phytoliths in prehistoric ash layers using a quantitative approach. In: J.D. Meunier, and F. Coline. (eds.), *Phytoliths: Applications in Earth Sciences and Human History*. A.A. Balkema Publishers, Lisse, pp. 251–266.

Bell, R.H.V. 1971. A grazing ecosystem in the Serengeti. *Scientific American* 225(1): 86 – 93.

Bender, P.A. and Brink, J.S. 1992. A preliminary report on new large mammal fossil finds from the Cornelia-Uitzoek site. *South African Journal of Science* 88: 512 – 515.

Brink, J.S. 1987. The archaeozoology of Florisbad, Orange Free State. *Memoirs of the National Museum, Bloemfontein* 24: 1 – 151.

Brink, J.S. 1988. The taphonomy and palaeoecologgy of the Florisbad spring fauna. *Palaeoecology of Africa* 19: 169 – 179.

Brink, J.S. and Lee Thorpe, J.A. 1992. The feeding niche of an extant springbok, *Antidorcas bondi* (Antilopini, Bovidae), and its palaeoenvironmental meaning. *South African Journal of Science* 88: 227 – 229.

Brink, J.S. and Rossouw, L. 2000. New trial excavations at the Cornelia-Uitzoek type locality. *Navorsinge van die Nasionale Museum, Bloemfontein* 16: 141 – 156.

Butzer, K.W. 1974. Geology of the Cornelia Beds. *Memoirs of the National Museum* 9: 7 – 32.

Churchill, S.E., Brink, J.S., Berger, L.R., Hutchinson, R.A., Rossouw, L., Stynder, D., Hancox, J., Brandt, D. Woodborne, S., Loock, J.C. Scott, L. and Ungar, P. 2000. Erfkroon: a new Florisian fossil locality from fluvial contexts in the western Free State,

South Africa. *South African Journal of Science* 96: 161 – 163.

Cooke, H.B.S. The fossil mammals of Cornelia, O.F.S., South Africa. *Memoirs of the National Museum* 9: 63 – 84.

Grün, R., Brink, J.S., Spooner, N.A., Taylor, L. Stringer, C.B. 1996. Direct dating of the Florisbad hominid. *Nature* 382: 500 – 501.

Hendey, Q.B. 1974. The Late Cenozoic Carnivora of the south-western Cape Province. *Annals of the South African Museum* 63: 1 – 369.

Horrocks, M., 2005. A combined procedure for recovering phytoliths and starch residues from soils, sedimentary deposits and similar materials. *Journal of Archaeological Science* 32, 1169-1175.

Lentfer, C.J., Boyd, W.E., 1998. A comparison of three methods for the extraction of phytoliths from sediments. *Journal of Archaeological Science* 25, 1152 – 1183.

Lentfer, C.J., Boyd, W.E., 1999. An assessment of techniques for the deflocculation and removal of clays from sediments used in phytolith analysis. *Journal of Archaeological Science* 26, 31 - 44.

McLean, B. and Scott, L.1999. Phytoliths in sediments of the Pretoria Saltpanand their potential as indicators of the environmental history at the site. In: T.C. Partridge (ed). *Tswaing-investigations into the origins, age and Palaeoenvironments of the Pretoria Saltpan*. Council for Geosciences, Pretoria. Pp 167 – 171.

Piperno, D. R., 1988. *Phytolith analysis: an archaeological and geological perspective*. Academic Press, London.

Scott, L. and Brink, 1992. Quaternary palaeoenvironments of pans in central South Africa: palynological and palaeontological evidence. *South African Geographer* 19(1/2): 22 – 34.

Scott, L and Rossouw, L. 2005. Reassessment of botanical evidence for palaeoenvironments at Florisbad, South Africa. *South African Archaeological Bulletin* 60(182): 96 – 102.

Mucina, L., Rutherford, M.C., Palmer, A.R., Milton, S.J., Scott, L. *et al*. 2006b. Nama-Karoo Biome. In: L. Mucina and M.C. Rutherford (eds.) 2006. The vegetation of South Africa, Lesotho and Swaziland. *Strelitzia* 19: 324 - 347. National Botanical Institute, Pretoria.

Scott, L. 1999. The vegetation history and climate in the Savanna Biome, South Africa, since 190000 KA: A comparison of pollen data from the Tswaing Crater (the Pretoria Saltpan) and Wonderkrater. *Quaternary International* 57-58: 215-223.

Scott, L. and Lee-Thorp, J. A. 2004. Holocene climatic trends and rhythms in Southern Africa. In: R.W.. Battarbee, F. Gasse., and C.E. Stickley (eds) *Past Climate Variability through Europe and Africa.* Dordrecht, the Netherlands: Kluwer Academic Publishers.

Scott, L. and Nyakale, M. 2002. Pollen indications of Holocene palaeoenvironments at Florisbad in the central Free State. South Africa. *The Holocene* 12(4): 497-503.

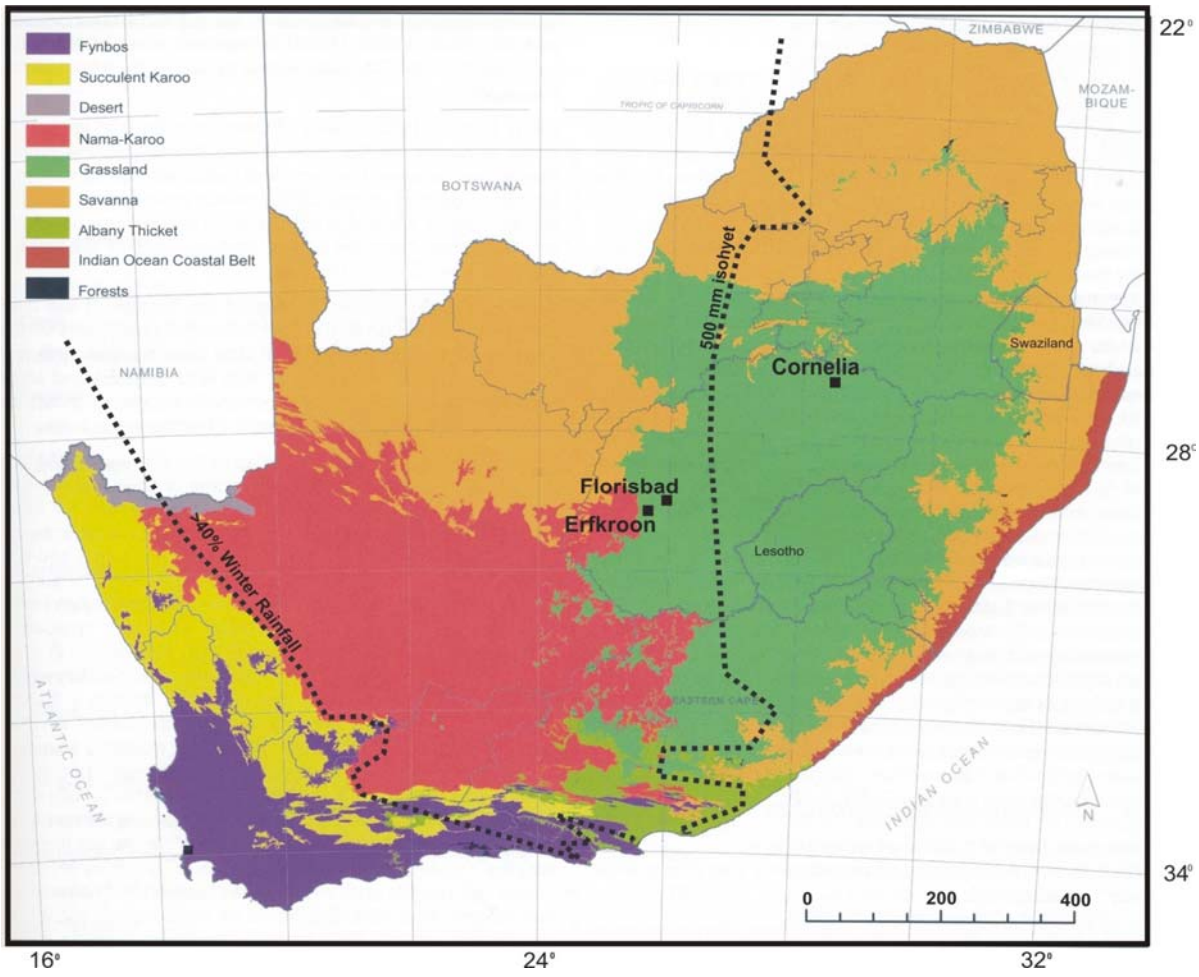

Figure 1. Map of fossil localities.

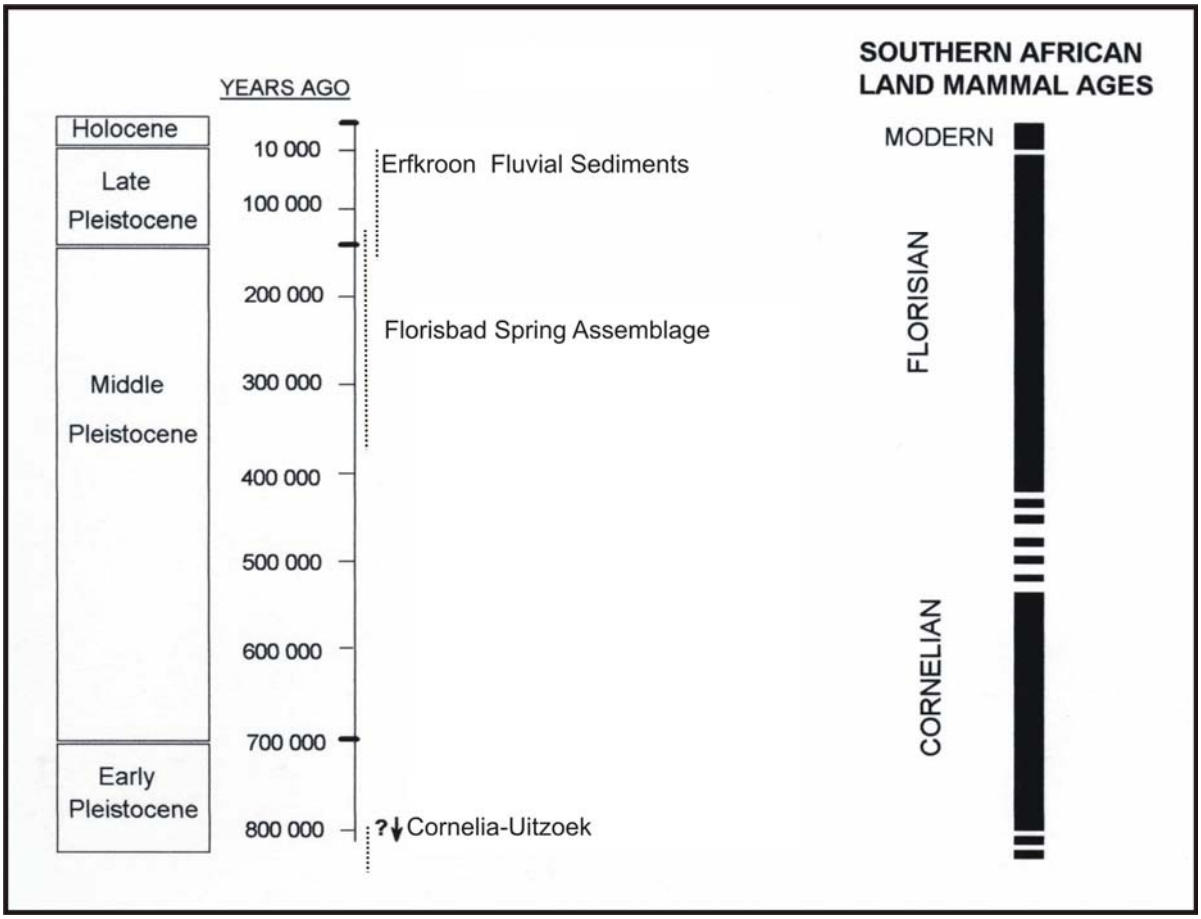

Figure 2. Temporal distribution of fossil localities.

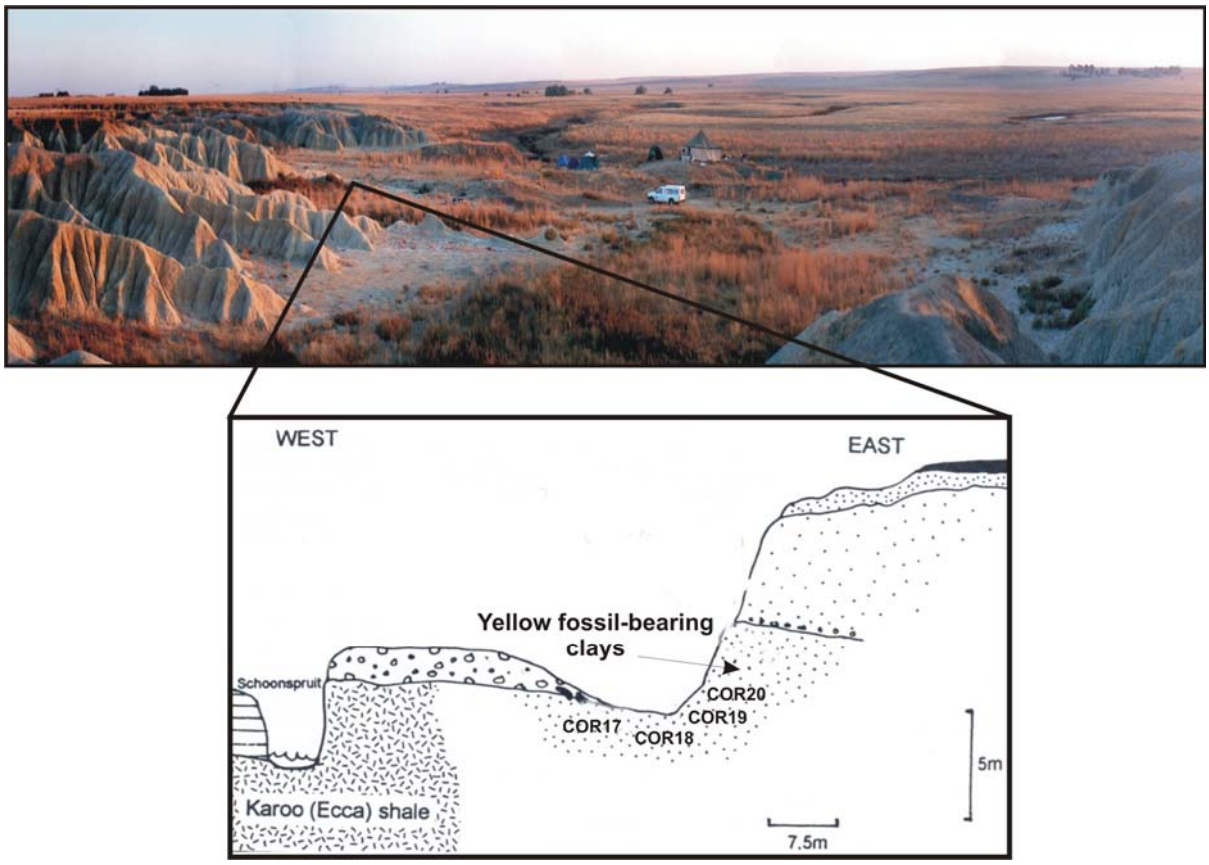

Figure 3. General view of Cornelia-Uitzoek with section diagram showing where samples were taken (after Butzer 1974).

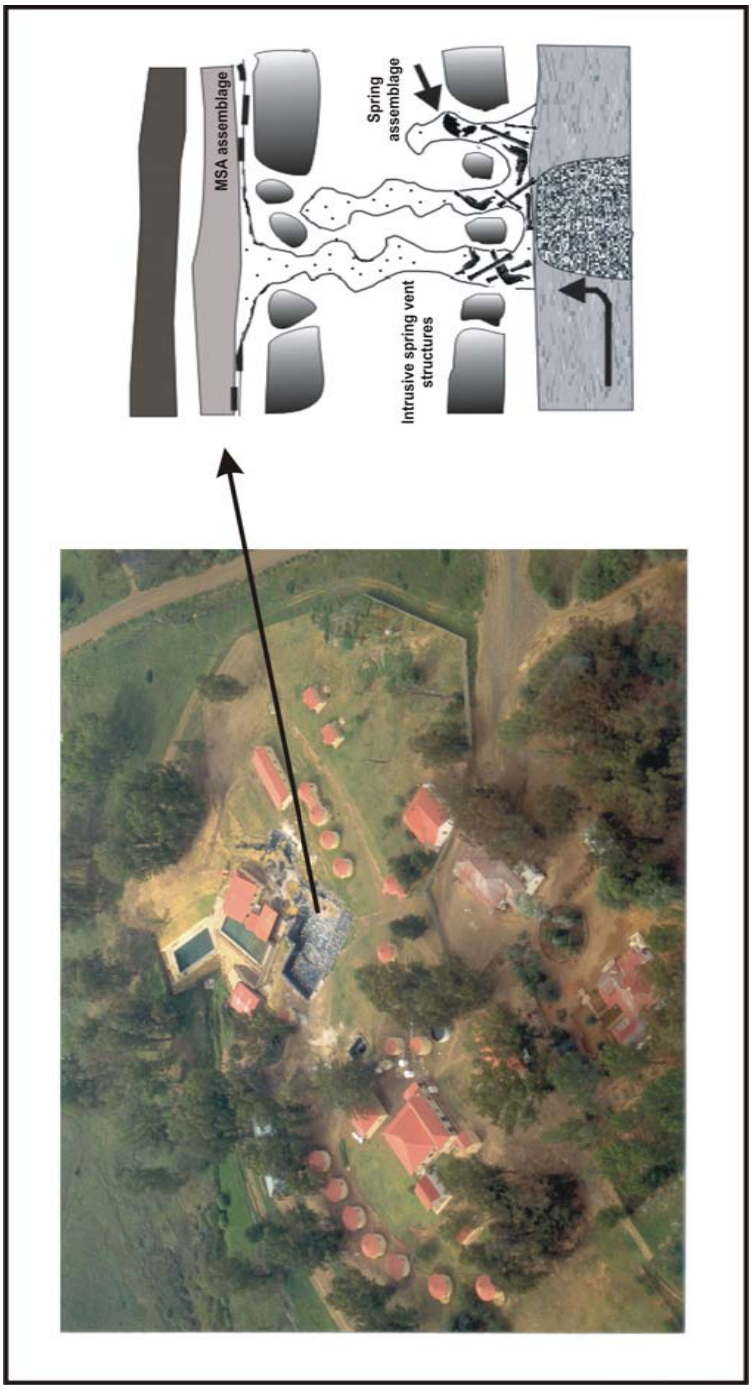

Figure 4. Aerial view of Florisbad with section diagram of the fossil-bearing sediments.

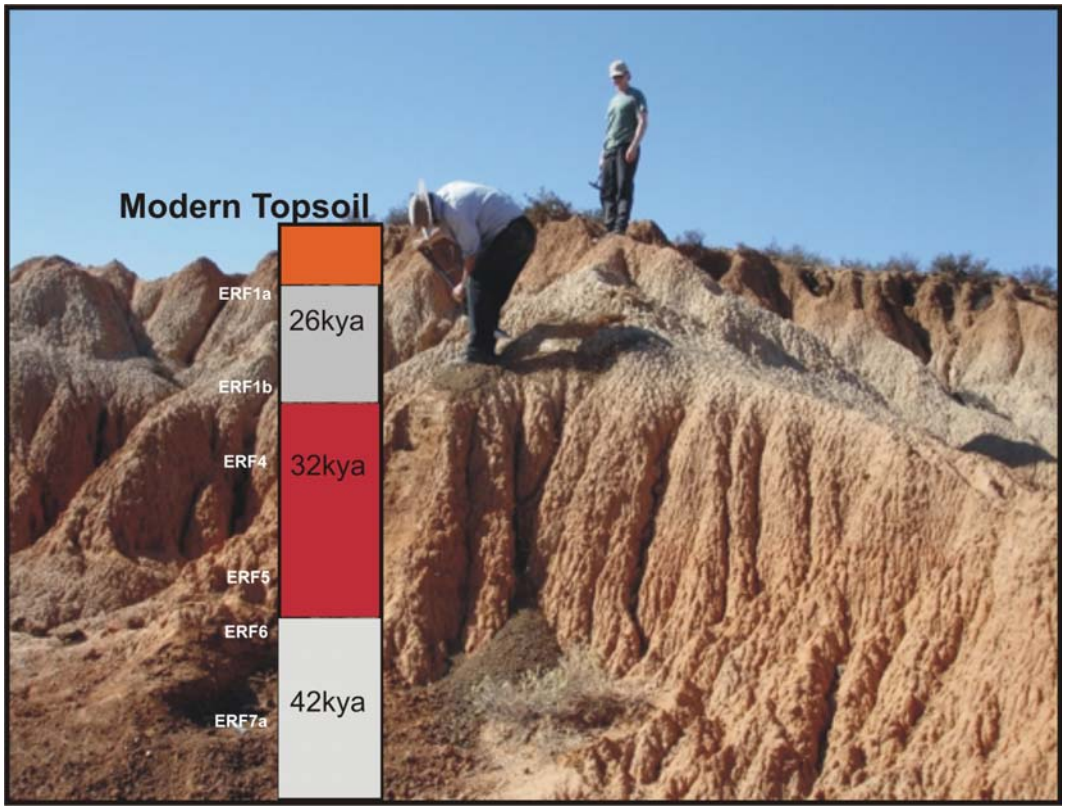

Figure 5. The section profile at Erfkroon where phytolith samples were collected.

Table 1. Number of phytoliths counted (raw counts).

	SUM	Bilobate Var1	Bilobate Var2	Bilobate Var3	Polylobate	Cross	Saddle Var1	Saddle Var2	Trapezoid	Rondel	Oblong
Cornelia Modern Soil	667	51	178	7	0	2	287	71	167	46	73
COR 20	512	57	41	12	0	5	231	48	26	29	51
COR 19	486	64	51	9	0	3	197	51	34	13	48
COR 18	498	37	77	11	0	4	179	63	98	14	12
COR 17	509	23	98	17	2	9	201	69	44	18	21
Florisbad Modern Soil	1091	124	178	56	67	45	238	142	157	15	57
FLO 59	423	77	44	13	7	4	61	32	102	6	67
FLO 1050	517	143	166	19	33	2	54	27	29	14	17
FLO 1051	535	97	145	11	6	7	109	53	59	26	13
Erfkroon Modern Soil	1055	98	199	24	28	33	284	217	89	13	59
ERF 1a	177	2	3	2	0	1	11	26	35	7	82
ERF 1b	296	6	2	0	0	0	37	46	53	20	120
ERF 4	316	3	7	0	0	2	54	67	61	32	87
ERF 5	213	9	6	3	0	1	53	22	32	12	56
ERF 6	203	12	24	7	0	5	44	37	56	2	15
ERF 7 a	197	9	13	2	0	0	46	26	15	11	58

Table 2. Phytolith counts normalized as percentages of the short-cell sum for each sample and incorporated into the modern dataset of GSSC-profiles created for the Habitat- and Rainfall-category.

	Bilobate Var1	Bilobate Var2	Bilobate Var3	Polylobate	Cross	Saddle Var1	Saddle Var2	Trapezoid	Rondel	Oblong	Reniform
COR 20	11.133	8.008	2.3438	0.000	0.977	45.117	9.375	5.078	5.664	9.961	2.344
COR 19	13.169	10.494	1.8519	0.000	0.617	40.535	10.494	6.996	2.675	9.877	3.292
COR 18	7.298	15.187	2.1696	0.000	0.789	35.306	12.426	19.329	2.761	2.367	0.592
COR 17	4.323	18.421	3.1955	0.376	1.692	37.782	12.970	8.271	3.383	3.947	1.316
FLO 59	18.203	10.402	3.0733	1.655	0.946	14.421	7.565	24.113	1.418	15.839	2.364
FLO 1050	27.660	32.108	3.6750	6.383	0.387	10.445	5.222	5.609	2.708	3.288	2.515
FLO 1051	18.131	27.103	2.0561	1.121	1.308	20.374	9.907	11.028	4.860	2.430	1.682
ERF 1a	1.130	1.695	1.1299	0.000	0.565	6.215	14.689	19.774	3.955	46.328	4.520
ERF 1b	2.027	0.676	0.0000	0.000	0.000	12.500	15.541	17.905	6.757	40.541	4.054
ERF 4	0.949	2.215	0.0000	0.000	0.633	17.089	21.203	19.304	10.127	27.532	0.949
ERF 5	4.225	2.817	1.4085	0.000	0.469	24.883	10.329	15.023	5.634	26.291	8.920
ERF 6	5.911	11.823	3.4483	0.000	2.463	21.675	18.227	27.586	0.985	7.389	0.493
ERF 7a	4.569	6.599	1.0152	0.000	0.000	23.350	13.198	7.614	5.584	29.442	8.629
Desert grasses	15.577	16.500	1.1923	0.885	0.000	18.923	24.346	16.846	3.462	0.000	2.269
Succulent Karoo grasses	3.500	23.413	3.5217	3.478	3.804	7.826	24.326	15.087	1.957	9.957	2.935
Nama-Karoo grasses	8.214	30.318	2.6235	4.762	5.310	22.600	9.388	7.071	2.800	5.976	0.141
Savanna grassland	17.071	36.586	2.6752	6.089	4.127	23.904	4.516	2.236	0.057	2.191	0.210
Grassland Biome	15.194	35.396	2.2985	7.276	4.858	18.022	1.634	3.522	3.194	6.903	0.955
Fynbos grasses	4.087	35.990	5.4904	3.827	3.260	8.644	4.269	16.808	4.212	5.779	6.606
Montane grassland	11.486	24.300	2.2143	3.614	0.886	1.671	0.686	24.629	6.314	13.243	11.116
High altitude grassland	21.833	7.556	0.6667	0.389	0.000	0.000	0.222	25.556	14.056	15.000	14.722
Damp soils	11.877	36.439	3.9268	5.148	5.556	6.605	0.593	10.890	3.146	12.927	3.378
Swamps/Vleis	13.952	40.286	5.0476	11.950	5.800	4.762	0.190	7.762	5.857	3.762	1.476
<500S	6.856	29.309	2.8557	6.845	4.433	27.784	15.742	2.320	2.340	0.247	0.344
>500S	16.665	35.693	3.1023	6.801	3.847	15.960	1.341	6.324	2.318	5.256	2.251
>40%W	3.888	33.496	5.4240	4.496	2.880	3.128	10.160	17.424	3.920	7.672	6.672

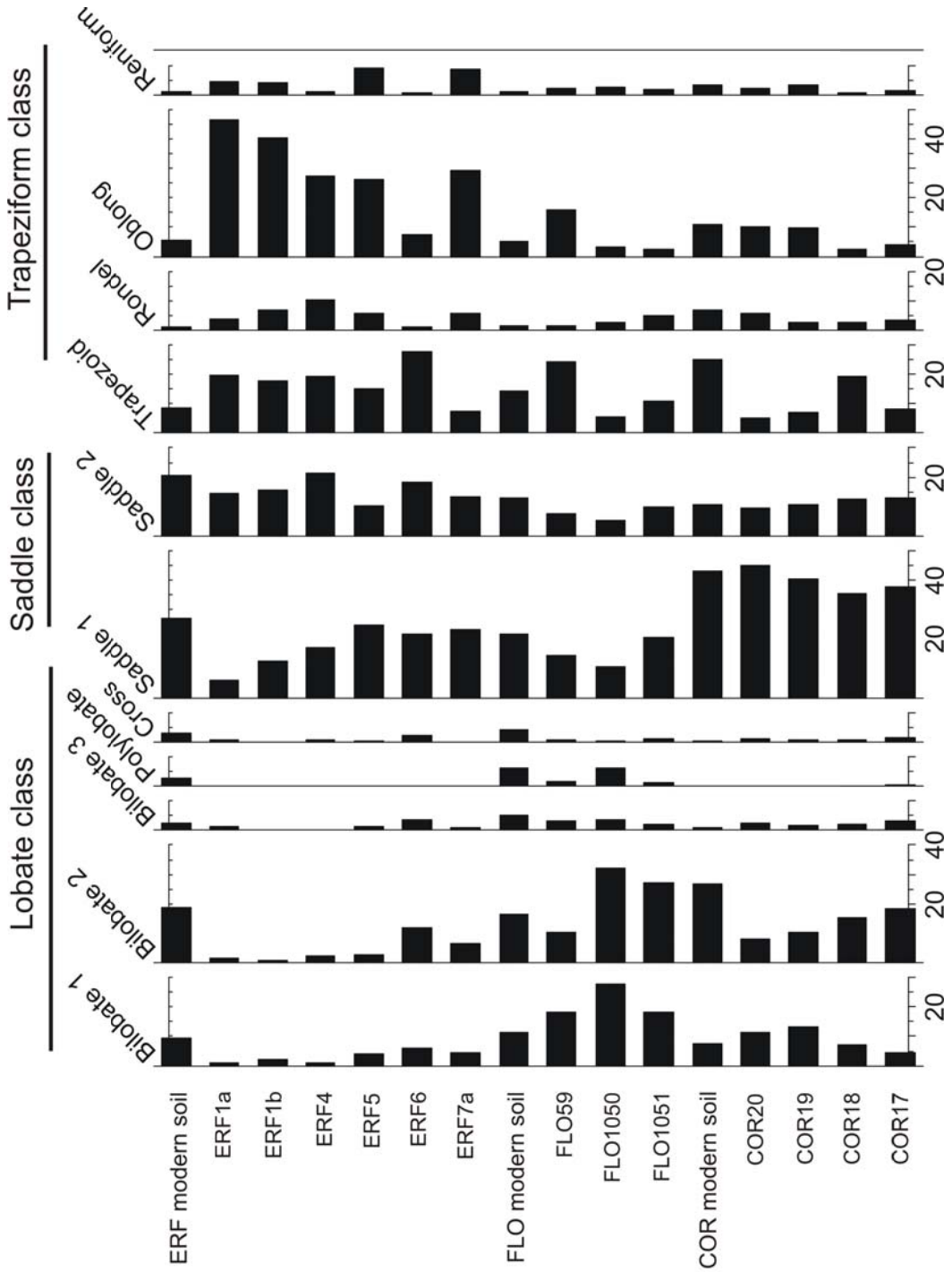

Figure 6. GSSC-phytolith diagram of the fossil samples.

Table 3. Dimension contributions to inertia in CA for Habitat-category.

Number of Dims.	Eigenvalues and Inertia for all Dimensions Input Table (Rows x Columns): 23 x 4 Total Inertia=.34959 Chi²=369.69 df=66 p=0.0000 Singular Values	Eigen-Values	Perc. of Inertia	Cumulatv Percent	Chi Squares
1	0.479321	0.229748	65.71865	65.7186	242.9542
2	0.301860	0.091119	26.06433	91.7830	96.3568
3	0.169488	0.028726	8.21702	100.0000	30.3774

Row Name	Row Coordinates and Contributions to Inertia Input Table (Rows x Columns): 23 x 4 Standardization: Row and column profiles Row Number	Coordin. Dim.1	Coordin. Dim.2	Mass	Quality	Relative Inertia
COR 20	1	-0.608337	0.318853	0.058549	0.996234	0.079304
COR 19	2	-0.485034	0.257252	0.057984	0.984192	0.050800
COR 18	3	-0.260308	0.033396	0.063976	0.637639	0.019767
COR 17	4	-0.499167	0.105973	0.057059	0.999230	0.042533
FLO 59	5	0.259288	-0.059080	0.045829	0.381179	0.024322
FLO 1050	6	-0.058854	0.078614	0.022498	0.377303	0.001645
FLO 1051	7	-0.199404	-0.023540	0.040654	0.950117	0.004934
ERF 1a	8	0.403362	-0.356605	0.042741	0.998439	0.035494
ERF 1b	9	0.180275	-0.267796	0.047282	0.985529	0.014302
ERF 4	10	-0.025594	-0.418848	0.055362	0.991784	0.028117
ERF 5	11	0.074759	0.206632	0.055940	0.620359	0.012455
ERF 6	12	0.035400	-0.274842	0.064285	0.585416	0.024121
ERF 7a	13	-0.056277	0.140098	0.049922	0.130301	0.024981
Desert grasses	14	-0.068093	-0.413223	0.058994	0.946516	0.031269
Succulent Karoo grasses	15	0.122765	-0.643750	0.047447	0.897641	0.064936
Nama-Karoo grasses	16	-0.447054	-0.006634	0.037069	0.988635	0.021440
Savanna grassland	17	-0.719679	0.312613	0.029188	0.998586	0.051476
Grassland Biome	18	-0.533927	0.458853	0.022822	0.978712	0.033060
Fynbos grasses	19	0.541753	0.178442	0.034352	0.998942	0.032003
Montane grassland	20	1.153730	0.340886	0.036031	0.999142	0.149293
High altitude grassland	21	1.318761	0.446426	0.038299	0.989605	0.214589
Damp soils	22	0.498439	0.327769	0.020299	0.884061	0.023374
Swamps/Vleis	23	0.415879	0.278873	0.013419	0.609666	0.015786

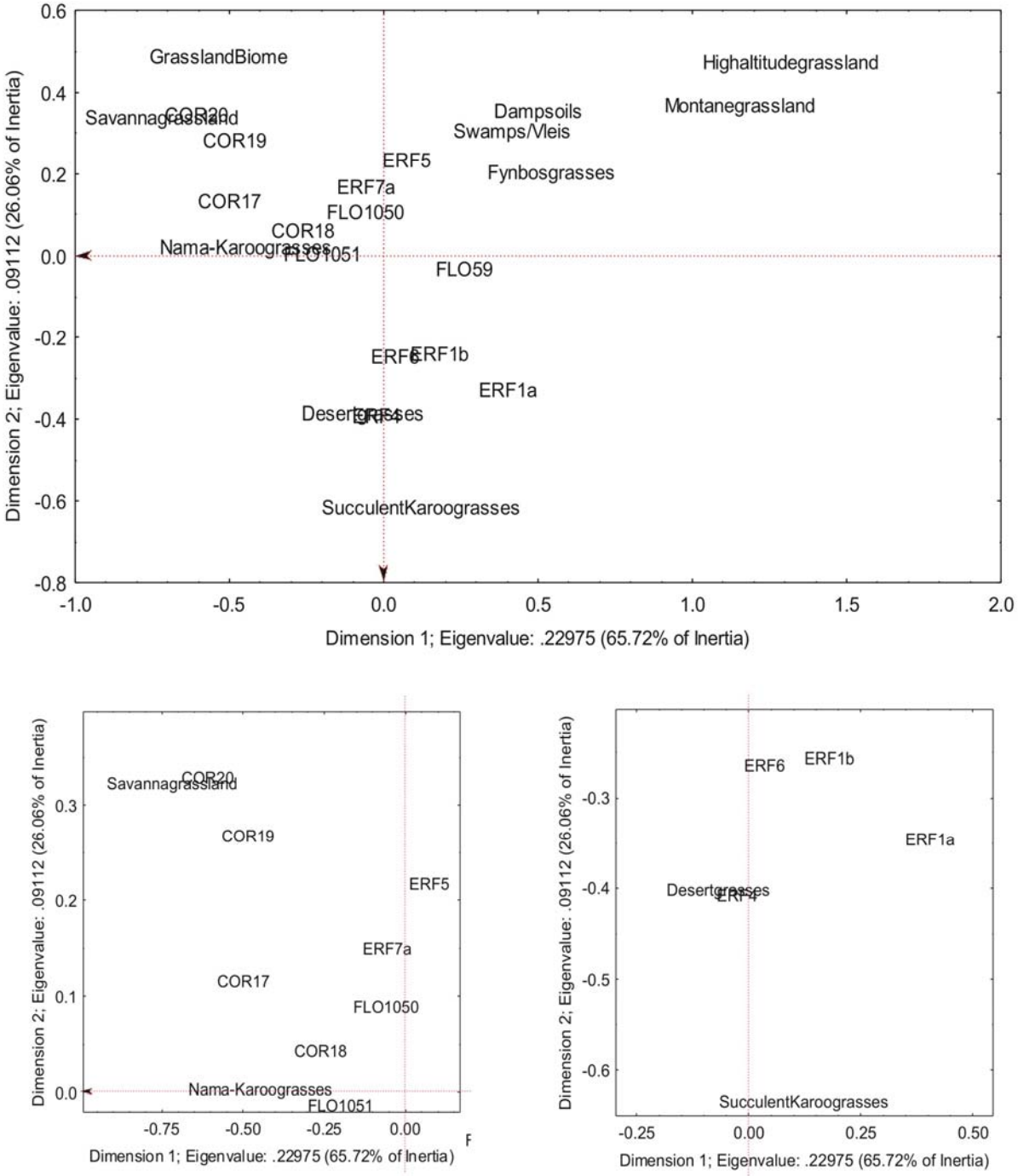

Figure 7. First CA. Two-dimensional matrix of data generated by the CA for the Habitat-category.

Table 4. Dimension contributions to inertia in CA for Rainfall-category.

Number of Dims.	Eigenvalues and Inertia for all Dimensions Input Table (Rows x Columns): 16 x 6 Total Inertia=.41851 Chi²=499.75 df=75 p=0.0000 Singular Values	Eigen-Values	Perc. of Inertia	Cumulatv Percent	Chi Squares
1	0.472815	0.223554	53.41695	53.4170	266.9522
2	0.319701	0.102209	24.42226	77.8392	122.0507
3	0.239707	0.057459	13.72960	91.5688	68.6139
4	0.148689	0.022109	5.28270	96.8515	26.4004
5	0.114789	0.013177	3.14848	100.0000	15.7346

Row Name	Row Coordinates and Contributions to Inertia Input Table (Rows x Columns): 16 x 6 Standardization: Row and column profiles Row Number	Coordin. Dim.1	Coordin. Dim.2	Mass	Quality	Relative Inertia
COR 20	1	-0.402270	-0.294684	0.069513	0.755935	0.054637
COR 19	2	-0.371858	-0.172917	0.070647	0.789039	0.035980
COR 18	3	-0.332637	-0.286168	0.064748	0.663602	0.044889
COR 17	4	-0.359714	-0.500981	0.057455	0.998434	0.052302
FLO 59	5	-0.038908	0.406459	0.069093	0.710918	0.038717
FLO 1050	6	-0.759956	0.871359	0.045840	0.960189	0.152493
FLO 1051	7	-0.528227	0.245271	0.053220	0.954562	0.045185
ERF 1a	8	0.830188	0.140048	0.077592	0.960356	0.136843
ERF 1b	9	0.656692	0.048944	0.077519	0.945992	0.084907
ERF 4	10	0.444117	-0.141091	0.072878	0.760838	0.049700
ERF 5	11	0.300703	-0.036442	0.075094	0.511108	0.032210
ERF 6	12	-0.007474	-0.112050	0.068067	0.044091	0.046520
ERF 7 a	13	0.342076	-0.053387	0.072691	0.456718	0.045585
<500S	14	-0.539176	-0.455542	0.044629	0.816430	0.065076
>500S	15	-0.555384	0.463915	0.040027	0.899577	0.055675
>40%W	16	0.335281	0.257656	0.040987	0.295400	0.059279

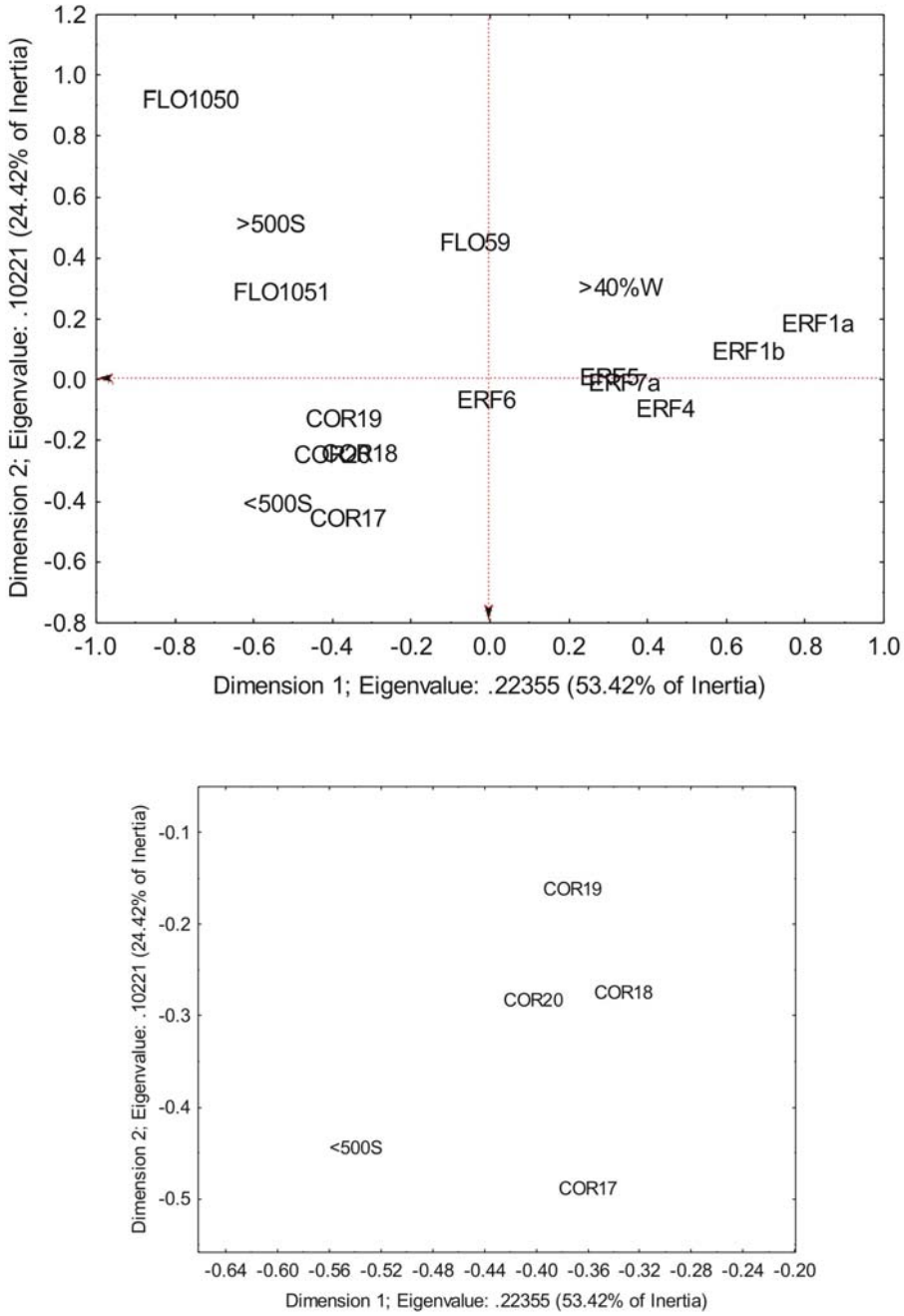

Figure 8. Second CA. Two-dimensional matrix of data generated by the CA for the Rainfall-category.